CONTENTS

Contents (continued)

Book Reviews

PARVUS

An Extendable Package of Programs for Data Exploration, Classification and Correlation

Authors: **M. Forina, R. Leardi, C. Armanino**, and **S. Lanteri**

- a software package for general pattern recognition
- comprehensive and efficient
- can be readily applied to a large range of problems in data analysis
- provides sophisticated statistical techniques for multivariate data analysis
- the programs can be subdivided into several functional groups:

  - data import
  - data manipulation and pre-processing
  - feature selection
  - data processing
  - classifying methods
  - correlation analysis
  - target factor analysis
  - regression analysis
  - nonlinear mapping
  - graphical presentation
  - and utilities

- can handle three main groups of problems:

  - explorative analysis and representation
  - classification
  - correlation

- available for IBM-PC and compatibles
- extensive program manual
- source code included
- US$ 645.00 / Dfl. 1325.00

AVAILABLE FROM:

Elsevier Scientific Software (JIC)
655 Avenue of the Americas
New York, NY 10010, USA
Phone: (212) 633 3950
Telex: 420643

or

Elsevier Scientific Software
P.O. Box 330
1000 AH Amsterdam
The Netherlands
Phone: (020) 5862 828
Telex: 18582

Write to us for further information on our other programs

No shipping charge if paid in advance
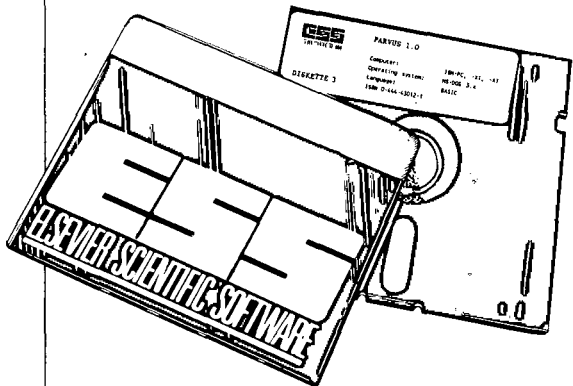
IBM-PC is a registered trademark of IBM

ELSEVIER SCIENTIFIC SOFTWARE

JOURNAL OF CHROMATOGRAPHY

Cumulative Author and Subject Indexes

An invaluable tool for locating published work, the CUMULATIVE AUTHOR AND SUBJECT INDEXES make the vast amount of information in the journal more easily accessible.

Supplied automatically to subscribers to the JOURNAL OF CHROMATOGRAPHY, the Indexes are also available separately for desk use.

Vols. 1 - 50 (1972)
US$ 87.50 / Dfl. 175.00

Vols. 51 - 100 (1975)
US$ 112.50 / Dfl. 225.00

Vols. 101 - 150
(Published as *J. Chromatogr.*
Vol. 293, 1984)
US$ 127.50 / Dfl. 255.00

Vols. 151 - 250
(Published as *J. Chromatogr.*
Vol. 263, 1983)
US$ 217.50 / Dfl. 435.00

Vols. 251 - 350
(Published as *J. Chromatogr.*
Vol. 453, 1988)
US$ 226.50 / Dfl. 453.00

Vols. 351 - 400
(Published as *J. Chromatogr.*
Vol. 401, 1987)
US$ 147.50 / Dfl. 295.00
PRICES QUOTED INCLUDE POSTAGE

JOURNAL

of

CHROMATOGRAPHY

INTERNATIONAL JOURNAL ON CHROMATOGRAPHY,

ELECTROPHORESIS AND RELATED METHODS

ELSEVIER
AMSTERDAM — OXFORD — NEW YORK — TOKYO

MATHEMATICAL MODELLING OF THE CONTINUOUS AFFINITY-RECYCLE EXTRACTION PURIFICATION TECHNIQUE

NOUBAR B. AFEYAN[a], NEAL F. GORDON[a] and CHARLES L. COONEY*

Department of Chemical Engineering, Massachusetts Institute of Technology, Cambridge, MA 02139 (U.S.A.)

SUMMARY

Continuous affinity-recycle extraction (CARE), a continuous protein purification unit operation, has been designed to address design and optimization criteria relevant for process scale chromatographic separation of proteins. The development and application of a mathematical model describing purification in the CARE process are described. The model incorporates adsorption–desorption kinetics into material balance equations describing the operation of two well-mixed reactors operating with recycle. An accurate mathematical model of CARE has aided in its development as a new unit operation for protein purification, in the assessment of its performance tradeoffs, and in its optimization.

INTRODUCTION

As the biotechnology industry undergoes a transition from research to product commercialization, cost reductions in process development and large-scale protein purification are emerging as key determinants to commercial success. Techniques used today for purification are mainly chromatographic in nature and employ equipment and material derived directly from the laboratory/bench scale. With these roots, it is common to find process chromatograms and adsorbents being evaluated based on resolution alone, with little regard to recovery or throughput. Process-scale chromatographic purification of proteins requires a different set of design and optimization criteria than those used for laboratory/research work. For example, final purity is a constraint and not an objective. The ultimate objective is minimum cost of a purified product that meet specifications which, in turn, implies maximal recovery and throughput. A different approach to the selection and design of unit operations for manufacturing, is to first consider the entire process at the largest scale, and then scale-down to an intermediate scale which can simulate, with confidence, the larger scales.

---

[a] Present address: PerSeptive Biosystems Inc., 60 Hamilton Street, Cambridge, MA 02139, U.S.A.

Due to the similarities in the physico-chemical properties of proteins found in typical fermentation or cell culture broth, very high levels of purity (required for most current commercial applications) can only be achieved by using a series of steps, each incrementally purifying the product via different separation mechanisms. This entire sequence of steps is often termed Downstream processing (DSP). DSP of a crude fermentation broth typically produces the final product with a very high purity but a correspondingly low recovery yield. In general, an average of 10–20% product loss per separation step is encountered; hence, the final recovery of a process with six DSP steps can be as low as 30%. This places a great impetus on integration of DSP steps in order to achieve the same purification with much higher overall recovery.

Protein purification is most often effected by chromatographic techniques. Adsorptive chromatography, which includes ion-exchange, affinity, reversed-phase and hydrophobic interaction chromatography, accounts for a large portion of the preparative chromatography applications. Traditionally, adsorptive chromatography is carried out using a fixed bed of adsorbent particles (i.e. column chromatography). While for small molecules, the importance of column length (i.e. number of theoretical plates) on resolution is well characterized, for macromolecules experimental evidence suggests a far lesser need for a large number of plates. Early reports of this observation showed that in surface mediated separations, columns of less than 5 cm long have 80% of the resolving power of 30-cm columns[1,2]. Among the adsorptive techniques, affinity chromatography, which uses biospecific interactions to purify the desired protein from a mixture, has been termed an "on–off" process[3], and is little more than solid–liquid extraction, a common unit operation in the chemical process industries. As such, a fixed bed is but one of alternative contactors which have been employed in other applications, such as: moving beds, simulated moving beds, counter current stirred contractors, etc.

An alternative to fixed bed affinity chromatography was recently proposed as a means of overcoming some of its operational limitations[4]. Continuous affinity-recycle extraction (CARE) was shown to allow continuous separation of an intracellular protein from a crude cell lysate following cell disruption without pre-clarification steps; the approach uses conventional chromatographic media. A schematic of the CARE system is shown in Fig. 1. CARE operates as follows. The sample is fed continuously to the adsorption stage where it contacts the adsorbent beads containing the affinity ligand. The desired product adsorbs while contaminants are washed out with wash buffer. The beads, with the adsorbed product, are then pumped to the desorbing stage where the addition of the desorbing buffer causes the detachment of the product from the affinity matrix. The bare beads are then recycled to the adsorption stage, while the product is removed with the desorbing buffer stream. Both vessels are well agitated; the sorbent is retained within the two vessels and the recycle loop by macroporous filters. The system can be operated continuously at steady state.

Initial experiments, where the enzyme β-galactosidase was recovered from a turbid liquor of lysed cells with no clarification (i.e. no debris removal), confirmed the technical feasibility of CARE. From an initial purity of 0.5%, a continuous product stream of 14% pure β-galactosidase was produced with 70% recovery[4]. An important advantage of CARE over conventional approaches is the early introduction of an affinity-based technique in a DSP train, and the omission of several steps which
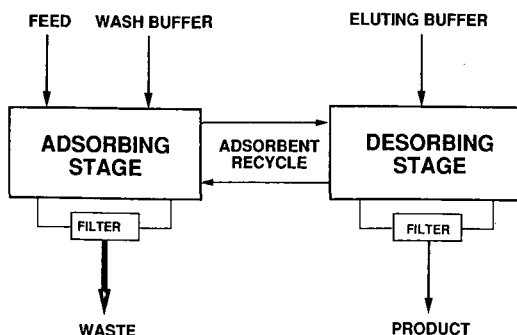
Fig. 1. Schematic of the CARE process.

would otherwise be required prior to the use of a fixed bed. This, in turn, can translate into higher overall product recoveries and lower cost of purification.

In addition to its performance advantages, the CARE technique is readily characterized mathematically. An accurate mathematical model of CARE has aided in its development as a new unit operation for protein purification, in the implementation of computer control for its continuous operation, and in its optimization. This paper describes the mathematical analysis of CARE, and various uses of the model.

MODEL FORMULATION

The strategy to model the CARE system is to mathematically describe the adsorption and desorption processes simultaneously with a material balance. The sorption rate parameters are estimated in batch experiments independent of purification in the CARE system. The methodology used to derive the rate parameters is described below as Microscopic formulation of the model. Descriptions of the sorption processes are then incorporated into a set of material balance equations describing the operation of two well-mixed vessels operating with recycle. This later section is described as a Macroscopic formulation. Purification performance then is predicted, by specifying flow-rate and feed-stream composition data.

Microscopic formulation
The literature is replete with mathematical models describing adsorption of solutes to porous, solid-phase supports[5-11]. A mathematical description must combine equations for the various mass transfer steps (film diffusion, internal pore diffusion) as well as the biochemical adsorption step. In general, one wishes to solve the equations for the decrease in solute concentration in the bulk solution, surrounding the porous support material, as a function of time.

The mathematical formulation employed here is a simple, lumped-parameter model[7]. This model does not explicitly distinguish between mass transport and intrinsic biochemical binding kinetics. However, as shown in this paper, this model describes the experimental system well.

Generalized adsorption model. This model is based on the isothermal sorption of a single solute onto porous particles, suspended in a well-mixed vessel. The bulk liquid

has a solute concentration, $c(t)$. The particles are spherical, with radius, R. The total volume is v, with liquid volume αv and adsorbent volume $(1 - \alpha)v$. The sorbate concentration in the particle is $q_i(r,t)$, where r is the radial position within the particle, and the solute concentration within the pore liquid is $c_i(r,t)$.

The mass balance for the adsorber is

$$\alpha\frac{\mathrm{d}c}{\mathrm{d}t} + (1 - \alpha)\frac{\mathrm{d}s}{\mathrm{d}t} = 0 \tag{1}$$

where s is the average solute concentration in the particle, which includes solute adsorbed to ligands at the pore surface as well as solute within the pore liquid. The two terms in eqn. 1 account for depletion of solute from the bulk liquid and solute uptake within the particles.

The rate of solute uptake within the particle is equated to the flux of solute into the pores, which is driven by a diffusive process described by Fick's Law:

$$\frac{\mathrm{d}s}{\mathrm{d}t} = 3\left(\frac{N_0}{R}\right) = 3\left(\frac{D_i}{R}\right)\left(\frac{\mathrm{d}c_i}{\mathrm{d}t}\right)_{r=R} \tag{2}$$

where D_i is the effective particle diffusion coefficient, and the quantity $3/R$ is the surface area per unit volume of particles.

The particle mass balance relates the solute diffusing into the pore with sorbate adsorbing at the pore surface.

$$D_i\left(\frac{\mathrm{d}^2c_i}{\mathrm{d}r^2}\right) + \frac{2}{r}\left(\frac{\mathrm{d}c_i}{\mathrm{d}r}\right) - \beta\left(\frac{\mathrm{d}c_i}{\mathrm{d}t}\right) - (1 - \alpha)\frac{\mathrm{d}q_i}{\mathrm{d}t} = 0 \tag{3}$$

The four terms in eqn. 3 represent the flux of solute into the pores, the depletion of solute in the pore liquid, and the adsorption of sorbate onto the pore surface, respectively.

The concentration of solute in the particle pores and in the bulk liquid is:

$$k(c - c_i)_{r=R} = D_i\left(\frac{\mathrm{d}c_i}{\mathrm{d}r}\right)_{r=R} \tag{4}$$

Finally, the rate of binding for affinity adsorption is commonly described by the following equation:

$$\frac{\mathrm{d}q}{\mathrm{d}t} = k_\mathrm{f}(Q_\mathrm{max} - q)c - k_\mathrm{r}q \tag{5}$$

Adsorption is second order in the forward direction and first order in the reverse direction. This rate equation corresponds to a Langmuir isotherm at equilibrium.

$$q_0 = \frac{Q_\mathrm{max}Kc}{(1 + Kc)} \tag{6}$$

In general, one wishes to solve for the decrease in solute concentration in the bulk solution as a function of time $c(t)$. An analytical solution to the equations developed above does not exist, hence one must resort to numerical techniques. Alternatively, one can lump all resistances to adsorption into a single parameter yielding a simplified and analytically solvable equation set.

Simplified lumped parameter adsorption model. The equations describing adsorption to porous solid phase supports, shown above, distinguish among the various resistances to adsorption. These resistances are: solute diffusion through a thin stagnant film surrounding the adsorbent particles, diffusion within the pores of the solid support, and the biochemical adsorption step itself.

These three resistances have been combined into the biochemical adsorption forward rate constant (k_f) with eqn. 5 representing the adsorption process. The solution for the bulk liquid concentration as a function of time is:

$$c(t) = \frac{[2c_0(N - b) + N^2 - b^2]D + 2c_0(b + N) + b^2 - N^2}{[4c_0 + 2b + 2N]D - 4c_0 - 2b + 2N} \tag{7}$$

where $b = Q_{max}(1 - \alpha) + 1/K - c_0$; $N = \sqrt{(b^2 + 4c_0/K)}$; and $D = \exp(Nk_f t)$.

This form of the solution to the adsorption equations was chosen for incorporation into the CARE model, because of its simplicity, both in number of required input parameters, and in its incorporation into a material-balance description of the CARE process. This solution requires the input of three adsorption parameters: two equilibrium and one kinetic.

Batch adsorption experiments were conducted with varying initial β-galactosidase concentration; bulk-liquid enzyme concentration (c) was measured as a function of time[12]. Rather than using equilibrium adsorption experiments to independently estimate the equilibrium adsorption parameters, batch adsorption rate data were fitted to eqn. 7 through non-linear regression yielding estimates for all three adsorption parameters. The estimated forward reaction rate constant (k_f) is not necessarily the true, intrinsic reaction rate constant; it is a parameter in which all resistances to adsorption, mass transfer and biochemical binding, have been incorporated. Similarly, the two estimated equilibrium parameters do not necessarily correctly predict the equilibrium adsorption isotherm, yet when used in conjunction with the rate constant yield good model agreement with experimental data.

The fit of the lumped parameter model to experimentally determined adsorption profiles is shown in Fig. 2. Good model agreement is obtained for both low (200 U/ml gel) and high (7000 U/ml gel) adsorbent loading. Although the three adsorption parameters result from an empirical fit to the data, this simple model predicts experimental adsorption data over a wide rage of adsorbent loading conditions.

Investigation of adsorption mechanism. Although, the adsorption of β-galactosidase to p-aminobenzyl-1-thio-β-D-galactopyranoside (PABTG)-Agarose has been successfully described using a lumped parameter approximation, this approach does not shed light on the mechanism of adsorption. One would anticipate that the rate of internal pore diffusion would control adsorption[5,13-15] since the affinity adsorbent is porous and fairly large (100 μm diameter). In addition, β-galactosidase is a large protein (mol.wt. *ca.* 460 000)[7]; its diffusion coefficient in bulk solution is small $(3 \cdot 10^{-8}$ cm^2/s)[16], and one would anticipate the effective diffusivity inside the pores to
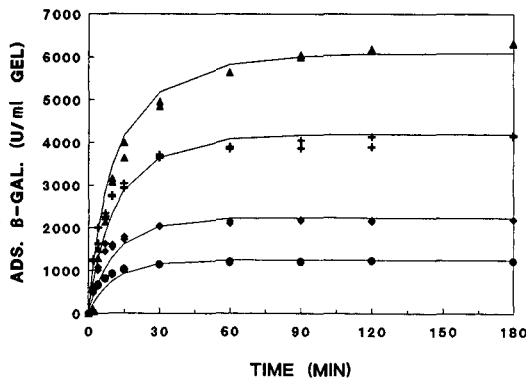
Fig. 2. Batch adsorption of β-galactosidase to PABTG-Agarose. Fit of lumped parameter adsorption model. Adsorption parameters: $Q_{max} = 7100$ U/ml; $K = 0.57$ ml/U; $k_f = 0.0013$ ml/U/min. Experiments performed in a batch vessel containing a total of 50 ml liquid volume; 0.5 ml adsorbent gel contacted with varying initial β-galactosidase concentrations ranging from 10 to 100 U/ml; samples were withdrawn periodically and the decrease in bulk β-galactosidase activity over time was determined. Initial β-galactosidase concentrations are: 13 U/ml: $\bullet$; 24 U/ml: $\blacklozenge$; 46 U/ml: $+$; 75 U/ml: $\blacktriangle$.

be even lower due to hindered diffusion. Finally, most affinity interactions are inherently fast, $e.g.$ relative to internal pore diffusion, and this is expected to be the case for the β-galactosidase affinity system employed here.

It was postulated previously that β-galactosidase, does not fully enter into the pores of the affinity support during adsorption[17] and adsorbs at the surface and entrance region to the pores, thus blocking further entry of molecules. As a consequence, it was felt that internal pore diffusion did not play a major role in determining adsorption rates since β-galactosidase was not penetrating into the pore.

In an attempt to verify this hypothesis, an experiment was performed where β-galactosidase was covalently immobilized, via cyanogen bromide activation[18] to Sepharose 4B. In this manner, the β-galactosidase molecule was immobilized in a position that could potentially block pore access as was believed to occur during adsorption of β-galactosidase to PABTG-Agarose. It was anticipated that the accessible volume fraction and possibly the effective diffusivity would decrease relative to unsubstituted Sepharose 4B.

A known volume of adsorbent gel was introduced into a solution of β-galactosidase of concentration c_0. At periodic intervals, samples were withdrawn and the β-galactosidase was determined by measurement of enzymatic activity (Fig. 3). β-Galactosidase concentration in the bulk fluid, from which it was sampled, decreased rapidly and then leveled off once the enzyme diffused into the interior of the adsorbent gel. The volume fraction of the gel accessible to β-galactosidase was calculated using eqn. 8.

$$\beta = \alpha\left(\frac{c_0 - c_f}{c_f}\right) \tag{8}$$

where $\alpha = (V_{bulk}/V_{gel})$.

As shown in Fig. 3, unsubstituted Sepharose, cyanogen bromide activated and blocked Sepharose (using ethanolamine) and Sepharose to which β-galactosidase had
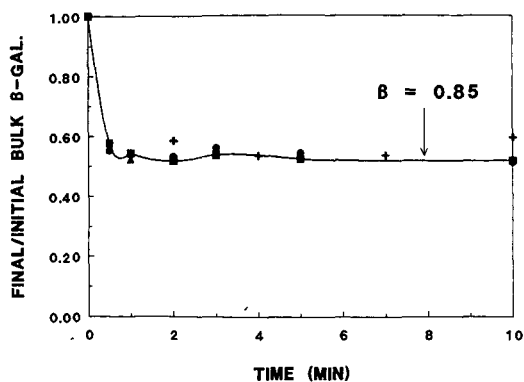
Fig. 3. Estimation of internal pore accessibility. Diffusion of β-galactosidase in Sepharose 4B. Base: + and ▲; CNBr activated: O; immobilized β-galactosidase: □. Experiments performed in 50-ml batch vessel; 50 ml of a 50% Sepharose gel suspension was contacted with an initial β-galactosidase concentration of 75 U/ml; samples were withdrawn periodically and the decrease in bulk β-galactosidase activity over time was determined.

been attached all behaved the same. The estimated value of β was 0.85, indicating, that β-galactosidase has access to the bulk of Sepharose 4B's internal volume. In summary, β-galactosidase has access to the interior of the adsorbent particle, transport to the interior is governed by a diffusive process, characterized by a small diffusion coefficient, the adsorbent particle itself, is large, and most enzyme–inhibitor interactions are inherently fast. Thus it is likely that internal pore diffusion limits the overall adsorption rate.

Finally, since adsorption is conducted in a well-mixed vessel, the boundary layer thickness, and hence external film diffusion resistance, should be minimal. In an attempt to validate this assumption, batch adsorption experiments[4], at varying agitation rates, were conducted in one of the CARE reactors. The results for β-galactosidase adsorption are shown in Fig. 4. There were no significant differences in the adsorption profiles, suggesting external film diffusion is fast relative to internal pore diffusion.

Desorption process. Desorption, of β-galactosidase, is accomplished by the introduction of borate ions, and is not associated with the pH change from 7 to 9. It has been shown that borate is a specific eluent for β-galactosidase, and since the ion concentration is orders of magnitude greater than the enzyme's (at pH 9), desorption from the ligand is not an equilibrium process[19]; rather desorption goes to completion. It is assumed that desorption is diffusion controlled in a similar manner to adsorption.

Given these assumptions, desorption of β-galactosidase from the affinity support is a much faster process than adsorption. During adsorption, the driving force, which is the difference between the bulk concentration and the pore liquid concentration in equilibrium with adsorbed enzyme, is typically low; on the order of 10 U/ml for the rate experiments. As enzyme adsorbs to the affinity ligand, the bulk enzyme concentration decreases and the equilibrium pore liquid concentration increases. As a result, the driving force for adsorption decreases and remains small over the entire time course of adsorption. In contrast, during desorption, the initial driving force is proportional to the adsorbed enzyme concentration which is typically
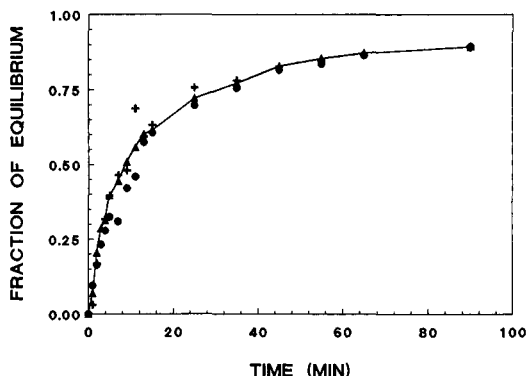
Fig. 4. Evaluation of external mass transfer. Adsorption at varying agitation rate. Experiments performed in a batch vessel containing a total of 50 ml liquid volume; 0.5 ml adsorbent gel contacted with an initial β-galactosidase concentrations of 20 U/ml; the vessels were agitated at varying rate (rpm) in a temperature controlled (25°C) shaker bath; samples were withdrawn periodically and the decrease in bulk β-galactosidase activity over time was determined. ●, 150; ▲, 250; +, 280 rpm.

on the order of 1000 U/ml. Both experiment and theory confirm that desorption is complete within one min[19]. Thus, desorption is described as taking place both instantaneously and completely.

Macroscopic formulation

     The equations describing sorption kinetics, developed above, form the basis of a mathematical model of the CARE process. Sorption kinetics are incorporated into a set of material balance equations, describing the conservation of total mass within the process as described below. The model, although developed for the β-galactosidase affinity purification system, is generalizable to any system where sorption kinetics can be mathematically described, non-specific adsorption is minimal and enzyme activity is maintained throughout the time course of the separation.

     Adsorption kinetics (at pH 7) can be modeled by eqn. 5, while desorption (at pH 9) is assumed nearly instantaneous and complete based on evidence described above. The macroporous filters, used to retain the adsorbent, offer little resistance to flow[19], thus the two stages are modelled as continuous, well-mixed vessels. The model treats
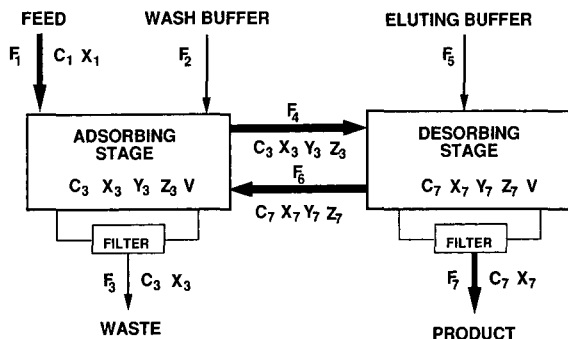
Fig. 5. Mathematical model parameters.

the feed material as a protein mixture and ignores non-proteinaceous contaminants.

The CARE model was developed with the parameters shown in Fig. 5. There are seven flow-rates (F_1–F_7), three free (unbound) enzyme concentrations (X_1, X_3, X_7), two bound enzyme levels (Z_3, Z_7) and three contaminant concentrations (C_1, C_3, C_7). This paper considers the case where the waste steam flow-rate (F_3) equals the sum of the feed (F_1) and wash (F_2) flow-rates; similarly, the eluting buffer flow-rate (F_5) is set equal to the product stream flow-rate (F_7), while the adsorbent recycle flow-rates (F_4 and F_6) are kept equal. Finally the adsorbent concentration in each vessel (Y_3 and Y_7) are kept constant and equal.

With these specifications, a steady state solution describing the CARE system can be derived. The material balances for the free enzyme (2 equations), the bound enzyme (2 equations) and the contaminant protein (2 equations) are coupled to eqn. 5 which describes the rate of product adsorption in the first stage.

Material balances for total enzyme (free and bound) are:

$$F_1 X_1 = F_3 X_3 + F_7 X_7 \tag{9}$$

$$F_1 X_1 + F_6 X_7 = (F_3 + F_4)X_3 + \left(\frac{V}{V_e}\right)F_4 Z_3 Y_3 \tag{10}$$

Accumulation of bound enzyme in the adsorption reactor is given by:

$$\frac{dZ_3}{dt}VY_3 = \left(\frac{V}{V_e}\right)F_4 Z_3 Y_3 \tag{11}$$

Adsorption kinetics (eqn. 5) are incorporated into eqn. 11

$$\left[k_f X_3(Q_{max} - Z_3) - \left(\frac{k_f}{K}\right)Z_3\right]VY_3 = \left(\frac{V}{V_e}\right)F_4 Z_3 Y_3 \tag{12}$$

Material balances for contaminants are:

$$F_1 C_1 + F_6 C_7 = (F_3 + F_4)C_3 \tag{13}$$

$$F_4 C_3 = (F_6 + F_7)C_7 \tag{14}$$

The set of equations described above suffice to completely specify CARE operation. The equations can be solved either explicitly or iteratively depending on how the problem is defined. There are four sets of parameters and variables that must be specified or predicted by the model. They are: F_1, C_1, X_1, V, (V/V_e); the adsorption parameters, k_f, K, Q_{max} (determined from independent batch adsorption experiments); operating variables (or controllable variables) F_2, F_4, F_5, Y; and, the performance variables, purification factor (PF), recovery yield (REC) and concentration factor (CF). The system's performance variables are defined as:

$$PF = \left(\frac{X_7}{X_1}\right)\left(\frac{C_7}{C_1}\right)^{-1} \tag{15}$$

$$\text{REC} = \left(\frac{X_7 F_7}{X_1 F_1}\right) \qquad\qquad\qquad (16)$$

$$\text{CF} = \left(\frac{X_7}{X_1}\right) \qquad\qquad\qquad\qquad (17)$$

The steady-state solution described above is useful in the design and optimization of CARE. In order to model the start-up period and predict system dynamics (*e.g.* for feedback control), the same equation set can be solved numerically (4th order Runge-Kutta method) for unsteady state operation.

MODEL USES

The purpose of the mathematical description of CARE, described above, is to help elucidate relations between system performance and the operating and design variables. By investigating these relations and the tradeoffs among the performance variables, one can gain the insight necessary to incorporate CARE into a protein recovery sequence. In this section three model applications are described: *e.g.* for design, parametric sensitivity, and optimization.

Design
The model may be used to design and specify the operating variables of CARE to achieve a desired performance. For given feed conditions (enzyme level, contaminant concentration and flow-rate), a desired level of final purity, recovery and concentration can be achieved by proper selection of flow-rates and amount of adsorbent. For example, the CARE model was solved for a base case with the performance measures specified as: PF = 30, CF = 5, REC = 90% and feed conditions being: $F_1 =$ 1 ml/min, $X_1 = 100$ U/ml (*ca.* 0.2 mg β-galactosidase) and $C_1 = 10$ mg/ml. An iterative solution of the equation set yields a set of operating conditions to achieve the specified performance (Fig. 6).

Surprisingly, the model predicts that for a specified level of adsorbent, above a minimum value, there can be two sets of wash (F_2) and bead recycle (F_4) flow-rates which satisfy the performance constraints. For the base case in this example, CARE, operated with 12.5 ml of affinity adsorbent beads in the adsorption stage, and $F_4 = 0.1$ ml/min and $F_2 = 1.2$ ml/min, is a unique solution. If one uses more beads, an additional degree of freedom is gained so that according to the model, a combination of high wash and bead recirculation flow-rates can give identical performance to a case with low flow-rates.

In order to maintain constant system performance, with the addition of more adsorbent, two approaches can be used. If the adsorbent recycle flow-rate is decreased, the amount of regenerated gel being returned to the adsorption reactor, per unit time, decreases and thus the amount of β-galactosidase recovered from the feed would decrease. At the same time, the residence time of the adsorbent in the adsorption reactor increases, and thus, specific adsorbent loading increases. In this manner, the recovery yield can be matched to what it was before the increase in the amount of adsorbent. Since the recycle flow-rate is lower, the wash flow-rate must be lowered in order to keep the same purification factor.
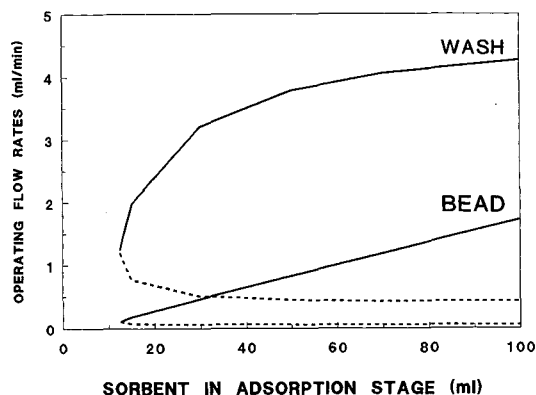
Fig. 6. Operating conditions which satisfy a specified performance. (———) Low loading, dynamic, (— — —) high loading, rear equilibrium.

A second mode of operation is the reverse approach of the first. Both the adsorbent recycle and wash flow-rates are increased. The higher wash flow-rate dilutes the β-galactosidase concentration in the adsorption reactor, hence lowering the driving force for adsorption. Since the adsorption rate decreases, the adsorbent recycle rate is increased to maintain the same level of recovery from the incoming feed. The low flow-rate case allows nearly maximal (equilibrium) loading of the sorbent, whereas the high flow-rate case involves very low (dynamic operation) sorbent loading. Realistically, the high flow-rate case underutilizes the media, uses excess wash buffer and requires high bead recycle rates which may subject the sorbent to excessive mechanical action.

The minimum level of sorbent required to achieve a given performance is a useful design criterion in comparing deviations from the base case. Fig. 7 shows the effect of varying the concentration, purification and recovery, on the minimum level of sorbent required. Typically, the cost of sorbent is an important factor in the economics of an affinity purification step. Hence, the increase in the "price" paid to achieve a higher performance in each case, is to be expected.

Sensitivity

The CARE model may also be used to evaluate a fixed design, and assess the effect of changes in operating variables on system performance. This sensitivity analysis provides further insight into the tradeoffs inherent in the CARE system.

Fig. 8 shows the sensitivity of recovery yield, to changes in three operating variables: wash, recycle and eluting buffer flow-rates. Similar profiles can be generated for purification and concentration factors and serve to illustrate the complex set of tradeoffs among the performance variables.

An alternative approach to sensitivity analysis involves changing only one of the operating-variable flow-rates and following the sensitivity to all three performance criteria simultaneously; Figs. 9–11 show the results of this analysis. In Fig. 9, the arrow points in the direction of increasing bead recirculation rate. When all other variables are kept constant, this change is seen to give rise to an increase in concentration factor, a corresponding linear increase in recovery, but a decrease in purification factor.
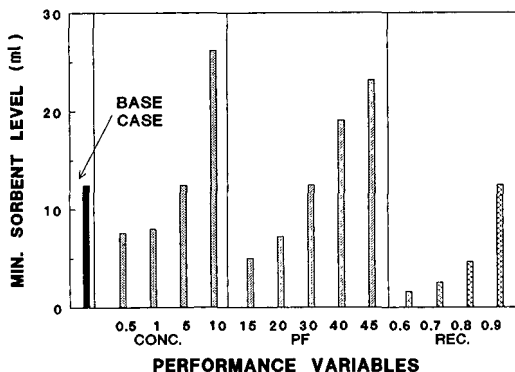
Fig. 7. Minimal amount adsorbent required.

A similar analysis is shown in Fig. 10 where the arrows points in the direction of decreasing elution buffer flow-rate, which in turn causes an increase in concentration factor but little change in recovery or purification factor. Finally, Fig. 11 shows the sensitivity to decreasing wash flow-rate which causes a sharp decrease in purification factor, an increase in recovery along with a small increase of concentration factor.

The sensitivity approach in using the CARE mathematical model results in the following generalized rules where the feed composition and flow-rate are held constant: to increase the purification factor, one must increase the ratio of adsorption reactor throughput relative to bead recirculation rate (*e.g.* increasing the wash flow-rate and/or decrease the bead recirculation rate). Concentration of the product can be achieved by decreasing the ratio of desorbing buffer flow-rate relative to the feed flow-rate. Finally, recovery is increased most effectively by decreasing the wash flow-rate and/or increasing bead recirculation. The existence of tradeoffs in performance suggest an opportunity for system optimization, once suitable objective functions are determined.

Optimization
A predictive mathematical model of the CARE process provides the opportunity
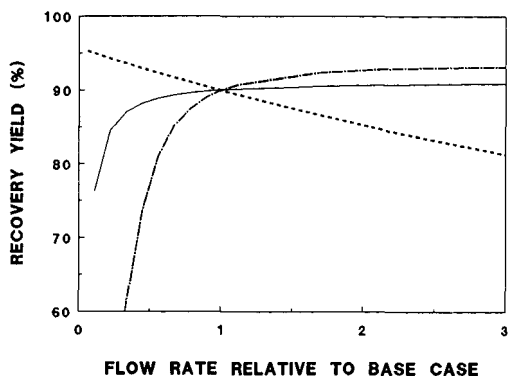
Fig. 8. Sensitivity of recovery yield to operating variables. ———, Borate, – – –, wash; – · – · –, bead.
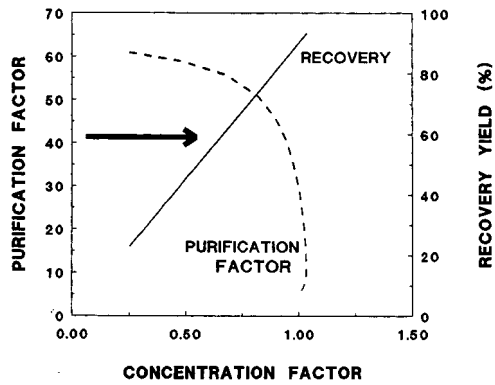
Fig. 9. Sensitivity of system performance to increasing bead recirculation rate.
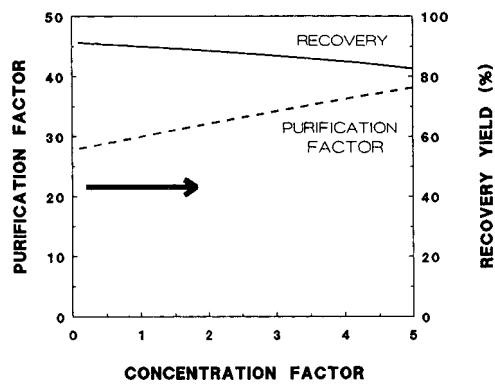
Fig. 10. Sensitivity of system performance to decreasing elution buffer flow.
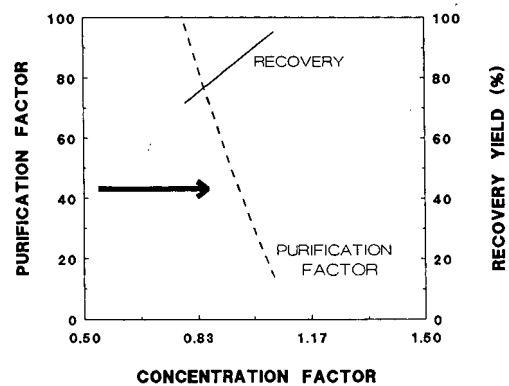
Fig. 11. Sensitivity of system performance to decreasing wash buffer flow.

for optimization. Optimization requires definition of an objective function. The optimum performance of CARE operating as a single step, is described here. In a broader sense, an entire DSP sequence, in which CARE has been incorporated, can be optimized to minimize cost for a fixed amount of product. Such work is in progress and will be the subject of subsequent publications.

Given the large number of "degrees of freedom" (three) in the CARE system as well as the many ways of measuring unit performance (PF, REC, CF), optimization needs to be coupled with the setting of system constraints. For example, one can maximize the purification factor while constraining recovery yield and concentration factor within certain boundaries. Scheme 1, illustrates this optimization strategy and two optimization cases have been considered. The first maximizes purification factor with the constraints of a minimum feed throughput rate of 10 ml/min, 70% minimum recovery yield and a maximum two-fold dilution of product. The second example shows a maximization of feed throughput constrained by a minimum 70% recovery yield, maximum 5-fold dilution and minimum 10-fold purification. The operating conditions required to achieve optimum results are shown in Scheme 1. These examples demonstrate the operational flexibility inherent in the CARE system's design.

These examples in addition to the sensitivity analysis discussed in an earlier section of this paper, provide the basis for the formulation of the following rule: system throughput can be increased by relaxing performance constraints (PF, REC, CF). In fact, any of the four performance measures can be increased by decreasing the constraints on one of the other three performance variables. A unique feature of the CARE system relative to packed bed adsorption is the ability to control unit performance. Control of CARE allows its optimization and continued operation at optimal levels despite variations in feed composition.

MODEL VALIDATION

The formulation of a mathematical model is strengthened after it has been experimentally validated. During the CARE model formulation stage, two key flow-rate ratios were found to influence unit performance. The ratio of the input flow to the adsorption contactor, relative to the adsorbent recycle flow governs the

CASE 1	CASE 2
OBJECTIVE: MAXIMIZE PF	OBJECTIVE: MAXIMIZE THROUGHPUT
CONSTRAINTS:	CONSTRAINTS:
1. Throughput > 10 ml/min	1. PF > 10
2. Recovery Yield > 70%	2. Recovery Yield > 70%
3. CF > 0.5	3. CF > 0.2
PERFORMANCE	**PERFORMANCE**
PF REC CF	PF REC CF
118 70% 0.5	10 70% 0.2
OPERATING FLOW RATES	**OPERATING FLOW RATES**
FEED WASH ELUTE RECYCLE	FEED WASH ELUTE RECYCLE
10 65.8 14.0 0.466	147 0 514 11.3

Scheme 1. Optimization examples.

purification. For a given feed flow-rate, an increase in the wash flow-rate dilutes the reactor contaminant concentration, and hence, the quantity of contaminants transported with the recycle stream to the desorption reactor. Similarly, decreasing the bead recycle flow-rate, increases the adsorbent reactor residence time. As a result, the amount of β-galactosidase adsorbed per unit of sorbent increases (assuming that equilibrium adsorption has not been reached), increasing the ratio of β-galactosidase to contaminants in the bead recycle stream. The ratio of feed to elution buffer flow-rates, the second important flow-rate ratio, determines whether product concentration or dilution occurs.

A qualitative assessment of the mathematical model was undertaken by a series of experiments designed to modify unit performance from a base case run. The results are shown in Table I. The two pertinent flow-rate ratios are normalized to the value in the base case. Steady-state performance is shown for each case. In order to improve the recovery yield, the amount of feed to the system was decreased. In a similar fashion, to improve purification factor, the first flow-rate ratio (feed + wash)/(gel recycle) was increased. Finally, in order to increase the concentration factor, the feed to eluting buffer flow-rate ratio was increased.

The results from an experiment conducted to investigate start-up dynamics serves to validate the quantitative aspects of the model. Fig. 12 shows the results from this experiment where adsorbent in the adsorption reactor was initially devoid of β-galactosidase; experimental conditions are listed in the figure caption. The enzyme concentration in the product stream slowly increases and approaches a steady state level after approximately 18 h of operation. This long start-up period is due to the time required to saturate the adsorbent as well as, the slow adsorbent recycle flow-rate between the two reactors. The waste stream enzyme concentration increases over time and levels off after approximately 10 h reflecting adsorbent saturation.

The solid lines in Fig. 12 indicate enzyme concentration predicted by the model. Recall that the model predictions are based on adsorption parameters (Q_{max}, K, k_f) obtained in independent batch adsorption experiments combined with flow-rates used in this experiment. Good model agreement is shown for both the dynamic and steady state stages of operation, and for β-galactosidase concentration in both the product and waste. Model predictions, of both β-galactosidase and contaminating protein

TABLE I

QUALITATIVE VALIDATION ON THE CARE MODEL

Experiment	Ratio of flow-rates		Performance		
	(Feed + wash) / (Gel recycle)	(Feed) / (Elute)	PF	CF[a]	REC. (%)
Base case	1	1	18	0.09	72
High recovery	1	0.15	13	0.02	77
High purification	5	0.77	31	0.04	50
High concentration	1.2	3.2	14	0.18	40

[a] A preconcentrated E. coli homogenate feed was used for these experiments. The concentration factors relative to the original homogenate are 0.9, 0.2, 0.4 and 1.8, respectively.
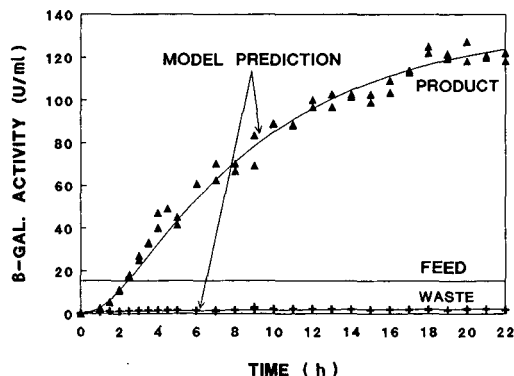
Fig. 12. Start-up dynamics in the CARE system. Reactor volume, 75 ml; gel volume fraction, 0.2; V_e/V, 1.05; F_1, 6.2 ml/min; F_2, 0; F_4, 0.18 ml/min; F_5, 0.60 ml/min, X_1, 15.4 U/ml; C_1, 0.35 mg/ml.

concentrations are compared with experimental results in Table II. Predictions of β-galactosidase concentrations in the various process streams, are matched closely by experimental results. However, their is an apparent contradiction between prediction and measurement of contaminant protein concentrations.

The protein concentration in the waste stream was found to be similar to that of the feed, indicating near total removal of incoming contaminating protein (e.g. β-galactosidase is a small portion of feed protein). However, it was not possible to experimentally validate the model prediction for protein in the product stream. Measurement of total protein concentration, using the standard Biorad dye reagent assay, accounts for all proteinaceous components, including the contribution due to β-galactosidase. The contaminant protein concentration reported in Table II, was

TABLE II

MODEL VS. EXPERIMENTAL RESULTS FOR START-UP EXPERIMENT

β-Galactosidase sp.act. (U/mg)	Contaminant protein (mg/ml)					
	Feed		Waste		Product	
	Model	Experimental	Model	Experimental	Model	Experimental
900	0.35	0.35	0.35	0.37	0.078	0.23
600	0.34	0.34	0.34	0.37	0.076	0.16
420	0.33	0.33	0.33	0.37	0.073	0.075
	β-Galactosidase (U/ml)					
	Feed		Waste		Product	
	Model	Experimental	Model	Experimental	Model	Experimental
900	15.4	15.4	2.3	2.0	124	122
600	15.4	15.4	2.3	2.0	124	122
420	15.4	15.4	2.3	2.0	124	122

estimated by subtracting the contribution of β-galactosidase to total protein from the measured total protein concentration. In order to perform this calculation, the β-galactosidase specific activity must be known. Values of specific activity ranging from 600 to 900 U/mg protein are reported for purified β-galactosidase preparations, obtained from Sigma.

Model predictions, when contrasted to experimental results in Table II, for Sigma's range of specific activity, show a poor fit. This poor fit can be accounted for in several ways. If their is a certain level of non-specific adsorption of contaminating proteins to PABTG-Agarose, contaminant carry-over between the two reactors would be greater than predicted by the model, and thus account for the discrepancy between the predicted and measured contaminant protein concentration in the product stream. However, electrophoretic gels [native polyacrylamide gel electrophoresis (PAGE), not shown] of the components that adsorb, and are subsequantly eluted from the adsorbent, show a single predominant band, corresponding to β-galactosidase. The significant level of non-specific adsorption of contaminants, that would be required to account for the apparent discrepancy with model predictions, was not detected.

An alternate, and more likely explanation, is that a portion of the β-galactosidase in the feed is not enzymatically active. Further, if the non-active component can adsorb to the affinity adsorbent, the resulting β-galactosidase specific activity would be lower than 600 U/mg, and thus, the contribution of β-galactosidase to the measured total protein would increase. The results listed in Table II, show that for a specific activity of 420 U/mg protein, for β-galactosidase, model predictions match experimental results. Although contaminant protein concentrations, and hence purification factors, cannot be reported with confidence, electrophoretic gels (native PAGE, not shown), have confirmed the high purity of the product stream, as predicted by the mathematical model.

NOMENCLATURE

c	bulk solute concentration
c_i	pore solute concentration
c_f	final bulk liquid concentration in diffusivity experiments
c_0	feed concentration
C_1	contaminant concentration in CARE feed stream
C_3	contaminant concentration in CARE waste stream
C_7	contaminant concentration in CARE product stream
CF	concentration factor

D_i effective particle diffusion coefficient
F_1 flow-rate of CARE feed stream
F_2 flow-rate of CARE wash stream
F_3 flow-rate of CARE waste stream
F_4 flow-rate of CARE gel recycle stream
F_5 flow-rate of CARE elution buffer stream
F_6 flow-rate of CARE gel recycle stream
F_7 flow-rate of CARE product stream
K adsorption equilibrium constant
k fluid film mass transfer coefficient
k_f forward reaction rate constant
k_r reverse reaction rate constant
N_0 flux of solute into particle
PF   purification factor
q average particle sorbate concentration
q_i particle local sorbate concentration
q_0 sorbate concentration in equilibrium with c_0
Q_{max} maximum sorbate concentration
R sorbent particle radius
REC   recovery yield
s average concentration in particle (including pore liquid)
t time
v volume
V CARE reactor volume
V_e CARE reactor volume external to retaining screen
V_{bulk} fluid volume excluding gel volume
V_{gel} gel volume
X_1 solute concentration in CARE feed stream
X_3 solute concentration in CARE waste stream
X_7 solute concentration in CARE product stream
Y_3 gel volume fraction in adsorption reactor
Y_7 gel volume fraction in desorption reactor
Z_3 particle sorbate concentration in adsorption reactor
Z_7 particle sorbate concentration in desorption reactor
α adsorbent volume fraction
β accessible particle volume fraction

REFERENCES

1 G. Vanecek and F. E. Regnier, *Anal. Biochem.*, 109 (1980) 345.
2 J. J. O'Hare, M. W. Capp, E. C. Nice, N. H. C. Cooke and B. G. Archer, in M. T. W. Hearn, F. E. Regnier and C. T. Wehr (Editors), *High-Performance Liquid Chromatography of Proteins and Peptides*, Academic Press, New York, NY, 1983, p. 23.
3 P. C. Wankat, *Large-Scale Adsorption and Chromatography*, Vol. 2, CRC Press, Boca Raton, FL, 1986.
4 E. Pungor, Jr., N. B. Afeyan, N. F. Gordon and C. L. Cooney, *Bio/Technology*, 5 (1987) 604.
5 F. H. Arnold, H. W. Blanch and C. R. Wilke, *Chem. Eng. J.*, 30 (1985) B9.
6 B. H. Arve and A. I. Liapis, *AIChEJ.*, 33(2) (1987) 179.
7 H. A. Chase, *J. Chromatogr.*, 297 (1984) 179.
8 C. M. Yang and G. T. Tsao, *Adv. Biochem. Eng.*, 25 (1982) 1.

9 D. J. Graves and Y. T. Wu, *Adv. Biochem. Eng.*, 12 (1979) 219.
10 S. Katoh, T. Kambayashi, R. Deguchi and F. Yoshida, *Biotech. Bioeng.*, 20 (1978) 267.
11 J. W. Eveleigh and D. E. Levy, *J. Solid-Phase Biochem.*, 2 (1977) 45.
12 G. R. Craven, E. Steers, Jr. and C. B. Afinsen, *J. Biol. Chem.*, 240 (1965) 2468.
13 K. Buchholz, *Biotech. Lett.*, 1 (1979) 451.
14 S. W. Carleysmith, M. B. L. Eames and M. D. Lilly, *Biotechnol. Bioeng.*, 22 (1980) 957.
15 D. D. Do, *Biotechnol. Bioeng.*, 26 (1984) 1032.
16 H. A. Sorber, *Handbook of Biochemistry, Selected Data for Molecular Biology*, Chemical Rubber Co., Cleveland, OH, 1968.
17 N. F. Gordon and C. L. Cooney, paper presented at *the 1987 AIChE National Meeting, New York, NY, November 16–20, 1989.*
18 S. C. March, I. Parikh and P. Cuatrecasas, *Anal. Biochem.*, 60 (1974) 149.
19 N. F. Gordon and C. L. Cooney, unpublished results.

SYSTEMATIC PROCEDURE FOR THE DETERMINATION OF THE NATURE OF THE SOLUTES PRIOR TO THE SELECTION OF THE MOBILE PHASE PARAMETERS FOR OPTIMIZATION OF REVERSED-PHASE ION-PAIR CHROMATOGRAPHIC SEPARATIONS

GARY K.-C. LOW*

Centre for Advanced Analytical Chemistry, CSIRO Division of Fuel Technology, Lucas Heights Research Laboratories, Private Mail Bag 7, Menai (Australia)

and

AKOS BARTHA[a], HUGO A. H. BILLIET and LEO DE GALAN

Department of Analytical Chemistry, Delft University of Technology, De Vries van Heystplantsoen 2, 2628 RZ Delft (The Netherlands)

(First received September 26th, 1988; revised manuscript received May 3rd, 1989)

SUMMARY

Separation selectivity of ionized solutes in reversed-phase ion-pair chromatography can be varied by manipulating a number of mobile phase variables. From a study of computer-simulated mixtures of differently charged solutes it became obvious that the selection of the parameter space for systematic solvent optimization is constrained principally by the nature of the charged species present in the mixture. For most sample mixtures there are preferred combinations of the mobile phase variables, leading to a significant reduction of the optimization search area. A systematic strategy is shown here for the determination of the charge type and the relative retention (hydrophobicity) of the components in samples for which this information is not known. The first part of the strategy identifies the weak acids and bases according to their retention behavior in two gradient separations at pH 2.5 and 7.5, respectively. The second part determines the presence of strong acids and bases by the same two gradients but "pulsed" with a negatively and a positively charged ion-pairing reagent, respectively. Solutes are classified according to their characteristic retention shifts using a sequential-elimination scheme. Solutes without retention shifts are classified as non-charged solutes.

INTRODUCTION

The use of computer-aided procedures for the optimization of separation selectivity in reversed-phase high-performance liquid chromatography (HPLC) has been extensively studied during the last few years[1-5]. The efforts of many research groups

---

[a] On leave from the University of Chemical Engineering, Veszprem, Hungary.

resulted in several commercial software packages[6-10]. However, the value and success of all these optimization strategies (including the trial-and-error aproaches) critically depends on the number and range of the mobile phase variables, which are selected to vary the retention and selectivity of the separation. The combination of these parameters and their limiting values defines the parameter space, in which the optimum separation conditions should be located. In all presently known HPLC optimization procedures[1-10], a preselected vector space is used. If the parameter ranges are too broad, many experiments may be required to find the optimum, while a too narrow parameter space often leads to a local (usually unsatisfactory) optimum.

The selection of an appropriate parameter space for sample mixtures containing non-charged solutes is relatively easy in reversed-phase HPLC, and involves almost exclusively the manipulation of either the type and/or the concentration of the organic modifier(s) in the mobile phase. The retention movement of the non-charged components is largely predictable with a decrease of solute retention when the organic modifier concentration is increased in the eluent. Simple isocratic or gradient scouting experiments can be used to determine the initial eluent compositions before starting the binary, ternary or quaternary solvent optimization procedure[6-12].

However, a wide range of typical samples such as ionic surfactants, drugs, reaction mixtures, environmental and biological samples often contain both non-charged and ionic or ionizable compounds. The separation of such sample mixtures usually needs the variation of a number of other mobile phase parameters (eluent pH, type and concentration of buffer, ionic strength, charge type, hydrophobicity and concentration of ion-pairing reagent). The increasing number (and/or range) of the mobile phase variables to be optimized necessitates the completion of many more chromatographic experiments and needs more complex instrumentation. Furthermore, most available optimization methods (except Simplex) permit the simultaneous optimization of only two or three parameters. Therefore, it is essential to reduce the parameter space as much as possible, by including (and varying) only those parameters which have a significant effect on the selectivity of the separation.

A number of recent publications have demonstrated the successful separation of sample mixtures containing solutes of different charge types using a mixture-design statistical approach along with predictive regression methods[13-15]. Generally, the three most important eluent parameters considered in these selectivity optimizations are the organic modifier, pairing ion concentrations and the eluent pH. The experimental designs described in refs. 13–15, depending on their philosophy, select different subspaces of the parameter space, as shown in Fig. 1 using a three-dimensional representation. However, the parameter space selected by these methods is correct for certain mixtures[16] and none of them is generally applicable.

Based on a study of the separations of many computer simulated sample mixtures of differently charged solutes it will be shown here that the optimization parameter space can be selected rationally if the nature (charge type and the relative hydrophobicity) of the sample components is known. A systematic and rapid procedure has been developed to obtain this information for solute mixtures, where it is not available a priori. The method is based on four specifically designed organic modifier gradients according to the unique retention shifts of charged solutes. The felicity of the scanning procedure is demonstrated by determining the solute types in complex synthetic solute mixtures.
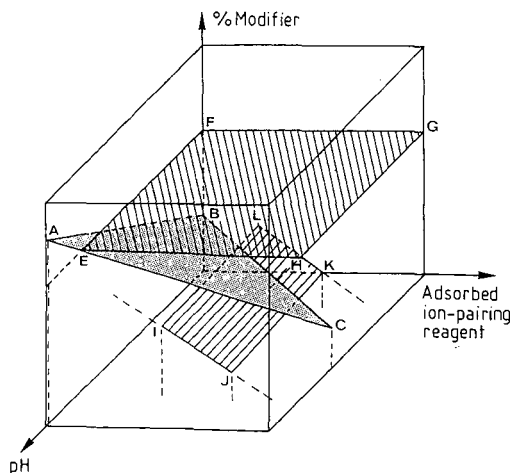
Fig. 1. Comparison of the parameter spaces selected for the optimization of reversed-phase ion-pair chromatographic separations according to the different mixture designs by (ABC) Goldberg et al.[13]; (ILKJ) Coenegracht et al.[14]; and (EFGH) Billiet et al.[15]. The three optimization parameters are eluent pH, organic modifier and ion-pairing reagent concentrations.

EXPERIMENTAL

Instrumental

Two HPLC systems were used in this work. The first consisted of two M6000A pumps, a M660 gradient controller, a M440 UV detector (all from Waters Chromatography Division, Milford, MA, U.S.A.), and a Rheodyne 7125 injector with a 20-μl loop (Rheodyne, Cotati, CA, U.S.A.). The second system was a HP 1090 liquid chromatograph with an autoinjector and a HP 1040A linear photodiode array detector. The latter was connected to a HP-85 desktop computer, equipped with a HP 7074A graphics plotter and a HP 9121 dual flexible disk drive (all from Hewlett-Packard, Waldbronn, F.R.G.).

The computer simulation programs for building the library of synthetic solute mixtures were developed in PRO/BASIC on a Waters 840 data management system (Digital Equipment Corp., Maynard, MA, U.S.A.).

Two different reversed-phase columns were used. The first was a 200 $\times$ 4.6 mm I.D. column, slurry packed with 5-μm ODS-Hypersil (Shandon Southern Products, Runcorn, U.K.). The second was a commercial Nova-Pak C_{18} (3 μm, 150 $\times$ 4.6 mm I.D.) column, purchased from Waters. A flow-rate of 2 ml/min was used throughout this work. Column temperature was maintained at 35°C for the Hewlett-Packard system (Nova-Pak C_{18}), and at room temperature for the Waters system (ODS-Hypersil).

Chemicals

Methanol was purchased from Rathburn (Walkerburn, U.K.). Distilled, deionized water was prepared with a Milli-Q water purification system (Millipore, Molsheim, France). Sodium bromide, disodium hydrogenphosphate and citric acid (J. T. Baker, Deventer, The Netherlands); tetrabutylammonium bromide and anhydrous

sodium hexane- and octanesulfonate (Janssen Chimica, Beerse, Belgium); "Gold Label" quality triethylamine (TEA) and phosphoric acid (85%, w/w) (Merck, Darmstadt, F.R.G.) were used without further purification. The solutes were of the highest quality available. Individual sample solutions were prepared in methanol–water (50:50, v/v) and combined in appropriate proportions to form synthetic mixtures.

Mobile phases and gradient sequence

For the ODS-Hypersil column buffers were prepared from citric acid and disodium hydrogenphosphate, balanced with sodium bromide to maintain a constant 50 mM concentration of counterions in the mobile phase. The final eluents for this column also contained 10 mM triethylamine phosphate. For the Nova-Pak C_{18} column 15 mM triethylamine phosphate was used. Buffers of pH 2.5 and pH 7.5 were made by directly titrating the organic base with phosphoric acid (10%, w/w).

Above a methanol concentration of 20% (v/v) an appropriate correction was made to the apparent pH[17]. The buffer concentrations in the aqueous eluents and in the methanol rich eluents were identical. The solubility of the citrate–phosphate buffer (containing also sodium bromide) allowed a maximum of 70% (v/v) methanol concentration. A higher methanol concentration limit of 90% (v/v) could be used with the TEA–phosphate buffer. Mixing of different proportions of the aqueous and aqueous-methanolic solutions gave acceptable ($\pm 5\%$) errors in the expected pH values.

Solutions (0.5 M) of the ion-pairing reagents were prepared in methanol–water (50:50) for the "pulse" injection experiments. A volume of 20 μl of the selected reagent were injected 45 s prior to the injection of the sample mixture (the solvent gradient was always started at the injection of the sample). The gradient run consisted of four sequences: (i) a linear gradient from 0 to high methanol concentrations at a given pH (2.5 or 7.5) in 15 min, (ii) isocratic elution at high methanol concentration for 5 min, (iii) reverse linear gradient from high methanol to the aqueous buffer in 5 min, and (iv) reequilibration of the column with the aqueous buffer for 2 min. This procedure gave practically no "ghosting" effects or irreversible pairing ion adsorption.

COMPUTER SIMULATION OF SYNTHETIC MIXTURES

In order to develop a rational approach to the optimization of the separation of mixtures which contain differently charged solutes an extensive library of the possible separation problems has been built by computer simulation. The problems are represented by the retention *vs.* pH behavior of different solute types in each sample mixture. Retention profiles of acids and bases were obtained using the equations derived by Horváth *et al.*[18]. The following pK_a values were used: 3.5–5.0 for weak acids (WA) and bases (WB), <1.5 for strong acids (SA), and >9.0 for strong bases (SB). For hydrophilic compounds the capacity factors (k') of the ionized and non-ionized forms of the same solute were 0.3–0.5 and 4.3–4.8, respectively. For the hydrophobic ones the ranges 8.5–9.0 and 13.5–14.0 were used. The k' values of the hydrophilic and hydrophobic non-charged (N) solutes were assumed to be 0.5 and 13.5, respectively.

Mixtures containing 1:1, 1:2 and 2:2 permutations of WA, WB, SA and SB of

different hydrophobicity were formed to yield synthetic mixtures of increasing complexity. Non-charged compounds either hydrophilic, hydrophobic or both were then systematically included in each of these mixtures to increase the complexity of the sample. To account for very closely related compounds in the mixtures, each compound type was represented twice, with marginally (5–10%) different k' values. Therefore, the simplest mixture contained two components of a single compound type (*e.g.* hydrophilic strong acid), while the most complex mixture contained six different solutes types, a total of twelve components. Altogether 648 different types of mixtures were simulated and evaluated.

RESULTS AND DISCUSSION

Rational selection of the mobile phase optimization parameters

A study of the separation problems represented by a large number of computer-simulated synthetic mixtures of increasing complexity, revealed that the selection of the optimization parameter space in reversed-phase ion-pair HPLC can be rationalized, and it is constrained by the nature of the charged species in the sample mixture.

The primary variables for the optimization of ion-pair chromatographic separations considered in this study are the type and concentration of the organic modifier, the eluent pH and the charge type and concentration of the ion-pairing reagent. In this discussion we will show that the selection of these retention controlling parameters and their combinations depend, primarily, on the nature (charge-type and relative hydrophobicity) of the solutes in the sample mixture.

Solutes can be classified according to their charge type within the 2.5–7.5 pH range. The constraint on the pH window is dictated by the chemistry of the currently available silica-based reversed-phase packing materials. In Fig. 2 the idealized reversed-phase retention behavior of different solute types is shown as a function of the eluent pH. Strong acids (SA) and bases (SB) are solutes which are fully ionized, whereas weak acids (WA) and bases (WB) are compounds which change their ionic state (and their retention) within this pH range. Compounds which are non-ionized within this pH gate are referred to as neutral (N) compounds. The terms "hydrophilic" and "hydrophobic" are relative terms referring to the order of elution of a solute in a given sample mixture. That is, the same compound can be classified as hydrophobic in one solute mixture, but as hydrophilic in another.

When examining a large number of simulated separation problems, we realized that a procedural strategy is needed to solve these problems rationally. First, by inspecting the problem, one must decide whether the retention gap between neighbouring solute peaks is to be decreased or increased. Second, one must select the optimization parameters which would affect the retention gap and provide the best overall selectivity (no more than three parameters are to be used at a time). Third, one must try to avoid very early and/or late elution of any of the components (all components are assumed to be of interest). Fourth, one must decide whether a reduced portion of the parameter space (which still contains the global optimum with respect to the selected mobile phase variables) could be used.

Several representative examples will be discussed below to demonstrate the advantages of this strategy, which selects the optimization parameter space according to the nature of the solutes in the sample mixture. The k' *vs.* pH plots are used to
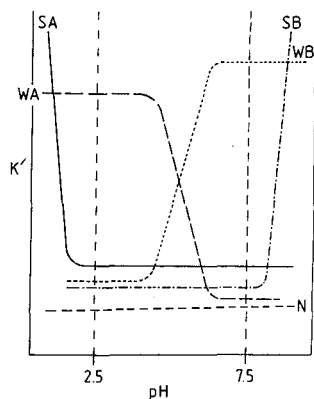
Fig. 2. Capacity factor (k') *vs.* eluent pH profiles of strong (SA) and weak (WA) acids, strong (SB) and weak (WB) bases and non-charged solutes (N) in an ideal reversed-phase chromatographic system.

illustrate the problem, and a three-dimensional representation of the selected combination of the optimization variables is used to visualize the resulting vector space.

The simple mixture shown in Fig. 3a consists of hydrophilic strong bases and hydrophobic neutrals. One of the important features of this sample is that there are no weak acids and bases present. Therefore, the eluent pH can be fixed at any practical value (*e.g.* low pH for basic compounds may give better peak symmetry). In order to close the retention gap between the early and late eluting solutes, a negatively charged ion-pairing reagent must be used to increase the retention of the lightly retained strong bases. (Alternatively, one could try another organic solvent, assuming that the eluent contains any at all, but experience shows that this option is more profitable with hydrophilic–hydrophobic non-charged solute combinations.) Once the bases have been moved away from the solvent front, the retention gap can be further decreased by increasing the concentration of the organic modifier. These considerations result in a simple line vector space (Fig. 3b). The search for an optimum composition can be simply performed by mixing the two low-pH eluents (lower and higher organic modifier concentrations, without and with an ion-pairing reagent, respectively) in different ratios.
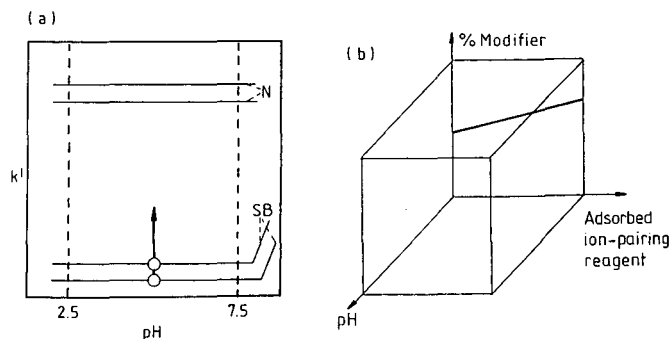
Fig. 3. Example 1. (a) k' *vs.* pH behavior of a simulated solute mixture, containing strong bases (SB) and non-charged (N) solutes; (b) the selected optimization parameter space (see text for discussion).

A more complex mixture is shown in Fig. 4a. This sample contains hydrophobic strong acids, hydrophilic weak acids and hydrophylic non-charged solutes. Again, the retention gap between the early and late eluting solutes should be closed. However, the organic modifier concentration cannot be increased, because this would shift the hydrophilic neutral solute to the solvent front. Therefore, the organic modifier concentration must be fixed at a level, which assures sufficient retention for the non-charged solutes. The retention gap can only be closed by decreasing the retention of the hydrophobic strong acid, with a similarly (negatively) charged ion-pairing reagent. Though in general the pH is varied to achieve separation of the weak acids, the high-pH region, where they are negatively charged, cannot be used in this case, because repulsion by the ion-pairing reagent will push these solutes to the solvent front. Again a fairly reduced optimization parameter space results (Fig. 4b).

It must be pointed out that none of the mixture designs shown in Fig. 1 is able to select these subspaces which, according to the reasoning given above, contain the global optimum.

Obviously, for most sample mixtures there are clear preferences as to which combinations of the mobile phase variables should be used, leading to a significant reduction of the optimization search area (see Figs. 3b and 4b). These preferences are directly related to the presence or absence of certain sample types, and can be described as rules. For example, the absence of weak acids and bases will always eliminate the need of pH variation. In this simplest form this rule reads: "if there is no WA and WB present then pH is fixed". A preliminary set of such rules has been derived in this study, as a part of a knowledge base of an expert system for ion-pair HPLC. Work is under way to develop a prototype expert system which can select the optimization parameter space by considering the solute types present.

In conclusion, the knowledge of the nature (not the exact identity) of the components in the mixture is decisive in the rational selection of the optimization parameter space. In some cases, this information is known *a priori*, but in most cases (reaction mixtures, new products, mixtures of metabolites) one might have only limit-
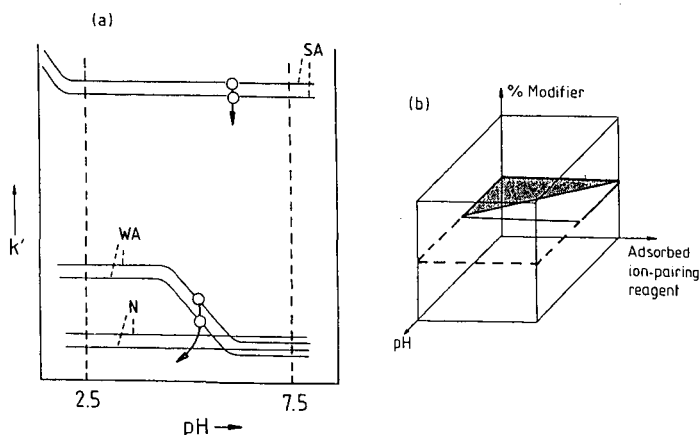
Fig. 4. Example 2. (a) k' *vs.* pH behavior of a simulated solute mixture, containing weak (WA) and strong (SA) acids and non-charged (N) solutes; (b) the suggested optimization parameter space (see text for discussion).

ed or no information about the solute mixture. Therefore, an efficient and easy to use method is needed to obtain rapid information about the nature of the components in the sample.

Determination of the nature of the components

In order to aid the rational selection of the optimization parameters in reversed-phase HPLC, we developed a systematic and rapid scouting procedure to determine the nature (hydrophobic or hydrophilic, non-charged or charged, weak or strong acid or base) (though not the exact identity) of the solutes in the mixture. The strategy is based on the unique retention shifts of the differently charged solutes (see Fig. 5), which occur when a positively or a negatively charged ion-pairing reagent is added to the eluent at a given pH. The retention behaviors of the different solute types in pH 2.5 and pH 7.5 eluents are shown on the two middle bars in Fig. 5. The bars on the left and the right sides show the retention shifts of the same solutes when negatively and positively charged ion-pairing reagents are used at pH 2.5 and pH 7.5, respectively. For example, the retention of a weak acid will be lower at high pH where it is ionized, but it will increase if a positively charged ion-pairing reagent is added to this high-pH eluent. Obviously, if retention data of a given solute are subsequently measured in all the four eluents, its charge type can be determined by matching the retention shifts with one of the patterns.
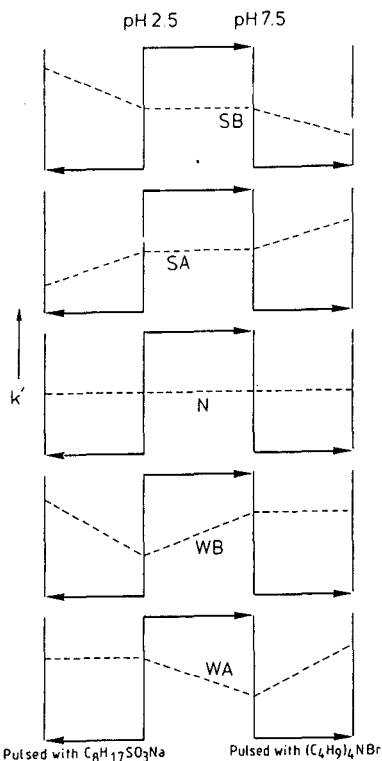
Fig. 5. Idealized retention shift patterns of different solute types, in the solute-type determination strategy proposed here.

The retention data can be collected either in isocratic or gradient mode, with respect to the organic modifier. The advantage of the gradient mode is that the column can be reequilibrated rapidly and *a priori* knowledge of the sample mixture is not required. Thus, four separate 0–90% organic modifier (methanol) gradient runs are used. Two gradients have their pH fixed at 2.5 and 7.5, respectively. They are expected to show retention shifts of the chromatographic peaks only if weak acids and/or bases are present. The two other gradients which involve a "pulse" injection (a technique described by Berry and Shansky[19] with a negatively and a positively charged ion-pairing reagent, respectively, will show retention shifts when strong acids and/or bases are present. The retention of the non-charged solutes is unaffected in all the four gradients.

The solutes are classified sequentially by an eliminative algorithm shown by its flowchart in Fig. 6. The strategy can be divided into two main parts: (i) differentiation between strong and weak (acid/base) solutes; (ii) differentiation between acids and bases and finding the non-charged solutes by simply eliminating the other possible solute types.

The fourth gradient may seem somewhat superfluous, since all solute types are already assigned. However, at low pH both SB and WB are positively charged, their retention increases with a negatively charged pairing ion, which prevents the un-ambiguous discrimination between these solute types. Furthermore, in complex mixtures containing very hydrophilic ionic components (eluting close to the solvent front) the repulsion effect of the "pulsed" pairing ion cannot be observed. In such cases the "pulse" with an oppositely charged pairing ion can produce positive retention shifts. The fourth gradient seems to eliminate this problem and also enhance the chances of discriminating all solutes from the non-charged ones.

In order to realize the benefits of this procedure, the majority of the solutes (more exactly their shifts) must be recognized in the sequential chromatographic runs. One can inject standards (if available) separately for peak identification, but this can be time and solvent consuming. Although this method was used in this study to validate the scanning strategy, it should be considered as a last resort, especially for the gradient method.

Peak tracking procedures based on the solute UV spectra can only be used when the spectra do not change with the eluent composition. An extensive use of mathematical techniques allowed for the ready identification of the components in a mixture of local anaesthetics, when an "isocratic" version of the scanning procedure was used[20].

However, the UV spectra of weak acids and bases can change significantly with the eluent pH. Therefore gradients at pH 2.5 and 7.5 can give different chromatograms at a constant detection wavelength. An example is shown in Fig. 7 for a mixture of a weak base (N-methylaniline) and a weak acid (phthalic acid). Both the magnitude of the UV signal and the UV spectra change dramatically with the ionization of the solutes. Therefore, a simple comparison of retention times and peak areas (and/or spectra) will not reveal peak identity in the two chromatograms.

On the other hand, one must realize that not all solutes have to be identified in order to reduce the range and/or number of the mobile phase optimization variables (*e.g.* the presence of only one hydrophilic non-charged solute may be enough to limit the organic modifier concentration of the mobile phase). The nature of the first and
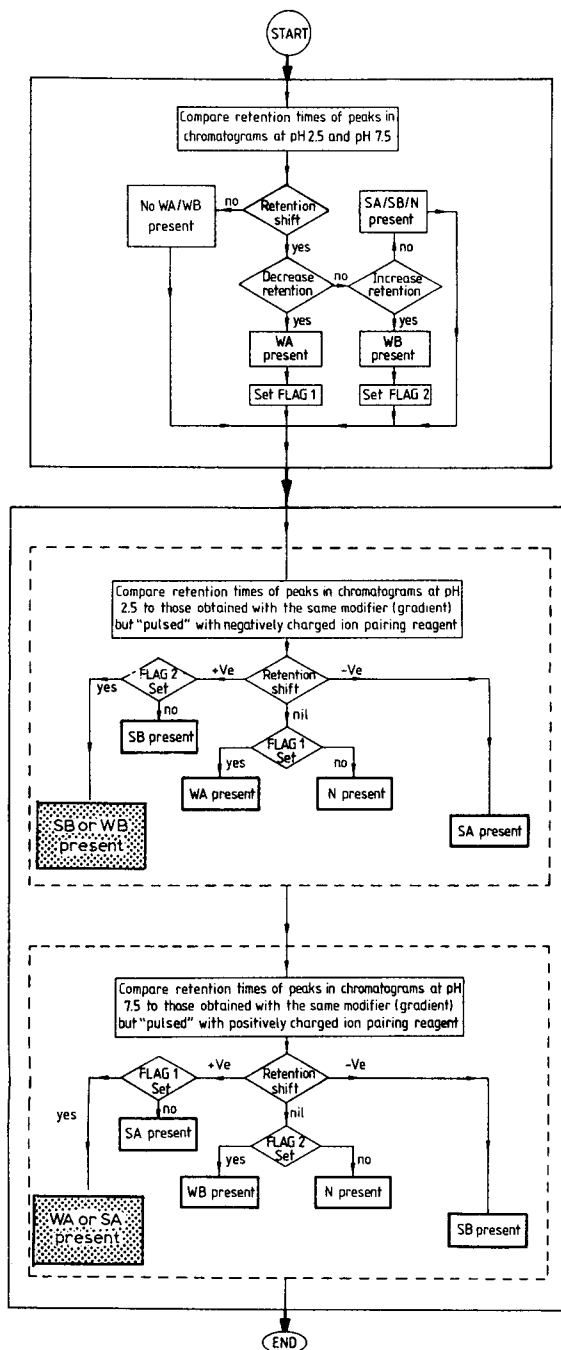
Fig. 6. Flow chart of the solute-type determination strategy.
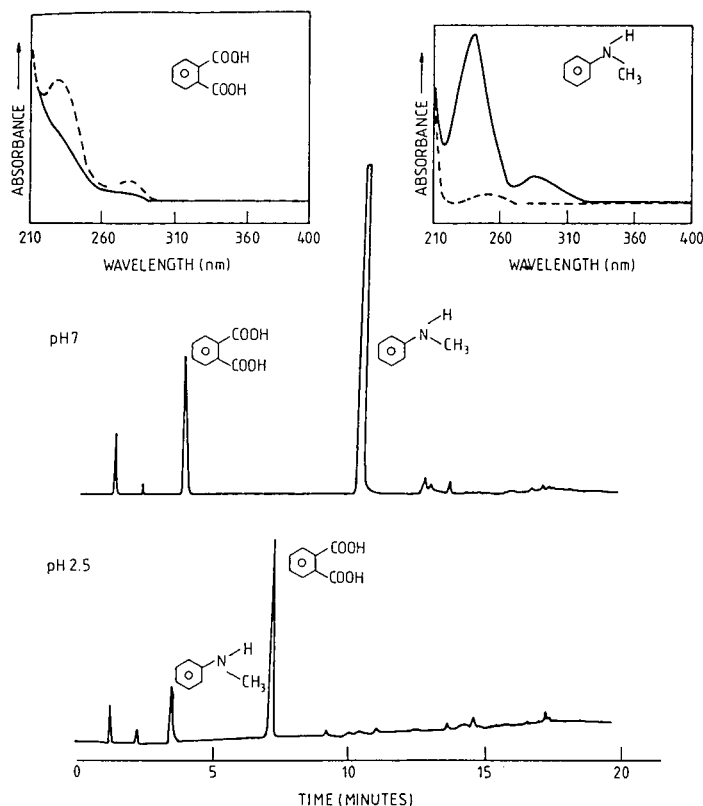
Fig. 7. Examples of changes of UV absorbance signals and spectra (insets obtained by a diode-array detector) of a weak acid (phthalic acid) and a weak base (N-methylaniline) with the eluent pH (solid lines, pH 7.0; broken lines, pH 2.5). Chromatograms were measured at 254 nm wavelength, using the triethyl-amine–phosphate buffer (15 mM) with a Nova-Pak C_{18} column.

last eluting peaks (at pH 2.5 and 7.5) is very important for the selection of the initial mobile phase conditions.

        In the case of mixtures containing one or two solute types, the retention shifts can be easily recognized and solute-type classification is relatively simple[21]. More complex sample mixtures require a retention shift-based successive elimination type computer program (currently under development[22]).

Experimental requirements for the solute-type determination
        A number of experimental requirements must be fulfilled before the proposed strategy can be used to classify the different solute types in an unknown mixture using the procedure outlined in Fig. 6: (a) the reversed-phase column must behave "ideally" towards the different classes of compounds in all chromatographic runs; (b) the retention of the charged solutes must be sufficiently altered by ionic repulsion and attraction when the ion-pairing reagent is added to ("pulsed" into) the eluent, throughout the whole of the chromatographic run; (c) the organic modifier concentration in the gradient scan must be sufficiently high so that very hydrophobic solutes can also be eluted, and the pH (2.5 or 7.5) during the modifier gradient must be stable.

    The requirements in point c can be fulfilled by the judicious selection of the
buffer system (see Experimental for details). Points a and b are discussed below.

    (a) Realization of "ideal" retention behaviour of charged solutes on reversed-
phase columns. The success of our strategy critically depends on whether the different
solute classes follow the idealized retention behavior shown in Fig. 2. To ascertain
this, the retention data of weak/stong acids/bases and non-charged solutes were mea-
sured as a function of the eluent pH (2.5–7.0) using isocratic (12.5% methanol) sol-
vents buffered with citric acid and disodium hydrogenphosphate on the ODS-Hy-
persil column (see Fig. 8a).

    The capacity factors of amphetamine and norephedrine (both strong bases with
pK_a values above 9) gave the largest deviation from the expected retention profile,
showing a minimum at around pH 3.3 rather than constant retention over the entire
pH range. Increased retention in the high-pH region is usually attributed to an ion-
exchange interaction of the positively charged amines with the dissociating silanol
groups[23–25]. The less pronounced increase of the retention of SBs at the lower pH
region (pH < 3.3) is more likely due to the citrate ions, which may act as ion-pairing
reagent with respect to the protonated base molecules. This reasoning is further sup-
ported by the decreasing retention of the negatively charged p-toluene sulfonic acid in
the same region, presumably caused by ionic repulsion between citrate and SA ions.
The retention profiles of N,N-dimethylaniline (WB) and 3,4-dihydroxyacetic acid
(WA) were as expected.

    The inclusion of organic amines (such as diethyl- or triethylamine) in the buffer
system was successfully used to suppress the anomalous behaviour of basic solutes
caused by the silanol groups on the surface of the octadecylsilica stationary phas-
es[23–25]. The mobile phase concentrations of these additives appear to vary in a range
of 5 to 25 mM, the upper limit being dependent on the peak asymmetry[13,14]. In our
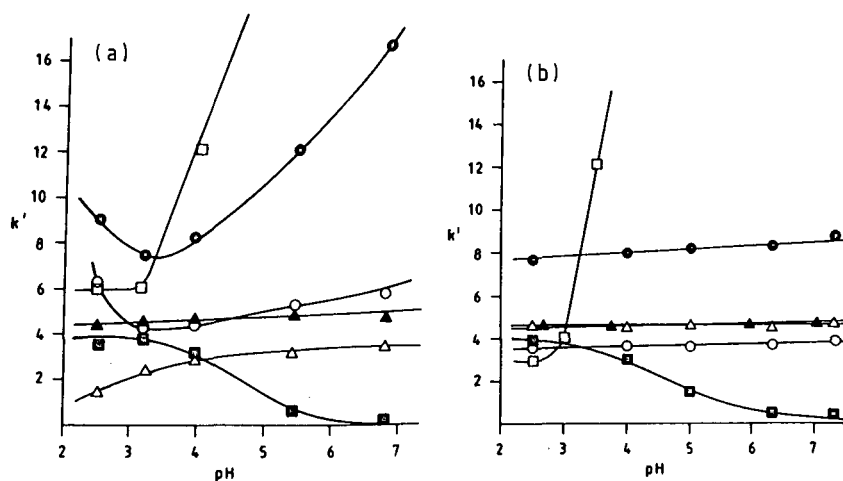
Fig. 8. Retention behavior of differently charged solutes on ODS-Hypersil column, using 12.5% (v/v)
methanol in 50 mM citrate-phosphate buffers (a) without the addition of triethylamine, and (b) with the
addition of 20 mM triethylamine phosphate. Solutes: □ = N,N-dimethylaniline (WB); ● = amphetamine
(SB); ▲ nitropropane (N); ○ = norephedrine (SB); △ = p-toluenesulfonic acid (SA); ▣ =
3,4-dihydroxyphenylacetic acid (WA).

case, 25 mM triethylamine phosphate completely eliminated the adverse silanol effects. However, it was also found to act as a positively charged ion-pairing reagent, having a serious impact on the second part of our strategy. It considerably toned down the expected retention shifts of charged solutes, when additional positively or negatively charged ion-pairing reagents were "pulsed" in the organic modifier gradients. Therefore, a lower (20 mM) triethylamine concentration was used finally, to realize the "ideal" retention behavior of the charged solutes, as shown in Fig. 8b. This eluent system, however, occasionally caused band broadening and/or peak splitting in the methanol gradients at pH 2.5, and allowed for the use of "pulsed" injections only at pH 7.0.

A more simple buffer system, prepared from 15 mM triethylamine and phosphoric acid was sufficient to normalize the retention behavior of the charged solutes on the other reversed-phase column (Nova-Pak C_{18}). With this organic buffer alone, higher final methanol concentration (90%), v/v) could be achieved in the gradient runs. However, due to the higher organic modifier concentration reduced ionic interactions were observed between the charged solutes and the ion-pairing reagents in the later part of the gradient. This additional problem will be discussed in section b below.

The procedure followed with these two columns can easily be generalized to evaluate whether other columns behave "ideally" in the selected buffer system (and allow for the use of our strategy). The retention of slightly and strongly retained strong acids and bases (see Fig. 8) must be determined at three different pH values (2.5, 5.0, 7.5), which could give immediate information on the behavior of the column. It is also advisable to include several non-charged solutes in the set, since their retention shifts can indicate inaccuracies of eluent preparation.

(b) Ionic attraction and repulsion of charged solutes by "pulsed" injection of the ion-pairing reagent. The basis of the "pulsed" injection method is to load a concentrated "slug" of ion-pairing reagent on the top of the reversed-phase column before the sample is introduced (and the organic modifier gradient is started)[19]. The ion-pairing reagent adsorbs on the hydrophobic surface of the packing material, and alters the retention of the charged solutes through ionic interaction. Bartha and co-workers[26–27] have demonstrated previously that the adsorption of the ion-pairing reagent decreases substantially with the increase of the organic modifier concentration of the mobile phase. Therefore, the ionic attraction/repulsion effect of the adsorbed pairing ion drops off significantly in the later part of the gradient, where it is increasingly removed from the column by methanol rich eluent. This phenomenon is clearly demonstrated by the retention data shown in Table I. For example, a more retained solute (which elutes also at higher methanol concentrations) such as N-ethylnaphthylamine shows marginal retention shift in the gradient at pH 2.5 when "pulsed" with sodium hexanesulfonate. The retention shift was considerably larger, when a more hydrophobic, more strongly adsorbed ion-pairing reagent, sodium octylsulfonate was used (see Table I). The retention of naphthalenesulfonic acid (SA) was also decidedly more affected in this latter case.

The results in Table I also indicate that even more hydrophobic pairing ions might be needed to effect significant retention movements for very highly retained ionic solutes. Work is in progress to explore this possibility[22]. Higher injection volumes and/or more concentrated solutions of the reagents have been tried with limited

TABLE I

TYPICAL RETENTION MOVEMENTS OF DIFFERENTLY CHARGED SOLUTES IN GRADIENT RUNS "PULSED" WITH DIFFERENT ION-PAIRING REAGENTS

Mobile phases buffered with triethylamine phosphate. Maximum methanol concentration during the gradient is 90% (v/v).

Compound	Solute classification	Modifier gradient at pH 2.5			Modifier gradient at pH 7.5	
		Non-pulsed	Pulsed		Non-pulsed	Pulsed
			$C_6H_{13}SO_3Na$	$C_8H_{17}SO_3Na$		$(C_4H_9)_4NBr$
Arginine phenylthiohydantoin	SB	7.25	8.38	10.85	7.54	6.34
N-Methylaniline	WB	3.38	6.64	9.55	10.26	10.33
N-Ethyl-naphthylamine	SB	9.40	9.57	11.67	10.59	9.68
Naphthaleneacetic acid	WA	12.78	12.73	12.72	9.56	10.55
1-Naphthalenesulfonic acid	SA	8.15	7.41	6.02	8.10	9.89
Ethyl iodide	N	12.34	12.41	12.40	12.34	12.35
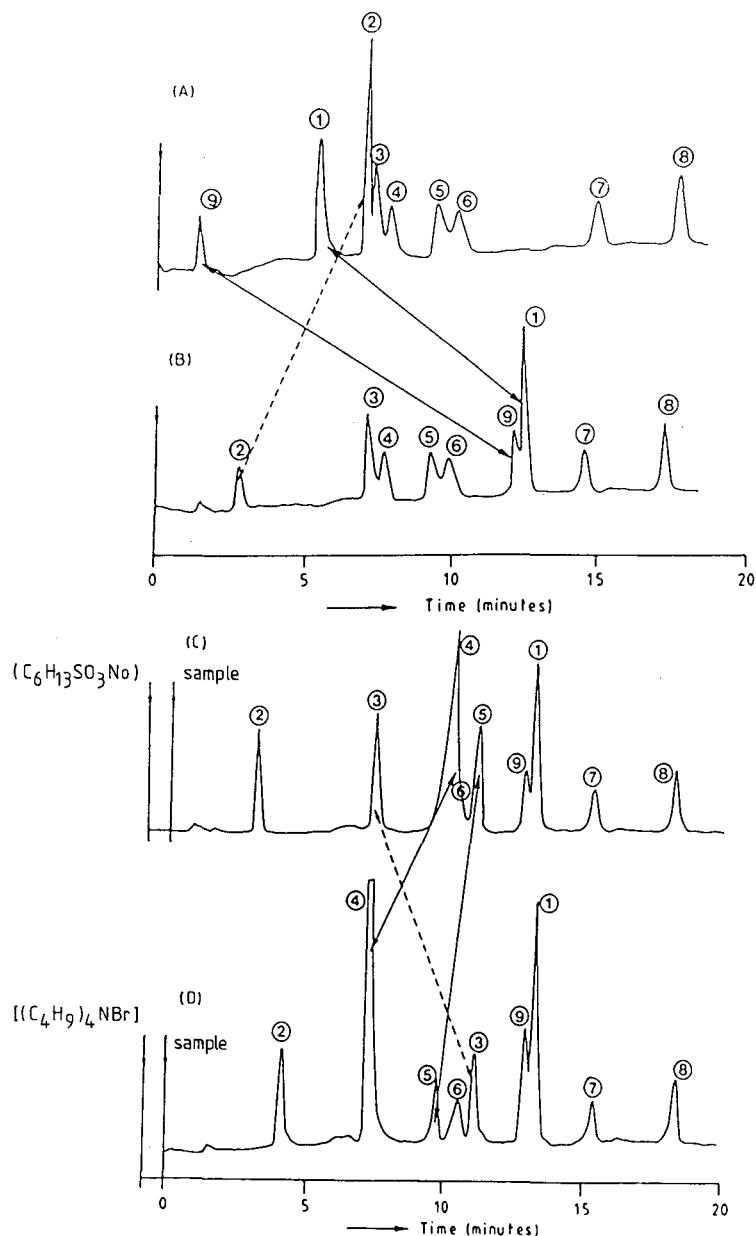
Fig. 9. Application of the solute-type determination strategy to an "unknown" mixture using the 50 mM citrate–phosphate (containing 20 mM triethylamine) buffer eluents on the ODS-Hypersil column. Chromatograms were obtained with 0–70% (v/v) methanol gradients at (A) pH 2.5; (B) pH 7.0; (C) pH 7.0 and "pulsed" with sodium hexylsulfonate; (D) pH 7.0 and "pulsed" with tetrabutylammonium bromide. Solutes: 1 = N-methylaniline (WB); 2 = 3,4 dihydroxyphenylacetic acid (WA); 3 = p-toluenesulfonic acid (SA); 4 = norephedrine (SB); 5 = amphetamine (SB); 6 = methyl iodide (N); 7 = ethyl iodide (N); 8 = propyl iodide (N); 9 = an impurity from N-methylaniline, which appears to be a WB.

success. Injection volumes larger than 20 μl were found to disturb the retention of the early eluting solutes (*e.g.* adrenaline, $k' < 1.5$), because of the disturbance effect caused by the solvent (methanol–water, 50:50) of the pairing ion slug. Limited solubility and long column equilibration times prevented the use of ion-pairing reagents in concentrations higher than 0.5 M.

Application of the solute-type determination procedure

The practical application of the solute-type determination strategy for two synthetic solute mixtures is illustrated in Figs. 9 and 10. Peaks which have moved during the scans were identified by the injection of standards in this validation of our procedure. The characteristic shifts of some solute types are indicated by arrows.

Results obtained on the ODS-Hypersil column with the citrate–phosphate buffer and using an earlier scheme of the solute-type determination strategy are shown in Fig. 9A–D. Chromatograms A and B were run at pH 2.5 and 7.0, respectively, without pairing ions. When these two chromatograms are compared, the increased retention of peaks 1 and 9 can be observed with the eluent pH, indicating that they must be weak bases. The decreased retention of component 2 reveals the presence of a weak
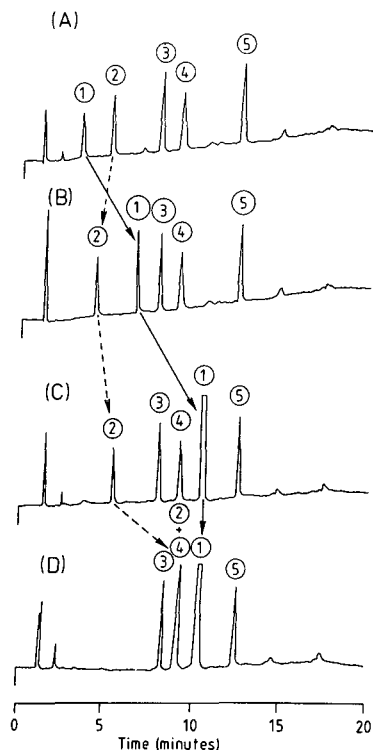
Fig. 10. Application of the solute-type determination strategy to a simple mixture using the triethylamine–phosphate buffered mobile phase on a Nova-Pak C_{18} column. The chromatograms were obtained with 0–90% (v/v) methanol gradients at (A) pH 2.5; (B) pH 2.5 and "pulsed" with sodium hexylsulfonate; (C) pH 7.5; (D) pH 7.5 and pulsed with tetrabutylammonium bromide. Solutes: 1 = N-methylaniline (WB); 2 = *p*-toluenesulfonic acid (SA); 3 = phenol (N); 4 = methyl iodide (N); 5 = ethyl iodide (N).

acid in this mixture. The remaining solutes do not change their retention with the pH and can be either strong acids/bases or non-charged solutes. A "pulsed" injection of a sodium hexanesulfonate in the gradient run at pH 7.0 (see chromatogram C) produced a positive retention shift of peaks 4 and 5 (compared to pH 7.0 without pulse) indicating that these components are strong bases. Similarly, a "pulsed" injection of tetrabutylammonium bromide at pH 7.0 (see chromatogram D) gave a pronounced positive shift for peak 3, indicating that this component is a strong acid. Therefore, out of nine components, two WBs (1, 9) and SBs (4, 5), one WA (2) and SA (3), and three Ns (6, 7, 8) are in the mixture. The most hydrophobic compound is peak 8 (N), and the least retained solute is either peak 2 (WA) or 9 (WB), depending on the final pH of the eluent.

Fig. 10A–D show the application of the solute-type determination strategy for a simple mixture, as given by the flowchart of Fig. 6. Triethylamine–phosphate buffer was used with the Nova-Pak C_{18} column. The highest methanol concentration at the end of the gradient is 90% (v/v). The buffer–methanol gradient was pulsed with sodium hexylsulfonate at pH 2.5 (Fig. 10B) and with tetrabutylammonium bromide at pH 7.5 (Fig. 10D). A notable feature of this example is that peak 1 (N-methylaniline) followed exactly the retention movement pattern of a WB, as outlined in Fig. 5. It is also noted that the confirmation of peak 2 as a SA is not conclusive until the completion of the fourth gradient, where a large retention increase occurs. Nevertheless, the consistent trend of the first three chromatograms indicated that peak 2 was likely an SA. The remaining solutes (3, 4, 5) in the mixture are non-charged (N) compounds.

Other applications of this solute-type determination strategy along with the extensive discussion of the problems of peak tracking, optimization parameter selection and subsequent mobile phase optimization can be found in refs. 20 and 21.

CONCLUSIONS

From the study of simulated mixtures of differently charged compounds we found that the nature (*i.e.* charge-type and relative hydrophobicity) of the components (not their exact identity) is important to decide what combination of eluent pH, organic modifier and pairing-ion concentration is to be selected for systematic optimization. Adapting the design of the eluent composition to the nature of the sample mixture often leads to a significant reduction of the optimization search area.

A systematic strategy, along with a sequentially eliminative algorithm was suggested and experimentally realized to determine the nature of the components in mixtures where this information in unavailable. A novel combination of aqueous buffer-methanol gradients at two different pH (2.5 and 7.5) values with the "pulsed" injection of ion-pairing reagents was used in this method. Since the classification of solute types (strong/weak acid/base, non-charged) is based on their "ideal" retention behavior in the reversed-phase chromatographic system, certain experimental requirements must be fulfilled for the successful application of this strategy. Both the reversed-phase column and the buffer system must be selected carefully, as shown for two commercial C_{18} colums of the same generic type.

ACKNOWLEDGEMENTS

REFERENCES

1 J. C. Berridge, *Techniques for the Automated Optimization of HPLC Separations*, Wiley, Chichester, 1985.
2 P. J. Schoenmakers, *Optimization of Chromatographic Selectivity – A Guide for Method Development*, Elsevier, Amsterdam, 1986.
3 J. L. Glajch and J. J. Kirkland, *Anal. Chem.*, 55 (1983) 319A.
4 H. J. G. Debets, *J. Liq. Chromatogr.*, 8 (1985) 2725.
5 L. de Galan and H. A. H. Billiet, *Adv. Chromatogr.*, 24 (1984) 35.
6 J. L. Glajch, J. J. Kirkland, K. M. Squire and J. M. Minor, *J. Chromatogr.*, 199 (1980) 57.
7 L. R. Snyder, J. W. Dolan and M.A. Quarry, *Trends Anal. Chem.*, 6 (1987) 106.
8 M. W. Dong, R. D. Conlon and A. F. Poile, *Am. Lab. (Fairfield, Conn.)*, 20 (5-6) (1988) 50.
9 T. O'Dwyer, P. DeLand, R. Smith, *Am. Lab. (Fairfield, Conn.)*, 20 (6) (1988) 40.
10 G. D'Agostino, L. Castagnetta, M. J. O'Hare and F. Mitchell. *J. Chromatogr.*, 338 (1985) 1.
11 L. R. Snyder, J. W. Dolan and J. R. Grant, *J. Chromatogr.*, 165 (1979) 3.
12 P. J. Schoenmakers, H. A. H. Billiet and L. de Galan, *J. Chromatogr.*, 205 (1981) 3.
13 A. P. Goldberg, E. Nowakowska, P. E. Antle and L. R. Snyder, *J. Chromatogr.*, 316 (1984) 241.
14 P. M. J. Coeneggracht, N. V. Tuyen, H. J. Metting and P. M. J. Coenegracht-Lamers, *J. Chromatogr.*, 389 (1987) 351.
15 H. A. H. Billiet, J. Vuik, J. K. Strasters and L. de Galan, *J. Chromatogr.*, 384 (1987) 153.
16 A. Bartha, Gy. Vigh, G. K. C. Low, H. A. H. Billiet and L. de Galan, presented at the *Pittsburgh Conference on Analytical Chemistry, Atlanta, GA, March 6–10, 1989*, paper P588.
17 J. L. M. van de Venne, J. L. H. Hendrikx and R. S. Deelder, *J. Chromatogr.*, 167 (1978) 1.
18 Cs. Horváth, W. R. Melander and I. Molnár, *Anal. Chem.*, 49 (1977) 142.
19 V. V. Berry and R. E. Shansky, *J. Chromatogr.*, 284 (1984) 318.
20 J. K. Strasters, F. Coolsaet, A. Bartha, H. A. H. Billiet and L. de Galan, *J. Chromatogr.*, submitted for publication.
21 A. Bartha, H. A. H. Billiet and L. de Galan, *J. Chromatogr.*, 464 (1989) 225.
22 A. Bartha and Gy. Vigh, in preparation.
23 K. E. Bij, Cs. Horváth, W. R. Melander and A. Nahum, *J. Chromatogr.*, 203 (1981) 65.
24 J. S. Kiel, S. L. Morgan and R. K. Abramson, *J. Chromatogr.*, 32 (1985) 313.
25 G. B. Cox and R. W. Stout, *J. Chromatogr.*, 384 (1987) 315.
26 A. Bartha and Gy. Vigh, *J. Chromatogr.*, 260 (1983) 337.
27 A. Bartha, Gy. Vigh, H. A. H. Billiet and L. de Galan, *J. Chromatogr.*, 303 (1984)

CHROM. 21 613

EXPERIMENTAL AND THEORETICAL DYNAMICS OF ISOELECTRIC FOCUSING

III. TRANSIENT MULTI-PEAK APPROACH TO EQUILIBRIUM OF PROTEINS IN SIMPLE BUFFERS

RICHARD A. MOSHER* and WOLFGANG THORMANN[a]

Center for Separation Science, Engineering Building 20, University of Arizona, Tucson, AZ 85721 (U.S.A.)
and
REINHARD KUHN[b] and HORST WAGNER

Institut für Analytik und Radiochemie, Universität des Saarlandes, D-66 Saarbrücken (F.R.G.)
(First received February 2nd, 1989; revised manuscript received May 3rd, 1989)

SUMMARY

Transient states in the isoelectric focusing of proteins in simple three-component buffer systems were examined by (i) analyzing the collected fractions from continuous flow electrophoresis at a range of operating conditions, (ii) photographing the behavior of colored proteins in capillaries, (iii) monitoring the electric field dynamics along a capillary with a potential gradient array detector and (iv) computer simulation. The good agreement between simulation and experimental data clearly reveals how the separation dynamics of the buffer system, *i.e.*, the formation of a natural pH gradient, produces the observed peaks and boundaries of protein during the approach to the steady state. The protein focusing dynamics are different, but characteristic, for each buffer system, with both transient double, and multiple, peaks being observed.

INTRODUCTION

Characterization of the transient processes in isoelectric focusing (IEF) is of interest in order to establish when the steady state is reached. A variety of procedures have been developed by a number of investigators for examination of these transient states. Repetitive optical scanning has been employed with rotating[1] and density gradient-stabilized[2] free fluid columns as well as gel filled columns[2]. Gels have also been segmented at various times during the course of an experiment and measure-

---

[a] Present address: Department of Clinical Pharmacology, University of Bern, CH-3010, Bern, Switzerland.
[b] Present address, Analytical Research and Development, Pharmaceutical Division, Sandoz Ltd., Basel, Switzerland.

ments of pH, conductivity, absorbance, radioactivity and biological activity made on segment eluates (see ref. 3 for a review). Additionally, Weiss *et al.*[4] have developed a theoretical description of sample behavior in the presence of pre-established, linear pH gradients.

Our prior studies of the dynamics of IEF have employed an amalgam of experimental and computer simulation data. In a first publication on the subject, a general separation mechanism was elucidated[5]. It was found that the focusing process proceeds in two phases, a relatively fast separation phase followed by a slow stabilizing phase during which a steady state is reached. The latter phase provides an explanation of the plateau phenomenon in IEF[6]. A second paper reported the impact of various electrode assemblies on the focusing process and the decay of the focusing pattern caused by cathodic, anodic or symmetrical drifts[7]. Those studies utilized low-molecular-weight components with the experimental investigations conducted in free solution in capillaries. In this third contribution on focusing dynamics, computer simulation and experimental data are employed to describe transient protein distributions during focusing in three-component buffer mixtures. Experiments were carried out in free solution using both continuous flow and capillary instruments.

MATERIALS AND METHODS

Instrumentation

The CapScan capillary-type apparatus with a linear potential gradient array detector along the focusing column has been described in detail elsewhere[5,8]. This instrument allows the electric field profile along the focusing axis to be recorded within 20 min, fully controlled by a desk top computer. Two different troughs of rectangular cross-section and 10 cm length were used, which have channel widths of 1 or 15 mm and a height of about 0.4 mm (ref. 8). Dialysis membranes with a molecular mass cut-off of 12 000–14 000 (Spectrapore No. 132709; Spectrum Medical Industries, Los Angeles, CA, U.S.A.), were used to isolate the focusing capillary from the electrode compartments. Small amounts of NaOH and phosphoric acid, 0.1 *M* each, were the respective cathodic and anodic electrolytes. A Kepco power supply APH 2000 M provided either constant voltage or current. Experiments were performed at room temperature.

Some of the continuous flow experiments were done with the Elphor VaP 22 (Bender and Hobein, Munich, F.R.G.). The instrument has a vertical, rectangular separation chamber (50 cm × 10 cm × 0.05 cm). Five buffer and four sample inlets are provided at the top of the chamber. A computer controlled reflectance scanner records absorbance at 280 nm along the separation axis just prior to the exit. Ninety fractions are collected. Experiments were performed at 4°C. Other experiments utilized a laboratory-made continuous flow device with chamber dimensions of 27 cm × 22 cm × 0.05 cm. Eight inlet ports and ninety outlet ports are provided. Experiments with this device were also performed at 4°C.

Computer simulations

The dynamic computer model of Mosher *et al.*[9] was used to simulate the behavior of proteins and buffer constituents. The one-dimensional approach assumes the absence of convective flows and thermal gradients. The specified initial conditions

TABLE I

ELECTROCHEMICAL PARAMETERS USED FOR COMPUTER SIMULATION

Component	pK_1	pK_2	Mobility · 10^4 $(cm^2/v \cdot s)$
Glutamic acid	2.16	4.29	2.97
Cycloserine	4.40	7.40	3.42
Histidine	6.02	9.17	2.85
Arginine	9.04	12.48	2.26
H_3O^+			36.27
OH^-			19.87

included the uniform distribution of all constituents, the diffusion coefficient and net charge–pH relationship of the proteins, the pK and mobility values of the buffer constituents, the current density and the electrophoresis time. The program predicts concentration profiles and pH and conductivity gradients as a function of time. Input data are summarized in Tables I and II.

Experimental procedures

Analytical grade chemicals were used. Human hemoglobin was prepared from fresh, washed red blood cells by standard techniques. Bovine serum albumin was

TABLE II

NET CHARGE *vs.* pH RELATIONSHIPS FOR HEMOGLOBIN AND ALBUMIN

Ionization data were adopted from ref. 10 for hemoglobin and from ref. 11 for albumin. The diffusion coefficient used for hemoglobin is[12] $6.8 \cdot 10^{-11}$ m²/s and for albumin is[13] $5.94 \cdot 10^{-11}$ m²/s.

pH	Net charge	
	Hemoglobin	Albumin
3.0	68.5	58
3.5	43.5	35.5
4.0	–	13
4.5	25.5	–
4.8	–	0
5.56	–	– 6.1
6.0	10.25	–
6.56	–	– 12.2
7.0	0	–
7.56	–	– 18.3
8.0	– 10.25	–
8.56	–	– 24.4
9.0	– 20.5	–
9.56	–	– 30.5
10.0	– 30.75	–
10.06	–	– 33.55
11.0	– 50	– 44
11.5	– 63.5	– 64
12	–	– 84

obtained from Pentex as a 35% solution. In the CapScan the progress of the experiment was followed by monitoring the dynamics of the electric field and/or photographically recording the distribution of hemoglobin and bromophenol blue-stained albumin. Data from the continuous flow instruments represent either measurements on collected fractions or were obtained with the scanner on the VaP 22. Buffer constituents were analyzed by thin-layer chromatography (TLC) using a mobile phase of ethanol–water–concentrated ammonia (70:25:5, v/v). Kieselgel 60 (0.2 mm) aluminum TLC plates and ninhydrin (0.1%) spray for chromatography were from Merck (Darmstadt, F.R.G.).

RESULTS AND DISCUSSION

The glutamic acid–histidine–arginine system

This system is comprised of 10 mM each of glutamic acid (Glu), histidine (His) and arginine (Arg) as the background buffers with 0.5 mg/ml albumin as the sample, which focuses in the boundary between Glu and His. Simulation, continuous flow and capillary data are shown in Figs. 1, 2 and 3, respectively, which collectively present the dynamics of this mixture. The three buffer components behave according to the focusing mechanism described previously[5], thus the presence of the protein at this concentration does not alter the behavior of the buffers, or the development of the pH gradient. Two schematic representations of the amino acid distributions are included above time points 10 and 30 in Fig. 1A. The boundaries referred to in the following discussion are indicated there.
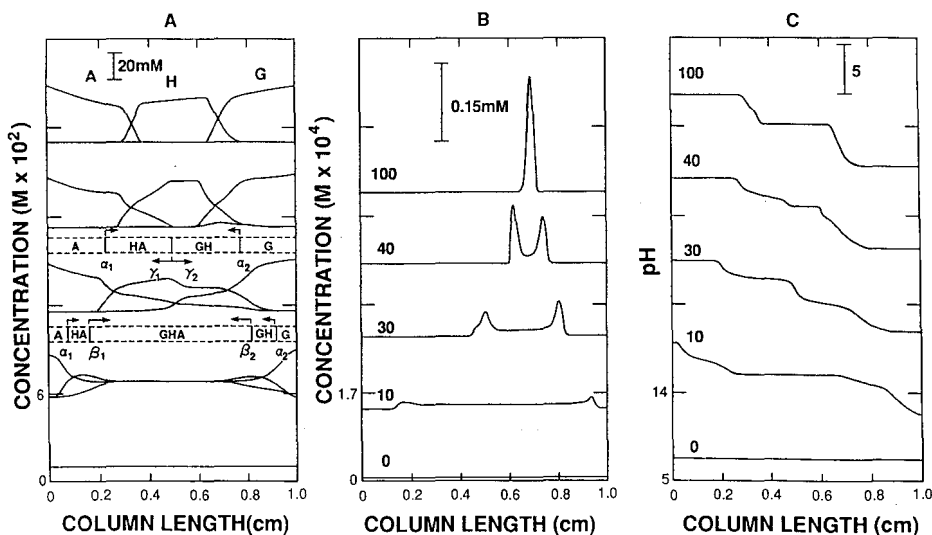
Fig. 1. Computer simulation data showing the focusing behavior of 0.5 mg/ml albumin in a buffer system composed of 10 mM each of glutamic acid (G), histidine (H) and arginine (A). (A) The transient behavior of the amino acids; (B) the albumin dynamics; (C) the development of the pH gradient. Profiles are shown after 0, 10, 30, 40 and 100 min of current flow (5 A/m^2) and are offset vertically by a constant amount to facilitate presentation. The focusing mechanism of the ampholytes is displayed schematically above the 10- and 30-min profiles. Migrating boundaries are indicated by vertical solid lines (5). Vectors indicate direction and relative velocity. The anode is to the right.

Fig. 1B depicts the computed albumin distribution at 0, 10, 30, 40 and 100 min after current application. On the anodic side, albumin accumulates in the boundary which demarcates the production of the pure Glu zone. On the cathodic side, the protein migrates with the boundary which marks the trailing end of the Glu distribution. These boundaries correspond to α_2 and β_1, respectively of Fig. 1A. The sharp anodic peak grows as it migrates toward the position of final focus. A sharpening of the cathodic protein peak occurs about 30 min after current application, at the time of the meeting of the two faster boundaries (β_1 and β_2), $i.e.$, the beginning of the establishment of the pure central histidine zone. During the evolution of this zone the cathodic protein peak continues to migrate with the same velocity as that of Glu (now the γ_2 boundary). The magnitudes of the two migrating protein peaks increase until they ultimately merge. This coalescence corresponds to the conclusion of the separation phase of the three buffer constituents. Thus, the protein and the buffer reach their final positions at the same time.

The experimental data shown in Figs. 2 and 3 qualitatively validate the computer predicted focusing scheme for continuous flow and capillary devices. The most obvious discrepancy is found in the continuous flow data, where the cathodic protein

FRACTION NUMBER
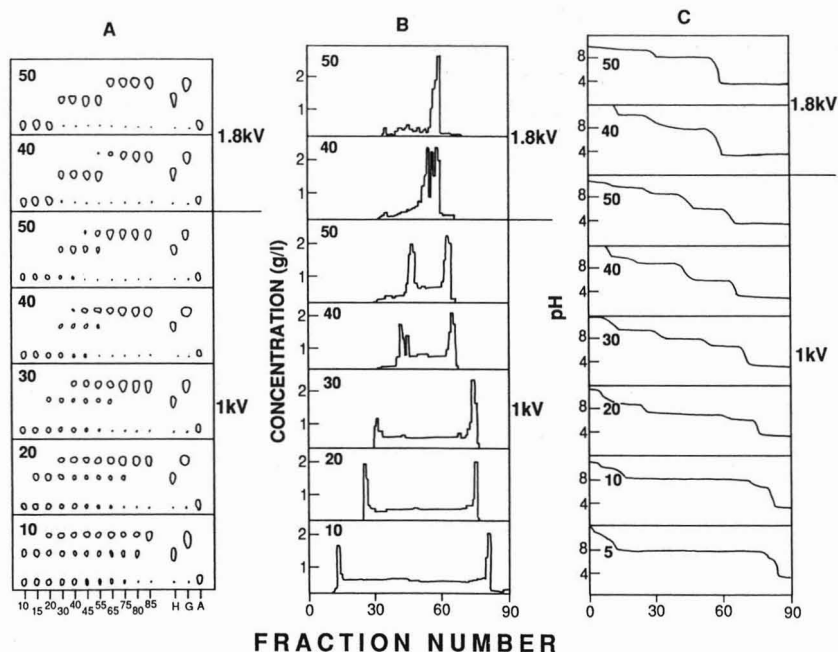
Fig. 2. Experimental data which show the focusing of 0.5 mg/ml albumin in a buffer system composed of 10 mM each of glutamic acid, histidine and arginine. These data were obtained with the laboratory made continuous flow instrument, utilizing cellulose acetate membranes, and 0.1 M phosphoric acid and 50 mM NaOH as anolyte and catholyte, respectively. (A) The distribution of the amino acids as a function of the residence time, indicated in minutes, and the applied voltage, 1 kV for the lower six time points and 1.8 kV for the upper two time points. These data are schematic representations of TLC separations. For each time point the first three lanes from the right contain the pure amino acids applied as references. Measurements on collected fractions provided the corresponding protein distributions shown in (B) and the pH distributions of (C). The anode is to the right.
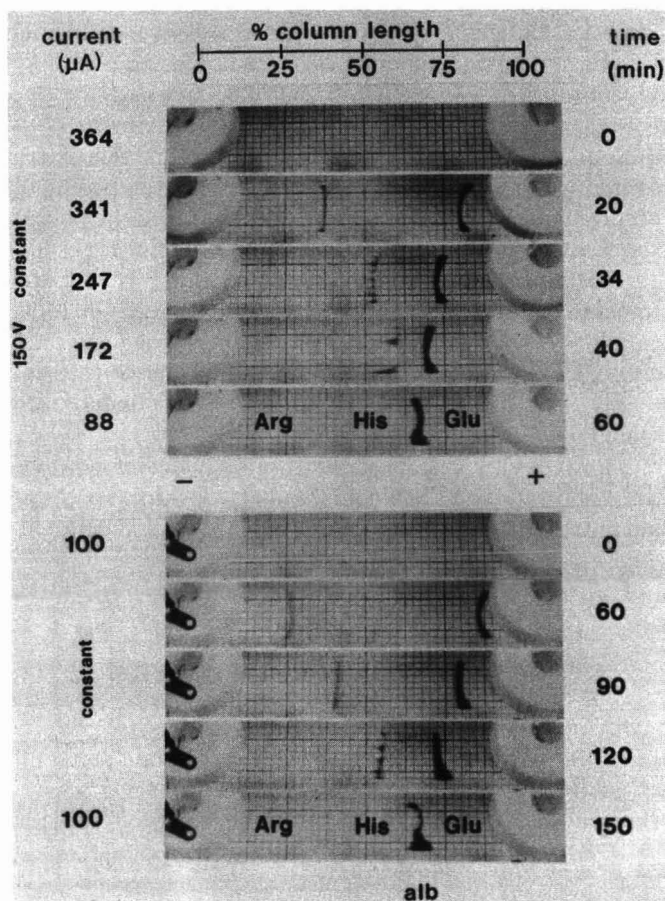
Fig. 3. The focusing of bromophenol blue-stained albumin in a ribbon-like capillary is presented at constant voltage (150 V) in the upper half of the figure and at constant current (100 μA) in the lower half. The initial buffer composition is the same as that in Figs. 1 and 2. The anode is to the right. Note that the weaker (cathodic) transient peak is interrupted by an organized, unidentified flow pattern at 34 and 40 min at constant voltage and at 120 min at constant current. The approximate steady state positions of the focused buffers are indicated by their respective abbreviations.

peak is relatively larger than predicted by the simulation. The reason for this is unclear. However, this peak in the capillary data, at both constant current and constant voltage, is much fainter than its anodic counterpart. In general, the theoretical predictions and experimental data correlate well and exhibit the focusing mechanism found in Ampholine-based configurations and referred to as the transient double peak approach to equilibrium[14]. The prediction by Dishon and Weiss[15] that non-linear pH changes are necessary to produce that mechanism is consistent with this data.

The glutamic acid–cycloserine–arginine system

Figs. 4–6 present the detailed focusing process of albumin (about 0.5 mg/ml) in a system consisting of Glu, cycloserine (Cser) and Arg (10 mM each). Panel A of Fig.
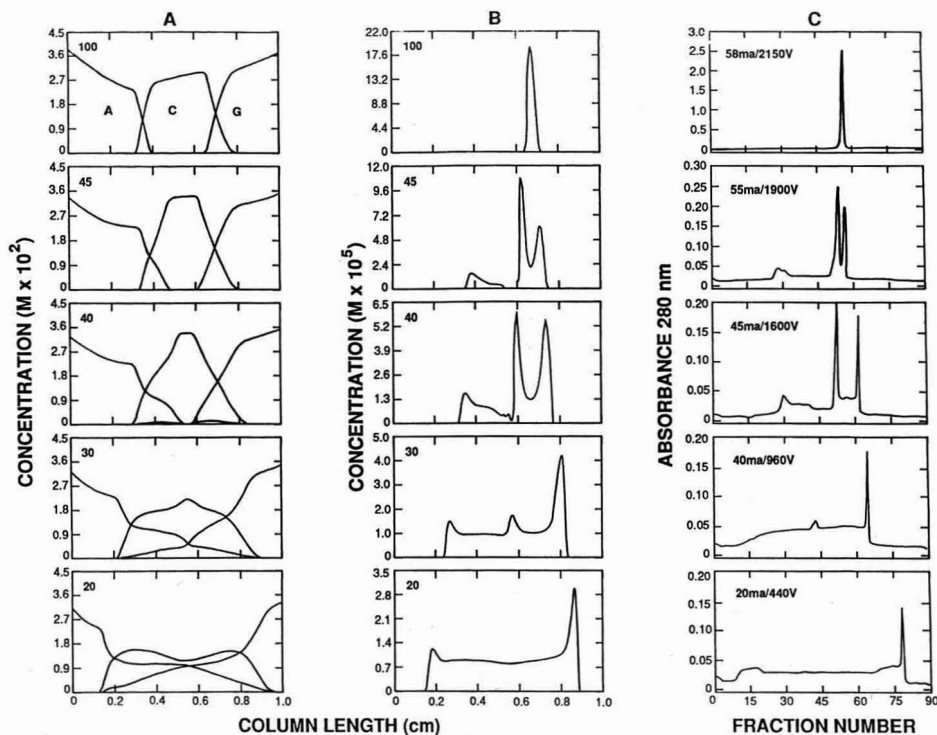
Fig. 4. Simulation and continuous flow experimental data which describe the focusing of albumin (0.5 mg/ml) in a buffer system composed of 10 mM each of glutamic acid (G), cycloserine (C) and arginine (A). (A) The simulated behavior of the buffer components after 20, 30, 40, 45 and 100 min of current flow (5 A/m^2). The anode is to the right. (B) The simulated behavior of albumin at the same time points. (C) Corresponding experimental data taken with scanner on the Elphor VaP 22, with a residence time of 11 min. The current and applied voltage when the scans were recorded are indicated in each panel. The upper three distributions were obtained in the presence of 0.3% hydroxypropylmethylcellulose (HPMC), whereas the lower two were taken in the absence of any additives.

4 shows the computer predicted behavior of the electrolytes which focus by the mechanism presented in Fig. 1A. The focusing of albumin (Fig. 4B and C) begins with a strong peak from the anode and a very weak counterpart at the cathode. These peaks are moving within boundaries α_2 and α_1, respectively. This is a different mechanism to that displayed in the Glu–His–Arg system, with the protein moving relatively more slowly in the anodic direction. The weak cathodic peak (α_1 boundary) is not visible in the capillary data (Fig. 5), either at constant voltage or at constant current.

The emergence of the pure zone of Cser marks the appearance of a new peak of albumin which migrates with the γ_2 boundary. This peak grows rapidly as it migrates toward the strong peak coming from the anode, surpassing it in size before the two meet. The focusing of albumin in this system thus displays three peaks or areas of increased protein concentration, which constitutes a second difference in comparison to the Glu–His–Arg system. Only a trace of albumin is present within the emerging Cser zone. The protein migrating within the α_1 boundary and in the transient zone
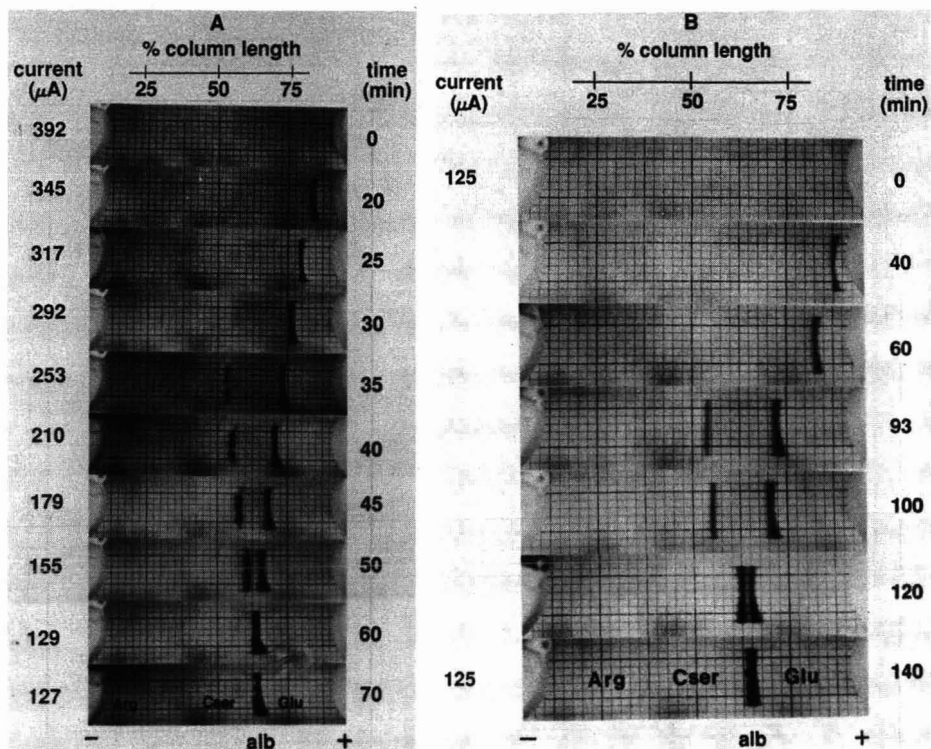
Fig. 5. The focusing behavior of 0.5 mg/ml bromophenol blue-stained albumin in a ribbon-like capillary in the Glu–Cser–Arg buffer system at constant voltage (150 V) (A) and at constant current (125 μA) (B). A strong band of protein appears suddenly between 30 and 35 min at constant voltage and between 60 and 93 min at constant current. The approximate steady state positions of the focused buffers are indicated by their respective abbreviations.

between boundaries α_1 and γ_1 slowly joins the major peak, the focusing of albumin being completed after the focusing of the ampholytes, a third difference from the Glu–His–Arg system. The data in Fig. 4C clearly confirm that the experimental behavior in the Elphor VaP 22 follows, in detail, the theoretical prediction. The capillary data (Fig. 5) also show the sudden appearance of the protein peak (in boundary γ_2) which appears upon the emergence of the pure, colorless Cser zone. This occurs between 30 and 35 min at constant voltage and 60 and 93 min at constant current.

Fig. 6 presents the computed (panel A) and experimental (panel B) behaviors of the electric field profiles for this system. The major boundaries (α_1 and α_2) which migrate away from each electrode are clearly visible as is the appearance of the pure central zone of Cser, which is just beginning at 30 min in the simulation data. In panel B the albumin makes a clear contribution to the steady state profile, in the boundary between Glu and Cser. Under the simulation conditions used, the protein makes no significant contribution to the potential gradient data. The current density in the experiment is about three-fold higher than that assumed for the simulation.

Fig. 7 presents simulation data, and experimental data obtained with the rib-
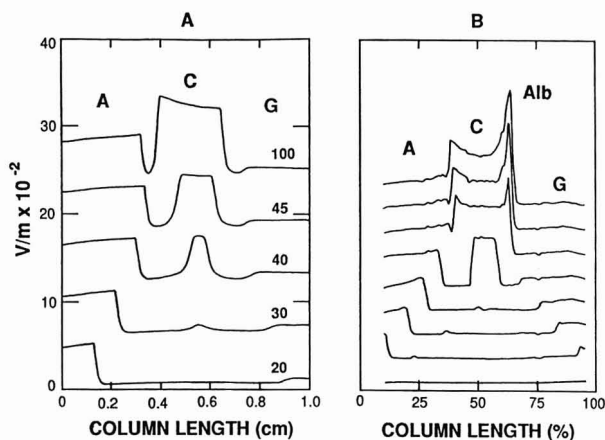
Fig. 6. Simulated (A) and experimental (B) voltage gradient profiles for the Glu–Cser–Arg system containing 0.5 mg/ml albumin. Successive time points are offset vertically to facilitate presentation. The anode is to the right. In (A) insufficient protein is present to have a visible impact on the profiles. In (B) the steady state concentration of the focused protein is high enough to affect the electric field in the Glu–Cser boundary. The positions of the focused buffers are indicated. Simulation conditions are the same as for Fig. 4. The CapScan experiment was performed at a constant current of 10 μA. The scans represent the electric field distribution at intervals of 40 min.
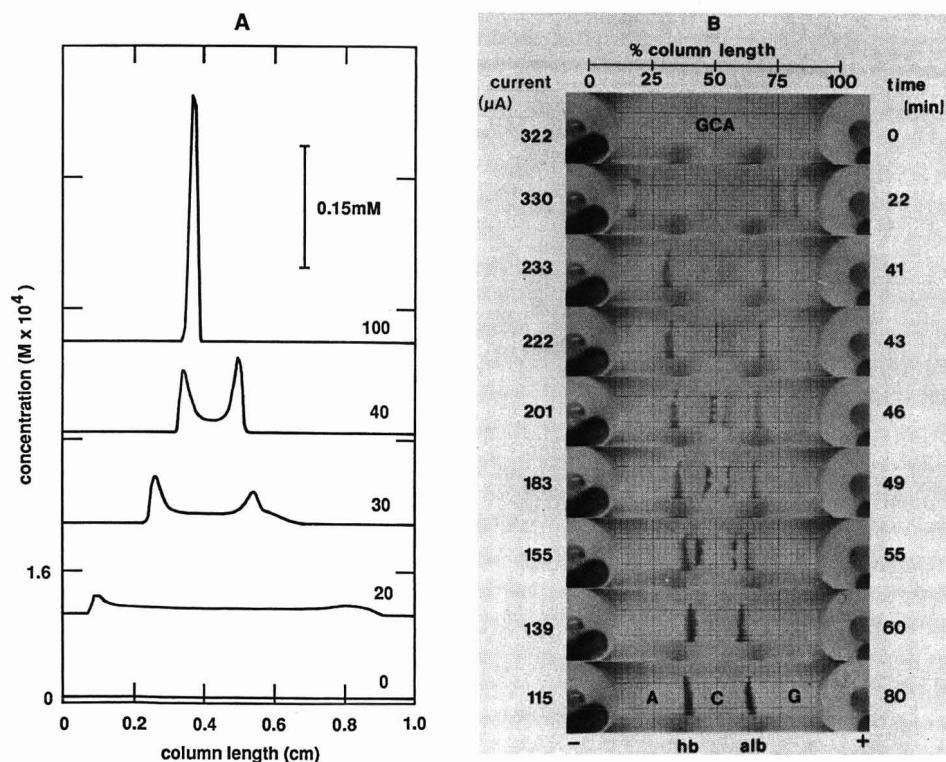
Fig. 7. The simulated focusing of hemoglobin in the Glu–Cser–Arg system (A). The time points are labelled in min of current flow (5 A/m^2). The anode is to the right. (B) The focusing of hemoglobin and bromophenol blue-stained albumin in the ribbon-like capillary. The focusing was accomplished under a constant 150 V.

bon-like capillary device, which show the focusing behavior of hemoglobin and albumin in the Glu–Cser–Arg system. Hemoglobin behaves much differently than albumin, showing a simpler, double-peak approach to equilibrium, as is the case for albumin in the Glu–His–Arg system. The peak which migrates away from the cathode is sharper than its counterpart from the anode, and moves within the α_1 boundary. The broad peak which leaves the anode migrates within the faster β_2 boundary. It undergoes a substantial sharpening when the pure zone of cycloserine begins to emerge (the appearance of the γ boundaries), after 30 min of current flow. It is clear from the simulation data that hemoglobin focuses faster than does albumin in this system, reaching its equilibrium position at approximately the same time as do the background buffers.

CONCLUSIONS

The model used to represent the electrophoretic behavior of proteins[9] accurately predicts the IEF behavior of hemoglobin and albumin in two different buffer systems. This model should prove valuable for the continued study of the fundamental behavior of proteins in this electrophoretic mode. It confirms that proteins will focus as rapidly, or nearly so, as do the background buffers in free solution. However, this will not be true in gels, because of the sieving effect of even the low %T gels commonly used for IEF. This means that the focusing mechanisms in gels will likely be different than those in free solution. The correspondence of the experimental results from continuous flow instruments and capillaries indicates the high degree of fluid stability present in these devices[16] and that the mechanisms presented hold for static as well as flowing solutions. However, a careful inspection of some of the migrating protein peaks in the capillary results in Figs. 3, 5 and 7 reveals a patterned disruption, e.g., the fainter albumin line in the 120-min time point in Fig. 3. These are observed when a system-dependent potential gradient is exceeded, and are presumably due to an organized, non-uniform, electrohydrodynamic flow. This effect has been observed in continuous flow instruments and is a function of the conductivity and dielectric gradients present[17]. Electroosmosis can be ruled out as the source of the instability because these patterned states can be observed in the presence of a.c. fields[18].

Focusing mechanisms are dependent upon the protein and the buffer system and independent of whether the experiment is performed at constant current or constant voltage. Hemoglobin and albumin display completely different focusing mechanisms in the Glu–Cser–Arg system, and albumin focuses differently when cycloserine is replaced with histidine. The multiple transient peaks displayed by albumin in the Glu–Cser–Arg buffer are quite unusual; such multiple peaks are only likely to be observed in simple buffer systems. More complex buffers will promote the more common mechanism characterized by two peaks and called the transient double peak approach to equilibrium[14].

ACKNOWLEDGEMENTS

REFERENCES

1 P. Lundahl and S. Hjerten, *Ann. NY Acad. Sci.,* 209 (1973) 94.
2 N. Catsimpoolas, *Ann. NY Acad. Sci.,* 209 (1973) 65.
3 P. G. Righetti, *Isoelectric Focusing: Theory, Methodology and Applications,* Elsevier Biomedical, Amsterdam, 1983.
4 G. H. Weiss, N. Catsimpoolas and D. Rodbard, *Arch. Biochem. Biophys.,* 163 (1974) 106.
5 W. Thormann, R. A. Mosher and M. Bier, *J. Chromatogr.,* 351 (1986) 17.
6 R. A. Mosher, W. Thormann and M. Bier, *J. Chromatogr.,* 351 (1986) 31.
7 R. A. Mosher, W. Thormann and M. Bier, *J. Chromatogr.,* 436 (1988) 191.
8 W. Thormann, A. Tsai, J. P. Michaud and M. Bier, *J. Chromatogr.,* 389 (1987) 75.
9 R. A. Mosher, D. Dewey, W. Thormann, D. A. Saville and M. Bier, *Anal. Chem.,* 61 (1989) 362.
10 E. J. Cohn, A. A. Green and M. H. Blanchard, *J. Am. Chem. Soc.,* 59 (1937) 509.
11 K. Linderstrom-Lang and S. O. Nielsen, in M. Bier (Editor), *Electrophoresis,* Vol. 1, Academic Press, New York, 1959, p. 85.
12 J. T. Edsall, in H. Neurath and K. Bailey (Editors), *The Proteins,* Vol. 1, Academic Press, New York, 1953, Pt. B, p. 637.
13 H. R. Mahler and E. H. Cordes, *Biological Chemistry,* Harper and Row, New York, 2nd ed., 1971, p. 87.
14 J. N. Behnke, S. M. Dagher, T. H. Massey and W. C. Deal, *Anal. Biochem.,* 69 (1975) 1.
15 M. Dishon and G. H. Weiss, *Anal. Biochem.,* 81 (1977) 1.
16 R. Kuhn, H. Wagner, R. A. Mosher and W. Thormann, *Electrophoresis,* 8 (1987) 503.
17 P. H. Rhodes, R. S. Snyder and G. O. Roberts, *J. Coll. Interface Sci.,* 129 (1989) 78.
18 W. Thormann and R. A. Mosher, in C. Schafer-Nielsen (Editor), *Electrophoresis '88,* VCH Verlagsgesellschaft, Weinheim, 1988, p. 121.

INDIRECT DETERMINATION OF O-ETHYL S-(2-DIISOPROPYLAMINO-ETHYL) METHYLPHOSPHONOTHIOATE IN AIR AT LOW CONCENTRATIONS

WILLIAM K. FOWLER* and JOSIAH E. SMITH, Jr.

Southern Research Institute, P.O. Box 55305, Birmingham, AL 35255-5305 (U.S.A.)

(First received March 21st, 1989; revised manuscript received July 3rd, 1989)

SUMMARY

This paper describes an indirect method for the quantification of the toxic military agent O-ethyl S-(2-diisopropylaminoethyl) methylphosphonothioate (VX) in the vapor state in air or other similar gases at ng/m^3 levels. The method begins with the passage of a gaseous sample through a filter impregnated with silver fluoride to convert the VX vapor to ethyl methylphosphonofluoridate. The latter compound is then trapped on a bed of Chromosorb 106, transferred to a smaller bed of the same sorbent, and desorbed thermally into a gas chromatograph equipped with a flame-photometric detector. The method is comparable in sensitivity to the principal alternative method, which is based on cholinesterase inhibition, and it is less subject to interference from common organic solvents and other cholinesterase inhibitors.

The detection limit was found to be limited by, and therefore dependent on, the nature and extent of any background substances that produced a significant chromatographic signal or response at the retention time of the analyte. In the absence of such substances, the instrument provided a response to 0.19 ng of VX that was thirty times larger than the peak-to-peak noise amplitude on the chromatographic base line. Moreover, the method bias (*i.e.*, 100% minus the percent VX recovery) was found to depend on VX concentration, with estimates of agent recovery ranging from 83% at a VX concentration of 0.67 ng/m^3 to 104% at a concentration of 0.084 ng/m^3. The relative standard deviation varied with VX concentration and with the nature of the test that was performed to estimate it. It ranged from 2.1% in one VX vapor-challenge test to 17% in an experiment involving spiked sampling tubes, and it was generally lower at the higher VX test concentrations.

INTRODUCTION

The very high toxicity of O-ethyl S-(2-diisopropylaminoethyl) methylphosphonothioate, also known as VX, mandates the requirement for an analytical method that can determine it at exceedingly low concentrations in air. Defense-related research over the past two or three decades has produced numerous analytical methods

for determining VX in a variety of matrices[1,2]. But methods based on the Schoene-mann reaction[1-3], on enzyme inhibition [1,2,4], and on gas chromatography (GC) with a variety of detectors [1,5-8] are by far the most commonly used approaches to trace-level determinations of VX in complex matrices.

Because of its very high sensitivity, the enzymatic technique (in conjunction with sampling into a glass impinger or bubbler filled with a liquid absorbing medium) has been evaluated for determining very low concentrations of VX vapor. But this technique responds rather indiscriminately to any substance that can inhibit or de-stroy the activity of the enzyme (cholinesterase); such inhibitors include, *e.g.*, many common organic solvents[1].

For this reason, a sensitive, yet specific method based on GC was sought. However, VX vapor exhibits a troublesome tendency to adsorb strongly (often irre-versibly) on any surface[9], a phenomenon that places extreme demands on the sam-pling device and on the gas chromatographic system with respect to inertness. Indeed, we have found that this adsorption problem leads to excessive inaccuracy and impre-cision even in the enzymatic method, where the VX presumably adheres to the inner surface of the impinger sampler.

In the method reported here, the adsorption problem is effectively circumvented by first converting the VX to ethyl methylphosphonofluoridate, which is much less strongly adsorbed on most surfaces. This compound is frequently referred to as the G-analogue of VX because of its structural similarity to the G-type chemical agents. The V-to-G conversion reaction involves the use of solid silver fluoride as the reagent and is depicted in Fig. 1. Although this reaction has been widely used for facilitating determinations of VX[1], its original use occurred in classified military studies that were conducted over two decades ago, and the authors have not located the names of the original investigators. Nevertheless, it appears probable that V-to-G conversion has not been used previously in conjunction with solid-sorbent sampling, gas chroma-tographic determinations, or ppt[a] concentrations of VX vapor in air.
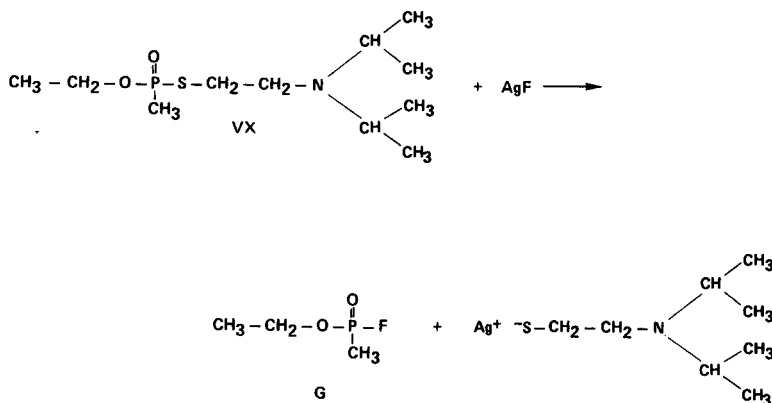
Fig. 1. Conversion of VX to its G-analogue (G).

---

[a] Throughout this article, the American trillion (10^{12}) is meant.

The method described in this publication entails the pumping of an air sample through a felt pad impregnated with silver fluoride, the collection of the G-analogue of VX in a solid-sorbent (Chromosorb 106) sampling tube, the transfer (by thermal desorption) of the collected G-analogue from the sampling tube to a much smaller transfer tube containing the same sorbent, and the thermal desorption of the G-analogue from the transfer tube into a gas chromatograph equipped with a flame-photometric detector in the phosphorus-specific mode. The only other method with comparable sensitivity is the impinger/enzymatic method, which is much more susceptible to interferences from common organic solvents and from other organophosphorus nerve agents than the method given here.

EXPERIMENTAL

The sampling tubes and the transfer tubes were constructed and conditioned essentially as described previously[10]. However, the glass blank for the sampling tube was 90 mm × 8 mm O.D. × 6 mm I.D., and the transfer-tube blank was 175 mm × 3 mm O.D. × 1.7 mm I.D. Moreover, the tubes were packed with unweighed portions of 60–80-mesh Chromosorb 106 (Alltech, Deerfield, IL, U.S.A.) to form either a 2-cm-long bed (*ca.* 180 mg) or a 5-cm-long bed (*ca.* 450 mg) in the sampling tube and a 1.5-cm-long bed (*ca.* 10 mg) in the transfer tube. Sampling rates up to about 4 l/min could be attained with the 8-mm-O.D. sampling tube that was packed with 2 cm of sorbent, whereas the 5-cm sorbent bed in this tube permitted sampling rates only up to about 1.5 l/min.

The V-to-G conversion filters were fabricated in three steps: (1) preparation of a solution of silver fluoride, (2) deposition of solid silver fluoride onto a felt pad, and (3) assembly of the filter unit at the inlet end of the sampling tube.

The silver fluoride solution was prepared by dissolving 37.5 g of $AgNO_3$ (Alfa Products, Danvers, MA, U.S.A.; purity = 99.9 + %) in 40.0 ml of deionized water. In a separate container, 12.5 g of $KF \cdot 2H_2O$ (Alfa Products; purity not specified) was dissolved in 44.0 ml of deionized water. The silver nitrate solution was then slowly added to the potassium fluoride solution as the latter was stirred. The resulting mixture was turbid and was therefore filtered through Whatman No. 42 filter paper before proceeding. A 12.5-ml aliquot of absolute ethanol was added to the filtrate with stirring; this treatment produced a brown precipitate, which was left as a suspension in the mixture. The above steps were carried out entirely with the use of polyethylene vessels. Moreover, the mixture, which was sufficient for the production of about 240 conversion filters, was invariably used immediately after its preparation and was thus never stored prior to use.

The reagent mixture was absorbed into the felt (Fiber-Taxis, Bellingham, MA, U.S.A., Type PE-9080 non-woven polyester felt) by pouring the mixture into each of two shallow polyethylene trays and immersing a 15 × 13 cm rectangle of felt in the solution of each tray. After a 30-s soak period, the felt pieces were removed from the reagent mixture, squeezed gently on a polyethylene surface to remove excess solution, placed in dry polyethylene trays, and dried in a forced-air oven at 50°C for 6 h. It was found that best results were achieved when the above manipulations leading to the drying step were performed as rapidly as possible, preferably within 5 min. After the drying step, circular pads of the impregnated felt were punched from the material

with a 5/16-in.-diameter arch punch, and the pads were sealed in a polyethylene jar and stored in the dark until ready for use in air sampling. All handling of the reagent or impregnated felt, either before or after drying, was performed with the use of long forceps and/or protective rubber gloves to avoid skin contact with the reagent.

Just prior to the collection of a sample, a conversion pad was installed in a 5/16-in. polypropylene union (Cole-Parmer, Chicago, IL, U.S.A.; Part No. N-06381-20) as shown in Fig. 2. A back-up filter pad of unimpregnated felt was used just
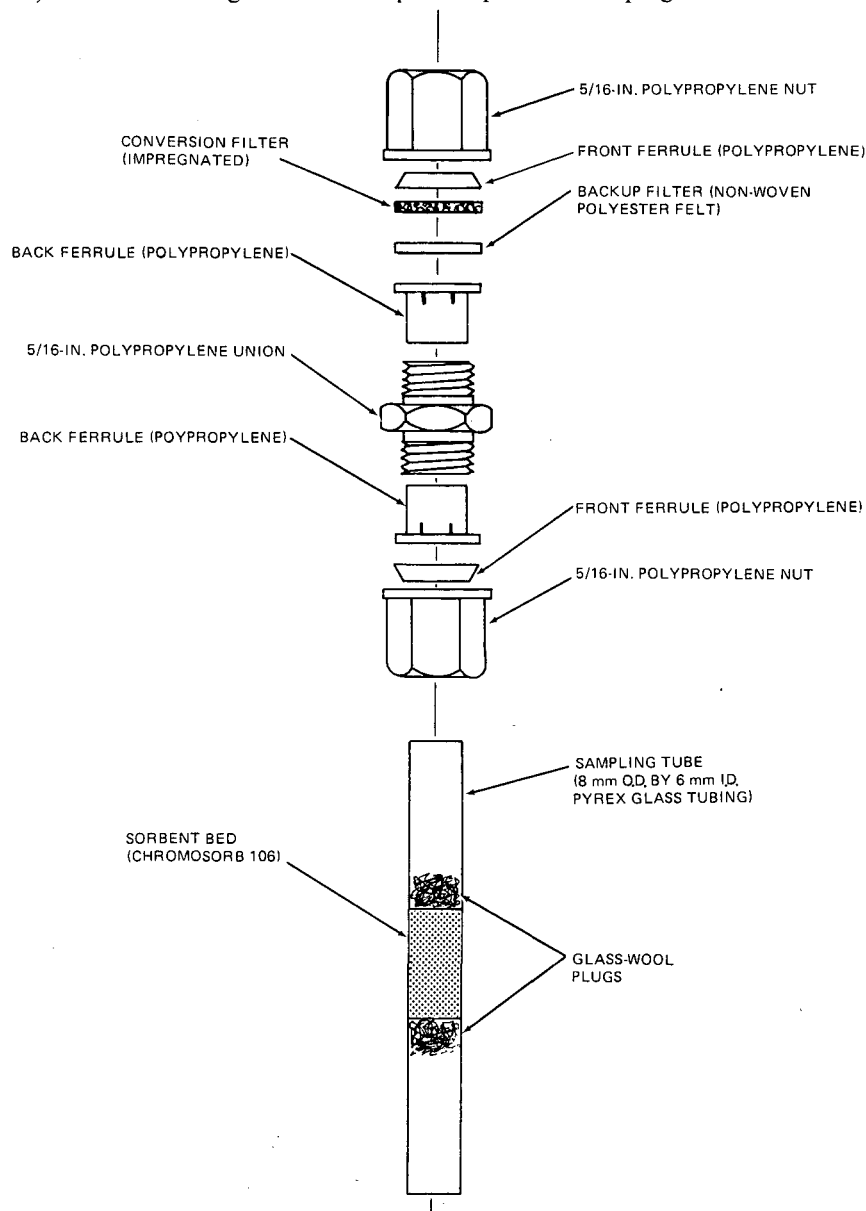
Fig. 2. Construction of the V-to-G conversion filter and attachment of the filter to the sampling tube.

beneath the impregnated pad to prevent loose particles of the solid silver fluoride reagent from being swept into the sampling tube. The union, with conversion pad installed, was then fitted onto the inlet end of a sampling tube (Fig. 2). In the apparatus of Fig. 2, the recess between the top of the uppermost polypropylene ferrule and the upper surface of the conversion pad (ca. 3–4 mm) was intended to be sufficient to prevent significant back-diffusion of spiked VX or G-analogue out of the device but not deep enough to allow substantial wall contact with incoming VX vapor during sampling.

The sampling tubes, the transfer tubes, and the V-to-G conversion filters are reusable, but their useful life depends on the conditions under which they are used. For example, chemically harsh gases (such as nitrogen dioxide, chlorine and ozone) and excessively high desorption temperatures will promote the deterioration of the Chromosorb 106 sorbent, and strong light will degrade the V-to-G conversion reagent. Although the vendor of the Chromosorb 106 recommends an upper temperature limit of 250°C, we have found that sorbent deterioration is rapid in this application at desorption temperatures above about 220°C.

Prior to the analysis step, the collected vapor samples were passed from the sampling tubes to the smaller transfer tubes by thermal desorption. This step was performed by first attaching the transfer tube to the sampling tube (after removal of the conversion filter) by means of a 5/16-to-1/8-in. stainless-steel Swagelok reducing union (Crawford, Solon, OH, U.S.A.) equipped with PTFE ferrules. Next, the free end of the transfer tube was connected to a vacuum sampling pump, which was switched on and adjusted to pump room air at 300 ml/min into the sampling tube and out through the transfer tube. With the pump running, the free end of the sampling tube was inserted into a 9-mm-I.D. hole bored through a small aluminum block that was maintained at 200°C. The sampling tube was kept inside the heated block for 2 min to ensure a quantitative desorption and transfer of G-analogue from the sampling tube to the transfer tube.

The G-analogue that accumulated in the 3-mm-O.D. transfer tube was desorbed thermally inside the hot injection port of a gas chromatograph the injection port of which had been modified in a manner similar to Method A of the previous publication[10]. Also described in this reference is the desorption procedure except that, in the current work, the transfer tube resided in the injection port for 15 s prior to the initiation of carrier gas flow. All desorptions, whether in the transfer step or in the analysis step, were carried out in the backflush direction. The GC instrumental conditions are summarized in Table I.

The instrumental response was calibrated by the spiking of sampling tubes with known amounts of VX, the thermal desorption of spiked VX (as its G-analogue) into the gas chromatograph, and the linear regression of response versus VX amount. The previously reported tube-spiking procedure[10] was used here except that the solvent used in preparing the standard solutions was cyclohexane rather than chloroform, as a matter of convenience. Additionally, the VX solution was deposited directly onto the V-to-G conversion pad, rather than onto the inner wall of the sampling tube, during the spiking procedure. The VX concentration ranges employed in calibrations were chosen to bracket the expected sample concentrations. The linear range of the instrument extended up to about 100 ng of VX per desorption.

Both VX and the G-analogue of VX in neat liquid form were supplied in several

TABLE I

GC INSTRUMENTAL CONDITIONS FOR DETERMINATIONS OF VX IN AIR

Instrument	Hewlett-Packard Model 5880A
Detector	Flame-photometric detector in the phosphorus-specific mode
Column	15 m × 0.53 mm I.D., DB-210 fused-silica capillary column with a 1.0-μm thick coating of the stationary phase
Chart speed	1.0 cm/min
Gas flows	
Carrier gas (He)	20 ml/min
Air	44 ml/min
Oxygen	20 ml/min
Hydrogen	80 ml/min
Temperatures	
Oven	60°C
Injection port	200°C
Detector	200°C

lots or batches by the U.S. Army. All batches were found to be in excess of 90% pure, and most were better than 95% pure, when assayed by GC with flame-ionization detection. Each working standard solution was prepared by serial dilution from a stock standard that had been prepared gravimetrically in a small volumetric flask. All solution concentrations were corrected for the less-than-100% purity of the starting materials. All reagents and solvent were of reagent grade except as otherwise noted.

Test atmospheres containing VX vapor were generated in an all-PTFE, diffusion-tube generator (constructed in-house) the output stream of which could be adjusted to any relative humidity and any temperature between room temperature and 50°C. In addition, NO_2 and SO_2 concentrations of (nominally) 0.01 ppm could be established when desired by bleeding in the respective gases from pressurized cylinders. (These gases were tested as potential sources of interference because they are known to be chemically aggressive substances.) The diffusion tube was about 14 cm long and 0.64 cm I.D.; its temperature was adjusted between 25 and 50°C to obtain VX vapor concentrations ranging from 3.9 to 51 ng/m³.

RESULTS AND DISCUSSION

Fig. 3 displays a chromatogram that resulted from spiking a sampling tube, through its attached V-to-G conversion filter, with 0.19 ng of VX and sampling outdoor air at 2 l/min for 50 min. Because the total air volume in this case was 100 l, this corresponded to the detection of VX in air at a concentration of 1.9 ng/m³ or about 0.18 ppt. Furthermore, as is evident from Fig. 3, even lower levels of VX could have been detected in this instance. The practical lower limit of detection may be expected to depend on the extent of interference from background constituents (atmospheric contaminants and sorbent degradation products) in most applications of the proposed method. Because the G-analogue response in Fig. 3 agreed closely with
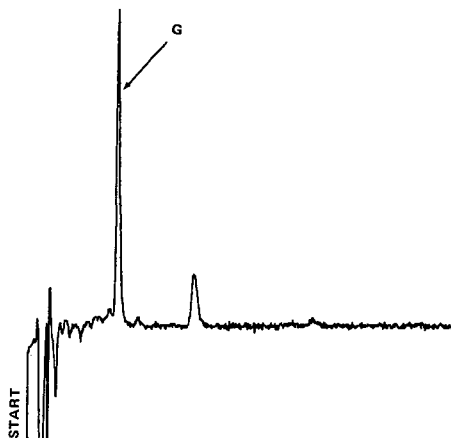
Fig. 3. Typical chromatogram obtained by spiking a sampling tube with 0.19 ng of VX, sampling air at 2 l/min for 50 min, and analyzing the tube for the G-analogue of VX. The retention time of the G-analogue (G) in this figure was 1.77 min.

the instrument-calibration responses for 0.19-ng VX spikes, a significant interference from coeluting background substances was unlikely.

The chromatogram of Fig. 3 reflects a loss of resolution that occurred as a result of the particular mode of thermal desorption that was employed in this study. Specifically, the G-analogue peak in this figure is approximately twice as wide as the G-analogue peak obtained by solution injection into the gas chromatograph under otherwise identical conditions. But this loss is still acceptable in many applications.

In a preliminary test of the proposed method, we sampled and determined VX vapor in the output stream from a VX vapor generator under various sets of conditions. In each test run under a given set of conditions, six replicate determinations of VX concentration were made. The first eleven test runs covered the VX concentration range from zero to 51 ng/m^3, as determined by the analytical method described in this paper. The last five runs were conducted at an essentially constant VX concentration (also as determined by the proposed method), which was about 12 ng/m^3. However, the generator output concentration appeared to be drifting, and it thus required an occasional minor adjustment between test runs. A gravimetric assay of the generator output concentration, based on measurement of the weight lost by the diffusion tube, was considered impractical because of the very small amount of weight lost by the tube during the course of these experiments. Because no suitable reference method was available for use in this work, no evaluation of method accuracy could be performed in this test. Except where noted otherwise below, sampling was conducted at 1.0 l/min for 2 h through sampling tubes containing 2 cm of sorbent.

The results of the test are given in Table II, where it can be seen that the relative standard deviations (R.S.D. values) of replicate determinations were less than 10% in all test runs. Moreover, no obvious effect due to relative humidity, temperature, NO$_2$, or SO$_2$ could be discerned.

As a further test of the method at lower effective VX concentrations, we spiked a set of five sampling tubes with different amounts of VX on each of four separate

TABLE II

RESULTS OF VX DETERMINATIONS IN SAMPLES COLLECTED FROM A VX-VAPOR GENERATOR

Run No.	Relative humidity (%)	Vapor temperature (°C)	Average found VX concentration (ng/m³)	R.S.D. (%)
1	<20	25	0	0
2	<20	25	3.9	3.8
3	<20	25	5.8	5.2
4	<20	25	9.2	4.0
5	<20	25	12	5.0
6	<20	25	13	4.6
7	<20	25	17	6.1
8	<20	25	23	2.1
9	<20	25	34	5.2
10	<20	25	51	5.7
11[a]	<20	25	10	8.4
12	<20	50	11	4.8
13	>80	25	14	6.7
14	>80	50	11	6.1
15[b]	<20	25	13	4.1
16[c]	<20	25	11	3.7

[a] In run No. 11, sampling was conducted at 0.20 l/min for 10 h.
[b] In run No. 15, the sampled VX vapor contained 0.009 ppm SO_2.
[c] In run No. 16, the sampled VX vapor contained 0.016 ppm NO_2.

days. The sampling tube used in this particular test contained Chromosorb 106 beds that were 5 cm, rather than 2 cm, in length. Because it was desired to test the capabilities of the method in the absence of atmospheric contaminants, each spiked sampling tube was fitted with a small charcoal filter at the inlet of the V-to-G conversion filter just prior to the initiation of air sampling to exclude airborne contaminants. Each day, the spiked tubes were allowed to sample outdoor air at 1.0 l/min for 24 h and were then promptly analyzed for VX. The VX spikes ranged in mass from zero (solvent only) to 0.96 ng each day, corresponding to VX concentrations ranging from zero to 0.67 ng/m³.

Table III displays the results of this test. In this table, the VX spike levels are expressed as the equivalent 'target concentrations', and the amounts of VX found by analysis of the various sampling tubes are similarly expressed as 'found concentrations'. The average found concentrations, the R.S.D. values of the found concentrations, and the average spike recoveries (expressed as percentages of the target concentrations) for the entire four-day period are also shown in Table III.

The R.S.D. values of Table III were clearly higher than those from the previous experiment (Table II), but even at these very low concentrations, they were still acceptable for applications not requiring high accuracy. Of course, the variability in spiking may have contributed significantly to the R.S.D. values of Table III but not to those of Table II. Note also that the found concentrations appeared to be positively biased at the low end of the concentration range and negatively biased elsewhere. But we observed this same behavior in similar tests involving other analytes and other

TABLE III

RESULTS OF THE DETERMINATION OF VX FROM SPIKED SAMPLING TUBES AFTER THE SAMPLING OF OUTDOOR AIR

Target VX concentration (ng/m^3)	Found VX concentration (ng/m^3)						Percent of target concentration
	Day 1	Day 2	Day 3	Day 4	Average	R.S.D. (%)	
0	0	0	0	0	0	0	100
0.084	0.11	0.096	0.075	0.075	0.087	17	104
0.17	0.16	0.16	0.12	0.14	0.14	13	85
0.33	0.29	0.32	0.25	0.29	0.29	10	88
0.67	0.50	0.63	0.52	0.58	0.56	11	83

solid sorbents. Although the source of the bias is currently unknown, its magnitude is acceptably small for many potential applications at these very low concentration levels, and its nature suggests that it was an experimental artifact rather than an inherent, unavoidable characteristic of the method.

In any event, it should be understood that the VX-recovery data of Table III merely approximate the true total accuracy of the method since these data reflect an unnatural error component (*i.e.*, that due to the error in spiking) and do not reflect a component due to the volumetric error in sampling.

The efficiency with which the V-to-G conversion filter converts VX to the G-analogue was also studied. The theoretical yield from the conversion of 1 ng of VX should be 0.47 ng of G-analogue. The actual yield from several replicate determinations was about 80% of this value, suggesting a conversion efficiency of 80%. But the response of the method to VX has been observed to be virtually constant under widely varying conditions (*e.g.*, Table II), suggesting that the conversion efficiency is largely unaffected by environmentally significant factors such as temperature and humidity.

The breakthrough volume of the G-analogue on Chromosorb 106 was not measured at room temperature becasue the data of Table III indicated little or no loss of G-analogue even after sampling 1440 l of air through sampling tubes containing 5-cm-long beds (*ca.* 450 mg) of Chromosorb 106. This implies a breakthrough volume of not less than 3.2 liters per milligram of Chromosorb 106, which is well above the limit on sample volume likely to be imposed by sample background concomitants that appear as extraneous peaks in the chromatograms. But when the sampling tube was maintained at 50°C, about 7% of a 1.8-ng VX spike was found, after conversion to the G-analogue, to have broken through a 2-cm-long (ca. 180-mg) bed of Chromosorb 106 (as the G-analogue) following the sampling of 160 l of air. This implies a breakthrough volume, at the 7% breakthrough level, of 0.89 l/mg at 50°C.

In the use of this method, it has been observed that the vapors from either liquid or solid chlorine/hypochlorite bleach will interfere with the method by producing a background constituent that coelutes with the G-analogue of VX. This constituent was identified by combined GC–mass spectrometry as *p*-dichlorobenzene, which is thought to arise from a reaction between Chromosorb 106 (a cross-linked polystyrene) and chlorine gas. In addition, the pesticide malathion appeared to undergo a reaction in the V-to-G conversion filter, yielding a phosphorus-containing product that eluted just before the G-analogue peak with a peak-to-peak retention time difference of 0.35 min between them. At a malathion concentration approaching that of VX, the peak overlap was significant.

However, the method reported here was found to be insusceptible to interference from milligram amounts of common organic solvents, *i.e.*, chloroform, methanol, ethanol, 2-propanol, *n*-hexane, cyclohexane, dichloromethane, 1,1,2-trichloro-1,2,2-trifluoroethane, acetone, ethyl acetate, formamide, carbon tetrachloride, benzene and toluene. Moreover, the reported chromatographic conditions were observed to successfully resolve the G-analogue peak from three other organophosphorus nerve agents —GA or tabun (ethyl N,N-dimethylphosphoramidocyanidate), GB or sarin (isopropyl methylphosphonofluoridate) and GD or soman (1,2,2-trimethylpropyl methylphosphonofluoridate). These represent distinct advantages for the method given here relative to the enzymatic method.

Because of the similarity of the G-analogue to the chemical agent GB, it is reasonable to expect that this method may be useful for simultaneous determinations of both GB and VX. Recent data have suggested that this is true, as GB has been found to pass through the V-to-G conversion filter efficiently, and the GB chromatographic peak is baseline-resolved from the G-analogue peak.

CONCLUSION

It was concluded that VX vapor can be determined with high sensitivity by converting it to a simpler compound (*i.e.,* the G-analogue of VX) during the sampling step, by trapping the G-analogue vapor on a Chromosorb 106 sampling tube, and by thermally desorbing the G-analogue into a gas chromatograph equipped with a flame-photometric detector. The accuracy and precision of the method were found to be adequate for many likely applications.

ACKNOWLEDGEMENTS

REFERENCES

1 E. V. Crabtree and E. W. Sarver, *Review of Analytical Procedures for GB, VX, and Their Degradation Products, EC-SP-76021,* Department of the Army, Aberdeen Proving Ground (EA), MD, January 1977.
2 S. J. Smith, *Talanta,* 30 (1983) 725.
3 U. Fritsche, *Anal. Chim. Acta.,* 118 (1980) 179.
4 H. O. Michel, E. C. Gordon and J. Epstein, *Environ. Sci. Technol.,* 7 (1973) 1045.
5 S. Sass and G. A. Parker, *J. Chromatogr.,* 189 (1980) 331.
6 S. Sass and T. L. Fisher, *Org. Mass Spectrom.,* 14 (1979) 257.
7 P. A. D'Agostino and L. R. Provost, *Biomed. Environ. Mass Spectrom.,* 13 (1986) 231.
8 P. A. D'Agostino, L. R. Provost and J. Visentini, *J. Chromatogr.,* 402 (1987) 221.
9 I. Lindgren and B. Jansson, *J. Chromatogr.,* 106 (1975) 385.
10 W. K. Fowler, C. H. Duffey and H. C. Miller, *Anal. Chem.,* 51 (1979) 2333.

MINIMIZING ADSORPTION OF PROTEINS ON FUSED SILICA IN CAPILLARY ZONE ELECTROPHORESIS BY THE ADDITION OF ALKALI METAL SALTS TO THE BUFFERS

JONATHAN S. GREEN[a] and JAMES W. JORGENSON*

Department of Chemistry, University of North Carolina, Chapel Hill, NC 27599-3290 (U.S.A.)

(First received July 18th, 1988; revised manuscript received May 8th, 1989)

SUMMARY

A method for minimizing the adsorption of proteins on fused-silica capillaries in capillary zone electrophoresis has been devised, involving the use of K^+ concentrations of 0.3 *M* and above in the operating buffer. The increased ionic strength results in a competition between K^+ and proteins for cation-exchange sites on the silica surface. The resulting increase in conductivity requires the use of lower voltages and capillaries of smaller diameter to allow adequate heat dissipation. With a voltage of 5 kV applied to a 50-cm capillary filled with a buffer of pH 9 containing 0.25 *M* potassium sulfate, a separation of five proteins was obtained. Two of these protein bands adsorbed irreversibly without added salt, but showed no apparent adsorption in the presence of 0.25 *M* potassium sulfate.

INTRODUCTION

Silica has been known for many years to possess cation-exchange properties[1]. These properties arise from the acidic nature of the silanol (Si–OH) groups, which make up a large proportion of the exposed surfaces of the silica. The groups are weakly acidic, leaving a negatively charged surface capable of ion exchange.

Proteins consist of numerous amino acids, many of which contain acidic or basic side-chains capable of giving substantial charge to a protein. Proteins can therefore be thought of as large "polyelectrolytes" which can ion exchange either as cations or as anions. Kopaciewicz *et al.*[2] showed that even at the isoelectric point (p*I*) of a protein it can still have regions of localized positive or negative charge. The proteins can orient themselves such that these regions of charge can make a close approach to an ion exchanger. It is not surprising, therefore, to find that proteins adsorb strongly on siliceous materials.

As early as 1954, Holt and Bowcott[3], studying the reactions of soluble silicic acid with proteins and heptadecylamine, suggested the formation of an ionic band between the basic amine functionality on the proteins and the silanoate (Si–O⁻) on the silicic

---

[a] Present address: E.I. DuPont de Nemours and Company, Medical Research Division, Biomedical Products Department, Experimental Station, Wilmington, DE 19898, U.S.A.

acid. In 1967, Weldes[4] atributed the interactions between proteins and alkali metal silicates with hydrogen bonding. Hydrogen bonding alone, however, cannot adequately explain the adsorption, as proteins fail to desorb from the silicates in the presence of high concentrations of urea[5], a reagent that generally disrupts hydrogen bonds. Messing[5] proposed a combination of the two mechanisms, on the basis that desorption of the protein with urea alone does not work, but that a mixture of urea and either dilute or concentrated acid results in nearly quantitative desorption. Messing[5] suggested that the urea breaks hydrogen bonds while the acid protonates the silanoates. Morrisey and Stromberg[6] suggested a hydrogen bonding interaction between the carbonyls in the proteins and the silica surface, although they failed to explain how this takes place at higher pH where the silica is highly ionized. Hiatt et al.[7] also proposed a hydrogen bonding interaction when they found a rabies virus with a net negative charge adsorbed on silica. Voegel et al.[8], and many others, simply refer to adsorption in a generic way without offering any proposed mechanism. Regardless of the exact mechanism(s) involved, much effort has been spent on attempts to deactivate silica to make it non-adsorptive toward proteins.

Initially, the need for surface deactivation in the liquid chromatography (LC) of biological macromolecules was circumvented by the use of carbohydrate-based supports and stationary phases. The principal advantage of these is their substantial hydrophilicity and the resulting lack of denaturation of the proteins. However, carbohydrate matrices are not well matched with current high-pressure LC systems, as they have poor mechanical stability and compress or collapse under typical operating pressures. Silica provides an abundant, easy to manufacture alternative as a support, but suffers from high adsorptivity toward many solutes.

Regnier and Noel[9] were among the first to formulate an acctable alternative in the form of a "carbohydrate" [3-(glycidoxypropyl)trimethoxysilane; GPTS] bonded to a controlled porosity glass (CPG) support. Chang et al.[10] used the GPTS as an intermediate coupling agent to which they bonded various ion-exchange, hydrophobic and hydrophilic groups, making a wide range of CPG-based packings. Since that time, many researchers have continued to pursue improvements in CPG- and silica-based packing materials for protein analyses[11], striving for biocompatability (no denaturation) and high recovery.

Our research has centred on the capillary zone electrophoresis (CZE) of proteins and peptides in glass and fused-silica capillaries. Short peptides, because of their limited number of charged groups, tend to migrate electrophoretically without significant adsorption. Proteins, however, possess so many ionic sites that adsorption to the capillary wall becomes significant. Walbroehl[12] predicted that capacity factors (k') as small as 0.05 are sufficient to reduce plate numbers for proteins 20-fold, making it a necessity that steps be taken to eliminate adsorption. The "glycophase" used by Regnier and Noel[9] has worked to some extent[13], but the efficiencies are still lower than predicted by theory, suggesting that some adsorptive sites might remain. Additional problems with the glycophase are the time required for column deactivation (several hours) and the limited lifetime of the deactivated surface (several days). An ideal solution would be one that required no pretreatment at all.

In traditional forms of ion-exchange chromatography, retained compounds can be eluted by increasing the ionic strength of the mobile phase. Following this line of reasoning, and assuming that Holt and Bowcott[3] were correct in their assertion of

ionic interaction-based adsorption, it should be possible to prevent adsorption in CZE by operating in buffers with high ionic strength. It is difficult to look at the effects of ionic strength in an electrophoretic system because of the number of possible complications and interferences which can confound data interpretation. During CZE, zone broadening and peak asymmetry can be caused by such things as sample concentration overloading[14] and the thermal effects arising from the joule heating that occurs in electrophoretic systems. This paper examines the effects of alkali metal chlorides on protein adsorption in fused-silica capillaries, using a "chromatographic" approach. In this way, the effectiveness of the salts can be examined in a straight-forward manner without complications from electrophoretic effects.

EXPERIMENTAL

Columns

Bare fused silica (50 cm × 75 μm I.D.) (Polymicro Technologies, Phoenix, AZ, U.S.A.) was used for all chromatographic runs, and bare fused silica (50 cm × 25 μm I.D.) (Scientific Glass Engineering, Austin, TX, U.S.A.) was used for electrophoresis. All columns were pretreated with 1 *M* KOH for 20 min, followed by 45-min rinses with each of 0.1 *M* KOH and water, using the method described by Lauer and McManigill[15]. In addition, the column was rinsed for 10 min with 0.1 *M* KOH, followed by 10 min with water and then 10 min with buffer after each series of injections. If protein adsorbed during a run, the column was rinsed for 5 min with 0.1 *M* KOH, followed by 5 min with water and then 5 min with buffer. This procedure will remove any adsorbed protein and provide a fresh surface for each subsequent injection.

Detection

A variable-wavelength ultraviolet absorption detector constructed in this laboratory was used. It includes a 30-W deuterium lamp (Hamamatsu, Middlesex, NJ, U.S.A.) as a source and an Instruments SA (Metuchen, NJ, U.S.A.) concave holographic grating monochromator to select the wavelength of interest. The wavelength for this work was 193 nm, corresponding to the peak UV absorption of proteins. Light was detected in the signal and reference paths by two end-on photomultiplier tubes (R759, Hamamatsu), connected to current amplifiers and to an IBM-PC computer for data acquisition and manipulation. Further details of the detector design will be published elsewhere.

Electrophoretic and chromatographic apparatus

The basic electrophoretic apparatus has been described in detail elsewhere[16]. The high-voltage power supply (RHR30PN30/RVC10, Spellman High-Voltage Electronics, Plainview, NY, U.S.A.) is capable of delivering up to ±30 kV. Electrophoretic injections were carried out by the electromigration technique described previously[16]. Electrophoresis was done at +5 kV. The chromatographic system was set up in a gravity-driven flow mode by placing the inlet buffer reservoir 23 cm higher than the outlet. Chromatographic injections were made by lowering the inlet buffer reservoir to the level of the outlet reservoir, replacing it with a sample vial, and raising the vial 23 cm for 5 s. The vial was then lowered to the height of the outlet

reservoir and replaced with the buffer reservoir, then raised back up 23 cm. Data acquisition was begun at this point.

Reagents

The buffer for chromatography and electrophoresis was 0.1 M 2-[N-cyclo-hexylamino]ethanesulfonic acid (CHES) (Sigma, St. Louis, MO, U.S.A.) of pH 9.0, containing varying amounts of KCl (J. T. Baker, Phillipsburg, PA, U.S.A.), NaCl (EM Science, Cherry Hill, NJ, U.S.A.), LiCl (Baker and Adamson, Morristown, NJ, U.S.A.) and CsCl (Aldrich, Milwaukee, WI, U.S.A.). All proteins were purchased from Sigma and were used as received. Additional salts used for comparison in absorbance studies were K_2SO_4 (Baker and Adamson), KNO_3 (Fisher Scientific, Fair Lawn, NJ, U.S.A.) and KBr (Harshaw Chemical, Solon, OH, U.S.A.).

RESULTS AND DISCUSSION

In order to determine the extent of adsorption and describe it in quantitative terms, k' (column capacity factor) was chosen as the best means of expressing the data:

$$k' = (t_R - t_m)/t_m \tag{1}$$

where t_R is the "retention time" of the protein (lysozyme) and t_m is the dead time as defined by elution of a neutral marker (acetone). The choices of a probe protein and a buffer system are important if one is to gain useful information from this study. It is necessary to select a protein that will adsorb under typical operating conditions, but should not adsorb so badly that drastic measures must be taken to reduce its adsorption. Lauer and McManigill[15] have shown that adsorption can be reduced by selecting a buffer pH that is above the isoelectric points (pI) of all proteins in solution. In such a system, the proteins have a net negative charge and are repelled from the negatively charged silica surface. If their idea is kept in mind, one can select a buffer pH that is far enough removed from the pI of lysozyme that it does not have an overall negative charge, but close enough to the pI that the number of adsorptive sites on the protein is reduced. CHES buffer, with a pH of 9.0, is only 2 pH units below the pI of lysozyme (11.0), so it satisfies the above requirements. Hence, the system selected for this study was lysozyme in 0.1 M CHES buffer.

As the chromatographic peaks in this system are broad, determination of minute changes in k' values would be impossible if the dead-time marker and protein were co-injected. It is important to measure minute changes in k', as Walbroehl[12] has predicted that k' values as small as 0.05 can reduce the efficiency of the electrophoresis of proteins 20-fold. Therefore, the data were collected by first injecting acetone dissolved in the buffer of interest, calculating the first statistical moment of the peak and calling that the "dead time", then injecting lysozyme and measuring its "retention time". This was repeated three times for each salt concentration. In an attempt to randomize any effects of the order in which salts were examined or the order of concentrations of salt, three sets of triplicate data were collected, alternately changing the order of salts and order of concentrations. The result was a total of nine pieces of data for each concentration of each salt. Following the nine sets of injections, a k' value was calculated using a statistical treatment outlined by Skoog and West[17]. Table

TABLE I

CAPACITY FACTORS AND ABSOLUTE STANDARD DEVIATIONS FOR 0.2% LYSOZYME RUN CHROMATOGRAPHICALLY IN 0.1 M CHES BUFFER OF pH 9.0

Each data value is the mean of nine trials.

Salt concentration (M)	Capacity factor (k')			
	LiCl	NaCl	KCl	CsCl
0.1	$-^a$	0.35 ± 0.13	0.49 ± 0.06	0.39 ± 0.11
0.3	0.10 ± 0.02	0.04 ± 0.03	0.02 ± 0.02	0.03 ± 0.02
1.0	0.00 ± 0.02	0.00 ± 0.03	-0.003 ± 0.007	0.00 ± 0.04

^{a} k' unmeasurable owing to irreversible adsorption.

I shows the k' values and their standard deviations for 0.2% lysozyme run in the four salts at three different concentrations. The negative k' value is an artifact of the lack of co-injection; occasionally, the dead-time marker had a slightly longer "retention time" than the solute when the two were injected separately. However, the negative value was smaller than its associated uncertainty.

There are considerable uncertainties associated with most of the data in Table I. Much of this is likely to arise from the dynamic nature of the capillary surface; between two sets of data, new silanols have formed as siloxane bonds have been hydrolysed. As stated earlier, the order in which data were collected was randomized, so that any effects of the progressive surface changes could be minimized.

In spite of the uncertainties in the data, there are some trends that are worthy of note. All four of the salts examined performed an equivalent job of preventing adsorption at a concentration of 1.0 M. At a concentration of 0.3 M, some differences begin to emerge. LiCl was the worst at preventing adsorption, giving a k' for lysozyme approximately three times higher than those given by the other salts. All of the other salts yield k' values that are significant but are approximately equal to each other. At a concentration of 0.1 M, K$^+$, Na$^+$ and Cs$^+$ all had high levels of adsorption, but it was not so severe as to be irreversible. Li$^+$, however, at 0.1 M concentration was so ineffective at minimizing adsorption that a solute peak was never observed. Li$^+$ is the most highly hydrated of these ions and, with its sphere of hydration included, it is effectively the largest in the alkali metal series. As the largest alkali metal ion, it is the most weakly bound. The expected order of effectiveness of the four salts is therefore Cs$^+$ > K$^+$ > Na$^+$ > Li$^+$. As Li$^+$ is clearly inferior and Cs$^+$ suffers from unacceptably high optical absorbance at short wavelengths, these two ions were eliminated. K$^+$ and Na$^+$ were essentially equal in their effectiveness, and K$^+$ was arbitrarily chosen for further studies.

Gooding and Schmuck[18] have shown that the choice of buffer anion in cation-exchange chromatography plays some role in solute retention. Hence it would seem logical to expect some type of effect in this study. A series of potassium salts were selected as buffer additives to investigate the effects of the anion chosen on solute retention. The four salts, KCl, KNO$_3$, KBr and K$_2$SO$_4$, all yielded equivalent k' values at potassium concentrations of 1.0, 0.3 and 0.1 M (0.5, 0.15 and 0.05 M in K$_2$SO$_4$), suggesting that in this system the anion does not have a measurable effect. The four salts, however, had widely varying optical absorbances (see Table II). KBr and KNO$_3$

TABLE II

ABSORBANCE OF 0.1 M POTASSIUM SALTS AT 193 nm IN WATER VS. WATER DRAWN THROUGH A 75-μm I.D. COLUMN

Salt	Absorbance	Salt	Absorbance
K_2SO_4	0.0178	KBr	6.36
KCl	0.1343	KNO_3	4.76

had absorbances more than two orders of magnitude higher than K_2SO_4. With such high absorbances, it was actually necessary to dilute these two salt solutions 100-fold and then to extrapolate back to the values reported in Table II. The extremely high absorbances result in stray light becoming a significant proportion of the remaining photocurrent, thereby pushing the detector into a region of poor linearity. Clearly, K_2SO_4 is far superior in transparency to the other salts which were examined. Given this fact, and the fact that there is no apparent difference in the abilities of the various potassium salts to prevent adsorption, it appears that K_2SO_4, at a concentration between 0.15 and 0.5 M (0.3–1.0 M in K^+), is the salt of choice for further work.

Capillary zone electrophoresis requires the use of high voltages, passing current through the buffer medium which fills the capillary tube, and generating joule heat which must be dissipated at the capillary walls. Using a typical capillary of I.D. 75 μm and a typical operating voltage of 20 kV, a buffer containing 0.3 M K^+ would pass current and generate heat well in excess of that which the system can tolerate. Three approaches can be taken to minimize the effects of the heat. The applied voltage can be lowered, but simple theory predicts that separation efficiency is directly proportional to applied voltage and analysis times are inversely proportional to applied voltage[19]. Consequently, lowering the voltage will probably lower the peak efficiencies and increase the analysis times. The column length can be increased, providing greater electrical resistance and thus lower joule heat, in addition to providing a greater surface area for heat dissipation. However, analysis times are proportional to the square of the column length, so this approach would result in significantly longer analysis times. Another approach is to reduce the inner diameter of the capillary, thereby increasing the surface area-to-volume ratio and improving the heat dissipating ability of the capillary. The problem with this approach is that it significantly shortens the path length of the on-column UV absorption detector, making detection of the zones more difficult. The only way to compensate for this is to increase the sample concentration or improve detection limits. In capillary electrophoresis it is necessary to keep the sample concentration approximately 100 times lower than the buffer and salt concentrations in order to prevent sample overloading[14], so care must be taken to avoid increasing the sample concentration too much. Fortunately, the increased ionic strength allows the use of increased sample concentrations.

Fig. 1 shows an electropherogram of a mixture of five proteins [1% (w/v) each] in 0.1 M CHES buffer (pH 9.0) containing 0.25 M K_2SO_4 and 0.001 M EDTA. The first two components are lysozyme and trypsinogen, both of which ordinarily show significant adsorption in a pH 9.0 buffer which does not contain any additional salt. As their isoelectric points are 11 and 9.3, respectively, both of these proteins still contain significant regions of positive charge at pH 9.0, making them likely to adsorb strongly
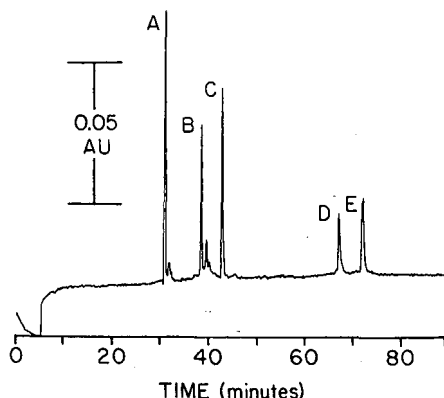
Fig. 1. Zone electrophoretic separation of five proteins on a 100 cm × 25 μm I.D. bare fused-silica column. (A) Hen-egg lysozyme, $N = 68\,000$; (B) bovine pancreatic trypsinogen, $N = 140\,000$; (C) horse heart myoglobin, $N = 78\,000$; (D) bovine milk β-lactoglobulin B, $N = 95\,000$; (E) bovine milk β-lactoglobulin A, $N = 95\,000$. The concentration of each protein is 1% (w/v) in 0.1 M CHES buffer containing 0.25 M K$_2$SO$_4$ and 1 mM EDTA at pH 9.0. Injection was for 3 s at 5 kV; electrophoresis at 5 kV. UV detection at 193 nm. The electropherogram was subjected to a nine-point Savitzky–Golay smoothing three consecutive times. (Reprinted with permission from ref. 20.)

on the capillary wall. Neither of them shows any evidence of serious adsorption in the presence of K$_2$SO$_4$. One advantage of this approach to the prevention of adsorption lies in the fact that no initial surface treatment was required, and no conditions that might be unfavourable for the column or proteins were required. The obvious drawbacks are the relatively long analysis time and the inordinately high protein concentrations in the original sample. Both problems could be solved with more sensitive detection, as a better detector would allow the use of even smaller diameter capillaries, allowing the application of higher voltages, and/or lower concentrations of protein, minimizing the likelihood of sample concentration overloading.

ACKNOWLEDGEMENTS

REFERENCES

1 K. K. Unger, *Porous Silica. Its Properties and Use as Support in Column Liquid Chromatography*, Elsevier, Amsterdam, 1977, p. 130.
2 W. Kopaciewicz, M. A. Rounds, J. Fausnaugh and F. E. Regnier, *J. Chromatogr.*, 266 (1983) 3.
3 P. Holt and J. Bowcott, *Biochem. J.*, 57 (1954) 471.
4 H. Weldes, *Adhes. Age*, 10 (1967) 32.
5 R. A. Messing, *J. Am. Chem. Soc.*, 91:9 (1969) 2370.
6 B. W. Morrissey and R. R. Stromberg, *J. Colloid Interface Sci.*, 46 (1974) 152.
7 C. W. Hiatt, A. Shelokov, E. J. Rosenthal and J. M. Galimore, *J. Chromatogr.*, 56 (1971) 362.
8 J. C. Voegel, N. De Baillou, J. Sturm and A. Schmitt, *Colloids Surf.*, 10 (1984) 9.
9 F. E. Regnier and R. Noel, *J. Chromatogr. Sci.*, 14 (1976) 316.
10 S. H. Chang, K. M. Gooding and F. E. Regnier, *J. Chromatogr.*, 120 (1976) 321.

11 K. K. Unger, B. Anspach and H. Giesche, *J. Pharm. Biomed. Anal.*, 2 (1984) 139.
12 Y. Walbroehl, *Ph. D. Dissertation*, University of North Carolina, 1986.
13 Y. Walbroehl and J. W. Jorgenson, *J. Chromatogr.*, 315 (1984) 135.
14 J. W. Jorgenson and K. D. Lukacs, *Clin. Chem.*, 27 (1981) 1551.
15 H. H. Lauer and D. McManigill, *Anal. Chem.*, 58 (1986) 166.
16 J. W. Jorgenson and K. D. Lukacs, *Science (Washington, D.C.)*, 222 (1983) 266.
17 D. A. Skoog and D. M. West, *Fundamentals of Analytical Chemistry*, Holt, Rinehart & Winston, New York, 3rd ed., 1976, p. 74.
18 K. M. Gooding and M. N. Schmuck, *J. Chromatogr.*, 266 (1983) 633.
19 J. W. Jorgenson and K. D. Lukacs, *Anal. Chem.*, 53 (1981) 1298.
20 H. H. Lauer and D. McManigill, *Trends Anal. Chem.*, 5 (1986) 11.

BAND BROADENING IN HIGH-PERFORMANCE LIQUID CHROMATOGRAPHIC SEPARATIONS OF ENANTIOMERS WITH SWOLLEN MICROCRYSTALLINE CELLULOSE TRIACETATE PACKINGS

I. INFLUENCE OF CAPACITY FACTOR, ANALYTE STRUCTURE, FLOW VELOCITY AND COLUMN LOADING

ANDREAS M. RIZZI

Institute of Analytical Chemistry, University of Vienna, Währingerstrasse 38, A-1090 Vienna (Austria)
(First received February 20th, 1989; revised manuscript received April 27th, 1989)

SUMMARY

The peak dispersion in high-performance liquid chromatographic columns packed with swollen crystalline cellulose triacetate was investigated as a function of the capacity factors of the analytes and their structures as well as of the flow-rate, column loading and degree of cross-linking of the adsorbent material. The main contribution to the plate height is attributed to the packed bed, arising from slow adsorption/desorption processes at certain, narrow parts of the surface. The results show the existence of at least two types of adsorption sites, which differ in the rate of the adsorption/desorption process: "quick"-type and "slow"-type sites. These types of sites are assumed to differ also in the types of interactions with the analytes. The narrow, "slow"-type sites are of decisive importance for chiral recognition.

INTRODUCTION

Triacetylated cellulose has been known for several years as a useful stationary phase for the chromatographic separation of optical isomers[1–16]. Nowadays, two different forms of cellulose triacetate (CTA) ar used in chromatography. First, CTA is used directly in a swollen crystalline state, called swollen microcrystalline cellulose triacetate (swcrCTA). This material is obtained by heterogeneous acetylation of microcrystalline cellulose and subsequent swelling in boiling alcohol, *e.g.*, ethanol[1,2,3,8]. It is assumed to form some type of "inclusion complexes" with several types of analytes[1,2]. The strength of the interaction, and therefore the retention on the stationary phase, is determined by the fit of the analyte to the chiral "cavities" of the swollen microcrystalline stationary phase. The geometric arrangement of the chiral environment in the "cavities" is determined by the microcrystalline structure of this material.

The second method of using CTA stationary phases is to coat the solved CTA material onto the surface of macroporous silica particles[14,17,18]. The silica particles

may be modified by chemically bonded aminopropyl or other groups. Solved and reprecipitated CTA loses its microcrystalline structure. The chiral recognition and discrimination properties of solved and reprecipitated CTA are quite different from those of the microcrystalline form[11,14].

Both materials are commercially available in a pressure-stable form, suitable for high-performance liquid chromatography (HPLC). swcrCTA particles are available with diameters down to 7–10 μm (refs. 3, 5 and 6) and can be used at pressures above 200 atm. These particle sizes are comparable with those of usual silica particles. Silica coated CTA materials are available in the particle sizes of ground silica and are highly pressure-stable due to the silica backbone.

CTA materials are widely utilized for chromatographic separations of enantiomers on the analytical and preparative scales[1–8,13]. The advantages of swcrCTA materials are the high enantioselectivity which can be obtained for many chiral analytes of different structural types and the high loadability[1,5]. A severe drawback is the large peak broadening often observed with these separations which leads to a low efficiency. In spite of the given enantioselectivity, in many cases there is insufficient chromatographic resolution, reduced detection limits by high dilution and a reduced peak capacity of the columns.

The enantioselectivity values obtained with coated CTA materials differ from those obtained with swollen crystalline materials. The former are smaller in many cases[14]. There is much less peak broadening with coated materials, however[14,17,18].

The problem of peak broadening on swollen crystalline CTA supports has briefly been stressed[1,2,5,8,16]. However, no systematic investigations have been described which deal with the dependence of the peak width on swcrCTA packings on the capacity factors of the analytes, the analyte structure, the eluent composition, the temperature and the pressure. In this paper, quantitative data are reported on the dependence of the theoretical plate height on the capacity factors of the analytes and on their structures, as well as on the flow-rate, the column loading and on the degree of cross-linking of the CTA material. The dependence on the eluent composition, the temperature and the pressure forms the subject of another paper[19].

THEORETICAL

In the last decade the theory of band spreading in chromatography has reached a level which allows one to understand and to predict with fair accuracy the peak broadening behaviour of analytes in normal and reversed-phase chromatography. The theory describes the dependence of the degree of peak broadening on parameters like the particle size, diffusion coefficient, solvent viscosity, temperature, flow velocity, capacity factor and the quality of packing (geometric arrangement of the particles in the packed bed)[20–25]. Today, it is clear that the plate height, H_i, results from at least four contributions, H_{di}, H_{ci}, H_{fi} and H_{bi} (refs. 20–22, 24, 26 and 27) which have different dependences on the flow velocity, u, the particle size, d_p, and the capacity factor, κ_i:

$$H_i = H_{di} + H_{ci} + H_{fi} + H_{bi} \qquad (1)$$

The index i indicates the solute and the subscripts d, c, f and b indicate the

)

contributions associated with dispersion due to axial diffusion, convection, mass exchange in the streaming part of the mobile phase and mass exchange in the fixed bed. H_b includes diffusion in the stagnant mobile phase, in the stationary phase and at the surface.

The following discussion of the band spreading process in swcrCTA packings starts from the plate-height equation given by Huber[22]

$$h_i = \frac{\varphi_d}{v_i} + \frac{\varphi'_c}{1 + \varphi''_c v_i^{-\frac{1}{2}}} + \varphi_f v_i^{\frac{1}{2}} \left(\frac{\kappa_i^*}{1 + \kappa_i^*}\right)^2 + \varphi_b v_i \cdot \frac{\kappa_i^*}{(1 + \kappa_i^*)^2} \tag{2}$$

where h_i is the reduced plate height and v_i is the reduced flow velocity

$$h_i = H_i/d_p \tag{3a}$$

$$v_i = u \cdot \frac{\varepsilon_m}{\varepsilon_f} \cdot d_p/D_{mi} \tag{3b}$$

where u is the linear flow velocity of the mobile phase, D_{mi} is the diffusion coefficient of the solute in the mobile phase, ε_m is the fraction of the column volume occupied by the mobile phase and ε_f is the fraction occupied by the flowing part of the mobile phase. The five geometry factors, φ_d, φ'_c, φ''_c, φ_f and φ_b, are constants for a given column depending on the geometry of the particles and the packing. The parameter κ_i^* is defined as the mass distribution coefficient between the fixed bed, b, and the flowing fluid, f

$$\kappa_i^* = \frac{Q_i^{(b)}}{Q_i^{(f)}} = \frac{\varepsilon_m}{\varepsilon_f}(\kappa_i + 1) - 1 \tag{4}$$

where κ_i is the mass distribution coefficient (capacity factor) between the stationary phase, s, and the mobile phase, m, and Q being the symbol for quantity.

It should be noted that h_f and h_b have different dependences on the capacity factor. Whereas $\left(\frac{\kappa_i^*}{1 + \kappa_i^*}\right)^2$ is an increasing function with increasing capacity factor, κ_i, $\frac{\kappa_i^*}{(1 + \kappa_i^*)^2}$ is a decreasing function with increasing κ_i^* values greater than one. Eqn. 2 describes experimental data on silica-based reversed-phase and normal-phase systems quite well[26–28].

This theoretical approach is, however, incapable of describing the effects actually observed with swcrCTA packing materials. Therefore eqn. 2 has to be extended. The measurements on swcrCTA, which are presented in detail later, reveal for many analytes dramatically elevated reduced plate heights. These plate heights are not correlated with the capacity factors of the analytes, but rather with their steric structures. This indicates that it is the mass exchange term in the chromatographic bed, h_b, which is essentially the main source of the increase in the plate height.

It is assumed that in the porous swollen crystalline packing material the motion of the analytes very near to narrow parts of the adsorbent is hindered. These narrow

parts may be of "cavity"-like or channel-like structure, or can be more generally described as adsorption sites where the adsorption/desorption process including the diffusion to these sites and the optimum positioning at these sites is slow.

For the following discussion it is assumed that the slow transport processes in the packed bed can be taken into account by splitting h_b into two contributions, h_b^{quick} and h_b^{slow}

$$h_b = h_b^{quick} + h_b^{slow} \tag{5}$$

where h_b^{quick} is assumed to be the h_b contribution observed normally, typical for small analytes not sterically hindered in their diffusion and motion near the surface or in narrow channels. It thus accounts mainly for the mass transport in the stagnant mobile phase in the large pores of the particles and is described by the term $\varphi_b v_i \cdot \dfrac{\kappa_i^*}{(1 + \kappa_i^*)^2}$ in eqn. 2; its value is expected to be small, as is found usually with porous silica particles[26-29]. The parameter h_b^{slow} is an additional contribution accounting for the slow transport and adsorption/desorption process near to or at some of the available adsorption sites. These sites, at which the entire process of adsorption/desorption is slow, are referred to as "slow"-type sites. (Since these sites are assumed to be narrow they are assumed to be decisive for chiral recognition in many cases.) The value of h_b^{slow} for a particular analyte can be regarded approximately as the difference between its measured h value and that of a small, not sterically hindered molecule, e.g., toluene.

In discussing the dependences of the reduced plate height on the capacity factor, κ_i, the temperature, T, the availability of the different types of adsorption sites (which is determined by the eluent composition) and on the flow velocity, u, in this and in the subsequent publication[19], respectively, it should be kept in mind that h_d, h_c, h_f and h_b^{quick} are also influenced by these parameters. However, the effects on these plate height contributions will be much smaller compared with that on h_b^{slow} and are therefore not always seen to have statistical significance within the precision of the data.

The influence of the particle size is not investigated here. Since h_b^{slow} is assumed to result predominantly from slow adsorption/desorption processes at the sites, and do not result from a slow diffusion velocity in the whole stagnant zone, the dependence of h_b^{slow} on d_p will probably differ from that of h_b^{quick}, which is known to be linearly dependent on d_p (see last term in eqn. 2; v is linearly dependent on d_p, therefore h_b^{quick} is also linearly dependent on d_p).

EXPERIMENTAL

Apparatus

Chromatographic experiments were carried out using an high-pressure liquid chromatographic pump (Model L-6200 intelligent pump; Merck-Hitachi, Tokyo, Japan), a syringe-valve injector (Model 7161; Rheodyne, Cotati, CA, U.S.A.) equipped with a 20-μl loop, a column oven (Model 655A-52, Merck-Hitachi) and an UV detector (Model L-4000, Merck-Hitachi) connected to an integrator (Model D-2000 chromato-integrator, Merck-Hitachi).

Columns

If not explicitly indicated otherwise, the data reported in the tables and figures refer to column I, prepacked with swcrCTA having a mean particle diameter of 10 μm (Hibar®, E. Merck, Darmstadt, F.R.G.), 250 mm × 10 mm I.D. Column II was prepacked with swcrCTA material of probably enhanced degree of cross-linking, mean particle diameter 7 μm (Macherey Nagel, Düren, F.R.G.), 250 mm × 4 mm I.D.

Reagents and samples

Absolute ethanol was of p.a. quality, methanol and cyclohexane of LiChrosolv® quality from E. Merck. Water used for the eluent preparation was distilled twice and purified by passing through a RP-8 column before eluent preparation. The eluent mixtures were premixed and degassed in an ultrasonic bath. The analyte samples were of the highest purity grade available or were received in a highly purified state as gifts from synthesis laboratories.

Procedure

All data refer to isocratic elution at constant temperature. After establishment of the thermal equilibrium, the constancy of retention data was about ± 1%. The void volume for the 250 mm × 10 mm I.D. column was estimated as 15 ml from the retention volume of the system peaks of water, methanol or propanol injected. All the calculations of the capacity factors are based on a void volume of 15.00 ml for all solvent mixtures. UV detection was performed at 254 nm.

RESULTS AND DISCUSSION

The porous structure of the packed bed

Crystalline CTA in the swollen state has a certain porosity. A system of macropores and micropores exists in the particles. Within the microporous system, narrow structured channels and cavities are expected. This results in a size exclusion mechanism for small molecules together with an adsorption mechanism. The porosity of this material is therefore different for different analytes.

The results of the determination of the porosity depend on the type of molecules used for the measurement. Using solvent components, the porosity will be higher the smaller are these solvent molecules. In the case of cyclohexane, it is likely in addition that the available pore volume is determined not only by the size of this molecule but also by its hydrophobicity, since cyclohexane does not penetrate the near vicinity of polar adsorption sites. This is illustrated in Table I, where the column porosity values, ε_m, are evaluated from the system peaks of solvents injected in a mobile phase of ethanol. The usually accepted substance for evaluation of V_0, tri-*tert*.-butylbenzene, is partially excluded from the pores available to methanol and water.

This discussion makes clear that a defined particle porosity cannot be given, because this obviously depends on the analyte (and even the solvent) structure. To avoid uncertainties in the calculation of the capacity factors, in this paper an uniform value of 0.76 is chosen for the column porosity, ε_m.

Plate height as a function of the capacity factor

In Fig. 1 and Table II the reduced plate height, *h*, is given as a function of the

TABLE I

COLUMN POROSITY, ε_m, FOR VARIOUS SOLVENT COMPONENTS

Eluent: ethanol–water (96:4, v/v). Temperature: 50°C. V_{column} = 19.635 ml.

V_0 marker	V_0 (ml)	ε_m
Water	15.0	0.76
Methanol	14.5	0.73
Ethanol	14.0	0.71
1-Propanol	12.4	0.63
Cyclohexane	12.0	0.61
Tri-tert.-butylbenzene	12.0	0.61

capacity factors of the analytes. No simple correlation is found between the peak broadening and the retention behaviour. This contradicts predictions of the dependence of the peak width from capacity factors based on the usual chromatographic
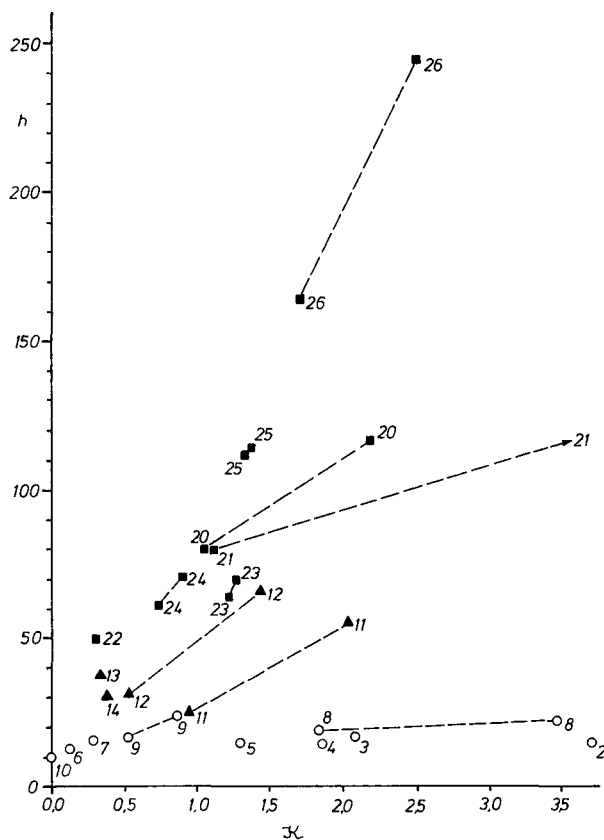
Fig. 1. Reduced plate height, h, for various non-chiral and chiral analytes as a function of their capacity factors. Enantiomers are connected by dotted lines. Symbols: ○, compounds with high efficiency; ▲ and ■, compounds with low or very low efficiency. Code numbers of the solutes as in Table II. Eluent: ethanol–water (96:4, v/v). Temperature: 50°C. Flow-rate: 1 ml/min.

TABLE II

DEPENDENCE OF THE REDUCED PLATE HEIGHT, h, ON THE CAPACITY FACTORS, κ, AND THE STRUCTURES OF THE ANALYTES

Non-trivial structures of analytes are given in Scheme 1. I and II indicate the first and second isomers eluted, α denotes the enantioselectivity coefficient. Eluent: ethanol–water (96:4, v/v). Temperature: 50°C. Flow-rate: 1 ml/min. Z = Benzyloxycarbonyl; FMOC = fluorenylmethyloxycarbonyl; Asn, Phe, Pro and Trp denote the amino acids asparagine, phenylalanine, proline and tryptophan, respectively.

Code No.	Solute		κ	h	α
High efficiency					
1	1,3,5-Tri-*tert.*-butylbenzene		<0	8	
2	Benzene		3.70	15	
3	Toluene		2.08	17	
4	Anthracene		1.85	16	
5	Nitrobenzene		1.30	15	
6	Resorcinol		0.12	13	
7	Benzylamine		0.29	16	
8	4-Phenyl-1,3-dioxolan-2-one	I	1.84	19	1.89
		II	3.47	22	
9	5-Phenyltetrahydrooxazol-2-one	I	0.53	17	1.62
		II	0.86	24	
10	2-Deoxyadenosine		0.0	9.8	
Low efficiency					
11	2,2'-Spirobiindan-1,1'-dione	I	0.95	25	2.14
		II	2.03	55	
12	2,2,2-Trifluoro-1-(9-anthryl)ethanol	I	0.53	31	2.72
	(TFAE)	II	1.44	66	
13	Barbital		0.34	38	
14	Z-Asn-methyl ester	L	0.38	30	
Very low efficiency					
20	Tröger's base	I	1.05	80	2.09
		II	2.19	117	
21	*o,o'*-Dimethyl-*o,o'*-di(bromomethyl)-	I	1.11	80	
	biphenylene	II	6.08	150	
22	*o,o'*-Dimethyl-*o,o'*-di(methoxycarbonyl)-	I	0.30	50	1.53
	biphenylene	II	0.46		
23	Z-Trp-methyl ester		1.22	64	1.04
			1.27	70	
24	FMOC-Pro-methyl ester	L	0.73	62	1.23
		D	0.90	71	
25	FMOC-Phe-methyl ester	D	1.33	112	1.03
		L	1.37	114	
26	FMOC-Trp-methyl ester	D	1.70	164	1.47
		L	2.50	245	

theory[22,26,28] and has to be explained by taking account of additional factors (*cf.*, eqn. 5).

In principle, these finding can be discussed on the basis of two different, but similar models. Both models assume that the large band spreading observed for many substances arises from slow diffusion of these solutes in the near surroundings
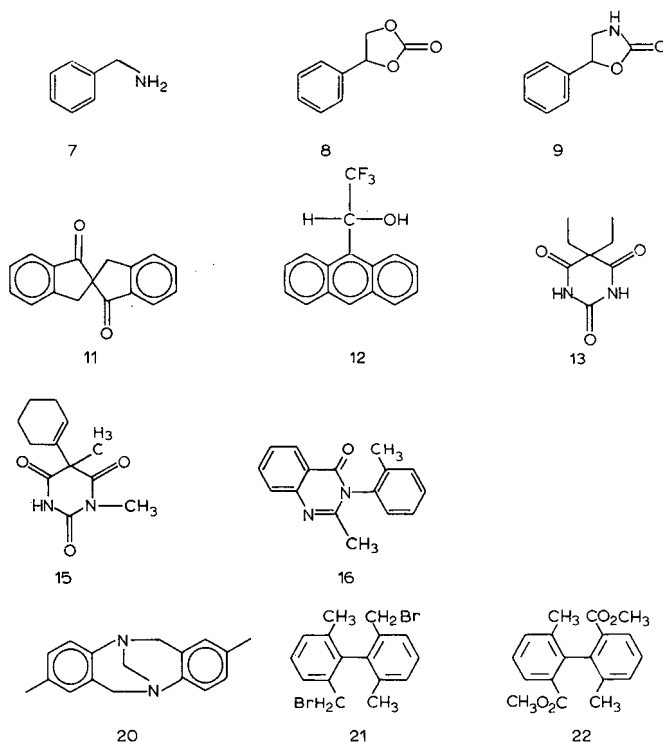
Scheme 1.

(environment) of narrow structured adsorption sites. These narrow sites do not necessarily have a "cavity"-like structure.

(i) The first model assumes that the adsorption sites are essentially of a single type. The type and strength of the interaction between the sites and the analytes depend mainly on the analyte structure and configuration. Similarly, the rate of the adsorption/desorption process of the analytes at the sites depends only on the structure (bulkiness) of the analytes. Thus the peak broadening is more or less a function only of the analyte structure. This model would be sufficient to explaining the band broadening data observed for different analytes.

(ii) The second model assumes that two main types of adsorption (binding) sites are operative. They differ essentially in the accessibility for the analytes and in the type and strength of the interaction with the analytes. One type of adsorption sites can be accessed easily: there the adsorption/desorption process is rapid. They are referred as "quick"-type sites. The other type of binding sites has a narrow environment; the adsorption/desorption process at these sites is hindered for bulky analytes and therefore slow. These sites are called "slow"-type sites. (Within this type of sites a certain distribution in the narrowness is likely.) In this model the peak broadening is a function not only of the bulkiness of the analyte structure alone but also of the type of bindings predominantly formed with the adsorbent, i.e., the type of binding site predominantly adsorbed on. Within this model, the overall plate height of a solute is

determined by the relative contribution of the narrow, "slow"-type adsorption sites to the total retention and by the individual diffusion velocity of the solute at these "slow"-type sites. For both factors the analyte structure is decisive.

Evidence in support of this second model is provided by the finding that non-polar aromatic compounds, in spite of their molecular size, always show low plate height values, and, secondly, by the observed dependence of the plate height and stereoselectivity data on the solvent composition, which is discussed in Part II[19]. A single type of site cannot account for these observations. This model is thus used to discuss the experimental data given in this paper.

The existence of different adsorption "principles" (generating different degrees of selectivity) for swcrCTA adsorbents[2,13] and different adsorption sites in coated CTA adsorbents[30] have been proposed before. It might also be concluded from the data reported recently by Roussel et al.[31] where for some types of racemic analytes the elution order of the enantiomers was found to be dependent on the analyte concentration. The assumption that in a more or less crystalline arrangement of the adsorbent the steric environment around different binding sites differs in narrowness has an high degree of probability.

It is clear from this discussion that the large plate height values observed for many solutes arise from the packed bed and can therefore be attributed as being a contribution to h_b.

Considering the plate height data in greater detail, the following pattern can be observed from Table II.

Some compounds (No. 1 and acidic compounds not included in Table II) are excluded from parts of the mobile phase volume due to their steric structure (tri-tert.-butylbenzene) or to their charges (organic acids). They are eluted slightly before the column void volume. Their h values are between 7 and 10, and thus lie above those obtainable with rigid silica particles of mean diameter 10 μm ($h = 4$–5). Nevertheless, packings of swollen CTA with h values of 7–10 have to be judged as excellent.

For non-polar aromatic compounds (benzene, toluene, naphthalene, anthracene), the reduced plate height values are found between 15 and 18. For these types of compounds no significant increase in plate height with increasing capacity factors is observed. [Such an increase is predicted by the chromatographic theory because of the dependence of h_f on the capacity factor, κ_i (cf., eqn. 2)[22,26,27]. However, the effect expected from theory is too small to be observed with statistical significance within this investigation.] It is characteristic for this adsorbent that larger aromatic molecules are adsorbed less strongly than is benzene. No significant correlation between h and the size of this type of analytes is found. Within the chosen model, it is concluded that non-polar aromatic compounds are thus predominantly adsorbed onto adsorption sites with rapid adsorption kinetics; h_b^{slow} is negligible for these compounds.

Similar h values between 10 and 20 are also found for aromatic compounds with (sterically) rather small polar side-functions (compounds 5–10, shown by circles in Fig. 1). This means that adsorption occurs either mainly onto the "quick"-type sites or, more probably, that the motion and steric orientation of parts of the molecules at the narrow sites is little hindered and therefore not slow.

Many analytes in Table II (compounds 11–26, shown by triangles and squares in Fig. 1) have strongly increased values of h. Fig. 1 shows that in these cases h and thus

h_b^{slow} is not uniquely correlated with the capacity factor but depends on the structures of the analytes. It is not completely clear which structural features are decisive for the adsorption kinetics. It seems that the total size of the whole molecule is decisive only in those cases where the molecule has a rigid structure (spirocompounds, Tröger's base). In the other cases, it is probably the steric feature of the polar group which is decisive. Planar analytes show relatively low h_b values. (Maybe the aromatic ring acts like an anchor at "quick"-type sites.) However, the number of different molecules investigated is too small for a subtle discussion of structure–efficiency relationships. In all cases of chiral analytes the more strongly retained enantiomer shows an higher value for the plate height. This is evidence in support of the assumption that the h_b^{slow} contribution is related to a process of adsorption and is not due to slow diffusion in a bulk environment.

Interpretation of these data —which is supported by the dependence of the plate height on the solvent composition reported in Part II[19]— leads to the assumption that "slow"- and "quick"-type sites differ in the type and strength of the interactions with the analytes, predominantly in the strength of the interaction with polar and non-polar groups of the analytes. These differences may be caused by differences in the polarizability of the sites and in their ability to undergo hydrogen bonding[30,32,33]. If the adsorption includes the motion into narrow structures, the narrow environment built by the adsorbent (including the eluent layer) interacts with the analyte and may represent a steric hindrance to the motion of the analyte or parts of it. Such sites may be therefore of the "slow"-type. Dependent on the steric structure of the analyte, the interactions are of different strengths (causing chiral separation if the strength differs between enantiomeric compounds). In narrow sites, the different strengths of interaction may cause differences also in the velocity of motion, and consequently in the plate height. The slope of the plate height $vs.$ capacity factor is not the same for all analytes, since (i) the steric hindrance in the narrow, "slow"-type sites is not equally strong for all compounds and (ii) the contribution of adsorption at the "slow"-type sites relative to that at the "quick"-type sites is dependent on the types of interactions being formed and therefore on the structures of the analytes.

From these data, it has become clear that the loss in efficiency can essentially be attributed to h_b^{slow}, which may be influenced to a certain extent by the swelling state of crystalline CTA. This point is discussed elsewhere[19]. The "quality of the packing procedure" does not influence h_b. It usually determines the h_c and h_f contributions which result from mixing processes in the streaming part of the mobile phase[20–24] and which are predominant in the most frequently used systems with rigid particles[26,27,29]. Since in swcrCTA packings the h_f term is found to contribute to a minor extent for most of the interesting solutes, one has to conclude that the problem of low efficiency in swcrCTA separations cannot be solved by improving the quality of the packing procedure.

Plate height as a function of the flow velocity

The dependence of the plate height on the flow velocity, u, for different analytes is given in Fig. 2. The following patterns can be observed.

The flow velocity corresponding to the minimum value of h, u_{min}, is found to be very low. Although linear velocities as small as 0.14 mm/s were applied, a real minimum was not seen. In the cases of TFAE (12) and Tröger's base (20) the curves
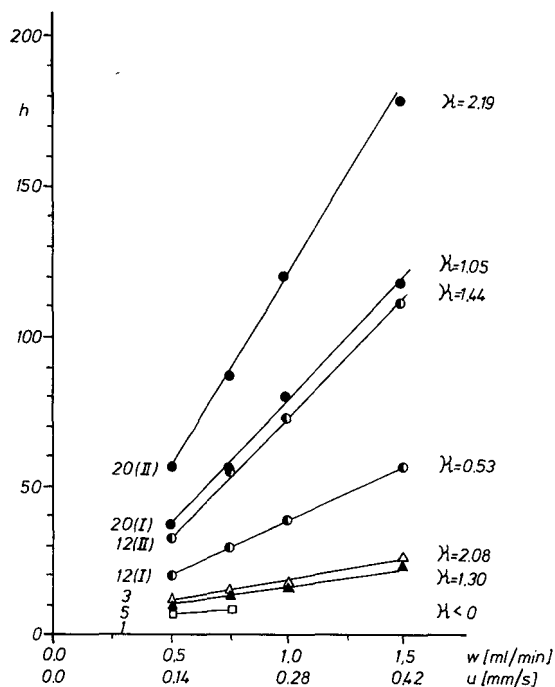
Fig. 2. Reduced plate height, h, as a function of the linear flow velocity, u. Code numbers of solutes as in Table II. Eluent and temperature as in Fig. 1.

observed result from extremely high contributions of h_b which cause the minimum in h to be shifted to very small values of u. The values of u_{min} and h_{min} depend on the magnitude of the h_b contributions and may therefore differ between different solutes. Undoubtedly, h_b is generally the main source of the small values of u_{min} and the large values of h_{min}. However, the extent of the observed shift of u_{min} for compounds **1, 3** and **5** is surprising, since for these h_b is not as high. It is likely that some other factors may be responsible for the very small values of u_{min}. First, the net diameter of the particles may be enhanced in the swollen state. The v_{min} values correspond, therefore, to lower u_{min} values. Secondly, using fibre-shaped particles, the tortuosity factor may be enhanced. This reduces the value of φ_d in eqn. 2 and thus reduces the contribution of h_d. Thirdly, with partially compressible particles like swcrCTA, it might be possible that the contributions h_c and h_f are lower than with rigid particles of the same diameter.

Concerning h_{min}, rather high values compared with alkylsilica or silica columns are expected. It is clear that these values result from the larger h_b contributions and from significantly increased h_d contributions at small values of u_{min}. However, h_{min} may also be overestimated to some extent by underestimating the d_p value of swollen particles.

Due to the predominant influence of h_b, which is known to increase linearly with u, the total plate height also increases approximately linearly with the flow velocity. This is seen in Fig. 2. The slopes of the plots of h vs. u reflect the different diffusion velocities at the adsorption sites which depend on the steric structures of the analytes.

The slopes are not correlated with the capacity factor values and are different for enantiomers in the general case.

The increase in h with increasing u is not very strong for analytes mainly adsorbed onto the "quick"-type adsorption sites, as expected from the previous discussion. For these analytes, the increase in h_f with u may also be important. However, the precision of the data is not sufficient to quantify the contribution of h_f to the total increase in h with u for these compounds.

Plate height and peak symmetry as a function of the analyte concentration

Generally, the peak symmetry obtained on the packing material and column used is excellent. At moderate concentrations, the symmetry factors, a, defined in Table III, usually lie between 1.10 and 0.85.

Although small, the asymmetry seems to be correlated with the retention mechanism. Non-polar analytes, mainly adsorbed onto the "quick"-type adsorption sites, show a slight leading in most cases, whereas the analytes which also penetrate to the narrow "slow"-type adsorption sites show a slight tailing. Depending on the analyte structure, this tailing is more or less pronounced.

These results can be interpreted by the following model. (i) At the narrow, "slow"-type adsorption sites a competitive adsorption mechanism is operative. In addition, these narrow sites may be not totally homogeneous in spatial configuration and thus not completely homogeneous in adsorption energies. The presence of adsorption sites having slightly different binding strengths causes a slight convex curvature of the adsorption isotherm which may be the source of the slight tailing observed. Because of the smallness of the effect, no significant shift of the capacity factor with loading can be observed. (ii) Aromatic compounds are assumed to adsorb preferentially onto the "quick"-type adsorption sites (*cf.*, the discussion above). To some extent, the "quick"-type adsorption sites may allow a second-layer or multi-layer adsorption of other molecules of the same type onto the first adsorbed ring, thus inducing a slight concave form of the adsorption isotherm. This interpretation is based on the correlation of tailing and leading with the different adsorption and band

TABLE III

REDUCED PLATE HEIGHT, h, AND PEAK SYMMETRY FACTOR, a, AS A FUNCTION OF THE ANALYTE CONCENTRATION

Eluent: ethanol–water (96:4, v/v). Temperature: 50°C. Flow-rate: 1 ml/min. Injection volume: 20 μl. The symmetry factor, a, was determined according to ref. 34 at 1/10 of the peak height; values >1 indicate leading, those <1 indicate tailing.

Code	Solute						
4	Anthracene		Q_{inj} (μg)	0.2	2.0	20.0	
			h	20	20	22	
			a	1.04	1.09	1.15	(leading)
12	TFAE		Q_{inj} (μg)	0.15	1.50	30.0	
		I	h	37	35	44	
			a	0.86	0.94	0.74	(tailing)
		II	h	71	72	76	
			a	—	0.72	0.80	(tailing)

broadening behaviours of the analytes. It must be pointed out, however, that these effects are very small and the peak shape is found to be highly symmetrical, very often to an higher extent than in most cases of reversed-phase chromatography.

Up to about 10 μg injected, the influence of the loaded mass on the plate height, peak symmetry or retention time of the peak maximum is statistically insignificant or unimportant (Table III). In the case of anthracene, the highest concentration given in Table III was about half the saturation concentration in ethanol.

Differences between different swollen crystalline cellulose acetate materials

Similar investigations to those described for the CTA material I have also been done for another CTA material, II, which is assumed to have an higher degree of cross-linking. Most likely, it is a cellulose 2.5-acetate. The main chromatographic differences between these two materials are as follows.

Material II yields strongly tailing peaks at 30°C. This tailing is eliminated nearly completely when working at 50°C.

With material I, the group of non-chiral, rather non-polar aromatic compounds (benzene, naphthalene, anthracene, toluene, ethylbenzene, chlorobenzene, nitro-benzene and anisole) have a very uniform dependence of h on κ (see Fig. 1). With material II, characteristic differences can be observed within this group as shown in Fig. 3. The larger analytes (anthracene, naphthalene, nitrobenzene, ethylbenzene) have similar behaviours to those on material I. The smaller ones (benzene, chlorobenzene and toluene) show a pronounced increase in h with κ. This means that hindered diffusion has to be assumed also for parts of the non-polar adsorption sites, especially for those which are accessible only to the smallest aromatic molecules. This may result from different steric structures and swelling states of the materials, due to a different degree of cross-linking.
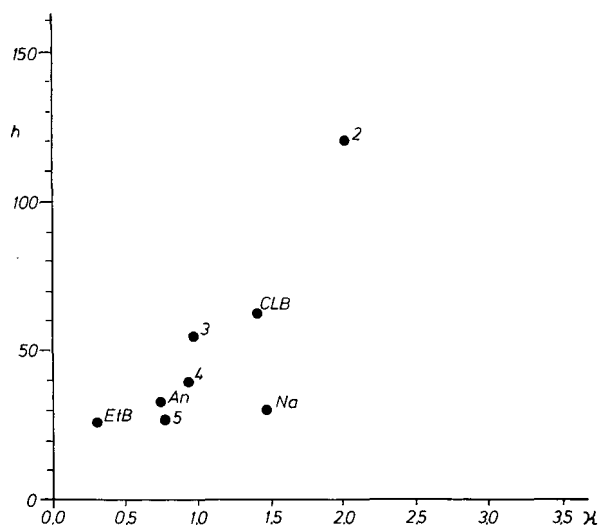
Fig. 3. Reduced plate height, h, as a function of the capacity factors, κ, for various non-chiral aromatic compounds using a cross-linked CTA material (II). EtB = Ethylbenzene; ClB = chlorobenzene; An = anisole; Na = naphthalene; code numbers for all other compounds as in Table II. Chromatographic conditions as in Fig. 1.

CONCLUSIONS

From the investigation of the dependence of the peak dispersion on the capacity factor and the structure of the analyte, one can primarily conclude that in columns packed with swcrCTA the most important contribution to the plate height arises from the slow mass exchange in the packed bed. Most probably, the source is a slow transport process at parts of the adsorption sites available, *e.g.*, diffusion and orientation at narrow sites, in narrow channels or cavity-like structures.

The steric structure of the analytes is found to be the decisive parameter which determines the plate height. The fact that relatively small h values can be found for some compounds, whereas for others very high values are observed, is interpreted by assuming the existence of at last two types of adsorption sites: "slow"- and "quick"-type sites. These types differ in the rate of the adsorption/desorption process including the diffusion in the vicinity of these sites. Both types of sites contribute to solute retention. The plate height, however, is predominantly determined by the "slow"-type sites. Since the relative contribution of the "slow"-type sites to the overall retention differs between different analytes depending on their structures, no correlation is found between plate height and capacity factor.

The different magnitudes of band spreading processes for analytes of different structures is illustrated together with the high enantioselectivity and the excellent peak symmetry obtainable with swcrCTA by the chromatograms in Fig. 4.

The dependence of the plate height on the flow-rate is approximately linear within the range of flow-rates applied. This is expected from the predominant contribution of the packed bed related mass-exchange term, h_b. The minima of the curves of h_i *vs.* u are shifted to very low flow velocities.

The axial diffusion contribution, h_d, and the mobile phase related contributions, h_c and h_f, cannot be determined individually. It is not yet clear whether for slightly
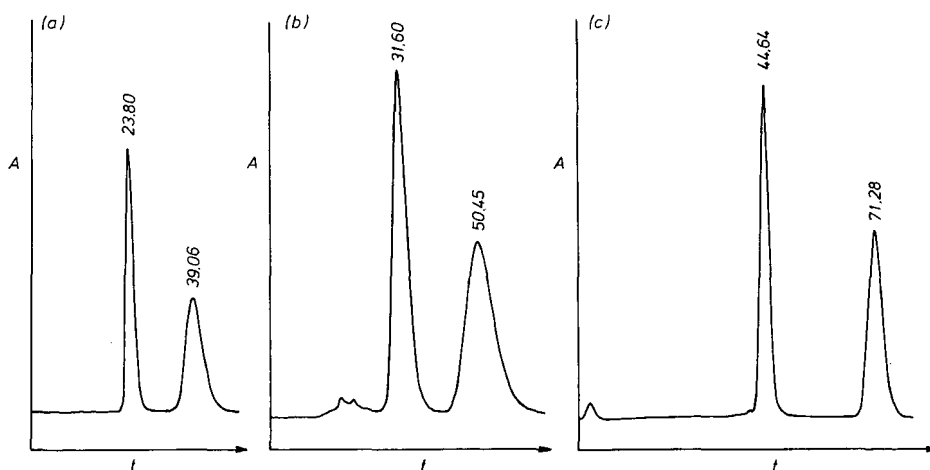
Fig. 4. Chromatograms of chiral analytes. (a) TFAE; (b) Tröger's base; (c) 4-phenyl-1,3-dioxolan-2-one. t = Time in min; A = UV absorption. Stationary phase: swcrCTA. Mobile phase: ethanol–water (96:4). Column: 250 mm × 10 mm I.D. Flow-rate: 1 ml/min. Temperature: 50°C. t in min.

compressible swcrCTA particles with enhanced tortuosity factors these contributions are strictly comparable with the corresponding terms for rigid silica particles. It is clear, however, that h_c and h_f are little enhanced in comparison to other packings with the same particle size. Thus, one has to conclude that the columns are well packed and that a better packing procedure will not decrease the peak broadening dramatically.

The dependence of h_b on the particle diameter has not been investigated here; h_b^{quick} is assumed to be linearly dependent on d_p, whereas this is not expected for h_b^{slow}. Since h_b^{slow} is in most cases the predominant plate height contribution, knowledge of the influence of the particle size on this term will be of considerable practical importance.

The peak symmetry is excellent even at high analyte concentrations. No significant increase in plate height can be observed up to 10 μg of analytes injected in 20 μl.

A detailed study of the plate height dependence on the eluent composition, the temperature and the pressure (which all influence the swelling state of the adsorbent) will be presented in the following paper[19].

ACKNOWLEDGEMENTS

REFERENCES

1 G. Hesse and R. Hagel, *Chromatographia*, 9 (1976) 62.
2 G. Hesse and R. Hagel, *Liebigs Ann. Chem.*, (1976) 996.
3 K. R. Lindner and A. Mannschreck, *J. Chromatogr.*, 193 (1980) 308.
4 K. Schlögel and M. Widhalm, *Chem. Ber.*, 115 (1982) 3042.
5 H. Koller, K.-H. Rimböck and A. Mannschreck, *J. Chromatogr.*, 282 (1983) 89.
6 G. Blaschke, H.-P. Kraft and H. Markgraf, *Chem. Ber.*, 116 (1983) 3611.
7 K. Schlögel and M. Widhalm, *Monatsh. Chem.*, 115 (1984) 1113.
8 A. Mannschreck, H. Koller and R. Wernicke, *Kontakte (Darmstadt)*, 1985/1 (1985) 40.
9 E. Francotte, R. M. Wolf, D. Lohmann and R. Mueller, *J. Chromatogr.*, 347 (1985) 25.
10 E. Francotte, H. Stierlin and J. W. Faigle, *J. Chromatogr.*, 346 (1985) 321.
11 K.-H. Rimböck, M. A. Cuyegkeng and A. Mannschreck, *Chromatographia*, 21 (1986) 223.
12 G. Blaschke, *J. Liq. Chromatogr.*, 9 (1986) 341.
13 J. Scharf, K. Schlögel, M. Widhalm, J. Lex, W. Tuckmantel, E. Vogel and F. Pertlik, *Monatsh. Chem.*, 117 (1986) 255.
14 T. Shibata, I. Okamoto and K. Ishii, *J. Liq. Chromatogr.*, 9 (1986) 313.
15 A. Hussenius, R. Isaksson and O. Matsson, *J. Chromatogr.*, 405 (1987) 155.
16 M. Krause and R. Galensa, *J. Chromatogr.*, 441 (1988) 417.
17 Y. Okamoto, M. Kawashima, K. Yamamoto and K. Hatada, *Chem. Lett.*, (1984) 739.
18 A. Ichida, T. Shibata, I. Okamoto, Y. Yuki, H. Namikoshi and Y. Toga, *Chromatographia*, 19 (1984) 280.
19 A. Rizzi, *J. Chromatogr.*, 478 (1989) 87.
20 J. C. Giddings, *Dynamics of Chromatography*, Part I, Marcel Dekker, New York, 1965.
21 J. F. K. Huber, *J. Chromatogr. Sci.*, 7 (1969) 85.
22 J. F. K. Huber, *Ber. Bunsenges. Phys. Chem.*, 77 (1973) 179.
23 G. J. Kennedy and J. H. Knox, *J. Chromatogr. Sci.*, 10 (1972) 549.
24 C. Horvath and H. J. Lin, *J. Chromatogr.*, 149 (1978) 43.
25 J. H. Knox and H. P. Scott, *J. Chromatogr.*, 282 (1983) 297.

26 J. F. K. Huber, J. Quaadgras and A. Rizzi, *8th Int. Symp. Column Liquid Chromatography, New York, May 1984,* Abstract No. 3pG3.
27 J. F. K. Huber, J. Quaadgras and A. Rizzi, in preparation.
28 E. Katz, K. L. Ogan and R. P. W. Scott, *J. Chromatogr.,* 270 (1983) 51.
29 J. F. K. Huber and A. Rizzi, *J. Chromatogr.,* 384 (1987) 337.
30 I. W. Wainer and M. C. Alembik, *J. Chromatogr.,* 358 (1986) 85.
31 C. Roussel, J.-L. Stein, F. Beauvais and A. Chemlal, *J. Chromatogr.,* in press.
32 I. W. Wainer, M. C. Alembik and E. Smith, *J. Chromatogr.,* 388 (1987) 65.
33 I. W. Wainer, R. M. Stiffin and T. Shibata, *J. Chromatogr.,* 411 (1987) 139.
34 L. R. Snyder and J. J. Kirkland, *Introduction to Modern Liquid Chromatography,* Wiley, New York, 1979, p. 222.

BAND BROADENING IN HIGH-PERFORMANCE LIQUID CHROMATO-GRAPHIC SEPARATIONS OF ENANTIOMERS WITH SWOLLEN MICRO-CRYSTALLINE CELLULOSE TRIACETATE PACKINGS

II. INFLUENCE OF ELUENT COMPOSITION, TEMPERATURE AND PRESSURE

ANDREAS M. RIZZI

Institute of Analytical Chemistry, University of Vienna, Währingerstrasse 38, A-1090 Vienna (Austria)
(First received February 20th, 1989; revised manuscript received April 27th, 1989)

SUMMARY

The peak dispersion in high-performance liquid chromatographic columns packed with swollen crystalline cellulose triacetate was investigated as a function of the eluent composition, the temperature and the pressure. The results provide support for a model which assumes the existence of at least two types of adsorption sites, "quick"-type and "slow"-type sites, which differ with respect to the rate of the adsorption/desorption process. The observed dependence of the peak dispersion on the temperature and the eluent composition can be understood as resulting from three factors: (i) changes in the diffusion velocity by changes in the solvent viscosity; (ii) changes in the three-dimensional structure of the adsorbent due to changes in the swelling state of the CTA adsorbent and (iii) changes in the availability and accessibility of the adsorption sites due to differences in the strength of the competitive adsorption of the solvent components.

INTRODUCTION

Swollen microcrystalline cellulose triacetate (swcrCTA) has been widely applied for liquid chromatographic separations of enantiomeric compounds 1,2. High enantioselectivity for many groups of compounds and high loadability are the main advantages of this adsorbent material. However, the large peak broadening usually observed results in reduced efficiency and limits the use of this material for analytical purposes.

In Part I [3] the peak broadening process on swcrCTA was systematically investigated with respect to the capacity factor of the analyte, analyte structure, flow velocity and column loading. It was concluded that in columns packed with swcrCTA the most important contribution to the plate height arises from the slow mass exchange in the packed bed. This is attributed to a slow transport process at narrow adsorption sites: slow diffusion and orientation at narrow sites, in narrow channels or in cavity-like structures.

The steric structure of the analytes was found to determine the plate height. From the dependence of the plate height on the capacity factors and the structures of the analytes, the existence of at least two types of adsorption sites was proposed: "slow"-type and "quick"-type sites, which differ in the rate of the adsorption/desorption process (including the diffusion in the vicinity of these sites). Both types of sites contribute to solute retention. Since the plate height is predominantly determined by the "slow"-type sites, no correlation was found between plate height and capacity factor.

In this paper quantitative data are reported on the dependence of the plate height on the eluent composition, the temperature and the pressure. The data provide strong support for the model presented previously[3].

The knowledge of the dependences investigated here may contribute to a deeper understanding of the adsorption mechanism on CTA materials, which is not yet clear. In addition these data provide a basis for a rational optimization of separations on swcrCTA adsorbents.

EXPERIMENTAL

The chromatographic equipment and experimental conditions were identical to those described previously[3]. The CTA column referred to in this paper was the previous column I.

RESULTS AND DISCUSSION

Capacity factor as a function of temperature

A good linear correlation is observed between ln κ and $1/T$, as is seen in Fig. 1. Similar slopes are obtained for most of the analytes, including analytes with dissimilar structures like anthracene, 2,2,2-trifluoro-1-(9-anthryl)ethanol (TFAE) and Tróg-
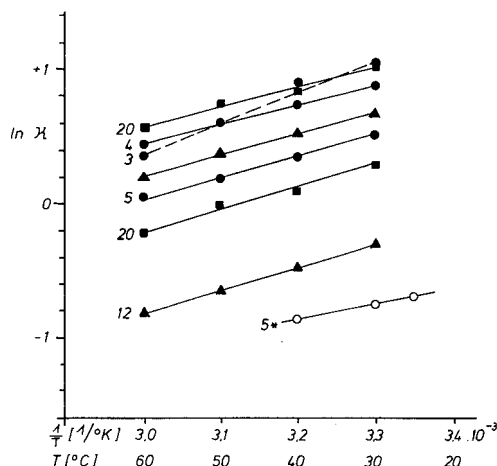
Fig. 1. Logarithm of the capacity factor as a function of the inverse of the temperature. Code numbers of solutes as in Table II. The open circles for compound 5 denote experimental data obtained from a octadecylsilica/ethanol–water system. Eluent: ethanol–water (96:4, v/v); flow-rate 1 ml/min.

er's base. An exception is toluene. The slopes are also similar to those obtained in reversed-phase systems using octyl-silica adsorbents.

A more detailed estimation of the temperature dependence for enantiomeric pairs reveals that the enantio- and stereoselectivity may either slightly increase or slightly decrease with temperature (Table I). This may be due to slight differences in the temperature dependence of the free enthalpy of adsorption for the two enantiomers at different binding sites, and/or to changes in the swelling state and thus in the structure of the narrow adsorption sites upon increase in temperature. Depending on the analyte structure, this may reduce the differences in adsorption strength between the enantiomers, or may even enhance it.

TABLE I

ENANTIOSELECTIVITY, α, AS A FUNCTION OF THE TEMPERATURE

Non-trivial structures of analytes are given in ref. 3. Code numbers are identical to those in ref. 3. Flowrate: 1 ml/min.

Code	Solute	Temperature (°C)			
		30	40	50	60
Eluent: ethanol–water (96:4, v/v)					
11	Spirobiindanone	2.29	2.24	2.14	–
12	TFMA	2.66	2.75	2.79	2.77
20	Tröger's base	2.07	2.13	2.14	2.21
Eluent: ethanol–methanol–water (76.8:20:3.2, v/v)					
8	Phenyldioxolanone	–	1.93	1.88	1.86
11	Spirobiindanone	2.10	2.06	2.03	2.00
12	TFAE	2.20	2.20	2.33	2.34
20	Tröger's base	–	1.60	1.68	1.75

Plate height as a function of the temperature

The influence of temperature on the plate height, h, is shown in Fig. 2. The influence of the temperature differs from analyte to analyte, depending on the adsorption mode. For aromatic benzene compounds adsorbed onto the "quick"-type adsorption sites[3] (circles in Fig. 2) the temperature effect is insignificant. However, a very pronounced temperature effect is observed for analytes with high contributions of the "slow"-type adsorption[3] (triangles and squares in Fig. 2). The steep decrease in h with increasing temperature is predominantly due to a gain in the diffusion velocity at the "slow"-type sites. This is caused by the decreasing strength of interactions between the analyte and its environment and partially by the lower viscosity of the solvents at higher temperatures. The slopes of the plots in Fig. 2 are similar for the enantiomers of TFAE and Tröger's base.

The decrease in h cannot be attributed simply to the reduction in the capacity factors: this would not explain the very steep descent observed in Fig. 2. The gain in efficiency has to be attributed to the increase in the diffusion velocity at "slow"-type
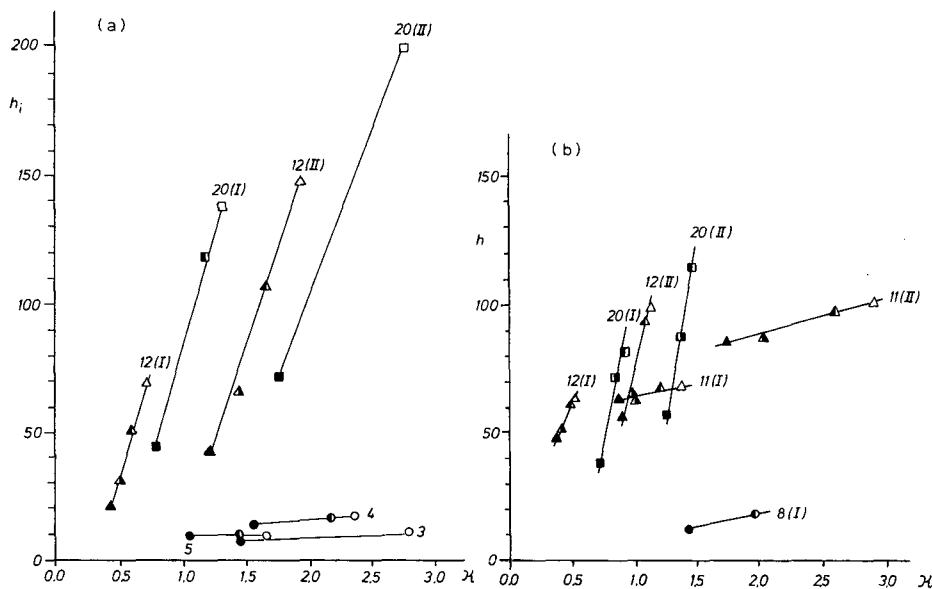
Fig. 2. Reduced plate height and capacity factor as a function of temperature. Temperatures: △, ○, □, 30; ⧫, ◐, ▮, 40; ▲, ◑, ▐, 50; ▲, ●, ■, 60°C. Code numbers of solutes as in Table II; I and II indicate the first and second enantiomers eluted. Flow-rate: 1 ml/min. Solvents: (a) ethanol–water (96:4); (b) ethanol–methanol–water (76.8:20:3.2).

sites, as mentioned before. Comparison of the data in Fig. 2a and b shows that the effect of the temperature on the plate heights of TFAE and Tröger's base is decreased by adding methanol to the eluent. This finding is in accordance with expectation, since methanol reduces the contribution of the "slow"-type sites to the total adsorption of the analytes (cf., next section).

Plate height as a function of the solvent composition

The dependence of the plate height, h, on the solvent composition is shown in Figs. 3 and 4 and in Table II. Various contents of methanol, propanol, water and cyclohexane in ethanol were investigated, and different effects are observed for different solvent components. From the behaviour of the substances as represented by a plot of h vs. [κ, %(v/v) moderator] (Fig. 4) some conclusions about the adsorption mechanism for the solutes can be made.

(i) Methanol. The plate height, h, decreases significantly with increasing methanol content in the mixture. Similarly, the capacity factors of all compounds investigated decrease. This influence of the methanol content is illustrated by a plot of h vs. κ in Fig. 4a. The gain in efficiency probably results from three sources. (a) The addition of methanol reduces the mean viscosity of the eluent mixture (cf., Table III) thus allowing an higher diffusion velocity of the analytes, which results in smaller values of h. (It mainly influences h_b^{slow}. A minor influence on h_c and h_f is expected to be insignificant in Fig. 4a.) (b) Each change in the solvent composition is assumed to change the swelling state of CTA. In this way the availability (important for the
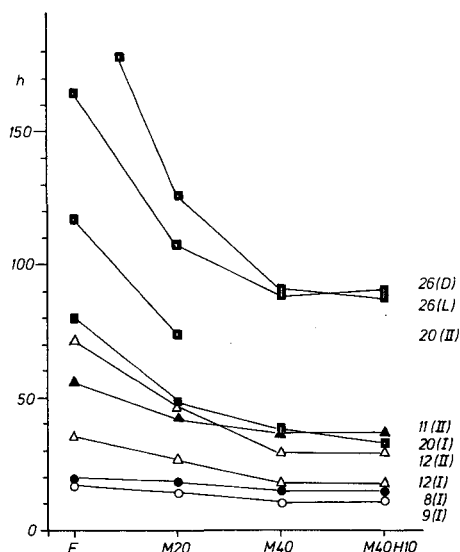
Fig. 3. Reduced plate height, h, as a function of the composition of the mobile phase. Code numbers of solutes as in Table II. Chromatographic conditions: temperature 50°C; flow-rate 1 ml/min. solvents: E = ethanol–water (96:4); M20 = methanol–ethanol–water (20:76.8:3.2); M40 = methanol–ethanol–water (40:57.6:2.4); M40H10 = methanol–cyclohexane–ethanol–water (40:10:48:2).

capacity factors and the selectivity) and the accessibility (important for the plate height) of the different types of adsorption sites is changed too. The importance and the direction of this influence on the plate height is not yet well understood. (c) With this type of packing material the elution power of an eluent component depends not only on the types of interactions with the solute and adsorbent, but also on its steric size. At narrow and therefore "slow"-type sites methanol is thus expected to be a stronger competitor for the adsorption of the analytes than is ethanol. Enhanced competition for the "slow"-type sites by methanol reduces the retention of the analytes and the relative influence of the slow kinetic. This results in a net decrease in h for those analytes, where, due to their structures, the adsorption onto "slow"-type sites results in high h_b^{slow} values.

Factors (b) and (c) are not independent of each other. The decreases in h_b^{slow} are found to be approximately proportional to the decrease in κ (Fig. 4a). It is therefore probable that the gain in efficiency upon the addition of methanol is mainly due to the effects mentioned in (b) and (c). The decrease in enantioselectivity for many analytes upon addition of methanol (Table IV) supports the assumption of changed relative contributions of "slow"- and "quick"-type adsorption sites, since it is likely that the narrow, "slow"-type sites are decisive for the chiral recognition. The finding that the addition of methanol also reduces the retention of non-polar aromatic hydrocarbons may indicate the importance of changes in the swelling state of CTA.

(ii) Cyclohexane. When increasing the content of cyclohexane in the mixture, the plate height remains approximately constant whereas the capacity factors generally decrease (Table II and Fig. 4b). It should be noted that cyclohexane as well as
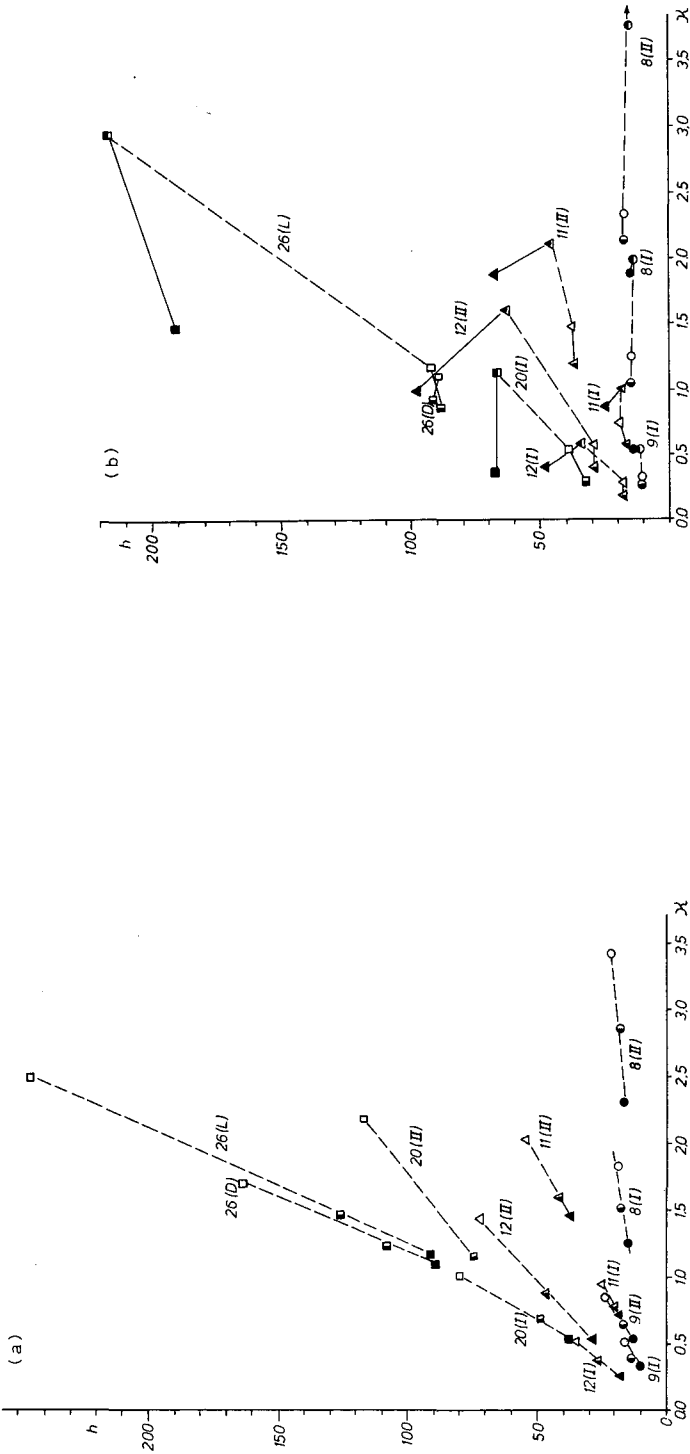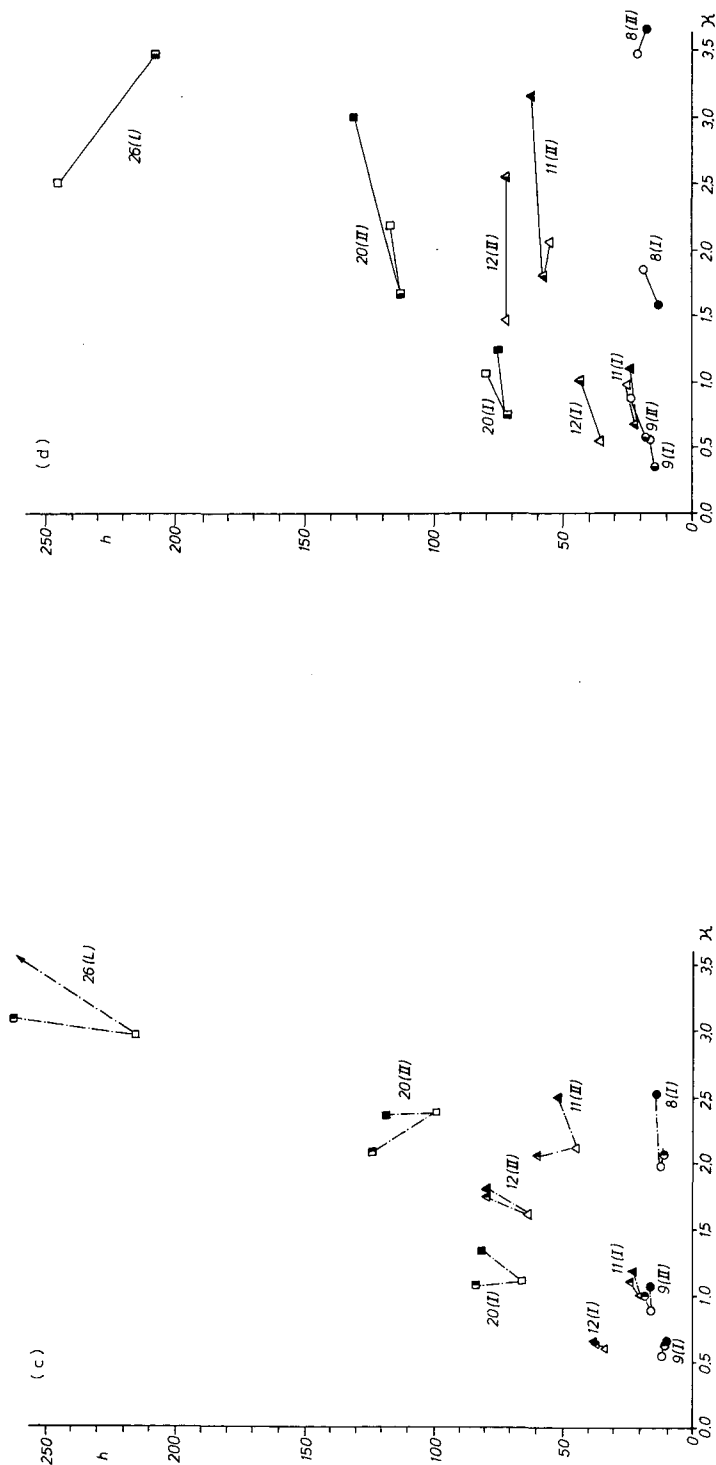
Fig. 4. Reduced plate height, h, and capacity factor, κ, as a function of the type and concentration of a second solvent component added to the ethanolic mobile phase: (a) methanol; (b) cyclohexane; (c) propanol; (d) water. Code numbers of solutes as in Table II. Symbols for the solvent systems: (a) ○, △, □, E = ethanol–water (96:4); ●, ▲, ■, M40 = methanol–ethanol–water (40:57.6:2.4). (b) ○, △, □, M40; ●, ▲, ■, M40H10 = methanol–cyclohexane–ethanol–water (40:10:48:2); ○, △, □, E; ●, ▲, ■, H20 = cyclohexane–ethanol–water (20:76.8:3.2); (c) ○, △, □, E; ●, ▲, ■, 2-P30 = 2-propanol–ethanol–water (30:67.2:2.8); (d) ○, △, □, E; ●, ▲, ■, W10 = ethanol–water (86.4:13.6); ●, ▲, ■, W20 = ethanol–water (79.8:23.2). Chromatographic conditions: temperature 50°C; flow-rate 1 ml/min.

TABLE II

REDUCED PLATE HEIGHT, h, AND CAPACITY FACTOR, κ, AS A FUNCTION OF THE COMPOSITION OF THE MOBILE PHASE

Non-trivial structures of analytes are given in ref. 3. Solvent systems: E = Ethanol–water (96:4); M20 = methanol–ethanol–water (20:76.8:3.2); M40 = methanol–ethanol–water (40:57.6:2.4); M40H10 = methanol–cyclohexane–ethanol–water (40:10:48:2); 1-P10 = 1-propanol–ethanol–water (10:86.4:3.6); 1-P30 = 1-propanol–ethanol–water (30:67.2:2.8); 2-P30 = 2-propanol–ethanol–water (30:67.2:2.8); W10 = ethanol–water (86.4:13.6); W20 = ethanol–water (76.8:23.2); H20 = cyclohexane–ethanol–water (20:76.8:3.2).

Code No.	Solute		Ethanol–methanol and ethanol–methanol–cyclohexane (system back pressure above 70 atm)							
			E		M20		M40		M40H10	
			κ	h	κ	h	κ	h	κ	h
1	Tributylbenzene		<0		<0	11	<0	13	<0	15
3	Toluene		2.08	17	1.92	11	1.71	12		
4	Anthracene		1.85	20	1.49	16	1.13	13	0.97	14
5	Nitrobenzene		1.30	15	1.21	9	1.10	9		
6	Resorcinol		0.12	13	0.07	9	0.04	8	0.02	8
8	Phenyldi-	I	1.84	19	1.53	18	1.26	15	1.05	15
	oxolanone	II	3.47	22	2.89	18	2.32	17	2.13	17
9	Phenyltetrahydro-	I	0.53	17	0.40	14	0.33	10	0.28	11
	oxazolone	II	0.86	24	0.66	17	0.55	13	0.53	14
11	Spirobi-	I	0.95	25	0.78	20	0.73	19	0.57	16
	indanone	II	2.03	55	1.59	42	1.46	37	1.19	37
12	TFAE	I	0.53	35	0.37	27	0.26	18	0.19	17
		II	1.44	72	0.88	47	0.55	29	0.40	29
20	Tröger's base	I	1.05	80	0.69	49	0.53	38	0.30	≤33[a]
		II	2.19	117	1.15	74	0.77	–	0.30	≤33[a]
26	FMOC-Trp	D	1.70	164	1.23	108	1.10	89	0.91	91
	methyl ester	L	2.50	245	1.46	126	1.16	91	0.85	88

Code No.	Solute		Ethanol–propanol (back pressure between 30 and 40 atm)							
			E		1-P10		1-P30		2-P30	
			κ	h	κ	h	κ	h	κ	h
1	Tributylbenzene		<0	11	<0		<0	14	<0	19
3	Toluene						1.84	9	2.40	13
4	Anthracene		1.99	12	1.85	11	1.93	13	2.06	12
5	Nitrobenzene						1.31	8	1.60	10
6	Resorcinol				0.13	9	0.16	9	0.17	8
8	Phenyldi-	I	1.98	13	1.98	12	2.06	11	2.52	14
	oxolanone	II	3.75	15	3.71	14	3.83	13	4.89	16
9	Phenyltetrahydro-	I	0.54	12	0.51	9	0.61	11	0.63	10
	oxazolone	II	0.88	16	0.83	14	0.99	18	1.07	16
11	Spirobi-	I	1.00	18	1.00	21	1.10	24	1.18	23
	indanone	II	2.10	45	2.05	48	2.02	60	2.49	54
12	TFAE	I	0.59	34	0.61	34	0.61	37	0.62	38
		II	1.60	63	1.68	67	1.73	79	1.78	79
15	Hexobarbital	I			0.89	30	0.99	≤38[a]	1.05	36
		II			1.29	35	1.39	≤47[a]	1.45	45
20	Tröger's base	I	1.11	66	1.09	67	1.07	84	1.31	82
		II	2.36	99	2.23	101	2.06	124	2.34	118
26	FMOC-Trp methyl ester	L	2.94	215			3.07	262	3.93	295

TABLE II *(continued)*

Code No.	Solute		Ethanol–water and ethanol–cyclohexane (back pressure between 30 and 40 atm)					
			W10		*W20*		*H20*	
			κ	h	κ	h	κ	h
1	Tributylbenzene		<0	9			<	13
3	Toluene		2.01	10			0.81	10
4	Anthracene		2.97	13			1.29	16
5	Nitrobenzene		1.23	8			0.50	10
6	Resorcinol		0.09	7			0.14	12
8	Phenyldi-	I			1.57	13	1.87	15
	oxolanone	II			3.66	17	4.06	18
9	Phenyltetrahydro-	I	0.34	15			0.55	15
	oxazolone	II	0.57	18			1.03	21
11	Spirobi-	I	0.67	22	1.08	24	0.86	25
	indanone	II	1.80	58	3.14	62	1.87	68
12	TFAE	I	0.99	43			0.40	48
		II	2.54	72			0.97	97
15	Hexobarbital	I	0.60	33	0.87	54		
		II	0.99	43	1.51	71		
20	Tröger's base	I	0.74	72	1.24	75	0.36	$\leqslant 67^a$
		II	1.67	113	2.99	131	0.36	$\leqslant 67^a$
26	FMOC-Trp methyl ester	L	3.45	207			1.54	190

[a] Incompletely resolved peak.

TABLE III

RELATIVE VISCOSITY (η/η_{water}) AND KINEMATIC VISCOSITY (η/ρ) AND DENSITY DATA FOR PURE AND AQUEOUS SOLVENTS AT 20°C[4]

η denotes the viscosity coefficient, ρ the density.

	η/ρ (cSt)	η/η_{water}	ρ (g/cm³)
Pure solvent			
Ethanol	1.525	1.201	0.789
Methanol	0.740	0.585	0.792
1-Propanol	2.773	2.223	0.803
2-Propanol	3.100	2.428	0.785
Cyclohexane	1.256	0.980	0.78
Water	1.004	1.000	1.000
Aqueous ethanol (%, v/v)			
96	1.674	1.339	0.801
90	1.885	1.539	0.818
86	2.021	1.671	0.828
80	2.229	1.877	0.843
76	2.361	2.011	0.853

TABLE IV

ENANTIOSELECTIVITY, α, AS A FUNCTION OF THE CONCENTRATION OF METHANOL AND CYCLOHEXANE IN THE ETHANOLIC MOBILE PHASE

Chromatographic conditions: flow-rate 1 ml/min; temperature 50°C. Solvent systems as in Table II.

Code No.	Solute	E	M20	M40	M40H10	H20	W10
8	Phenyldi-oxolanone	1.88	1.89	1.84	2.03	2.18	–
9	Phenyltetrahydro-oxazolone	1.62	1.64	1.65	1.87	1.88	1.68
11	Spirobiindanone	2.14	2.04	2.01	2.08	2.17	2.69
12	TFAE	2.72	2.38	2.17	2.11	–	2.57
15	Hexobarbital	1.45	1.46	1.39	1.25	1.11	1.65
16	Methaqualon	1.53	1.67	1.74	1.86	1.57	1.61
20	Tröger's base	2.08	1.67	1.43	$\leqslant 1.20^{a}$	$\leqslant 1.20^{a}$	2.26
22	o,o'-Disubstituted biphenylene	1.58	1.42	$\leqslant 1.20^{a}$	$\leqslant 1.20^{a}$	–	2.00
26	FMOC-Trp methyl ester	1.47	1.18	1.06	1.07	–	–

[a] Unresolved peak: the value given is the limit, where a partial resolution would be seen.

methanol is a stronger displacer than is ethanol on swcrCTA adsorbents. The non-polar and rigid cyclohexane is assumed to be a stronger competitor than ethanol for the adsorption of analytes onto non-polar sites which are concluded to be mainly of the "quick"- type. These non-polar sites are responsible for the strong adsorption of non-polar aromatic compounds (benzene, toluene, naphthalene) (cf., Fig. 1 in ref. 3). Since the competitive effect of cyclohexane mainly affects the "quick"-type sites, its addition induces a decrease in κ but has only a minor influence on the plate height. In cases where the relative importance of "quick"-type sites is reduced significantly, the plate height even increases, due to the enhancement of the relative importance of the adsorption onto the "slow"-type sites (Fig. 4b). The increase in enantioselectivity for many analytes upon the addition of cyclohexane (Table IV) again provides support for this assumption of changed relative contributions of the "slow"- and "quick"-type adsorption sites. The divergent influence on the capacity factors of enantiomers (8) and changes in the elution order of enantiomers (26) indicate that changes in the swelling state may be important, too.

(iii) Propanol. Different effects on the capacity factors are observed when 1-propanol or 2-propanol is added. The addition of 1-propanol induces a small increase or a small decrease in the capacity factors. On the other hand a significant increase in κ is always observed with 2-propanol. This is probably due to the reduced competition from 2-propanol originating from steric effects but may also be due to small changes in the swelling state of the CTA material. In all cases the plate height increases (Fig. 4c) since the addition of propanol induces a large increase in the solvent viscosity. This seems to be the main effect with 1-propanol. In the case of 2-propanol the opposite effect to that discussed for methanol may also be of importance.

(iv) Water. The addition of water strongly influences the capacity factors of the solutes. In spite of a large increase in solvent viscosity, it has, however, only a slight influence on the efficiency (Fig. 4d).

The addition of water most probably has a strong influence on the swelling state of CTA, and thus on the availability and accessibility of adsorption sites. The relative importance of the "slow"-and "quick"-type sites for the adsorption of the analytes is therefore changed (as described above for methanol). A decrease in h, expected for this effect, may just be balanced by the effect resulting from an increased viscosity.

However, other explanations might be valid too. Since no measurements are available which focus on the changes in the swelling state and on the preferential adsorption of water or ethanol onto CTA, it is not clear whether the addition of water does influence the viscosity of the solvent layers in the "cavities" significantly, or not. The changes in retention of analytes are partially due to changes in the activity coefficients of the solutes in the mobile phase upon the addition of water. This is especially valid for the rise in the capacity factors at higher concentrations of water. In this case the relative importance of the "slow"- and "quick"-type sites for the adsorption of the analytes would remain unchanged. This might be an alternative explanation for the constancy of h.

Influence of column pressure and column stability

During the first period of use of a column, the back pressure at a given temperature increased continuously. After cleaning the bottom frit of the column, the back pressure was significantly reduced and became very stable. Changes in the solvent composition had no significant additional influence on the back pressure and on the plate height after changing back to the solvent used originally. This implies that changes in the swelling state of CTA were reversible within the range of solvent mixtures investigated.

The increase in back pressure during the first period was utilized to investigate the influence of the pressure on the retention and on the efficiency. Both the retention and the efficiency are influenced as shown in Table V. The capacity factor decreases

TABLE V

REDUCED PLATE HEIGHT, h, AND CAPACITY FACTOR VALUES, κ, AS A FUNCTION OF THE BACK PRESSURE OF THE COLUMN

Eluent: ethanol–water (96:4, v/v). Temperature: 50°C. Flow-rate: 1 ml/min. 1 atm $= 1.0133 \cdot 10^5$ Pa.

Code No.	Solute		ΔP (atm)			
			25–30		90–95	
			κ	h	κ	h
4	Anthracene		1.99	12	1.85	20
8	Phenyldi-	I	1.98	13	1.84	19
	oxolanone	II	3.75	15	3.47	22
9	Phenyltetrahydro-	I	0.54	12	0.53	17
	oxazolone	II	0.88	16	0.86	24
12	TFAE	I	0.59	34	0.53	35
		II	1.60	63	1.44	72
20	Tröger's base	I	1.11	66	1.05	80
		II	2.36	99	2.19	117
26	FMOC-Trp methyl ester	L	2.94	215	2.50	245

with increasing pressure, whereas the plate height increases. Most probably, some of the narrow structured sites ("cavities") become less accessible in a "compressed" state. This reduced accessibility leads to reduced capacity factors and a significant increase in h.

CONCLUSIONS

In this paper the influence of the temperature and the eluent composition on the theoretical plate height is investigated. The data show that an increase in temperature greatly improves the efficiency by affecting the diffusion velocity at the "slow"-type sites. Probably it also causes some changes in the swelling state of the packed bed.

Changes in the solvent composition affect the elution strength and the mean viscosity of the solvent as well as the swelling state of the adsorbent. The relative contribution of the "slow"-type sites for the overall adsorption is changed in these ways. With the addition of methanol and water, the importance of the "slow"-type sites generally decreases. These sites seem to be more polar than the "quick"-type sites and are very important for enantioselective recognition. The addition of methanol consequently leads to a decrease in the plate height of the analytes and in their retention. 1- and 2-propanol cause a small increase in the plate height, predominantly due to viscosity effects. They may also affect to some extent the swelling state of the packing. Cyclohexane is predominantly a competitor at the rather non-polar "quick"-type sites. Thus it increases the relative importance of the "slow"-type sites for several analytes, causing a small increase in the plate height connected with a decrease in retention.

Stereorecognition seems to occur mainly when adsorption onto the narrow "slow"-type sites is involved. The availability of these sites, and therefore their relative contribution to the overall retention, is determined by the competitive adsorption of solvents on this type of sites and by the swelling state. In both ways the eluent composition is a decisive factor for the enantioselectivity of the system. Methanol most often causes a decrease in enantioselectivity, whereas water and cyclohexane cause an increase.
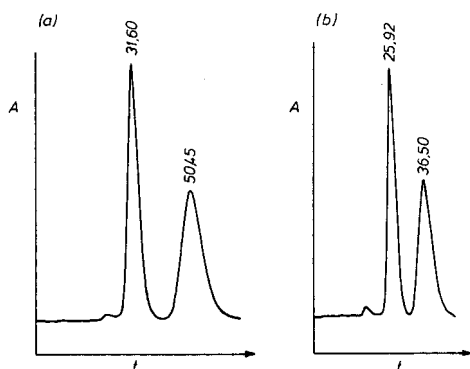
Fig. 5. Chromatograms of racemic Tröger's base obtained with different mobile phases. t = time in min; A = UV absorption. Stationary phase: swcrCTA. Mobile phases: (a) ethanol–water (96:4); (b) methanol–ethanol–water (20:67.2:12.8). Column: 250 mm × 10 mm I.D. Flow-rate: 1 ml/min. Temperature: 50°C.

For practical use it is important that changes in the swelling state induced by changes in the solvent composition are fully reversible within the range of solvent composition investigated.

There was a certain influence of pressure on the plate height. Obviously the packed bed is still compressible to a small extent which affects the adsorption kinetics onto the "slow"-type sites.

The chromatograms in Fig. 5 illustrate the influence of the eluent composition on the peak width and the chromatographic resolution of racemic Tröger's base.

The detailed study of the plate height dependence on the four variables structure [3], retention [3], eluent composition and temperature provides interesting information about the mechanisms of adsorption and chiral recognition on swollen crystalline CTA materials. The consequences for the optimization of separations of optical isomers by choosing an appropriate eluent composition, temperature and flow-rate for an improvement in the efficiency will be discussed in detail in a forthcoming paper [5].

REFERENCES

1 G. Blaschke, *J. Liq. Chromatogr.*, 9 (1986) 341.
2 T. Shibata, I. Okamoto and K. Ishii, *J. Liq. Chromatogr.*, 9 (1986) 313.
3 A. Rizzi, *J. Chromatogr.*, 478 (1989) 71.
4 *CRC Handbook of Chemistry and Physics*, CRC Press, Boca Raton, FL, 1980.
5 A. Rizzi, *J. Chromatogr.*, 478 (1989) 101.

EVALUATION OF THE OPTIMIZATION POTENTIAL IN HIGH-PERFORMANCE LIQUID CHROMATOGRAPHIC SEPARATIONS OF OPTICAL ISOMERS WITH SWOLLEN MICROCRYSTALLINE CELLULOSE TRIACETATE

ANDREAS M. RIZZZI

Institute of Analytical Chemistry, University of Vienna, Währingerstrasse 38, A-1090 Vienna (Austria)

(First received February 27th, 1989, revised manuscript received April 27th, 1989)

SUMMARY

Quantitative data concerning the effect of temperature, solvent composition and flow-rate on the enantioselectivity, efficiency and retention for optical isomers on swollen crystalline cellulose triacetate are reported. Based on these data, the optimization potential of the named variables for the separations of optical isomers is discussed with respect to the chromatographic resolution as well as to the analysis times and the detection limits for the analytes. The trends observed can serve as guidelines for the derivation of optimization strategies.

INTRODUCTION

Triacetylated cellulose material has been used for several years as a stationary phase for the chromatographic separation of optical isomers[1–18]. Due to the current high interest in the role of optical isomers in biochemical processes, separation techniques for enantiomeric compounds are developing rapidly. This has led also to a renaissance in the use of cellulose triacetate (CTA). Its chemical structure allows various types of interactions with functional groups commonly encountered in drugs, thus enabling chiral recognition and discrimination for a variety of analytes of different structural types and sizes. This explains the wide field of applications of CTA chromatography to pharmaceutically active substances, which have been reviewed recently by Blaschke[12] and Shibata *et al.*[14].

CTA can be used either in a swollen microcrystalline state or as a layer coated on porous silica particles. Both types have quite different chromatographic behaviours, especially stereoselectivity and efficiency. The differences in stereoselectivity have been discussed by Shibata *et al.*[14].

This paper deals with the evaluation of the optimization potential of different variables in chromatography with swollen microcrystalline cellulose triacetate (swcr-CTA). The dependence of the plate height, enantioselectivity, capacity factors and the resolution on the eluent composition and on the process variables, temperature and flow velocity, has been investigated systematically. The implications of these findings are discussed for a rational optimization of the chromatographic separations.

A thorough optimization of a separation may be of enhanced interest for routine analysis methods or where preparative scale separations are performed.

EXPERIMENTAL

Apparatus

Chromatographic experiments were carried out using a high-pressure liquid chromatographic pump (Model L-6200 intelligent pump; Merck-Hitachi, Tokyo, Japan), a syringe-valve injector (Model 7161; Rheodyne, Cotati, CA, U.S.A.) equipped with a 20-μl loop, a column oven (Model 655A-52, Merck-Hitachi) and an UV detector (Model L-4000, Merck-Hitachi) connected to an integrator (Model D-2000 chromato-integrator, Merck-Hitachi).

Column

A prepacked column (250 mm × 10 mm I.D.) filled with swcrCTA with a mean particle diameter of 10 μm was used (Hibar®; E. Merck, Darmstadt, F.R.G.).

Reagents and samples

Organic solvent components were obtained from E. Merck. Methanol and hexane were of LiChrosolv® quality, absolute ethanol of p.a. quality. Water used for the eluent preparation was distilled twice from a quartz apparatus and additionally purified by passing through a RP-8 column. The eluent mixtures were premixed and degassed in an ultrasonic bath.

The analyte samples were obtained in the highest purity grade available or were received in an highly purified state as gifts from synthesis laboratories.

Procedure

All the data refer to isocratic elution at the given temperature. After establishment of the thermal equilibrium, the constancy of retention data was about $\pm$1%. The void volume of the column was estimated from the retention volume of the system peaks of injected water, methanol or propanol and was approximately 15 ml. All the calculations of the capacity factors are based on a void volume of 15.00 ml for all solvent mixtures. UV detection was performed at 254 nm.

BASIC MODEL

Retention mechanism, capacity factor and stereoselectivity

swcrCTA differs significantly in its adsorbent characteristics from other packing materials. As this material provides different types of adsorption sites, different mechanisms of adsorption seem to exist. The retention of an analyte is determined by its structure in a way which is not completely understood and for which only some empiric rules can be given.

Interactions both between polar structures and between non-polar structures seem to be important. Obviously, the molecular volume plays an important role in this respect. For molecules with sterically large structures, like *tert.*-butyl groups, an exclusion from most of the adsorption sites is observed, *e.g.*, for tri-*tert.*-butylbenzene. Similarly, in ethanolic eluents, charged organic analytes are eluted before the column

void volume[19]. For non-polar aromatic and polyaromatic hydrocarbons the retention decreases with increasing size of the molecule. Generally, however, the retention is not simply correlated with the molecular size. Obviously, the configuration of the analytes plays an important role in the retention, otherwise this material would not be of great use for enantiomeric separations.

Prior to the presentation of the results a model concerning the adsorption mechanism is briefly discussed which can serve as a basis for the interpretation and discussion of the experimental data in the next section. The model has been derived to a significant extent from peak dispersion data for swcrCTA adsorbents[19,20]. Those investigations reveal that with respect to the mass-exchange kinetics, at least two (but maybe more) different types of adsorption sites are operative: "quick"-type and "slow"-type sites. These types differ in the kinetics of the adsorption/desorption process, mainly due to the different diffusion velocities very near to the adsorption sites. The adsorption sites differ also in their availability for different analytes and probably in the strength of interaction with polar groups in the analyte molecule. (The existence of a mixed adsorption mechanism, *i.e.*, of different types of sites with respect to the type and strength of interaction, has been proposed by Scharf *et al.*[13]. It is likely that the differences in the kinetic features and in the types of interactions are correlated: the sites which form stronger interactions with polar groups in the analytes seem to be of the "slow"-type[19].

Concerning the peak broadening process, the observed plate height is predominantly dependent on the kinetics of the adsorption/desorption proces. Hindered diffusion to (and at) narrow (maybe "channel"-like or "cavity"-like) structures of the swollen absorbent is probably responsible for the slow kinetics, which is observed for most analytes. The plate height of an analyte is determined (i) by the accessibility of the adsorption sites which influences the velocity of motion of the analytes to and at the sites, and (ii) by the relative contributions of "slow" (narrow)- and "quick"-type (broad) sites to the retention of the analyte. The most important parameter influencing the plate height of the analytes is therefore their molecular structure, since the structure determines the steric size and the types of interactions predominantly formed, and thus the diffusion velocity and the type of sites at which the analyte is preferentially adsorbed. The plate height is therefore not simply correlated with the capacity factors of the analytes. Any change in the accessibility and in the availability of the different types of sites, *e.g.*, by changes in the eluent composition, influences the overall plate height.

The retention of analytes is determined by the activity coefficients of the analytes in the mobile phase, and by the availability of the different adsorption sites. The availability depends on the swelling state of CTA and on the strength of the competitive adsorption effects of the solvent components at the adsorption sites. With the exception of the changes in the swelling state, this behaviour is analogous to other types of adsorption chromatography. Since both types of interactions, namely those between polar structures and those between non-polar structures, are operative, polar and non-polar solvent components act as competitors for adsorption. As regards the strength of the competitive effect, the size of the solvent molecules seems to play a major role. The solvent composition also influences the swelling state of the swcrCTA packing, and thus the number of different adsorption sites available. Owing to all these facts, no simple dependence of the capacity factors on the "hydro-

phobicity" and the "polarity" parameters of the eluent mixture is found, in contrast to reversed-phase chromatography with alkylsilica adsorbents and aqueous mobile phases.

For the steric discrimination of enantiomers, narrow adsorption sites seem to be decisive. Most probably these sites are identical with those observed as "slow"-type sites from the point of view of the kinetics of mass exchange. The solvent composition affects the availability of these narrow sites either by the competitive adsorption of solvent components or by influencing the swelling state of the packing material. In these ways the solvent composition has a strong influence on the stereoselectivity.

The dependence of the capacity factor, κ, enantioselectivity coefficient, α, and theoretical plate height, H, on temperature, eluent composition and flow-rate is reported in detail in the following section.

RESULTS AND DISCUSSION

For the optimization of separations of enantiomers in high-performance liquid chromatography (HPLC) the most frequently used criterion is sufficient resolution of the optical isomers, obtained in the shortest possible analysis time, with the lowest possible sample dilution. In this paper the following definition of the chromatographic resolution, R_S, is used

$$R_S = (\alpha - 1) \cdot \frac{\kappa_I}{1 + \kappa_I} \sqrt{\frac{N_I + N_{II}}{2}} \tag{1}$$

where κ denotes the capacity factors of the analytes, the indices I and II refer to the first and second eluted isomer, respectively, α denotes the enantioselectivity coefficient and N the plate number with respect to the indicated enantiomer.

The reason for using the mean value of N in eqn. 1 is the observation that the plate numbers of the two isomers are most often considerably different when using swcrCTA packings. This allows (i) the correlation to be kept between the numerical values of R_S and the separation effect obtained more or less unchanged in the usual manner (for symmetric peaks of equal height, a R_S value of 6 means approximate "baseline separation"), and (ii) calculation of the minimum plate number, $\bar{N}_{min}$, which is necessary to obtain a certain resolution, in a simple way. This would not be as simple when applying a more fundamental equation[a] for the resolution of peaks with strongly

---

[a] The chromatographic resolution of two peaks with very different plate numbers is defined in a more appropriate way by

$$R_S = \frac{t_{Rj} - t_{Ri}}{\bar{\sigma}_t}$$

where $\bar{\sigma}$ is the mean standard deviation of the two peaks. Substituting the retention time and the peak standard deviation by operational parameters leads to:

$$R_S = (\alpha_{ji} - 1) \cdot \frac{2\kappa_i}{(1 + \kappa_i)\sqrt{N_j} + (1 + \kappa_j)\sqrt{N_i}} \sqrt{N_i N_j}$$

different peak widths. However, for the discussion of the trends in resolution and analysis time, in this paper, the approximation of eqn. 1 is acceptable.

The minimum analysis time is defined in this context by

$$t_{R,min} = (L_{min}/u) (1 + \kappa_{II}) = (\bar{H}\bar{N}_{min}/u) (1 + \kappa_{II}) \tag{2}$$

where H denotes the theoretical plate height, L the column length and u the linear flow velocity.

Optimization of the separation can be carried out by tuning at least one of the three decisive chromatographic parameters, α, κ, and/or N. Thus, the knowledge of the quantitative dependence of these chromatographic parameters from the variables, eluent composition, temperature and flow-rate, is a prerequisite for any rational optimization.

The chiral analytes shown in Table I were used for this investigation.

Optimization potential of the temperature

The influence of the temperature on the capacity factor, the enantioselectivity and the plate height is given in Table II. The capacity factors decrease with increasing temperature for all the analytes investigated. A good linear correlation is obtained between $\ln \kappa$ and $1/T$. The slope of this plot is similar to that observed in reversed-phase chromatography[20]. No effects, specific to CTA, were found with respect to this general trend.

Considering the enantioselectivity at different temperatures, a small increase is observed for some analytes (TFAE, Tröger's base), whereas for others (spirobi-indanone, phenyldioxolanone) a slight decrease is observed. Probably the temperature increase causes some changes in the swelling state. This influences the structure of the adsorbent and thus to a certain degree the accessibility of the adsorption sites. In this way the enantioselectivity may be enhanced or reduced.

The plate height generally decreases dramatically at higher temperatures (Fig. 1), because of the increased diffusion velocity. Exceptions are those solutes where the kinetics of mass exchange is rapid even at low temperatures, *e.g.*, phenyldioxolanon. In these cases the decrease is not as dramatic, but comparable to the effects found in reversed-phase chromatography with ODS packings.

The strong influence of the temperature on all of the chromatographic parameters (κ, α, H) means that the temperature is a most important optimization parameter. The decrease in capacity factors in combination with the increase in plate number, and sometimes also in enantioselectivity, makes the use of elevated temperatures favourable in those cases where no racemization of analytes takes place at elevated temperatures. It allows reduced analysis times, increased peak heights and thus lower detection limits for the analytes.

The influence of the temperature on the chromatographic resolution may differ, as is seen in Table III. At constant enantioselectivity the effect of a decreasing capacity factor is by far overcompensated by the increase in N, for most analytes showing medium or low efficiency. In these cases (TFAE, Tröger's base) the resolution is therefore much improved with increasing temperature. Parallel to the improvement in the chromatographic resolution, the minimum analysis time is reduced significantly (Table III). With methanol–ethanol mixed mobile phases the temperature effect is less

TABLE I

STRUCTURES OF CHIRAL COMPOUNDS USED AS TEST ANALYTES

The given capacity factor values, κ_I, refer to the first enantiomer eluted and are measured with the eluent ethanol–water (96:4, v/v) at 50°C.
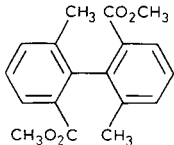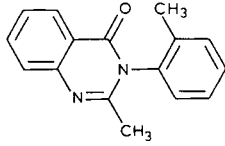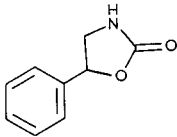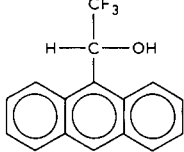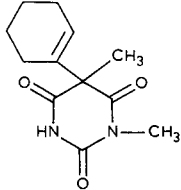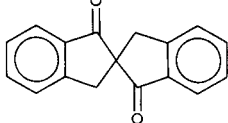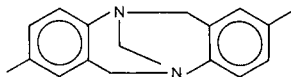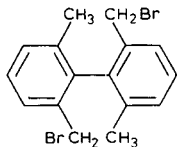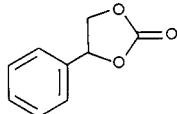
Code No.	Solute	κ	Structure
1	o,o'-Dimethyl-o,o'-di(methoxycarbonyl)biphenylene	0.26	
2	Methaqualone	0.27	
3	5-Phenyltetrahydrooxazol-2-one	0.53	
4	2,2,2-Trifluoro-1-(9-anthryl)ethanol (TFAE)	0.57	
5	Hexobarbital	0.83	
6	2,2'-Spirobiindan-1,1'-dione	0.95	
7	Tröger's base	1.05	
8	o,o'-Dimethyl-o,o'-di(bromomethyl)biphenylene	1.11	
9	4-Phenyl-1,3-dioxolan-2-one	1.84	

TABLE II

PLATE HEIGHT, H, CAPACITY FACTOR, κ, AND ENANTIOSELECTIVITY, α, FOR VARIOUS CHIRAL ANALYTES AS A FUNCTION OF THE TEMPERATURE

The code numbers of the solutes are as in Table I. The indices I and II indicate the first and second isomers eluted. Flow-rate: 1 ml/min.

Code	Solute	T (°C)	κ_I	H_I	κ_{II}	H_{II}	α
Eluent: ethanol–water (96:4, v/v)							
4	TFAE	30	0.73	690	1.94	1470	2.66
		40	0.61	520	1.68	1060	2.75
		50	0.52	320	1.45	660	2.79
		60	0.44	220	1.22	435	2.77
7	Tröger's base	30	1.33	1370	2.75	1980	2.07
		40	1.09	1180	2.32	1800	2.13
		50	0.99	800	2.12	1170	2.14
		60	0.80	445	1.77	710	2.21
Eluent: ethanol–methanol–water (76.8:20:3.2, v/v)							
4	TFAE	30	0.51	630	1.12	980	2.23
		40	0.49	610	1.08	950	2.23
		50	0.42	510	0.98	650	2.34
		60	0.38	480	0.89	560	2.38
6	Spirobiindanone	30	1.37	670	2.88	1000	2.11
		40	1.23	690	2.54	1010	2.06
		50	1.00	610	2.03	870	2.03
		60	0.86	400	1.72	840	1.99
7	Tröger's base	40	0.92	790	1.47	1160	1.60
		50	0.82	720	1.38	870	1.68
		60	0.71	385	1.24	570	1.76
9	Phenyloxolanone	40	1.98	180	3.83	170	1.94
		50	1.73	–	3.26	–	1.88
		60	1.44	110	2.68	150	1.86

pronounced than with a pure ethanolic eluent, since the addition of methanol causes an improvement in the efficiency itself (cf., next section).

In cases where the enantioselectivity decreases with increasing temperature or those which show an high efficiency even at low temperatures, the resolution slightly decreases with increasing temperature (phenyldioxolanone, spirobiindanone). The positive effect with respect to the analysis time and the detection limit remains.

At temperatures above 60°C and at flow-rates > 0.42 mm/s, the long-time stability of the packing with respect to efficiency may be reduced and should be controlled. A slight increase in the plate height may result from a strong compression of the swollen bed. At 50°C and flow-rates of 0.28 mm/s ($\approx$ 1 ml/min with a column of 10 mm I.D.) no significant loss in efficiency with time was observed over a period of several months.
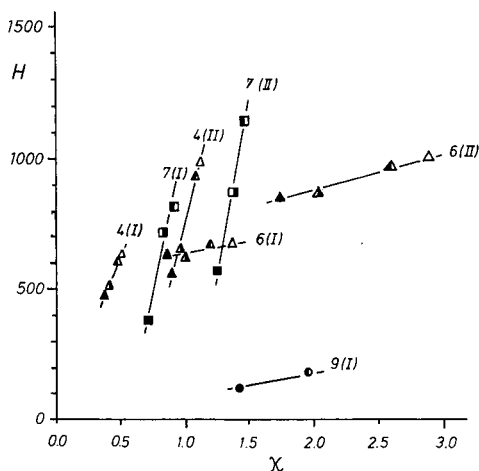
Fig. 1. Plate heights, H, and capacity factors, κ, as a function of the temperature. Code numbers of solutes as in Table I. Temperature codes: △. ○, □ 30°C; ◢, ◖, ◼ 40°C; ▲, ◕, ◪ 50°C; ▲, ●, ◼ 60°C. Eluent: methanol–ethanol–water (20:76.8:3.2, v/v); flow-rate 1 ml/min.

TABLE III

CHROMATOGRAPHIC RESOLUTION, R_S, AND ANALYSIS TIME, $t_{R,min}$, AS A FUNCTION OF COLUMN TEMPERATURE

$t_{R,min}$ = Minimum analysis time defined in eqn. 2; $t_{R(25)}$ = analysis time using a column of length 25 cm; flow-rate 1 ml/min.

		T (°C)			
		30	40	50	60
Eluent: ethanol–water (96:4, v/v)					
4 TFAE	R_S	11.4	12.6	14.8	15.8
	$t_{R,min}$	23.2	19.2	15.0	12.6
	$t_{R(25)}$	44.1	40.2	36.8	33.3
7 Tröger's base	R_S	7.6	7.8	9.2	11.5
	$t_{R,min}$	32.6	38.3	30.5	21.7
	$t_{R(25)}$	56.3	49.8	46.8	41.6
Eluent: ethanol–methanol–water (76.8:20:3.2, v/v)					
4 TFAE	R_S	7.3	7.2	8.2	8.1
	$t_{R,min}$	26.1	25.9	21.7	21.0
	$t_{R(25)}$	31.1	31.2	29.7	28.4
3 Spirobiindanone	R_S	11.2	10.2	9.6	9.9
	$t_{R,min}$	31.8	31.2	28.4	24.7
	$t_{R(25)}$	58.2	53.1	45.5	40.8
7 Tröger's base	R_S	—	4.7	5.5	7.3
	$t_{R,min}$	—	47.4	39.2	27.7
	$t_{R(25)}$	—	37.1	36.7	33.6
10 Phenyloxolanone	R_S	—	23.4	—	22.5
	$t_{R,min}$	—	18.6	—	14.7
	$t_{R(25)}$	—	72.5	—	55.2

Influence of the mobile phase composition

The eluent composition can be varied within certain limits. These limits are given on the one hand by the solubilities of the analytes in the eluent mixture and on the other hand by the solubility of the CTA material in the solvent and by the stability of its swollen state. The spectrum of the solvent components which can be used conveniently includes mainly alcohols, water, alkanes and some ethers. No ketones or chloro-alkanes should be used.

This paper shows the results of an investigation of the influence of methanol, 1-propanol, 2-propanol, water and cyclohexane at various concentrations mixed with ethanol. The composition of these mixed phases is given together with their abbreviations in the Appendix. Fig. 2 shows the dependence of ln κ of several analytes on the concentration of methanol in methanol–ethanol mixed mobile phases. Fig. 3 shows the capacity factors of the second eluted enantiomers for all analytes of Table I and for some non-chiral, non-polar aromatic hydrocarbons in various mixed mobile phases. Fig. 4 shows the corresponding enantioselectivity coefficients, α, and Fig. 5 the corresponding plate height values, H.

(i) Methanol. For all solutes investigated, a decrease in the capacity factor with increasing methanol content in methanol–ethanol mixed mobile phases is observed. In most cases a fairly linear correlation of ln κ with the volume fraction of methanol is found (Fig. 2). The slopes of such plots are sometimes different for different compounds, reflecting differences in the molecular sizes and in the adsorption mechanisms, as discussed above.

It is noteworthy that the addition of methanol causes a decrease in the capacity factors not only for polar but also for non-polar solutes (Fig. 3b). With swcrCTA adsorbents, the elution power of an eluent component is determined not only by the strength of the competitive interaction with the binding sites and by the strength of interaction with the solute, but also by its steric size. Methanol is a stronger competitor than ethanol for the adsorption of the solutes at narrow adsorption sites. Secondly, the addition of methanol changes the swelling state of the adsorbent and in this way the number of adsorption sites available. Both these effects overcompensate by far the
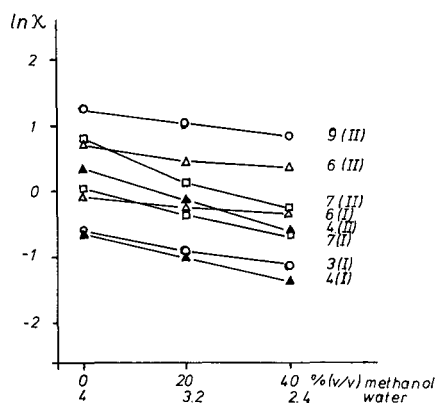
Fig. 2. Dependences of the logarithm of the capacity factors of various analytes on the volume fraction of methanol in methanol–ethanol–water mixed mobile phases. Code numbers of solutes as in Table I. Chromatographic conditions: flow-rate 1 ml/min; temperature 50°C.
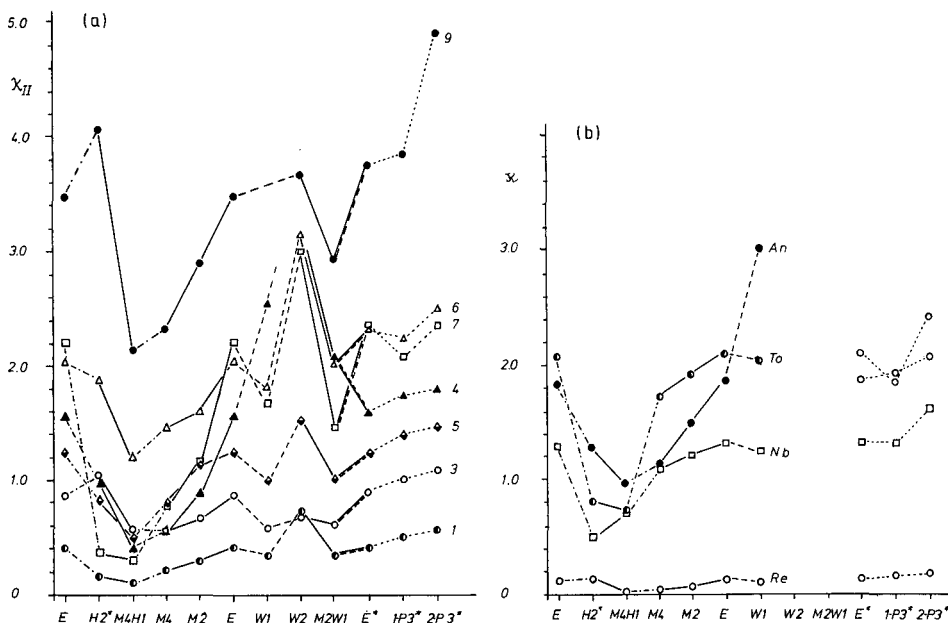
Fig. 3. Capacity factors of the second enatiomers eluted of various analytes obtained at various mobile phase compositions. (a) Compounds listed in Table I. Code numbers of solutes as in Table I. (b) Non-chiral, non-polar aromatic hydrocarbons: An = anthracene; To = toluene; Nb = nitrobenzene; Re = resorcinol. Solid lines: methanol content changed. Dotted lines: propanol content changed. Broken lines: water content changed. $— \cdot — \cdot —$, Cyclohexane content changed. Eluent codes as in the Appendix. Chromatographic conditions: Flow-rate 1 ml/min; temperature 50°C. The asterisks indicate a lower pressure drop, as specified in Table IV.
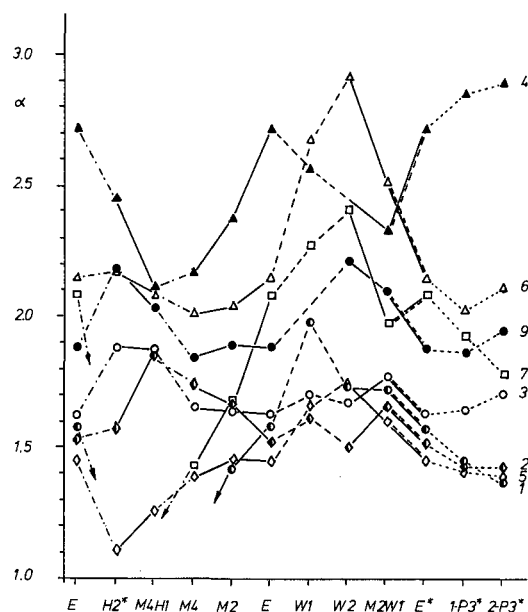
Fig. 4. Stereoselectivity, α, at various compositions of the mobile phases. Symbols and chromatographic conditions as in Fig. 3. Eluent codes are given in the Appendix.
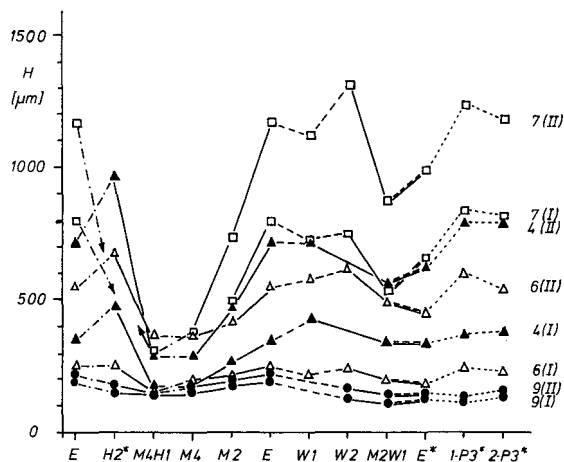
Fig. 5. Plate height, H, at various compositions of the mobile phase. Symbols and chromatographic conditions as in Fig. 3. Eluent codes as in the Appendix.

increase in the mobile phase activity coefficients of non-polar solutes (resulting from the lower solvation power of methanol for these types of analytes in comparison to ethanol), which, alone, would cause an increase in the capacity factors.

The enantioselectivity generally decreases upon addition of methanol (Fig. 4). This can be understood by assuming methanol to be a competitor especially for the narrow sites, which are most important for chiral recognition, and, further, that in the altered swelling state the number of narrow sites available is smaller.

Of great consequence is the strong decrease in plate height upon the addition of methanol (Fig. 5). This effect is found for all substances with exception of those compounds (phenyldioxolanone, phenyloxazolone) where low plate height values were found even before. Obviously, the reduced importance of the narrow sites, where the adsorption kinetics is slow, causes changes in the same direction as a reduction in viscosity.

The addition of methanol offers similar advantages as does the elevation of temperature: shorter analysis time, improved detection limit and little altered, or only slightly reduced, resolution. This is illustrated in Table IV, which shows that the decrease in the chromatographic resolution is small, since the gain in efficiency balances the loss in enantioselectivity in most cases.

(ii) Cyclohexane. In most cases, the addition of cyclohexane to the eluent leads to a decrase in retention. The magnitude of this effect is dependent on the analyte structure. It results either from an enhanced competitive adsorption of this solvent component at non-polar adsorption sites, and/or from the improved solvation power of the mixed solvent for non-polar analytes (reduced mobile phase activity coefficient). It should be mentioned in this context that methanol as well as cyclohexane are stronger displacers than ethanol on swcrCTA materials.

With the addition of cyclohexane an improvement in stereoselectivity is often observed. (Exceptions are TFAE and hexobarbital, where a slight decrease in α is observed, and Tröger's base, which cannot be resolved in systems with cyclohexane.) The influence of cyclohexane on the plate height is rather small. The increased plate

TABLE IV

CHROMATOGRAPHIC RESOLUTION, R_S, AND MINIMUM ANALYSIS TIME, $t_{R,min}$, AS A FUNCTION OF THE SOLVENT COMPOSITION

Flow-rate: 1 ml/min. Temperature: 50°C. Eluent code as given in the Appendix.

Code	Solute		Eluent				
			E	M2	M4	M4H1	W1
Back pressure with pure ethanol: 90–95 atm[a]							
9	Phenyldioxanone	R_S	20.0	20.7	18.6	20.9	—
		$t_{R,min}$	20.2	16.9	16.1	13.5	—
		$t_{R(25)}$	67.1	58.4	49.8	47.0	—
3	Phenyloxazolone	R_S	7.6	7.4	7.6	8.6	6.9
		$t_{R,min}$	22.0	20.2	18.5	16.1	20.4
		$t_{R(25)}$	27.9	24.9	23.3	23.0	23.6
6	Spirobiindanone	R_S	15.0	13.8	13.5	13.1	18.8
		$t_{R,min}$	18.2	16.8	16.5	15.0	13.4
		$t_{R(25)}$	45.5	38.9	36.9	32.9	42.0
4	TFAE	R_S	14.4	10.1	8.0	6.1	6.7
		$t_{R,min}$	16.0	16.8	17.4	20.8	19.1
		$t_{R(25)}$	38.3	28.2	23.3	21.0	53.1
7	Tröger's base	R_S	9.0	5.6	3.8	—	9.1
		$t_{R,min}$	32.1	34.4	41.7	—	26.4
		$t_{R(25)}$	48.0	32.3	26.6	—	40.1
5	Hexobarbital	R_S	—	5.5	4.6	—	6.4
		$t_{R,min}$	—	34.6	35.2	—	28.0
		$t_{R(25)}$	—	31.8	26.9	—	29.9

Code	Solute		E	1-P3	2-P3	H2	W2	M2W1
Back pressure with pure ethanol about 30 atm[a]								
9	Phenyldioxanone	R_S	25.0	26.5	27.5	30.1	31.1	28.6
		$t_{R,min}$	17.1	16.4	19.3	15.2	13.5	12.3
		$t_{R(25)}$	71.3	72.5	88.4	75.9	69.9	58.8
3	Phenyloxazolone	R_S	9.4	10.4	12.2	11.8	—	9.0
		$t_{R,min}$	17.9	17.3	15.3	15.5	—	16.1
		$t_{R(25)}$	28.2	29.9	31.1	30.5	—	24.0
6	Spirobiindanone	R_S	17.2	14.4	16.7	14.2	26.8	19.9
		$t_{R,min}$	16.3	20.1	18.8	18.3	13.9	13.6
		$t_{R(25)}$	46.5	48.3	52.4	43.1	62.1	45.2
4	TFAE	R_S	15.1	15.6	16.0	8.2	—	15.0
		$t_{R,min}$	15.5	15.7	15.7	21.7	—	18.4
		$t_{R(25)}$	39.0	40.9	41.7	29.6	—	46.1
7	Tröger's base	R_S	10.6	7.5	7.1	—	12.6	7.9
		$t_{R,min}$	28.6	36.7	42.3	—	28.4	27.8
		$t_{R(25)}$	50.4	45.9	50.1	—	59.9	36.5
5	Hexobarbital	R_S	—	5.0	4.9	—	7.0	6.6
		$t_{R,min}$	—	43.3	45.3	—	32.5	27.1
		$t_{R(25)}$	—	35.9	36.8	—	37.6	29.9

[a] A small influence of the back pressure on the capacity factors, the enantioselectivities and the plate heights is observed[19]. The significance of the differences in the back pressure values given can be judged by comparing the data sets obtained with the eluent E.

heights in several cases probably result from the limited access of cyclohexane molecules to narrow "slow"-type adsorption sites.

The increase in enantioselectivity connected with a decrease in retention is of great practical importance for reducing the analysis time and improving resolution (Table IV).

(iii) 1-Propanol and 2-propanol. The addition of propanol induces a moderate increase in the capacity factors of all analytes investigated. This effect is especially pronounced for rather small analytes with polar structures, *e.g.*, phenyldioxolanone). It seems to be quite the opposite of the effect observed with methanol. 2-Propanol generally shows a stronger effect than 1-propanol.

The enantioselectivity is little influenced by the addition of propanol within the range of 0–30% (v/v).

The plate height generally increases (opposite effect with methanol). At least partially, this effect is caused by an increase in the viscosity of the eluent.

Generally, the addition of propanol does not offer substantial advantages. In special cases the slight increase in selectivity might be of importance.

(iv) Water. The influence of water strongly depends on its concentration in ethanol and on the solute structure. At low concentrations [10% (v/v) water added] the solute capacity factors decrease in most cases. As with methanol, this effect may be due to changes in the swelling state of CTA and to a competitive effect at the narrow adsorption sites (which are probably important for the more polar interactions). Unlike methanol, however, water increases the enantioselectivity considerably.

At higher concentrations of water [20% (v/v) added] the retention increases in many cases. This effect depends on the analyte structure and is expected owing to the increase in the mobile phase activity coefficient. It is especially pronounced for analytes with large non-polar parts.

That both effects, reduction of the available free adsorption sites as well as the increase in activity coefficients, are operative is demonstrated by phenyldioxolanone, where the capacity factor of the first enantiomer eluted decreases, whereas that of the second increases.

Surprisingly, the plate height is little influenced by the addition of water in the concentration ranges described and for the analytes investigated. This may be due to a compensation of viscosity effects and displacement effects from the narrow adsorption sites.

The increase in enantioselectivity is the most important potential of water in the optimization of separations on CTA.

(v) Ternary mixtures. A useful combination of advantageous effects may be obtained by using ternary mobile phases of the type ethanol–methanol–cyclohexane and ethanol–methanol–water. In both these solvents the advantages of dramatically reduced capacity factors and significantly reduced band broadening (by methanol) can be combined in most cases with an enhanced enantioselectivity (by water or cyclohexane). This allows one to influence the analysis time, resolution and detection limit in the desired direction (*cf.*, Table IV).

The chromatograms of the racemic analytes Tröger's base, hexobarbital and TFAE in Fig. 6 illustrate the influence of the solvent composition on the chromatographic resolution and the analysis times.

When interest is not restricted only to chiral separations, CTA adsorbents offer

an high potential for tuning the selectivity also between different compounds by rather small changes in the mobile phase composition, as is seen from Fig. 3.

Optimum flow velocity and optimum column length

The plate height contribution which results from the mass exchange in the packed bed, H_b (*cf.*, refs. 21 and 22), is found to be the predominant contribution to the total plate height, H_{tot}[19,20]. H_b is known to increase approximately linearly with the flow velocity[21-25]. Because of the predominance of this linear contribution of H_b one also observes an approximately linear increase in the total plate height, H_{tot}, with u at flow velocities higher than u_{min} (Fig. 7). The high contribution of H_b causes the minimum of H to be situated at very low flow velocities, lower than 0.139 mm/s. (This value corresponds to 0.5 ml/min in a column with 10 mm I.D. and to about 0.09 ml/min in a column with 4 mm I.D) Fig. 7 illustrates the dependence of H on the flow velocity for analytes with different steric structures. The slope is not correlated with the capacity factor, as usual, but with the structure of the analyte, as has been pointed out in the first section and in ref. 19. Fig. 7 demonstrates the high potential of improving the separation by applying low flow velocities. However, its use results in very long analysis times.

In the range above u_{min} the total plate height, H_{tot}, can be expressed in most cases to a good approximation by

$$H_{tot} = a_i u \tag{3}$$

where a_i is the structure- and solvent-dependent slope. Such a simple linear dependence of H on u has interesting implications. Assuming N_{min} to be the minimum plate number
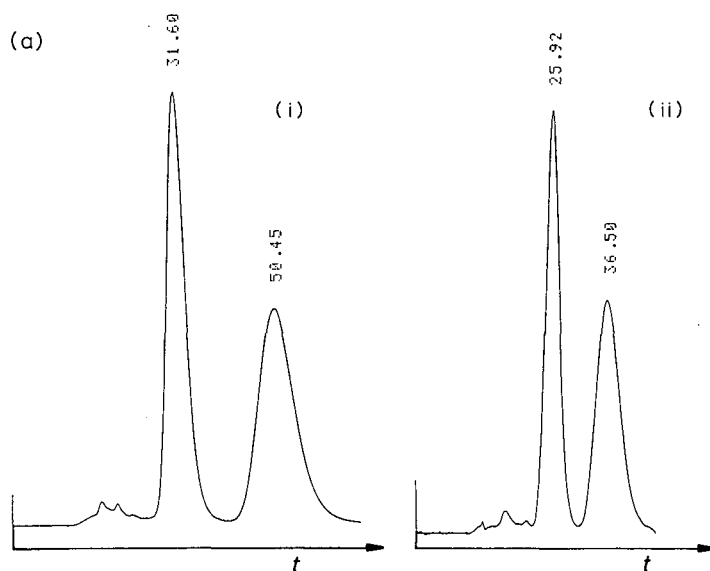
Fig. 6.
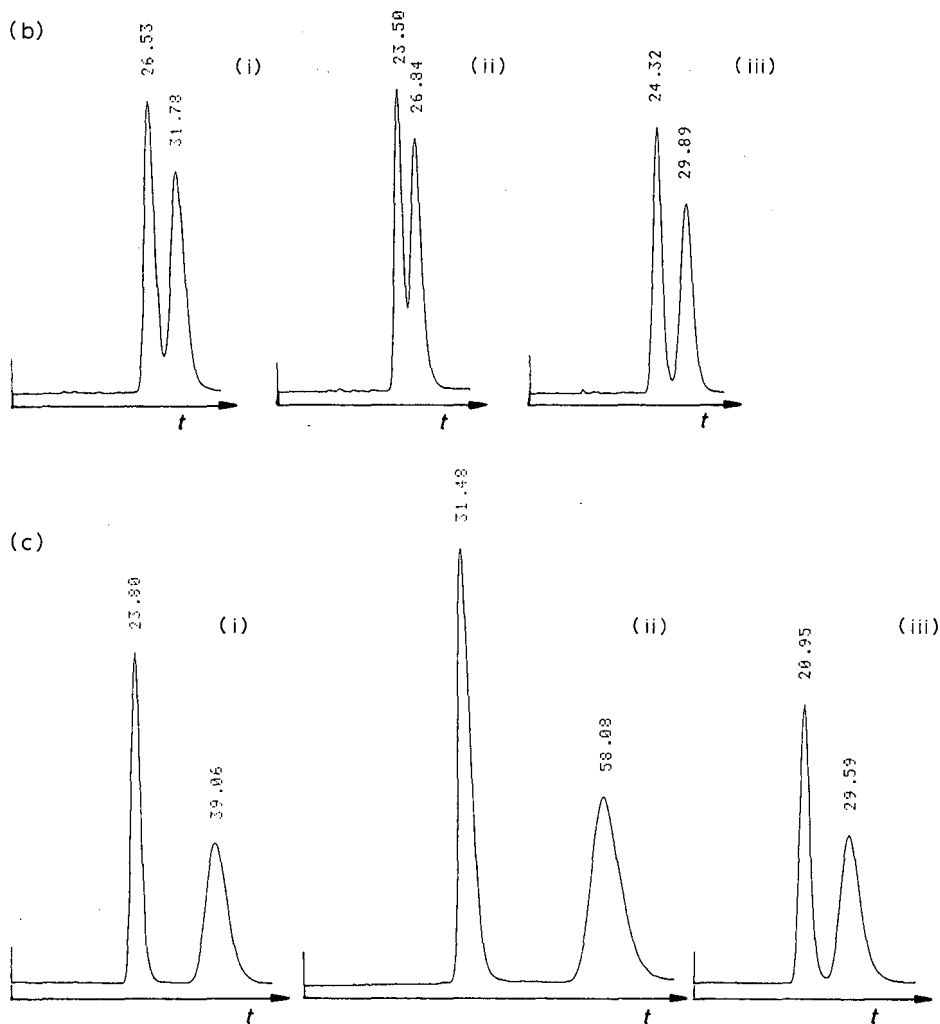
Fig. 6. Chromatograms of optical isomers as a function of the solvent composition. (a) Tröger's base: (i) ethanol–water (96:4) (E); (ii) methanol–ethanol–water (20:67.2:12.8) (M2W1). (b) Hexobarbital: (i) methanol–ethanol–water (20:76.8:3.2) (M2); (ii) methanol–ethanol–water (40:57.6:2.4) (M4); (iii) methanol–ethanol–water (20:67.2:12.8) (M2W1). (c) TFAE: (i) ethanol–water (96:4) (E); (ii) ethanol–water 86.4:13.6) (W1); (iii) cyclohexane–ethanol–water (20:76.8:3.2) (H2). Retention times in minutes. Flow-rate: 1 ml/min. Temperature: 50°C. Injection volume: 20 μl.

needed for a desired resolution in a given chiral separation problem, the minimum column length, L_{min}, which allows to obtain $\bar{N}_{i,min}$ at a certain value of $\bar{H}_i$, is given by eqn. 4:

$$L_{min} = \bar{N}_{i,min}\,\bar{a}_i u \tag{4}$$

If one is able to adjust the column length to L_{min}, e.g., by using small combinable columns one obtains for the minimum analysis time:

$$t_{Ri,min} = \bar{N}_{i,min}\,\bar{a}_i\,(1 + \kappa_{i,II}) \tag{5}$$
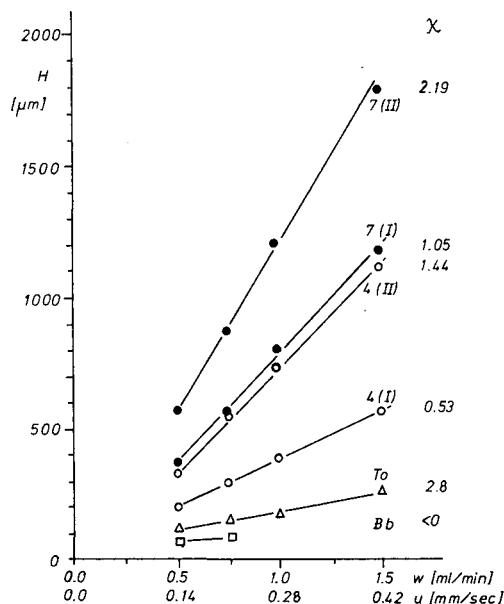
Fig. 7. Plate height as a function of the linear flow velocity, u. Code numbers of solutes as in Table 1; Bb = tri-*tert.*-butylbenzene; To = toluene. Eluent: ethanol–water (96:4, v/v). Temperature: 50°C.

In this case, and unlike the usual chromatographic situation, the analysis time is no longer a function of the flow velocity, but only of $\bar{N}_{i,min}$ and $\bar{a}_i$, the mean value of the H/u slopes of the two enantiomers. This may be an interesting aspect for highly repetitive analyses or in preparative separations, where an adjustment of the column length to the given problem might be worthwhile.

Column loadability

The loadability of swcrCTA packed columns is generally high. With concentration overloading, previous investigations[19] showed that the peak symmetry, plate height and elution time of the peak maximum is not significantly influenced up to an injected mass of 10–20 μg in a 250 mm × 10 mm column, with 20-μl injection volumes. The corresponding concentration is near the solubility limit for several substances.

Very recently, results differing from these have been reported for other types of analytes (substituted phenylthiazolinethiones)[26]. There, a slight tailing and a slight shift of the elution time of the peak maximum has been observed. Since this effect was found to differ for two enantiomers, or even to be in opposite directions, the enantioselectivity was found to be considerably influenced by the loading. In such a case the quality of a separation under concentration overloading cannot be predicted on the basis of the data obtained with low concentrations.

However, the injectable mass and the throughput can be considerably increased (further) by using volume overloading. To calculate the maximum allowable injection volume without loss in resolution, it is assumed that the chromatographic resolution is little affected (<5%) up to an injection volume equivalent to σ_{vi}, the standard

TABLE V

CALCULATED VALUES FOR THE MAXIMUM ALLOWABLE INJECTION VOLUME, V_{inj}max (5%), WHICH AFFECTS THE CHROMATOGRAPHIC RESOLUTION OF ENANTIOMERS BY NOT MORE THAN 5% IN A swcrCTA COLUMN (250 mm × 10 mm I.D.) AND APPROXIMATE MAXIMUM ALLOWABLE INJECTION VOLUME, V_{inj} max (t.b.), AT WHICH THE FIRST PEAK ELUTED JUST TOUCHES THE SECOND ONE

Temperature: 50°C. Eluent: ethanol–water (96:4, v/v). Pressure drop: 70 atm.

Code	Solute	$V_{inj}\ max(5\%)\ (\mu l)$	$V_{inj}\ max(t.b.)\ (ml)$
9	Phenyldioxolanone	1170	≈15
3	Phenyloxazolone	600	≈0.6
6	Spirobiindanone	920	≈7
4	TFAE	880	≈5.2
7	Tröger's base	1740	≈2

deviation of the analyte peak in volume units. This maximum allowable injection volume depends on type and structure of the analyte and on the temperature and the solvent composition, as was pointed out in the discussion of the efficiency in CTA columns. Table V shows these maximum allowable injection volumes for a 25 cm × 1 cm I.D. column.

In preparative scale separations, however, volume overloading is usually extended until the peaks are just touching. The maximum allowable injection volume in this sense depends on the resolution which can be obtained under the conditions chosen. For non-tailing peaks, these injection volumes are evaluated approximately by extrapolation and are given in Table V.

Pressure stability

The pressure stability of the column tested was excellent, especially after cleaning the bottom frit after the first 2.5 l of eluent had passed through the column at elevated temperature. At a temperature of 50°C and a flow velocity of 0.28 mm/s (1 ml/min), the back pressure, enantioselectivity, plate height and peak symmetry were constant and reproducible. It is important that changes in the solvent composition had no significant additional influence on the increase in the back pressure and plate height after reverting to the original solvent. Obviously, the changes in the swelling state were fully reversible.

CONCLUSIONS

The adsorption mechanism and the mass exchange process in swollen crystalline CTA packings are found to be different from those usually observed with silica and alkylsilica adsorbents. The plate heights are strongly dependent on the structures of the analytes but not on their capacity factors. The influence of temperature and solvent composition on the plate height, stereoselectivity and retention are often quite dissimilar to those usually observed.

The following general trends are found within the range of temperature or solvent composition investigated. Enhanced temperature induces improved efficiency, reduced retention and slightly increased or decreased stereoselectivity. Addition of

methanol, propanol, water and cyclohexane as solvent components to ethanol results predominantly in the following effects: (i) methanol [up to 40% (v/v)], improved efficiency, reduced retention and reduced stereoselectivity; (ii) cyclohexane [10 and 20% (v/v)], improved stereoselectivity, reduced retention and approximately constant or slightly reduced efficiency; (iii) propanol [up to 30% (v/v)], in some cases enhanced stereoselectivity, increased retention and reduced efficiency; (iv) water [up to 20% (v/v)], strongly enhanced stereoselectivity, approximately constant efficiency and reduced or enhanced retention, depending on the water concentration and the hydrophobicity of the solutes. The addition of two mobile phase modifiers allow one to combine the advantages of the single solvent components: (v) methanol–cyclohexane or methanol–water yield enhanced stereoselectivity, improved efficiency and reduced retention.

A reduction of the flow velocity strongly improves the efficiency. This effect is observed down to u_{min}, which lies at very low flow velocities of about 0.14 mm/s. The approximate linear dependence of the plate heights on the flow velocity means that the minimum analysis time is independent of the flow velocity.

The minimum analysis time is determined by the minimum column length needed to obtain sufficient resolution in a given chromatographic separation problem. It is determined therefore by the stereoselectivity and by the capacity factor of the second eluted enantiomers and the mean plate number for a given pair of enantiomers. Tables III and IV contain also the analysis time for columns of a constant length of 25 cm. This analysis time depends only on the capacity factors of the analytes. These data are useful for realistic cases where the column length cannot be varied and when the resolution obtained is sufficient.

From the point of view of chromatographic practice, it is important that a significant reduction of the analysis time can be achieved in most cases by increasing the temperature and by adding methanol, cyclohexane and/or water. This procedure allows in addition a significant lowering of the detection limit by improving the efficiency and by reducing the capacity factors of the analytes.

The stability of the pressure and column efficiency was good with the column investigated. Owing to the low plate height contribution arising from the dispersion in the streaming part of the mobile phase, the column has to be judged as a well packed high-performance column.

APPENDIX

Composition (%, v/v) of mixed mobile phases and their abbreviations:

E	Ethanol–water (96:4)
H2	Cyclohexane–ethanol–water (20:76.8:3.2)
M4H1	Methanol–cyclohexane–ethanol–water (40:10:48:2)
M4	Methanol–ethanol–water (40:57.6:2.4)
M2	Methanol–ethanol–water (20:76.8:3.2)
W1	Ethanol–water (86.4:13.6)
W2	Ethanol–water (76.8:23.2)
M2W1	Methanol–ethanol–water (20:67.2:12.8)
1P3	1-Propanol–ethanol–water (30:67.2:2.8)
2P3	2-Propanol–ethanol–water (30:67.2:2.8)

REFERENCES

1 G. Hesse and R. Hagel, *Chromatographia*, 9 (1976) 62.
2 G. Hesse and R. Hagel, *Liebigs Ann. Chem.*, (1976) 996.
3 K. R. Lindner and A. Mannschreck, *J. Chromatogr.*, 193 (1980) 308.
4 K. Schlögel and M. Widhalm, *Chem. Ber.*, 115 (1982) 3042.
5 H. Koller, K.-H. Rimböck and A. Mannschreck, *J. Chromatogr.*, 282 (1983) 89.
6 G. Blaschke, H.-P. Kraft and H. Markgraf, *Chem. Ber.*, 116 (1983) 3611.
7 K. Schlögel and M. Widhalm, *Monatsh. Chem.*, 115 (1984) 1113.
8 A. Mannschreck, H. Koller and R. Wernicke, *Kontakte (Darmstadt)*, 1985/1 (1985) 40.
9 E. Francotte, R. M. Wolf, D. Lohmann and R. Mueller, *J. Chromatogr.*, 347 (1985) 25.
10 E. Francotte, H. Stierlin and J. W. Faigle, *J. Chromatogr.*, 346 (1985) 321.
11 K.-H. Rimböck, M. A. Cuyegkeng and A. Mannschreck, *Chromatographia*, 21 (1986) 223.
12 G. Blaschke, *J. Liq. Chromatogr.*, 9 (1986) 341.
13 J. Scharf, K. Schlögel, M. Widhalm, J. Lex, W. Tuckmantel, E. Vogel and F. Pertlik, *Monatsh. Chem.*, 117 (1986) 255.
14 T. Shibata, I. Okamoto and K. Ishii, *J. Liq. Chromatogr.*, 9 (1986) 313.
15 A. Hussenius, R. Isaksson and O. Matsson, *J. Chromatogr.*, 405 (1987) 155.
16 M. Krause and R. Galensa, *J. Chromatogr.*, 441 (1988) 417.
17 Y. Okamoto, M. Kawashima, K. Yamamoto and K. Hatada, *Chem. Lett.*, (1984) 739.
18 A. Ichida, T. Shibata, I. Okamoto, Y. Yuki, H. Namikoshi and Y. Toga, *Chromatographia*, 19 (1984) 280.
19 A. Rizzi, *J. Chromatogr.*, 478 (1989) 71.
20 A. Rizzi, *J. Chromatogr.*, 478 (1989) 87.
21 J. F. K. Huber, *Ber. Bunsenges. Phys. Chem.*, 77 (1973) 179.
22 L. R. Snyder and J. J. Kirkland, *Introduction to Modern Liquid Chromatography*, Wiley, New York, 1979, p. 222.
23 J. C. Giddings, *Dynamics of Chromatography*, Part I, Marcel Dekker, New York, 1965.
24 G. J. Kennedy and J. H. Knox, *J. Chromatogr. Sci.*, 10 (1972) 549.
25 C. Horvath and H. J. Lin, *J. Chromatogr.*, 149 (1978) 43.
26 C. Roussel, J.-L. Stein, F. Beauvais and A. Chemlal, *J. Chromatogr.*, in press.

SLOW ISOMERIZATION OF SOME PROLINE-CONTAINING PEPTIDES INDUCING PEAK SPLITTING DURING REVERSED-PHASE HIGH-PERFORMANCE LIQUID CHROMATOGRAPHY

J. C. GESQUIERE* and E. DIESIS

Service de Chimie des Biomolécules, CNRS URA 1309, Institut Pasteur de Lille, 1 rue Calmette, 59019 Lille (France)

M. T. CUNG

Laboratoire de Chimie-Physique Macromoléculaire, CNRS UA 494, Institut Polytechnique de Lorraine, 1 rue Granville, 54001 Nancy (France)

and

A. TARTAR

Service de Chimie des Biomolécules, CNRS URA 1309, Institut Pasteur de Lille, 1 rue Calmette, 59019 Lille (France)

(Received March 20th, 1989)

SUMMARY

A slow conformational equilibrium, commensurable with the retention times, was shown to induce peak broadening or peak splitting during reversed-phase high-performance liquid chromatography of several medium-sized peptides. Elution at 50°C resulted in sharp unique peaks, while at sub-ambient temperature well resolved peaks were observed. Linear peptides which show this phenomenon had a Pro–Pro bond, but the phenomenon was also observed in the case of a cyclic peptide containing two non-vicinal proline residues.

INTRODUCTION

Reversed-phase high-performance liquid chromatography (HPLC) is.the most appropriate method to assess the purity of synthetic peptides. The observation of more than a single peak is usually attributed to the presence of impurities which have occurred as a result of side reactions during the different steps of the synthesis, or to misfunctioning of the HPLC apparatus such as uneven sample distribution or non-uniform eluent flow in the column. However, when a molecule exists in several conformations having different retention factors and when the relaxation times are commensurable with the time-scale of the chromatographic process, peak broadening, distortion of peak shape and eventually peak splitting can occur and be misinterpreted. We report in this communication several cases of medium-sized synthetic peptides (Table I) for which such unusual chromatographic behaviours were observed during usual reversed-phase gradient HPLC as a consequence of a slow conformational equilibrium[1].

TABLE I

AMINO ACID SEQUENCES OF PEPTIDES I–XII

<Glu = Pyroglutamic acid.

No.	Amino acid sequence
I	Met–Ser–Ile–Pro–Pro–Glu–Lys
II	Ile–Pro–Met–Ser–Ile–Pro–Pro–Glu–Lys
III	Leu–Ala–Ile–Pro–Pro–Lys–Arg–Leu–Asn
IV	Arg–Pro–Pro–Gly–Phe–Ser–Pro–Phe–Arg (bradykinin)
V	His–Asp–Leu–Pro–Lys–Ala–Val–Val–Lys–Leu–Glu–Pro–Pro–Trp–Ile–Gln
VI	Thr–Pro–Lys–Lys–Ile–Lys–Pro–Pro–Leu–Pro–Ser–Val–Thr–Lys
VII	Pro–Asp–Pro–Pro–Gln–Pro–Asp–Phe–Pro–Gln–Leu–Asn–Ser–Asp
VIII	<Glu–Glu–Lys–Pro–Tyr–Trp–Pro–Pro–Pro–Ile–Tyr–Pro–Met
IX	<Glu–Gly–Leu–Pro–Pro–Gly–Pro–Pro–Ile–Pro–Pro
X	Trp–Arg–Arg–Ala–Tyr–Asp–Ile–Pro–Pro–Pro–Val–Asp–Ile–Ser–Asp–Pro–Arg–Phe–Pro–Gly–Asn–Glu–Pro–Lys

XI

```
Cys ── Leu ── Pro ── Arg ── Glu ── Pro ── Gly ── Leu ── Cys
 |                                                    |
S ── Acm                                           S ── Acm
```

XII

```
Cys ── Leu ── Pro ── Arg ── Glu ── Pro ── Gly ── Leu ── Cys
 |                                                    |
S ─────────────────────────────────────────────────── S
```

MATERIALS AND METHODS

Chromatography

The apparatus consisted of two Model 302 pumps, a Model 704 system manager, a Model 116 UV detector and a Model 231 automatic sample injector (Gilson medical electronics). The 100-5 Nucleosil C_{18} Macherey-Nagel) column (300 mm × 4 mm I.D.) was immersed in a constant temperature bath.

Except where stated to the contrary, peptides were eluted at a flow-rate of 0.7 ml/min using a 15-min linear gradient from 3 to 50% acetonitrile in aqueous 0.01 M phosphate buffer, pH 3.5. The column effluent was monitored at 215 nm. For preparative purposes, 1-mg samples were injected and fractions were collected in tubes immersed in a refrigerated bath; the tubing in and out of the detector was made as short as possible.

Peptide synthesis

Peptides IV (bradykinin) and IX (bradykinin potentiator C) were obtained from Bachem. All other peptides were prepared in our laboratory using classical solid-phase methodology[2].

Briefly, peptides were synthesized on chloromethylpolystyrene 1% divinylbenzene resin, using N^α-*tert.*-butyloxycarbonyl (Boc) and benzyl side-chain protection as follows : Ser (benzyl, Bzl), Glu (OBzl), Lys (2-Cl-Z), Arg (tosyl, Tos), Cys (acetamidomethyl, Acm), Tyr(2-Br-Z). The first amino acids were anchored as their caesium

salts. Syntheses were performed on an Applied 430 (Applied Biosystems, Foster City, CA, U.S.A.) apparatus, starting with 0.5 mmol of aminoacyl-resins (average loading : 0.6 mmol/g).

Each synthetic cycle consisted of: (i) a 20-min deprotection with 50% trifluoroacetic acid–dichloromethane (after incorporation of Met or Trp residues, 2% dithioethane was added until the end of synthesis); (ii) neutralization with 10% diisopropylethyl amine–dichloromethane and (iii) coupling with preformed symmetrical anhydride (1 mmol) for 24 min in dimethylformamide (DMF). Boc-Arg (Tos), Boc-Asn and Boc-Gln were coupled as their preformed 1-hydroxybenzotriazole (HOBT) esters (2 mmol) for 40 min in DMF and recoupled for 40 min in dichloromethane.

Peptidyl-resins were cleaved by treatment with HF using p-cresol as a scavenger, and dimethyl sulphide was added during cleavage of peptides containing Met or Trp residues[3]. Peptides were purified by gel filtration on TSK HW40 Trisacryl® and their purity was checked by amino acid analysis after acid hydrolysis (5.6 M HCl, 24 h).

Cyclization

After removal of acetamidomethyl groups by mercuric acetate treatment at pH 4, peptide XI (10^{-5} M solution) was oxidized by air bubbling at pH 8 to give XII.

RESULTS AND DISCUSSION

Linear peptides containing one Pro–Pro bond

A typical HPLC profile for these compounds is shown in Fig. 1. Two peaks in a 4:1 ratio were observed and collected separately, and can be attributed to the presence of two different molecular species in the sample. Both peaks were subjected to amino acid analysis and fast atom bombardment (FAB) mass spectroscopy, yielding identical amino acid compositions and molecular weights. Each peak was collected and stored at room temperature during several hours. When reinjected under the same conditions, both gave the same profiles as shown in Fig. 1, suggesting the occurrence of a conformational equilibrium. Moreover, examination of the profiles showed that the two peaks had coalesced, suggesting that the region located between them contains molecules which have experienced a conformational inversion during elution,
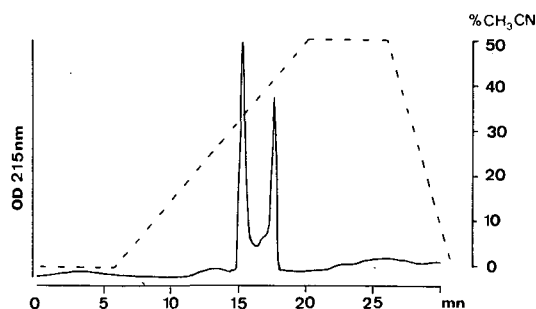
Fig. 1. HPLC profile of peptide I. Column: Nucleosil 100-5 C_{18}. Eluents: A = phosphate buffer pH 3.5 containing 3% acetonitrile; B = phosphate buffer pH 3.5 containing 50% acetonitrile. Flow-rate: 0.7 ml/min. Temperature: 20°C.
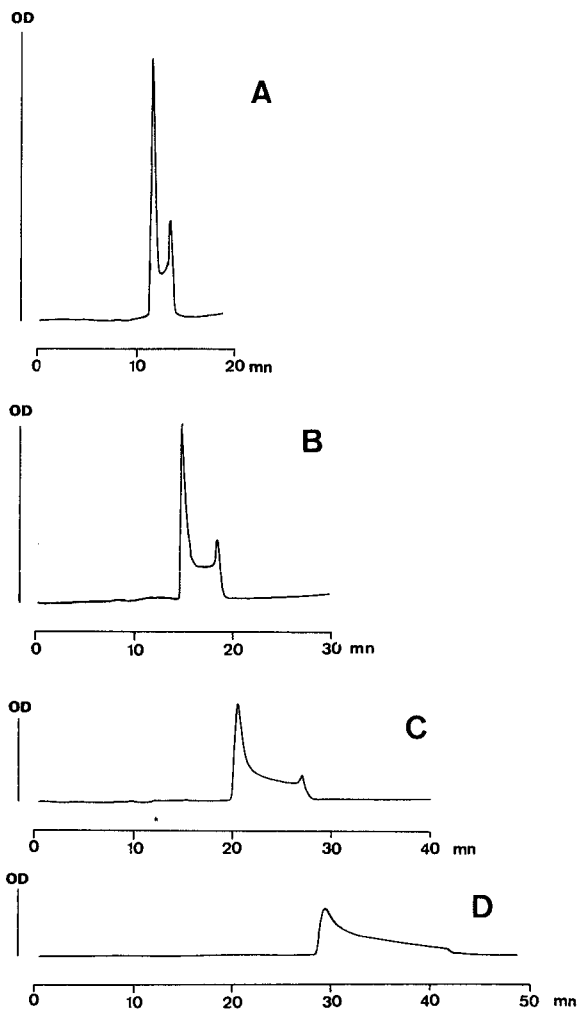
Fig. 2. HPLC profiles of peptide I as a function of gradient slope. Eluents and flow-rate as in Fig. 1. Gradient slope: times from 100% solvent A to 100% B, (A) 15, (B) 30, (C) 60 and (D) 120 min.

and that significant on-column isomerization of conformers occurred at room temperature during the chromatographic process.

There are several possible ways of influencing this phenomenon.

Effect of gradient slope. A change in the retention time of the peptide can be achieved by modification of the flow-rate under isocratic conditions, or, as was done here at constant flow-rate, by changing the slope of the gradient. Results are shown in Fig. 2, examplified with peptide I. Predictably, as the retention time increased, the probability that a molecule would undergo a conformational inversion increased simultaneously, resulting in broadening of the region between the peaks.

Effect of temperature. Increasing or lowering the column temperature had a dramatic effect on elution profiles as is seen in Fig. 3 with peptide I. Lowering the
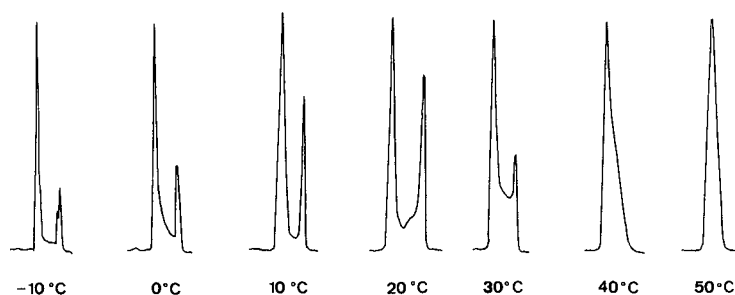
Fig. 3. HPLC profiles of peptide I as a function of temperature. Eluents and flow-rate as in Fig. 1. Gradient: 100% solvent A to 100% B in 15 min.

temperature of the column decreased the rate of isomer interconversion, whereas the retention times were only slightly affected. As a consequence, the separation between the two peaks improved. At 0°C the rate of on-column interconversion was slow enough to allow an almost baseline separation of the two conformers. As expected, increasing the column temperature above room temperature had the opposite effect, and at 50°C the rate of interconversion was high enough to yield a single symmetrical
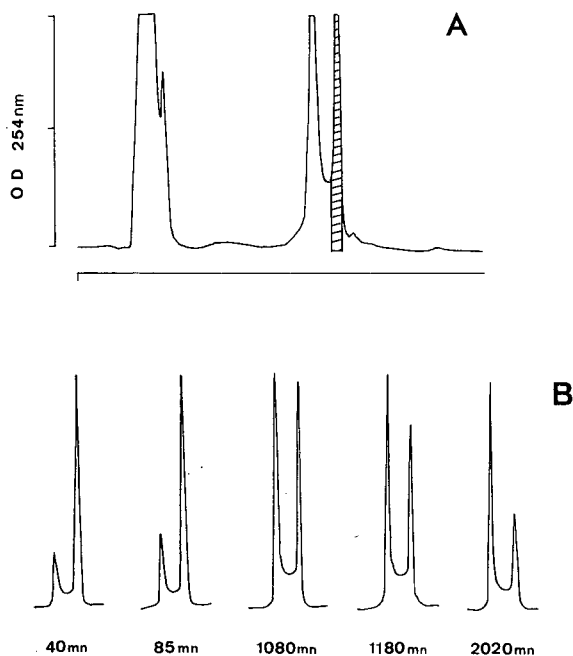
Fig. 4. Preparative low-temperature HPLC separation of peptide I conformers and reisomerization. (A) Isolation of the minor isomer. Column: Nucleosil 100-5 C_{18}. Eluent: phosphate buffer pH 3.5 containing 3% acetonitrile for solvent (A) and 50% acetonitrile for solvent (B). Flow-rate: 0.7 ml/min. Temperature: $-10°C$. Gradient: 5 min A then to 100% B in 15 min. Amount injected: 1 mg peptide in 20 μl 5% acetic acid. The peak collected, corresponding to the minor isomer, is shaded. (B) Reisomerization of the minor conformer as a function of time.

peak. However, this peak remained broad, indicating that, even at this temperature, the conformational equilibrium was still interfering with the chromatographic process.

Isolation of conformers. The almost complete separation of the two conformers which was observed at 0 and 10°C under analytical conditions prompted us to attempt their separation on a semipreparative scale. A solution of 1 mg of peptide I in 20 μl of 5% acetic acid was injected onto the column which was maintained at − 10°C. As seen in Fig. 4A, two separated peaks were obtained which were collected and maintained at − 10°C. Aliquots of the slower eluting peak, which corresponds to the minor isomer, were reinjected over a period of 48 h to observe the return to the equilibrium. As shown in Fig. 4B, a mixture containing equal quantities of both isomers was obtained after 18 h and after 48 h the profile was almost identical to that observed under equilibrium conditions.

Other linear, Pro–Pro containing peptides

Following these observations, we tested ten different linear peptides containing at least one Pro–Pro bond and found several types of behaviours.

Two peptides (II and III) had HPLC profiles very similar to that observed with peptide I; the two peaks were also in the same ratio of 4:1, the slower eluting being in each case the minor conformer.

Four peptides containing Pro–Pro bonds (IV–VII) showed no peak splitting even at low temperature. Among them is bradykinin (IV), a well known peptide with a Pro–Pro bond. A first explanation is that both conformers had similar retention times. However, we were not able to separate any conformers of IV, when using different eluting buffers or organic modifiers, even at temperatures as low as − 10°C.

It is thus more likely in the case of these peptides that a single conformer is thermodynamically favoured or that certain Pro–Pro bonds are prone to rapid isomerization.

Three peptides had more than one Pro-Pro bond : VIII (Pro–Pro–Pro), IX (Pro–Pro–X–Pro–Pro–X–Pro–Pro) and X (Pro–Pro–Pro–Pro). In these cases, the HPLC profiles at 0°C were more complex as four or eight different conformers are likely to coexist and some, at least, will display different chromatographic behaviours. However, elution at 50°C resulted in single sharp peaks for these three peptides.

Cyclic peptides

A second type of slow conformational equilibrium was observed in the case of the cyclic peptides XII. During cyclization of XI, which was performed by air oxidation in dilute solution after removal of Acm protecting groups, a very broad peak was observed by HPLC analysis of the reaction medium. At this point, a slow conformational equilibrium was suspected. This was confirmed by performing HPLC at different temperatures (Fig. 5): a single sharp peak was obtained at 50°C while a well resolved doublet containing two isomers in a 1:1 ratio was observed at 0°C. When the linear peptide XI was examined under the same conditions, no alteration of peak shape was detected.
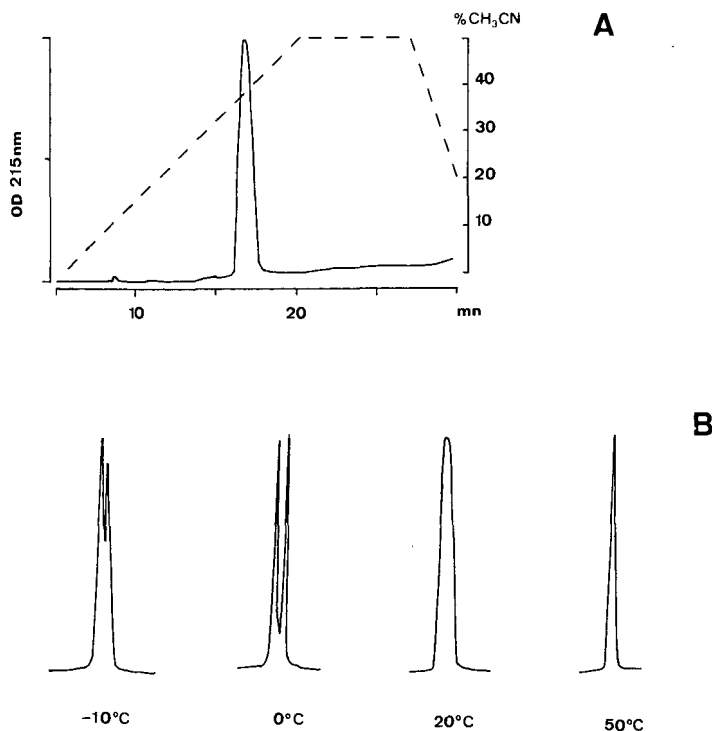
Fig. 5. HPLC of peptide XII. Eluents and flow-rate as in Fig. 1. (A) Profile at 20°C. (B) Profiles as a function of temperature.

DISCUSSION

The development of rapid methods of chromatography such as HPLC has dramatically decreased the time of chromatographic processes. Not surprisingly, slow isomerization of molecules can thus interfere more frequently with their chromatographic behaviours.

We have searched the relevant literature for similar observations. Melander *et al.*[4] have studied in detail the effect of *cis–trans* isomerization of proline dipeptides in reversed-phase chromatography. Their results clearly show that the slow isomerization of the imido peptide bond is responsible for peak splitting under isocratic conditions. They also provided a theoretical framework for the treatment of on-column reactions and introduced the use of low-temperature HPLC to characterize such equilibria.

However, to our knowledge, only one paper by Rusconi *et al.*[5]describes in detail a similar phenomenon in the case of a medium sized linear peptide (VIII), tryptophyllin (<Glu–Glu–Lys–Pro–Tyr–Trp–Pro–Pro–Pro–Ile–Tyr–Pro–Met).

Except for the proline-containing dipeptides which were analysed under isocratic conditions with very short retention times, all the longer peptides giving rise to this phenomenon have at least one Pro–Pro bond in their sequence.

Among proteogenic amino acids, proline is known to play an unique rôle be-
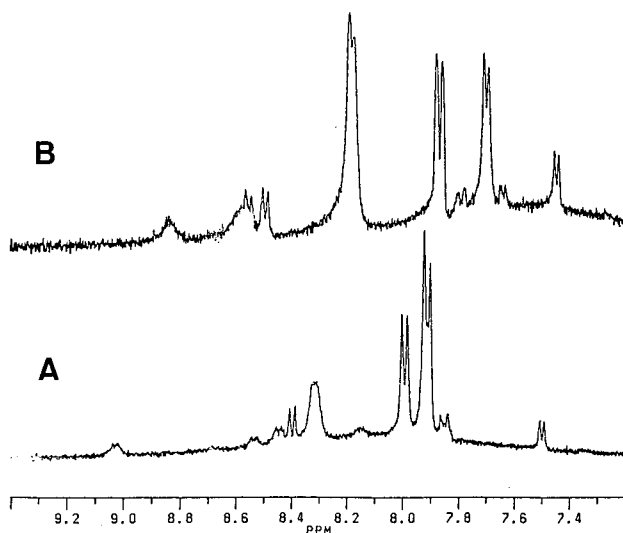
Fig. 6. NH region of the NMR spectra of peptide 1 (solution in [^{2}H$_6$]dimethyl sulphoxide). (a) Just after dissolution (preponderance of *cis*-isomer); (B) four days after dissolution (preponderance of the all-*trans*-isomer).

cause its side chain is linked to the α-nitrogen atom. As a result, *cis* isomers of these peptide bonds are only slightly less stable than *trans* isomers and both isomers are generally observed during NMR studies of small proline-containing peptides. Thus when the NMR spectrum of the NH region of peptide I was examined (Fig. 6), the presence of *cis-trans* isomers was observed, corresponding respectively to Ile–Pro and Pro–Pro bonds. This observation is consistent with the fact that the isomerization rates of both structures are slow when compared to the NMR time-scale. However, among the different possible *X*-Pro peptide bonds, only the Pro–Pro bond appears to be endowed with an exceptionally slow *cis–trans* isomerization rate comparable with the chromatographic time-scale. As an example, this slow *cis–trans* isomerization rate was recently proposed[6] to explain why the folding of porcine RNase differs significantly from the general folding pattern of other RNases. In porcine RNase, the change Tyr[115] → Pro[115] leads to a Pro[114]–Pro[115] bond which is found only in the porcine enzyme.

Determination of the kinetics of unfolding and refolding made it possible to determine an activation enthalpy of 22 kcal/mol (92 kJ/mol) and a half-life of 900 s at 10°C. This value is compatible with our chromatographic observations.

However, it should not be considered inevitable that the sole presence of a Pro–Pro bond in a peptide will induce a peak distortion, given that four peptides, including bradykinin (IV) gave rise to no peak distortion.

In the cyclic peptide XII, no Pro–Pro bond is present. The observations that the chromatographic properties of the linear peptide XI were not affected by temperature variations indicate that steric constraints upon cyclization are responsible for the decrease in the isomerization rate. A similar observation involving a proline-containing cyclic peptide has been reported[7] in the case of conotoxin MI (Gly–Arg–Cys–Cys–His–Pro–Ala–Cys–Gly–Lys–Asn–Tyr–Ser–Cys–NH$_2$) but not with closely re-

lated α-conotoxins. In this case also, HPLC at low temperature (0°C) gave a complete separation of the two possible forms, while a single sharp peak was observed at 60°C.

CONCLUSIONS

Slow *cis–trans* isomerization of particular peptide bonds such as Pro–Pro bonds or steric constraints induced by cyclization may be responsible for alteration of the chromatographic behaviour of medium-sized peptides.

Increasing the column temperature allows the peptide to be eluted as a single sharp peak and thus its purity can be assessed while still performing the elution at a reasonable speed. Lowering the temperature of the column and using the most rapid elution conditions compatible with isomer separation allows a baseline separation of the conformers. It might be of great interest to use this method to study separately the physicochemical properties of each conformer. Moreover, such peptides may prove to be valuable substrates in a study of the properties of the enzyme peptidyl-prolyl *cis–trans* isomerase discovered and purified from pig kidney, as this enzyme, which catalyses the *cis–trans* isomerization of proline imidic peptide bonds during refolding of proteins[8], accepts Pro–Pro-containing chain segments as substrates.

REFERENCES

1 J. C. Gesquiere, E. Diesis and A. Tartar, in G. Jung and E. Bayer (Editors), *Peptides 1988*, Walter de Gruyter, Berlin, New York, 1989, pp. 112–114.
2 R. B. Merrifield, *J. Am. Chem. Soc.*, 85 (1963) 2149–2154.
3 J. P. Tam, W. F. Heath and R. B. Merrifield, *J. Am. Chem. Soc.*, 105 (1983) 6442–6455.
4 W. R. Melander, J. Jacobson and C. Horvath, *J. Chromatogr.*, 234 (1982) 269–276.
5 L. Rusconi, G. Perseo, L. Franzoi and P. C. Montecucchi, *J. Chromatogr.*, 349 (1985) 117–130.
6 R. Grafl, K. Lang, A. Wrba and F. X. Schmid, *J. Mol. Biol.*, 191 (1986) 281–293.
7 W. R. Gray, J. E. Rivier, R. Gaylean, L. J. Cruz and B. M. Olivera, *J. Biol. Chem.*, 258 (1983) 12247–12251.
8 G. Fischer and H. Bang, *Biochim. Biophys. Acta*, 828 (1985) 39–42.

INDIRECT DETECTION OF INORGANIC ANIONS BY HIGH-PERFORMANCE LIQUID CHROMATOGRAPHY: USE OF PAPAVERALDINIUM AS AN ULTRAVIOLET ABSORBING AGENT

P. DORLAND

Central Hospital Pharmacy, 7 Rue du Fer à Moulin, 75005 Paris (France)

M. TOD

Avicenne Hospital, 125 Route de Stalingrad, 93009 Bobigny (France)

and

E. POSTAIRE* and D. PRADEAU

Department of Analytical Development, Central Hospital Pharmacy, 7 Rue du Fer à Moulin, 75005 Paris (France)

(First received January 2nd, 1989; revised manuscript received May 9th, 1989)

SUMMARY

An indirect UV detection method, using tetrabutylammonium hydroxide and papaveraldine perchlorate as counter ion and ion interaction reagent, respectively, is described. Water analysis and drug monitoring in the treatment of childhood epilepsy with bromides are presented as possible applications. As a result of analytical difficulties, a so-called "overload effect" was studied and a theoretical mechanism for this is proposed.

INTRODUCTION

Ion chromatography was first used to analyse ionic species[1]. However, this technique has the drawbacks of the fragility and cost of the column and the need for a thermostatic system. In addition, in the Dionex system, the suppressor column has to be regenerated after a few hours of use. Although a very low limit of detection can be reached, ion chromatography needs special apparatus and careful maintenance.

Indirect detection has been used for about 10 years. This simple technique allows the detection and quantification of compounds that are outside the scope of other detection techniques[1–3]. An ultraviolet-absorbing ion interaction reagent (IIR) is added to the mobile phase and then distributed to the stationary phase. This agent forms ion pairs with solutes of opposite charge which are eluted and detected easily through absorbance of the IIR[4]. The detection mechanism for this kind of chromatography is complex and has already been described by Stranahan and Deming[5,6].

In this study, ion-pair chromatography with indirect detection was chosen because with this method it is possible to assay inorganic anions with conventional apparatus. C_{18} columns were used because their efficiency and mechanical behaviour are better than those of ion-exchange resins. Many parameters (mobile phase

composition, solvent concentration, pH, ionic strength) can be modified when a C_{18} stationary phase is used. Such flexibility allows better optimization of the chromatographic conditions while setting up the assay. Further, the use of each column over an extended period is possible because of the stability of the stationary phase. Two major applications were considered: first, water analysis needs a fast, automatable technique in order to assay several anions simultaneously, and second, this technique allows the assay of blood bromide. Analytical difficulties appeared in the quantification of anions and in the choice of an internal standard, wich led us to study a so-called "overload effect".

EXPERIMENTAL

Reagents

Papaveraldine was synthesized from papaverine[7,8]. The perchlorate salt was obtained by dissolving 353 mg of papaveraldine base in 20 ml of 0.7% (w/v) perchloric acid, diluting to 100 ml with distilled water and heating at 90°C until dissolution was complete. Crystallization occurred after filtration within 24 h at 4°C (90% yield).

Tetrabutylammonium hydroxide (TBAH) [40% (w/v) aqueous solution] was obtained from Sigma, (Paris, France), acetonitrile (LiChrosolv, for chromatography) from Merck (Paris, France), mineral anions and citric acid (Normapur quality) from Prolabo (Paris, France) and water [high-performance liquid chromatographic (HPLC) grade] from FSA (Loughborough, U.K.).

Preparation of the mobile phase

A 50-mg amount of papaveraldine perchlorate was added to 850 ml of $7 \cdot 10^{-3}$ M sodium citrate buffer (pH 3.2) and dissolved by sonication, then 1.75 g of TBAH were added and the solution was mixed with 150 ml of acetonitrile. The resulting mobile phase was filtered on a 0.22-μm filter (GWMP; Millipore, France). The final pH was about 3.5.

Chromatographic procedures

The column was first washed with acetonitrile–water (50:50, v/v), then loaded with the mobile phase for 1 h in order to achieve adsorption of TBAH and papaveraldine on the C_{18} stationary phase. The mobile phase used during this operation was discarded. The system was then recycled and equilibrated for 24 h.

Apparatus

A Model 850 modular system from DuPont (Paris, France) was used, consisting of an HPLC pump, a thermostatic module set at 35°C and a variable-wavelength detector set at 325 nm. Peak areas and peak heights were determined with a Shimadzu Model CR5A integrator (Touzard et Matignon, France). The column used was a 10-μm C_{18} μBondapak (250 × 4.6 mm I.D. from Waters (Paris, France).

Calculations

The number of theoretical plates, N, was calculated using the equation $N = 5.54(t_R/\delta)^2$, where δ is the peak width at half-height and t_R is the retention time[9].

The displacement ratio (DR) was calculated from[10,11]

$$DR = \frac{\text{papaveraldine peak concentration}}{C_{\max}}$$

with (from ref. 9):

$$C_{\max} = \frac{Q_{\text{inj}}}{V_{\text{R}}} \sqrt{\frac{N}{2\pi}} \tag{13}$$

where Q_{inj} is the amount of anion injected, V_{R} the retention volume and the papaveraldine peak concentration = peak absorbance/εl (where ε = molar absorbance coefficient and l = length of the detector cell).

Study of overload effect

Response factors for internal standards and anions have to be strictly independent. In order to study this property, we examined the linearity and parameters of calibration graphs for NaCl with or without added NaNO$_3$. Four calibration graphs were prepared in $7 \cdot 10^{-3}$ M citrate buffer: (A) $5 \cdot 10^{-4}$–$50 \cdot 10^{-4}$ M NaCl solution; (B) $5 \cdot 10^{-4}$–$50 \cdot 10^{-4}$ M NaCl solution containing 10^{-2} M NaNO$_3$; (A') $5 \cdot 10^{-5}$–$1 \cdot 10^{-3}$ M NaCl solution; and (B') $5 \cdot 10^{-5}$–$1 \cdot 10^{-3}$ M NaCl solution 10^{-3} M NaNO$_3$. The different sample concentrations represented by A, B, A' and B' were injected alternately to minimize the time-dependent variability of the elution equilibrium. Two further solutions of 10^{-2} and 10^{-3} M NaNO$_3$ were injected alternately with the above solutions in order to study the response to nitrate alone and in the presence of chloride.

Procedures used for blood bromide assay

The mobile phase was similar to that described above with papaverinium fluoride as the detection agent because it is more soluble than perchlorate: 10^{-4} M papaverinium fluoride was added to 900 ml of $7 \cdot 10^{-3}$ M sodium citrate buffer, then $2.5 \cdot 10^{-3}$ M TBAH added and the solution was mixed with 100 ml of acetonitrile. The extraction of bromide from blood (98% yield) was performed on whole blood: 1 ml of methanol was added to 500 μl of blood, shaken for 30 s and centrifuged at 1000 g for 10 min. A 100-μl volume of the supernatant was diluted with 2 ml of distilled water and 20 μl of the mixture were injected. Cl$^-$ and Br$^-$ anions were identified by standard additions to the samples.

RESULTS AND DISCUSSION

Effects of the solvent

The chromatograms show successively a first peak corresponding to the void volume, either positive or negative depending on the composition of the injection solvent; a double system peak, first negative, then positive, the size of which depends on the composition of the injected sample; a positive peak, wich may be used to detect the injected anion, corresponding to the desorption of the excess IIR previously adsorbed during the elution of the anion along the column, and a final negative peak corresponding to the retention time of the perchlorate anion.

TABLE I

RETENTION CHARACTERISTICS LIMIT OF DETECTION (SIGNAL-TO-NOISE RATIO = 3) AND LIMITING CONCENTRATIONS

Parameter	$H_2PO_4^-$	NO_2^-	Cl^-	Br^-	NO_3^-	I^-	SO_4^{2-}
t_R (min)	5.5	5.8	6.5	7.1	7.6	9.5	18.9
k'	2.06	2.22	2.61	2.94	3.22	4.28	9.50
N (plates/m)	14 000	15 500	19 500	23 200	24 200	6700	18 300
L.O.D. (mg/l)	9.5	2.7	1.4	3.2	2.5	4.8	3.8
European Pharmacopoeia (mg/l)	5	0.005	50	—	10	—	50

Retention characteristics

Table I and Fig. 1 give data and chromatograms for the seven anions studied in aqueous solution. The efficiency of the separation is about 20 000 theoretical plates per metre. This system is therefore among those with the best performance. The linearity of the method was studied over a range of 50 nmol injected. The calibration graph (peak height *versus* amount injected) shows good linearity from 1 to 25 nmol injected. Good and easy quantification was obtained from measurements of peak heights.

Within-day reproducibility

Successive injections of various concentrations of NaCl gave satisfactory results for peak-height variability (Table II).
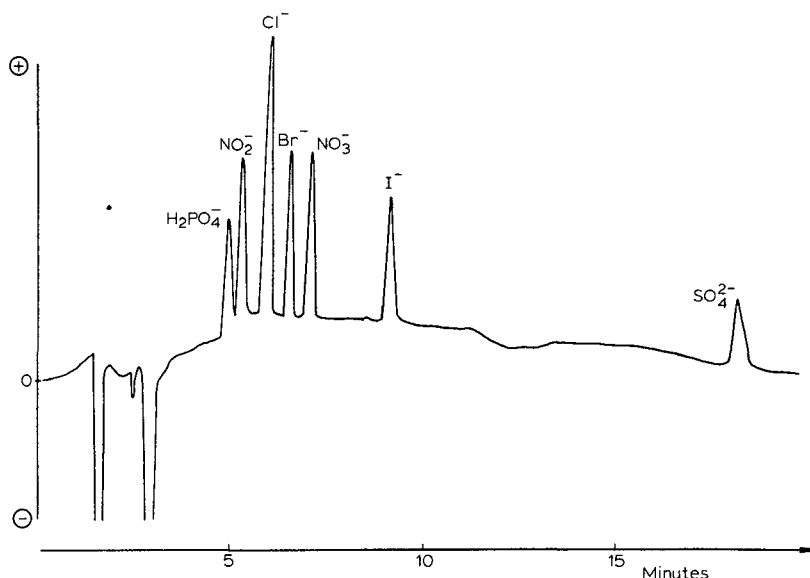
Fig. 1. Separation of phosphate, nitrite, chloride, bromide, nitrate, iodide and sulphate anions. For conditions, see text.

TABLE II

WITHIN DAY REPRODUCIBILITY

Chloride sample concentration (M)	Coefficient of variation (%) (n=7)
$2 \cdot 10^{-4}$	8.06
$5 \cdot 10^{-4}$	2.76
10^{-3}	3.9
$4 \cdot 10^{-3}$	2.68

Choice of the retention counter-ion

Two counter ions (tetrabutylammonium hydroxide and a detection agent) were adsorbed on the C_{18} stationary phase. Both retain the injected anions by electrostatic interactions. TBAH, called the retention counter ion, is the more effective retention agent. It was present at a concentration twenty times higher than that of the detection agent. Its adsorption to the stationary phase is easily reversible, in contrast to the long-chain alkylammonium[1]. It is important to use the hydroxide form rather than another salt, as this is eluted less readily.

A comparison of the effect of various concentrations on the retention efficiency showed that a steady state is reached at about 3.0 μM (Table III).

TBAH has no absorbance at the wavelength used for detection.

Choice of papaveraldine perchlorate

This detection agent gives a strong background signal at 325 nm and permits the indirect detection of anions. In order to obtain a high enough solubility of papaveraldine, a salt form was used. We chose the perchlorate, which did not interfere with the anions tested. The weak solubility of the salt meant that the maximum possible concentration of the detection agent was $1.1 \cdot 10^{-4}$ M. This concentration gives an absorbance of about 1, which offers an optimum dynamic reserve[10,11]. However, the retention of anions is insufficient at this concentration, and another counter ion is required (TBAH).

Choice of detection wavelength and limit of detection

Studying the signal-to noise ratio across the UV spectrum we found that the limit of detection (L.O.D.) was constant and maximal corresponding to an absorbance of 0.6–1.2 throughout the wavelength range 200–360 nm (Table IV). The detection

TABLE III

CHOICE OF THE RETENTION COUNTER-ION CONCENTRATION

Mobile phase: 10^{-2} M citrate buffer–acetonitrile (80:20, v/v), containing 10^{-4} M papaveraldine perchlorate and TBAH. Sample KBr concentration: 10^{-3} M.

TBAH (mM)	t_R Br^- (min)
2.6	11
2.9	12
3.2	12.5
4.5	12.5

TABLE IV

CHOICE OF THE DETECTION WAVELENGTH

Wavelength (nm)	Absorbance (a.u.f.s.)	Peak height	Noise	Signal-to-noise ratio	L.O.D. $(10^{-5}\ M)$
365	0.6	776	1	776	4
362	0.8	792	1	792	4
354	1.06	896	2	448	7
350	1.24	880	3	293	10

wavelength chosen, *i.e.*, 325 nm, which is an absorbance maximum, gave good reproducibility, owing to the minimal variability in absorbance. Table I gives the L.O.D.s for the anions studied.

Proportion of eluent modifier

A certain amount of acetonitrile (15% minimum) is necessary in order to dissolve the papaveraldine. Increasing this concentration decreases the retention of the anions studied. The lack of solubility of papaveraldine perchlorate in methanol prevents its substitution for acetonitrile.

Composition of the buffer and pH of the eluent

The pH of the eluent had to be around 3 in order to maintain the papaveraldine in an ionized state ($pK_a = 5$). Therefore, citrate buffer ($pK_a = 3.13$) was chosen. An inorganic buffer, interfering with the separation, had to be avoided. The pH has a major influence on the retention and detection of weak acids, for example $H_2PO_4^-$ and NO_2^- (pK_a 2.15 and 3.35, respectively). Increasing the pH of the eluent increases their retention and response factors because of the greater ionization.

Furthermore, an increase in the buffer concentration, *i.e.*, in the ionic strength, decreases the retention of all anions. The buffer adopted allows good resolution of the seven anions tested.

Overload effect

Table V gives the peak areas for Cl⁻ in the four solutions A, B, A′ and B′. The

TABLE V

OVERLOAD EFFECT

Solution	Area of chloride peak								
	NaCl concentration (M)								
	$5 \cdot 10^{-4}$	$10 \cdot 10^{-4}$	$20 \cdot 10^{-4}$	$50 \cdot 10^{-4}$	$5 \cdot 10^{-5}$	$10 \cdot 10^{-5}$	$20 \cdot 10^{-5}$	$50 \cdot 10^{-5}$	$100 \cdot 10^{-5}$
A	73	130	246	590					
B	55	101	193	468					
Ratio B/A	0.753	0.777	0.785	0.793					
A′					354	673	1310	3230	6420
B′					340	646	1250	3076	6110
Ratio B′/A′					0.927	0.943	0.946	0.952	0.953

TABLE VI

OVERLOAD EFFECT: t-TEST ON CALIBRATION GRAPHS FOR SOLUTIONS A, B, A' AND B'

Calibration graph	Slope	Intercept	r	t-test
A	11.33	$1.5 \cdot 10^{-3}$	0.999	$t = 16.55$ Degree of freedom $= 3$
B	9.04	$9.6 \cdot 10^{-4}$	0.999	Slopes significantly different.
A'	63.66	$3.4 \cdot 10^{-4}$	0.998	$t = 4.4$ Degree of freedom $= 3$
B'	60.53	$3.8 \cdot 10^{-4}$	0.999	Slopes alike

peak areas were lowered on addition of NO_3^- but only with 10^{-2} M NO_3^- (solutions A and B). This is characteristic of an overload effect. This was demonstrated (i) by the decrease in the slope (a) of Cl^- calibration with 10^{-2} M NO_3^- ($a = 11.3$ and 9.04, for solutions A and B, respectively) (see test in Table VI and Figs. 2 and 3); (ii) by the calculation of the ratio R:

$$R = \frac{X}{Y} = \frac{Cl^- \ area/NO_3^- \ area}{Cl^- \ concentrations/NO_3^- \ concentration}$$

which theoretically should be constant, but whereas this is true for low Cl^- concentration with 10^{-3} M NO_3^- (Table VII), R decreases and is more variable with higher anion concentrations (Table VII); and (iii) conversely, the peak area obtained for 10^{-2} M NO_3^- alone is higher than in the presence of chlorides.

The overload effect demonstrates the influence of the environment on response factors[12]. The comparison of the DR of NaCl solutions with and without nitrate shows a decrease in DR when 10^{-2} M NO_3^- is present (Table VIII). Further, it is noteworthy
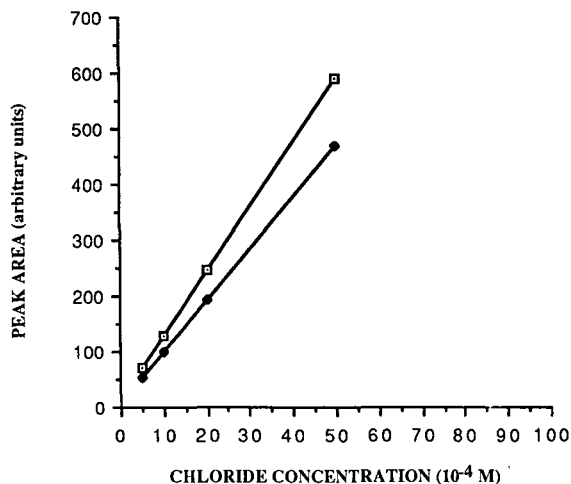
Fig. 2. Calibration graphs for solutions (□) A and (●) B.
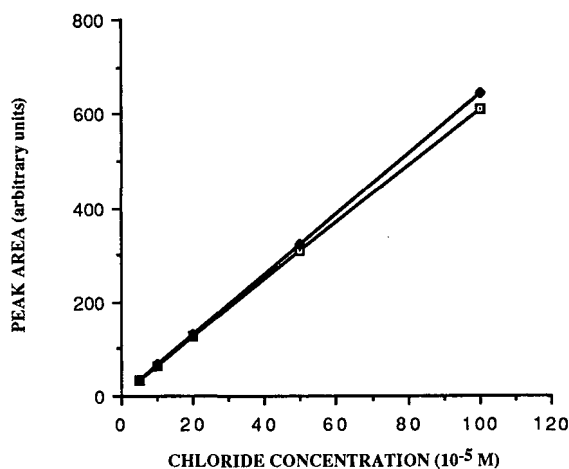
Fig. 3. Calibration graphs for solutions (●) A′ and (□) B′.

that the average value of DR is about 10^{-2}. The injection of a sample anion at a concentration of 10^{-2} M gives rise to ion pairs at a concentration of $10^{-2} \times 10^{-2}$ $= 10^{-4}$ M, which is precisely the concentration of the detection agent. Hence all papaveraldine present at the injection site binds with the anions to be assayed. Injection of larger amounts of anions gives rise to a displacement of papaveraldinium which is no longer proportional to the amount injected. Moreover, the detection mechanism results from a dynamic equilibrium between anions and the detection agent forming ion pairs. This equilibrium is governed by the mass equilibrium law. Hence a competition for binding with papaveraldinium occurs between the different anions studied. The overload effect causes a decrease in the DR for other anions and thus a decrease in peak height. This could explain the observations concerning peak height reported by Barber and Carr[4]. Indeed, they noticed a decrease in retention time and an unproportional decrease in peak height when the amount injected was increased (amounts ranging from 5 to 50 nmol were injected). One could reduce the overload effect by increasing the concentration of papaveraldine and thus the DR. However, this is inconsistent with the optimization of the L.O.D. Indeed, a minimum

TABLE VII

OVERLOAD EFFECT: SOLUTIONS B′ AND B

Overload effect[a]	NaCl concentration (M) (B′)					NaCl concentration (M) (B)			
	$5 \cdot 10^{-5}$	$10 \cdot 10^{-5}$	$20 \cdot 10^{-5}$	$50 \cdot 10^{-5}$	$100 \cdot 10^{-5}$	$5 \cdot 10^{-4}$	$10 \cdot 10^{-4}$	$20 \cdot 10^{-4}$	$50 \cdot 10^{-4}$
X	0.035	0.065	0.134	0.312	0.672	0.0328	0.0468	0.105	0.256
Y	0.05	0.1	0.2	0.5	1	0.05	0.1	0.2	0.5
X/Y	0.698	0.646	0.671	0.624	0.672	0.656	0.468	0.526	0.512

[a] $X = Cl^-$ peak area/NO_3^- peak area; $Y = Cl^-$ concentration/NO_3^- concentration.

TABLE VIII

MECHANISM OF OVERLOAD EFFECT

Chloride concentration (M)	DR (10^{-4} M)		DR (A) − DR (B) (10^{-4} M)
	Sol. A	Sol. B	
5 · 10^{-4}	11.22	7.59	3.63
10 · 10^{-4}	9.97	8.01	1.96
20 · 10^{-4}	9.62	7.89	1.72
50 · 10^{-4}	8.39	7.16	1.23

L.O.D. can be obtained by decreasing the concentration of the detection agent as given by[10,11]

$$\text{L.O.D.} = \frac{C_m}{R \cdot DR}$$

where C_m is the IIR concentration in the mobile phase and R the dynamic reserve. The only way to obtain a minimum L.O.D. is therefore to increase the dynamic reserve.

Bromide blood assay

The treatment of epilepsy with bromides has recently been reintroduced for children for whom classical treatment has failed[13]. The therapeutic efficiency zone is narrow (20–25 mM)[8] and, further, it is necessary to determine the dosage for each epileptic syndrome. Hence the availability of a bromide blood assay with a millimolar sensitivity would be of interest. A small modification of the technique described above allows such an assay.

The retention time of bromide is 10 min and the limit of detection, coefficient of variation and selectivity are similar to those described above. The calibration graph for whole blood is linear from 5 to 50 mM. Fig. 4 shows a chromatogram corresponding to a 35-day treatment with a mixture containing sodium, potassium and ammonium bromides in equal parts. The peak corresponding to the normal Cl⁻ blood level appears at $t_R = 9$ min. Valproic acid, often used in the treatment, did not interfere with other anions because of its high pK_a with respect to the pH of the mobile phase.

Water analysis

Table I gives concentration limits for five anions in haemodialysis water (European Pharmacopoeia) with the corresponding L.O.D. using our method. This is sensitive enough to quantify concentrations near the limits for chlorides, nitrates, phosphates and sulphates. The existence of the overload effect implies that accurate quantification of an unknown sample containing many anions is difficult and requires a calibration using the standard addition method.

CONCLUSION

Some interesting applications are possible using this method, which permits the separation of seven anions in 20 min. The usable working range is 2 · 10^{-5}–2 · 10^{-4}
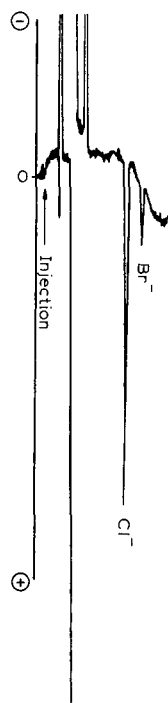
Fig. 4. Blood bromide assay. Bromide concentration, 10 mM.

M with an overloading anion concentration of 10^{-3} M. In water analysis, performing a limit test would simply consist of comparing the sample with a standard solution containing phosphate, chloride, nitrate and sulphate anions at the limiting concentration. The method is suitable for blood bromide assays because of the low anion concentration in the diluted blood sample. This method is already being used for pharmaceutical and clinical studies.

REFERENCES

1 P. R. Haddad and A. L. Heckenberg, J. Chromatogr., 300 (1984) 357–394.
2 G. Schill and J. Crommen, Trends Anal. Chem., 6 (1987) 111–114.
3 M. Sun-Il and E. S. Yeung, Anal. Chem., 57 (1985) 2253–2256.
4 W. E. Barber and P. W. Carr, J. Chromatogr., 260 (1983) 89–96.
5 J. J. Stranahan and S. N. Deming, Anal. Chem., 54 (1982) 1540–1546.
6 A. Sokolowski, Chromatographia, 22 (1986) 177–182.
7 A. Burger, in R. H. F. Manske (Editor), The Alkaloids —Chemistry and Physiology, Vol. 9, Academic Press, New York, 1967, pp. 32–41.
8 G. Schill and D. Weslerlund, in R. W. Frei and J. F. Lawrence (Editors), Chemical Derivatization in Analytical Chemistry, Vol. 2, Plenum Press, New York, 1982, p. 43.
9 R. Rosset and M. Caude, Manuel Pratique de Chromatographie en Phase Liquide, Masson, Paris, 1982.
10 T. Takeuchi and E. S. Yeung, J. Chromatogr., 370 (1986) 83–92.
11 T. Takeuchi and E. S. Yeung, J. Chromatogr., 366 (1986) 145–152.
12 B. A. Bidlingmeyer and C. T. Santanasia, Anal. Chem., 59 (1987) 1843–1846.
13 S. Livinston and P. H. Pearson, Am. J. Dis. Child., 25 (1953) 717–720.

CHROM. 21 620

DETERMINATION OF ACTIVITY COEFFICIENTS OF BINARY LIQUIDS BY CAPILLARY GAS CHROMATOGRAPHY WITH THERMAL DESORPTION MODULATION FOR DIRECT HEADSPACE SAMPLING

MINQUAN ZHANG[a] and JOHN B. PHILLIPS*

Department of Chemistry and Biochemistry, Southern Illinois University, Carbondale, IL 62901-4409 (U.S.A.)

(Received March 29th, 1989)

SUMMARY

Activity coefficients of the binary liquid mixtures benzene–toluene and acetone–chloroform were determined using thermal desorption modulation for direct headspace sampling into a capillary gas chromatograph. A thermal desorption modulator is a short, heated section at the head of the column. An electrical current pulse applied to a thin conductive film heats the modulator section and the stationary phase within it, releasing any retained substances as a concentration pulse which flows into the column. The modulator acts like an automatic and highly reproducible small-volume injector for a continuously flowing sample stream. Short-term relative standard deviations obtained using this technique are approximately 2%.

INTRODUCTION

Classical methods for the determination of the activity coefficients of volatile liquids in solution are laborious and time-consuming[1]. In addition, their accuracies and precisions are not as good as desired[2]. Gas–liquid chromatography has been used to determine the activity coefficients of volatile solutions at infinite dilution in the stationary phase in a column[3-7]. This method is faster and simpler than classical methods, but is can only be applied to binary systems in which the solvent is a gas–liquid chromatographic stationary phase and the solute is near infinite dilution. Arnikar *et al.*[8] proposed a headspace sampling method which can be used with a variety of solvent–solute combinations and for a wide range of concentrations. However, the instrumentation is complicated. A simplified procedure was employed by Barrett and Stewart[9], but the vapor injection and difficult temperature control make the method not very precise or accurate.

The increasing use of headspace methods in aroma analysis has already led to the development of many new headspace sampling techniques to circumvent problems with solvent extraction or distillation methods. Basically, there are two kinds of

---

[a] Permanent address: Xinjiang Engineering Institute, Urumqi, China.

headspace sampling, indirect (combined sampling and enrichment by condensation or sorption) and direct[10]. For example, Curvers et al.[11] investigated the possibilities and limitations of dynamic headspace sampling as a preconcentration technique for the trace analysis of organics. Jentzsch et al.[12] introduced a headspace sample directly into the chromatographic column by pressurizing the headspace vessel for quantitative gas chromatographic (GC) analysis.

Multiplex chromatography can directly accept large volume samples provided that the bulk of the sample is suitable for use as a mobile phase[13]. This technique has several advantages over conventional chromatography, including an improved detection limit for samples of low concentration. The most important advantage for headspace samples is the ease and high precision of sample introduction. For example, Koel et al.[14] used the technique to follow the sample concentration from an exponential dilution flask.

Thermal desorption modulation has been used with multiplex gas chromatography for direct sampling of the headspace above a plastic sample[13]. We have now applied the same technique to measure the activity coefficients of binary liquids. Two systems, benzene–toluene and acetone–chloroform, were investigated. The method is simple, highly reproducible and easily computer automated.

EXPERIMENTAL

Apparatus

Experiments were performed using a Perkin-Elmer Model 3920 gas chromatograph with a flame ionization detector for the benzene–toluene system and a Varian Model 2700 gas chromatograph with an electron-capture detector for the acetone–chloroform system. The instrument design is shown in Fig. 1. The injection port was modified to hold the sampler as shown in Fig. 2. The laboratory computer system has been described previously[13]. The analytical column was a Supelcowax 10 (Supelco, Bellefonte, PA, U.S.A.) fused-silica open-tubular column (25.0 m × 0.250 mm I.D.) with a film thickness of 0.25 μm. The modulator was prepared by applying an electrically conductive paint to an 8-cm section at the head of the column. The modulator's resistance was 1.6 Ω. Its design and construction have been described previously[13]. The modulator was outside the oven with only enough of it extending
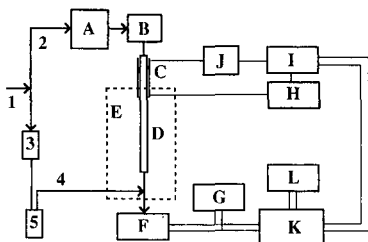
Fig. 1. Schematic diagram of the capillary GC instrument including thermal desorption modulator. A = Sample holder; B = manometer; C = thermal desorption modulator; D = column; E = oven; F = detector (flame ionization or electron-capture); G = recorder; H = power supply; I = optically coupled switch; J = resistor; K = computer; L = plotter; 1 = nitrogen gas supply; 2 = carrier gas; 3 = flow switch; 4 = make-up gas; 5 = flow controller.
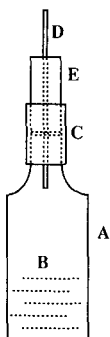
Fig. 2. Sample holder. A = Glass tube; B = sample; C = rubber tube connector; D = capillary tube; E = shrinkable tubing.

into the heated zone to avoid the presence of any cold stationary phase between the modulator and column. A U-shaped mercury manometer was placed between the column and the sampler to monitor the sample pressure. The pressures of all samples were equal. The computer controlled the modulator current from a 40 V d.c. power supply using an OPTO 22 Model ODC5P optically coupled switch.

Materials

Analytical-reagent grade benzene, toluene, acetone and chloroform were purchased from Fisher Scientific. Nitrogen, helium and hydrogen were of prepurified grade from Air Products.

Procedures

Liquid samples were placed into a 4.0-mm diameter glass tube. A 2.0 cm × 250 μm I.D. capillary was connected to the liquid sample holder as shown in Fig. 2. The ratio of the inside diameters of the reservoir glass tube and the capillary was large enough for the vapor concentration gradient along the reservoir to be neglected. A capped reservoir containing a particular molar fraction mixture was equilibriated in the injector for 30 min, then its cap was removed, the capillary restrictor installed and the whole sampler placed quickly in the injector.

A series of modulation pulse chromatograms were obtained from headspace gases above liquid mixtures with molar fractions varying from 0 to 1. Either a recorder connected directly to the gas chromatograph or a plotter connected to the computer could be used to record chromatograms.

Conventional injection chromatograms were also obtained. The recorder chart speed (1.0 cm/min) was much lower than that used in our method (2.5 cm/min). The injection splitting ratio was 1:10. Other chromatographic conditions were as specified in Fig. 3. A series of solutions with benzene molar fractions from 0 to 1 were placed in septum-capped bottles, which were then placed into an oven at 50°C for 40 min. A small vent needle was inserted through each septum to allow all samples to return to atmospheric pressure. The vent needle was removed and a syringe inserted through the septum. Pumping the syringe slowly ten times promoted mixing of the vapors. A 5-μl headspace sample was then withdrawn and injected through the injection port as soon as possible. A series of conventional chromatograms were thus obtained.

RESULTS AND DISCUSSION

Fig. 3 is a typical chromatogram obtained from a series of modulation pulses generated by computer. From the peak heights of components in the solution and the pure states, activity coefficients were calculated over the whole concentration range.

The activity coefficients a_A and a_B of substances A and B in a solution are $a_A = f_A/f_A^0$ and $a_B = f_B/f_B^0$, where f_A and f_B are the fugacities of components A and B in solution and f_A^0 and f_B^0 are the fugacities of the pure components A and B. If the vapor pressures of A and B are low, one can assume that the law of ideal gases applies and the fugacities are equal to the presures, and therefore $a_A = p_A/p_A^0$ and $a_B = p_B/p_B^0$, or $r_A x_A = p_A/p_A^0$ and $r_B x_B = p_B/p_B^0$, where r_A and r_B are the activity coefficients of A and B, x_A and x_B are molar fractions of A and B in solution, p_A and p_B are the partial pressures of the components in equilibrium with the solution and p_A^0 and p_B^0 are saturated vapor presures of the A and B in the pure state.

If we take the saturated vapors at the same volume and temperature and assume that peak height is proportional to concentration, then peak height is proportional to vapor pressure. Hence $p_A/p_A^0 = h_A/h_A^0$, $p_B/p_B^0 = h_B/h_B^0$, $r_A = h_A/x_A h_A^0$ and $r_B = h_B/x_B h_B^0$, where h_A and h_B are the peak heights of the vapors of A and B in equilibrium with the solution and h_A^0 and h_B^0 are the peak heights of the vapors of A and B in equilibrium with pure liquids A and B.

It is difficult to inject a desired volume of vapor into a GC column precisely, especially a capillary column. However, it is easy to effect precise sample introduction using a thermal desorption modulator.

Repeated modulation pulses give almost constant peak heights for the vapors of components A and B in equilibrium with their solution at each molar fraction. Only five pairs of peaks were averaged to calculate the results in Table I. It is possible to improve the precision by averaging more pulses if the experiment is run for a longer time. The variation due to sample introduction through the modulator appears to be random and can be eliminated or reduced by signal averaging. Signal averaging by repeated pulsing of the modulator is convenient and reproducible using thermal desorption modulators controlled by a computer. Signal averaging by conventional GC, however, is diffucult and of poor reproducibility.

Repeated pulsing of the modulator is very simple, requiring no external devices or extra operations to transfer a very small volume into the capillary GC column. The modulator continuously samples the concentration of the headspace vapor analytes in
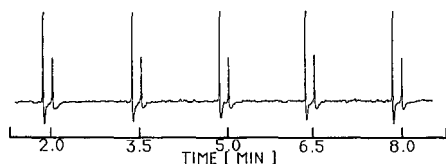
Fig. 3. Typical chromatogram obtained using the thermal desorption modulator for direct headspace sampling. Molar fraction of benzene, 0.60; data acquisition rate, 4 Hz; modulation pulse duration, 120 ms; pulse interval, 90 s; carrier gas flow-rate, 1.6 ml/min; detector make-up flow-rate, 27.0 ml/min; sample holder temperature, 50°C; column temperature, 120°C; detector temperature, 250°C; recorder chart speed, 2.5 cm/min.

TABLE I

ACTIVITY COEFFICIENTS IN BENZENE–TOLUENE BY THERMAL DESORPTION MODULA-
TOR INPUT CAPILLARY GC

Molar fraction		Mean peak height (mm)		R.S.D. (%)		Activity coefficient	
x_A	x_B	A	B			r_A	r_B
1.00	1.00	53.2		0.2			
0.80	0.20	47.4	11.1	0.2	1.0	1.11	1.38
0.60	0.40	38.2	19.2	0.5	1.1	1.20	1.19
0.40	0.60	28.4	27.0	0.9	0.8	1.33	1.12
0.20	0.80	15.0	34.2	1.5	0.7	1.41	1.06
0.00	1.00		40.2		0.6		
Average				0.7	0.8		

a flowing stream. Once the controlling parameters have been set, the process can run automatically.

Fig. 3 shows that the peaks are different in shape to those obtained with conventional GC. First a positive peak is observed, followed by a negative peak or vacancy. Together they look like the derivative of a conventional chromatogram. The positive peaks are due to desorption of analyte from the modulator stationary phase on heating, and the vacancies are due to readsorption of fresh analyte on the stationary phase on cooling the modulator.

The baseline of the modulator-generated chromatogram is determined by the steady-state sample concentrations, not zero concentration. Concentrations above the steady state are represented by positive peaks whereas concentrations below the steady state are vacancies. Some of the baseline noise is due to the constant bleeding of analyte through the detector[15].

The peaks are very sharp even though the recorder chart speed is faster than that used in conventional injection GC (2.5 vs. 1.0 cm/min). This modulation technique generates very sharp injections and is limited by band broadening in the column whereas our manual injection technique (split injection) generates broader peaks.

Sufficient time must be allowed between modulation pulses for the modulator to return to its initial state. Generally, the higher the capacity factor of the sample in the modulator, the longer the pulse interval should be because it will take a longer time to refill the modulator after each thermal desorption pulse. The 90-s repetition period in Fig. 3 is substantially longer than this required refill time. An improvement in signal averaging efficiency could be obtained by decreasing this time period.

The results obtained using this technique are in good agreement with those obtained using the conventional GC method. They are presented in Tables I, II and III for comparison. There are some differences in the activity coefficients of the acetone–chloroform system because the temperature used in our work (50°C) was different from that cited in the literature (35°C)[16,17].

The short-term relative standard deviation (R.S.D.) is often better than 1%, as in Tables I and III, but cannot be relied upon to be better than about 2%. Our syringe injection method will not give results with an R.S.D. better than about 4%.

TABLE II

ACTIVITY COEFFICIENTS IN BENZENE–TOLUENE BY CONVENTIONAL INJECTION CAPILLARY GC

Molar fraction		Mean peak height (mm)		R.S.D. (%)		Activity coefficient	
x_A	x_B	A	B			r_A	r_B
1.00	0.00	54.6		3.5			
0.80	0.20	50.2	11.3	3.8	4.5	1.15	1.36
0.60	0.40	40.0	19.3	3.2	4.1	1.22	1.17
0.40	0.60	28.7	27.0	4.5	2.4	1.30	1.09
0.20	0.80	15.5	34.5	3.0	3.3	1.42	1.04
0.00	1.00		41.4		3.8		
Average				3.6	3.6		

TABLE III

ACTIVITY COEFFICIENTS IN ACETONE–CHLOROFORM WITH THERMAL DESORPTION MODULAR INPUT

Molar fraction		Mean peak height (mm)		R.S.D. (%)		Activity coefficient[a]	
x_A	x_B	A	B			r_A	r_B
1.00	0.00	22.1		0.3			
0.80	0.20	17.3	4.9	1.2	1.8	0.98 (0.97)	0.65 (0.63)
0.67	0.33	13.3	9.0	1.2	1.0	0.90 (0.93)	0.74 (0.71)
0.50	0.50	9.0	15.0	1.0	0.9	0.81 (0.84)	0.81 (0.78)
0.33	0.67	5.1	19.2	1.7	0.5	0.70 (0.70)	0.79 (0.83)
0.20	0.80	2.8	27.4	3.6	1.6	0.63 (0.62)	0.93 (0.93)
0.00	1.00		37.0		0.4		
Average				1.5	1.0		

[a] Values from ref. 16 in parentheses.

Determinations run on separate days still have a 2% R.S.D. using the modulator sample input technique, and the R.S.D. increase further when determinations are run on separate days using the syringe injection technique.

This method should be useful for measuring the activity coefficients of other solutions or for measuring other solution parameters such as partition coefficients and enthalpy changes. Reaction kinetics can be investigated by monitoring the effluent from a flow-through micro-reactor. Also, it should be applicable to reaction gas chromatography using a thermal desorption modulator as a micro-reactor and to catalytic gas chromatography using a catalyst as an absorbent within a modulator.

ACKNOWLEDGEMENTS

REFERENCES

1 F. Daniels, J. M. Williams, P. Bender, R. Alberty and C. D. Cornwell, *Experimental Physical Chemistry*, McGraw-Hill, New York, 6th ed., 1962, p. 54.
2 E. R. Adlard, M. A. Khan and B. T. Whitham, in R. P. W. Scott (Editor), *Gas Chromatography 1960*, Butterworths, London, 1960, p. 252.
3 A. L. M. Keulmans, *Gas Chromatography*, Reinhold, New York, 1st ed., 1957, p. 171.
4 P. E. Porter, C. H. Deal and F. H. Stross, *J. Am. Chem. Soc.*, 78 (1956) 2999.
5 A. Kwantes and G. W. A. Rijnders, in D. H. Desty (Editor), *Gas Chromatography*, Butterworths, London, 1958, p. 125.
6 S. Evered and F. H. Pollard, *J. Chromatogr.*, 4 (1960) 451.
7 S. Kenwerthy, J. Miller and D. E. Martire, *J. Chem. Educ.*, 40 (1963) 541.
8 H. J. Arnikar, T. S. Rao and A. A. Bodhe, *J. Chem. Educ.*, 47 (1970) 826.
9 R. Barrett and T. Stewart, *J. Chem. Educ.*, 49 (1972) 492.
10 H. Hachenberg and A. P. Schmits, *Gas Chromatographic Headspace Analysis*, Heyden, New York, 1977, p. 23.
11 J. Curvers, Th. Noy, C. Cramers and J. Rijks, *J. Chromatogr.*, 289 (1984) 171.
12 D. Jentzsch, H. Kruger, G. Lebrecht, G. Dencks and J. Gut, *Fresenius Z. Anal. Chem.*, 236 (1968) 112.
13 J. B. Phillips, D. Luu, J. B. Pawliszyn and G. C. Carle, *Anal. Chem.*, 57 (1985) 2779.
14 M. Koel, M. Kaljurand and E. Küllik, in A. Zlatkis (Editor), *Advances in Chromatography 1982 (Las Vegas, NV)*, Chromatography Symposium, Houston, TX, 1982, p. 43.
15 S. Mitra and J. B. Phillips, *J. Chromatogr. Sci.*, 26 (1988) 620.
16 J. V. Zawidzki, *Z. Phys. Chem. (Leipzig)*, 35 (1900) 129.
17 R. C. Weast (Editor), *Handbook of Chemistry and Physics*, Chemical Rubber Company, Cleveland, OH, 51st ed., 1970-71, p. D146.

CHROM. 21 630

SENSITIVE FLUORESCENCE LABELLING FOR ANALYSIS OF CARBOXYLIC ACIDS WITH 4-BROMOMETHYL-6,7-METHYLENEDIOXYCOUMARIN

HIDEO NAGANUMA* and YUKINORI KAWAHARA

Product Development Laboratories, Sankyo Co. Ltd., 2-58, Hiromachi 1-chome, Shinagawa-ku, Tokyo 140 (Japan)

(First received December 28th, 1988; revised manuscript received May 17th, 1989)

SUMMARY

A fluorescence labelling reagent, 4-bromomethyl-6,7-methylenedioxycoumarin (BrMDC), was synthesized from sesamol and citric acid by Pechman condensation followed by bromination. Nanomole amounts of saturated aliphatic fatty acids were converted into the corresponding fluorogenic esters in the presence of anhydrous potassium carbonate and a crown ether as a catalyst and were separated by reversed-phase high-performance liquid chromatography (HPLC). Quantitative studies revealed that *n*-caproic acid was esterified completely at low temperature and with sufficient reproducibility. The detection limit was just below 15 fmol per injection at a signal-to-noise ratio of 3. The fluorescence quenching of the BrMDC derivative was the lowest in conventional mixed solvent systems in comparison with those of two previously reported coumarin compounds. BrMDC was also applied to the simultaneous analysis of some acidic non-steroidal anti-inflammatry agents by reversed-phase HPLC.

INTRODUCTION

A large number of biologically interesting substances contain carboxylic moieties, both as intermediates and end-products, from endogenous metabolism of carbohydrates or lipids. Several xenobiotics represented by drugs also possess carboxylic groups. In therapeutic drug monitoring to design an individualized dosage regimen or in the investigation of pharmacokinetic–pharmacodynamic relationships, reliable and sensitive analytical methods for the drug itself and/or its active metabolites in biological specimens are required[1,2]. High-performance liquid chromatography (HPLC) is now widely use for the trace analysis of numerous organic substances because it provides rapid and sufficient resolution even when two or more closely related analogues exist homogeneously. In early work, some fatty acids or their methyl esters were also successfully separated directly by carbon number using reversed-phase bonded columns[3–5]. With such substances, however, which do not have any chromogenic substituents, detection has to depend on their refraction or weak

absorption near the extreme ultraviolet region. This has hindered the application of
HPLC to the trace analysis of carboxylic acids in biological systems[6].

Chemical derivatization of specific functional groups to give UV-sensitive or
strong fluorogenic probes overcame this disadvantage and improved the detectability
of the compounds of interest[7]. Durst et al.[8] first employed p-bromophenacyl bromide
(p-BPB) as a labelling reagent for calboxylic acids to achieve sensitive UV detection in
HPLC, and this was extended to the resolution diastereomers of some long-chain
unsaturated fatty acids[9]. Dünges and co-workers introduced 4-bromomethyl-7-
methoxycoumarin (BrMMC), a highly sensitive fluorescence labelling reagent, for
both thin-layer chromatography[10,11] and HPLC[12,13], and since then various other
fluorescence probes have been developed, e.g., 1-bromoacetylpyrene (BAP)[14], 4-bro-
momethyl-6,7-dimethoxycoumarin (BrDMC)[15], 9-anthryldiazomethane (ADAM)[16],
4-bromomethyl-7-acetoxycoumarin (BrMAC)[17], 3-bromomethyl-6,7-dimethoxy-1-
methyl-2(1H)-quinoxalinone (BrMQ)[18] and p-(9-anthroyloxy)phenacyl bromide[19].
Among these, BrMMC and ADAM have been commonly applied to the trace analysis
of biologically important acid compounds such as prostaglandins[20,21] in enzymatic
preparations.

In this paper, we report the preparation of 4-bromomethyl-6,7-methylenedioxy-
coumarin (BrMDC), a fluorescence labelling reagent for caboxylic acids, which
possesses a more fluorogenic 6,7-methylenedioxycoumarin moiety than in previously
reported coumarin compounds, and its applicability to the simultaneous analysis of
a series of fatty acids and some acidic non-steroidal anti-inflammatry agents
(NSAIDs) by reversed-phase HPLC.

EXPERIMENTAL

Materials

3,4-Methylenedioxyphenol (sesamol) and 4-bromomethyl-6,7-dimethoxycou-
marin (BrDMC) were purchased from Aldrich (Milwaukee, WI, U.S.A.), 4-bromo-
methyl-7-methoxycoumarin (BrMMC), aspirin, ketoprofen and ibuprofen from
Wako (Osaka, Japan) and all C_3–C_{19} saturated fatty acids, naproxen, indomethacin
and the crown ethers 18-crown-6, dicyclohexano-18-crown-6, dibenzo-18-crown-6
and kryptofix 222 from Sigma (St. Louis, MO, U.S.A.). Loxoprofen was prepared and
supplied by the Chemical Research Laboratories of Sankyo (Tokyo, Japan)[22].
Flurbiprofen was purchased as commercially available tablets (Furoben; Kaken
Pharmaceutical, Tokyo, Japan) and extracted and purified in our laboratories.
4-Methyl-6,7-methylenedioxycoumarin for fluorescence spectral studies was prepared
according to Fukui and Nakayama[23]. All other chemicals for synthesis were of
guaranteed reagent grade and all organic solvents for chromatographic purpose were
of special grade for HPLC, obtained from Wako.

Instruments

Proton nuclear magnetic resonance (¹H NMR) spectra were measured on
a Model JNM-GX270 spectrometer (Jeol, Tokyo, Japan) at 270 MHz and chemical
shift values (δ) were expressed in parts per million downfield from tetramethylsilane as
internal standard. IR spectra were recorded on a Model 60-SX Fourier transform
infrared spectrometer (Nicolet Japan, Tokyo, Japan). Mass spectra were measured

with a Model DX-300 mass spectrometer (Jeol, Tokyo, Japan). The HPLC system consisted of a Model 655 solvent delivery pump unit (Hitachi, Tokyo, Japan) and a Model F-1000 fluorescence spectrophotometer (Hitachi), which was linked to a Model C-R3A chromatographic integrator (Shimadzu, Kyoto, Japan). The sample was applied to a μBondapak C_{18} reversed-phase packed column (300 mm × 3.9 mm I.D.) (Millipore-Waters, Milford, MA, U.S.A.) by a WISP 710B automatic sample processor (Millipore-Waters).

Determination of fluorescence quantum yield

Fluorescence spectra of 6,7-substituted 4-methylcoumarins in various solvents were measured on a Model RF-540 fluorescence spectrophotometer (Shimadzu). The fluorescence intensity was evaluated as the integrated area under the spectrum and the relative fluorescence quantum yield was calculated according to Weber and Teale[24] using quinine sulphate as a reference.

Synthesis of 4-carboxymethyl-6,7-methylenedioxycoumarin (I)

4-Carboxymethyl-6,7-methylenedioxycoumarin (I) was prepared according to Baker et al.[25]. Finely powdered crystalline citric acid (250 mmol) was poured stepwise at 70°C into 67.5 ml of sulphuric acid. To the ice-cold solution was added an equal number of moles of finely ground sesamol, keeping the temperature below 5°C. A further 29 ml of sulphuric acid were poured in gradually and stirred gently overnight. The reaction mixture, diluted with 50 ml of chilled water, was filtered and the remaining brown material was washed sequently with 0.01 M sulphuric acid, 2 M sodium hydroxide solution and 2 M hydrochloric acid. After being kept stationary overnight, the ash-coloured precipitate was separated by centrifugation and recrystallized from acetonitrile to give I as faintly white prisms; yield 33–51%, m.p. 170°C. Analysis: calculated for $C_{12}H_8O_6$, C 58.07, H 3.25; found, C 57.96, H 3.08%. ^{1}H NMR (perdeuterated dimethyl sulphoxide: 3.96 (2H, s, $-CH_2COO-$), 6.23 (2H, s, $-OCH_2O-$), 6.39 (1H, s, $=C=CH-CO-$), 7.02 (1H, s, aromatic), 7.26 ppm (1H, s, aromatic). Mass spectrum: m/z 248 (M^+), 204 (base peak). IR (KBr pellet): 3050, 2920, 1720, 1410, 1280, 1040, 940 cm^{-1}.

Synthesis of 4-bromomethyl-6,7-methylenedioxycoumarin (BrMDC, II)

To 10 mmol of I suspended in 7.5 ml of acetic acid was gradually added an equimolar amount of acetic acid containing 10 mmol of bromine, the solution was refluxed for 1 h. After cooling, the resulting crude material was subjected to silica gel column chromatography and eluted with acetone. The main fraction was evaporated to dryness and the residue was recrystallized from methanol to give II as yellow prisms; yield 76%, m.p. 241°C. Analysis: calculated for $C_{11}H_7O_4Br$, C 46.46, H 2.47, Br 28.23; found, C 46.93, H 2.34, Br 27.86%. ^{1}H NMR (perdeuterated acetone): 4.79 (2H, s $-CH_2Br$), 6.20 (2H, s, $-OCH_2O-$), 6.50 (1H, s, $=C=CH-CO-$), 6.94 (1H, s, aromatic), 7.32 ppm (1H, s, aromatic). Mass spectrum: m/z 283 (M^+), 175 (base peak). IR (KBr pellet): 3070, 2920, 1730, 1450, 1270, 1040, 630 cm^{-1}.

Preparation of n-caproic acid derivatives (III) as fluorescence reference

The authentic BrMDC derivative of n-caproic acid was synthesized on a semi-micro preparative scale in order to evaluate its reactivity. To a solution of

n-caproic acid (1.2 mmol) in 5 ml of acetonitrile were added BrMDC (0.6 mmol) and triethylamine (1.2 mmol). The resulting solution was allowed to stand at 40°C for 1 h, then, evaporated to dryness *in vacuo*. The residue was purified on a silica gel column with *n*-hexane–dichloromethane (50:50) as eluent. The main fraction was evaporated to dryness *in vacuo* and the residue was purified by repeated recrystallization from methanol to give III as white needles; yield 53%, m.p. 106°C. Analysis: calculated for $C_{17}H_{18}O_6$, C 64.14, H 5.70; found, C 64.33, H 5.58%. ^{1}H NMR (deuterochloroform): 0.91 (3H, t, J = 6.8 Hz, $-CH_3$), 1.31–1.72 [6H, m, $-(CH_2)_3-$], 2.45 (2H, t, $-OCOCH_2-$), 5.20 (2H, s, $-CH_2OCO-$), 6.09 (2H, s, $-OCH_2O-$), 6.36 (1H, s, $=C=CH-CO-$), 6.86–6.88 ppm (2H, m, aromatic). Mass spectrum: m/z 318 (M$^+$), 220 (base peak). IR (KBr pellet): 3080, 2840–2960, 1740, 1720, 1270, 1170, 1030 cm^{-1}.

Analytical derivatization of carboxylic acids

Fatty acids or NSAIDs for working standards were prepared as solutions in ethanol or acetone. An aliquot (0.1–100 nmol) was dispended into a 15-ml brown tube and evaporated to dryness *in vacuo*. To the residue were added a 500 µl solution of acetonitrile containing BrMDC (1.0 mM, corresponding to at least a 5-fold excess over the acids) and a crown ether (1.0 mM, saturated with an excess of finely powdered potassium carbonate and then sonicated briefly) as to become 1 ml of acetonitrile mixture. The reaction mixture was heated at 40°C for 1 h, then 100 µl of acetic acid–acetonitrile (1:9) was added in order to consume the remaining reagent and to stabilize the derivative formed. After cooling to ambient temperature, a 10-µl aliquot of the reaction mixture was applied to HPLC.

Chromatographic conditions

Optimum separation of C_3–C_{19} straight-chain fatty acid derivatives with BrMDC could be achieved by using µBondapak C_{18} as an analytical reversed-phase column and three different mobile phases, *i.e.*, acetonitrile–water (50:50, 70:30 and 90:10, v/v), containing 1.5% acetic acid. By using same column and acetonitrile–water (50:50, v/v) containing 1% acetic acid as the mobile phase was also separated six NSAID derivatives with BrMDC. All solvents were degassed by brief sonication just before use and then pumped isocratically at 2 ml/min under ambient temperature. The detection wavelengths were adjusted to 355 nm excitation and 435 nm emmision. The sensitivity range of the fluorescence detector was varied between 0.5 and 20.

RESULTS AND DISCUSSION

Synthesis of 4-substituted 6,7-methylenedioxycoumarin as a fluorescence probe

Many fluorescence labelling reagents are known for the sensitive chromatographic determination of carboxylic acids[10,14–19]. ADAM[21] and BrMMC[20] have been used extensively for the trace analysis of prostanoids in biological specimens. However, these reagents had the disadvantages that the former was unstable[8,21] and the fluorescence intensity of the latter derivatives was affected by solvents[26]. It is well recognized that electron-donating substituents at the 6- or 7-position of the coumarin moiety, such as alkylamino, hydroxy and alkyloxy, contribute to enhancing the fluorogenecities and show significant Stokes shifts[27,28].

In order to overcome the drawbacks of the previous fluorescence probes, we

therefore examined the effect of the solvent on the fluorescence properties of several 6-
or 7-substituted 4-methylcoumarins, and found that a 6,7-methylenedioxy substituent
possessed about a 2–10 times higher relative fluorescence quantum yield than the
7-monomethoxy analogue, as shown in Table I. The smaller difference in the
fluorescence quantum yields among aqueous solvents such as ethanol, acetonitrile and
water suggested less quenching in their mixed solvent systems, which might make them
utilizable as mobile phases for reversed-phase HPLC.

We have already demonstrated that N-(6,7-methylenedioxy-4-methyl-3-cou-
marinyl)maleimide (MDCM), a labelling reagent for thiol groups, gave a higher
sensitivity than DACM, because it showed less quenching in aqueous mixed solvents
used as HPLC mobile phases[29]. These findings strongly suggested that BrMDC, with
an active vinylogous halocarbonyl at the 4-position of the coumarin moiety, might be
also be also applicable as a labelling reagent for carboxylic acids. BrMDC could be
readily prepared from sesamol and citric acid by a two-step reaction, i.e., condensa-
tion[25] of a phenolic alcohol with an α-keto acid followed by bromination under mildly
acidic conditions, although the overall reaction yield was low (25–39%). The reagent
proved to be stable at room temperature for at least 6 months with protection from
light.

Fluorescence characteristics of BrMDC derivatives

A carboxylic acid is easily esterified with a β-halocarbonyl group under alkaline
catalysis[30]. Durst et al.[8] demonstrated that inorganic alkaline crown ethers might be
effective as solid–liquid phase transfer catalysts because of the small amount of reagent
required, quantitative reactivity and low solvent effect. We first compared the
derivatization efficiencies of BrMDC by combining seven aprotic solvents and four
crown ethers, 18-crown-6, dicyclohexo-18-crown-6, dibenzo-18-crown-6 and krypto-
fix 222, as catalysts. The first two crown ethers adequately catalysed the formation of
ester derivatives with n-caproic acid. The reaction velocity was the highest in
acetonitrile, followed by acetone, tetrahydrofuran and dichloromethane, in that order;
no fluorescent product could be obtained in methanol or water. Consequently,
18-crown-6 saturated with potassium carbonate in acetonitrile was chosen as the

TABLE I

COMPARISON OF MAXIMUM FLUORESCENCE EMISSION WAVELENGTHS (λ) AND REL-
ATIVE FLUORESCENCE QUANTUM YIELDS (Φ_f) OF 6- AND 7-SUBSTITUTED COUMARINS
IN VARIOUS SOLVENTS

Fluorescence properties of 4-methyl-7-methoxycoumarin are taken from ref. 28.

Solvent	4-Methyl-6,7-methylenedioxycoumarin		4-Methyl-7-methoxycoumarin	
	λ (nm)	Φ_f	λ (nm)	Φ_f
Diethyl ether	385	0.029	368	0.003
Dichloromethane	398	0.09	372	0.02
Ethanol	406	0.38	374	0.11
Acetonitrile	404	0.10	370	0.01
Acetic acid	405	0.51	375	0.18
Distilled water	410	0.88	381	0.58

catalyst for the subsequent study. The fluorescence characteristics of n-caproic acid ester derivatives with BrMDC, BrMMC and BrDMC were compared in acetonitrile–water mixtures as shown in Fig. 1.

The BrMDC derivative gave a higher fluorescence than equimolar amounts of the other two fluorescent derivatives, and its quenching on increasing the concentration of acetonitrile was the least, as expected from a spectral study. The reaction kinetics of BrMDC with n-caproic acid are shown in Fig. 2.

The derivatization reaction was completed almost quantitatively within 1 h at 40°C. A constant amount of n-caproic acid (250 nmol) was titrated with various amounts of BrMDC, as shown in Fig. 3. The results confirmed that the derivatization occurred in a 1:1 molar stoichiometric manner as already reported for β-halocarbonyl[8].

We further intend to study application of BrMDC to the quantitative analysis of acidic compounds in biological specimens. During a preliminary study on some acidic NSAIDs, it was found that equimolar BrMDC could not achieve complete derivatization with solvent extracts from biological fluids, such as human plasma and urine. This might be due to the coexistence of undesirable reactive substances or a small amount of water remaining in the extracts. On the other hand, none of interference peaks derived from the reagent could be found in the eluate for most carboxylic acids of interest, even when a large excess of BrMDC (2 μmol or more per reaction cuvette) was present. Therefore, it seemed preferable that the derivatization should be performed with an adequate excess of reagent, which was therefore set at 0.5 μmol, corresponding to at least a 5-fold excess over the total amount of acids expected, in further chromatographic studies.
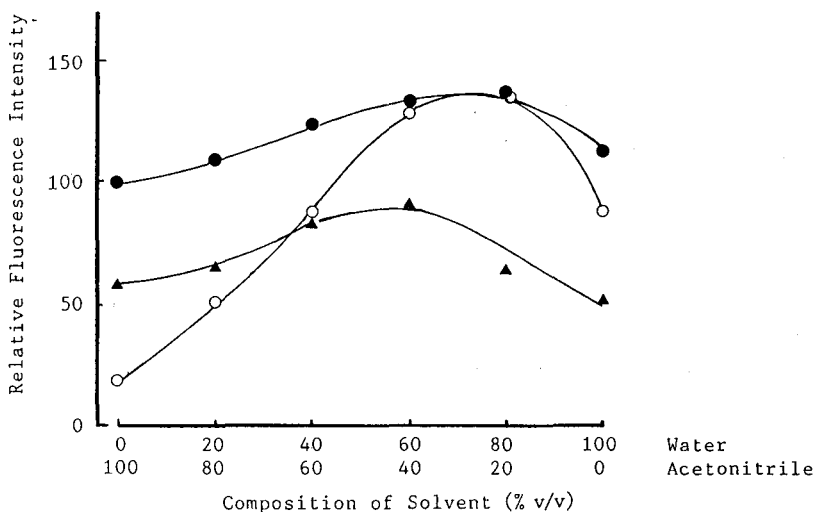
Fig. 1. Relative fluorescence intensity of derivatives of n-caproic acid with (●) BrMDC, (○) BrMMC and (▲) BrDMC in acetonitrile–water mixtures. A 40-nmol amount of n-caproic acid was derivatized with each fluorescence probe as described in the text and 5-μl aliquots of the reaction mixtures were applied to 20 × 20 cm silica gel thin-layer plates and developed with n-hexane–ethyl acetate (50:50). The corresponding reaction products were scraped off and reconstituted in aqueous acetonitrile to give a final concentration of 40 nM. The fluorescence intensity of the BrMDC derivative in distilled water is arbitrarily expressed as 100.
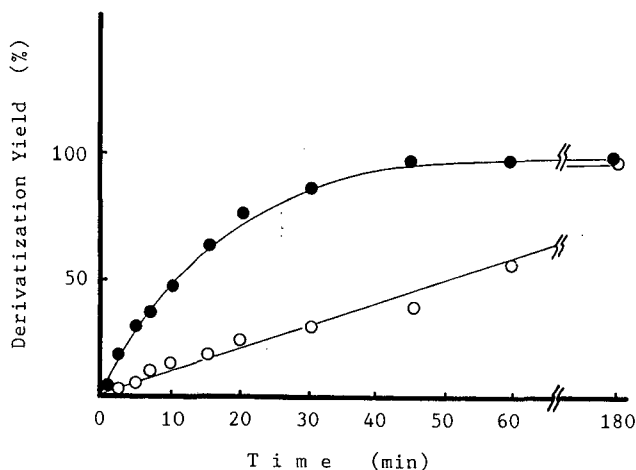
Fig. 2. Time course of the development of the fluorescence of n-caproic acid derivative with BrMDC. (●) 40°C; (○) room temperature. The derivatization yield was obtained from the fluorescence response against that of a synthetically prepared derivative (III).

Chromatographic application

A reversed-phase HPLC separation of BrMDC derivatives of thirteen aliphatic fatty acids could be achieved within 15 min per run by using three different mobile phases, as illustrated in Fig. 4.

The derivatives were almost completely resolved from each other, except the propionic acid derivative, which was eluted relatively faster than others and was overlapped by reagent peaks. The accuracy and the validity of the derivatization were
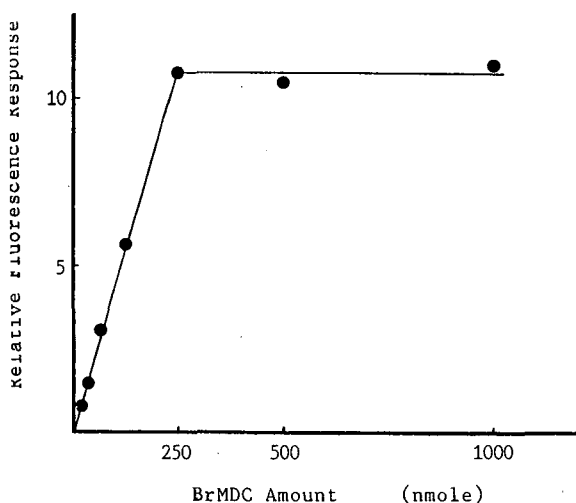
Fig. 3. Quantitative titration curve of n-caproic acid with BrMDC. A constant amount of n-caproic acid (250 nmol) was derivatized with different amounts of BrMDC (15–1000 nmol) and subjected to HPLC. The relative fluorescence response (ordinate) is represented in arbitrary units.
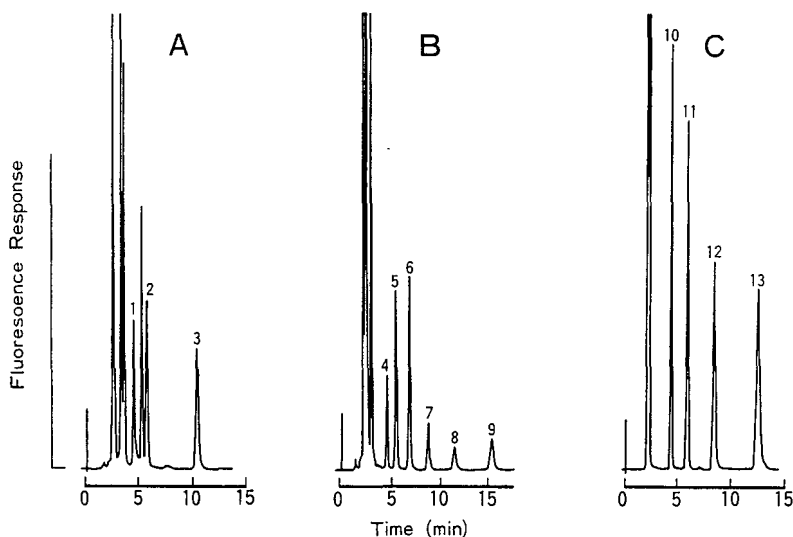
Fig. 4. Chromatographic separations of BrMDC derivatives of saturated fatty acids. Peaks: 1 = C_3; 2 = C_4; 3 = C_6; 4 = C_7; 5 = C_8; 6 = C_9; 7 = C_{10}; 8 = C_{11}; 9 = C_{12}; 10 = C_{13}; 11 = C_{15}; 12 = C_{17}; 13 = C_{19}. HPLC conditions: column, μBondapak C_{18} (300 mm × 3.9 I.D.); mobile phase, acetonitrile–water, (A) 50:50, (B) 70:30 and (C) 90:10, containing 1.5% acetic acid; flow-rate, 2.0 ml/min (isocratic); temperature, ambient; detection, excitation at 355 nm, emission at 435 nm; detector sensitivity, 0.5.

examined by five replicated analyses at different amounts of *n*-caproic acid, as shown in Table II.

The calibration graph of amount of acid *versus* integrated peak area of the fluorescent response was linear over the range 0.10–25 nmol and passed through the origin (r = 0.999). All the results for *n*-caproic acid were sufficiently accurate, with coefficients of variation of not more than 7%. The detection limit of the *n*-caproic acid derivative as a representative compound was as low as 15 fmol per injection when the signal-to-noise ratio was 3. This sensitivity is similar to those of previously reported fluorescence probes[11,12,17].

Some commercially available NSAIDs could also be derivatized with BrMDC. The derivatives of aspirin and five propionate anti-inflamatory agents in the

TABLE II

DERIVATIZATION REPRODUCIBILITY OF BrMDC WITH *n*-CAPROIC ACID

Each value is expressed as the mean ±S.D. of five replicate determinations.

Amount of n-caproic acid (nmol)		Coefficient of variation (%)
Added	Found	
25	25.2 ± 0.6	2.34
5	5.15 ± 0.12	2.33
1	0.94 ± 0.04	4.04
0.1	0.103 ± 0.007	6.98
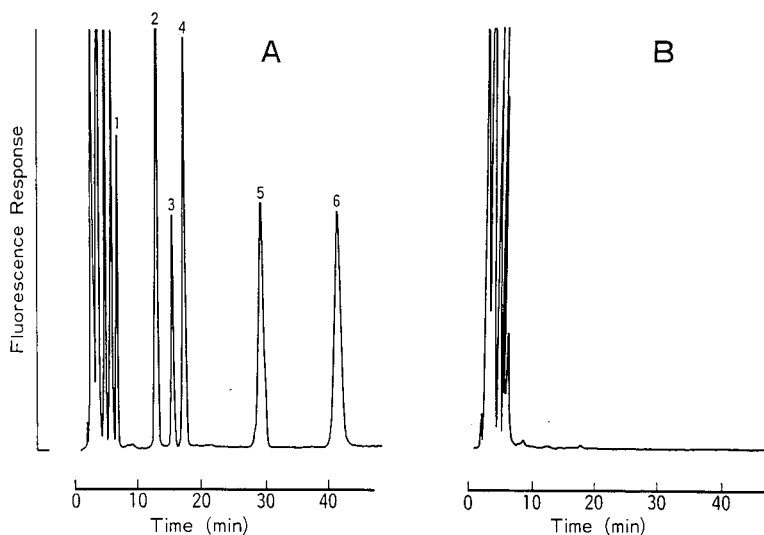
Fig. 5. Chromatographic separation of BrMDC derivatives of commercially available acidic NSAIDs. (A) Authentic NSAID mixture. Peaks: 1 = aspirin (25.2); 2 = loxoprofen (37); 3 = ketoprofen (72); 4 = naproxen (197); 5 = flurbiprofen (37); 6 = ibuprofen (44 pmol per injection). (B) Blank of reaction mixture containing only reagents. HPLC conditions: mobile phase, acetonitrile–water (50:50) containing 1% acetic acid; detector sensitivity, 2; other conditions in Fig. 4.

pharmacokinetically interesting concentration range (1–10 μg/ml) were adequately separated under the same isocratic conditions, as shown in Fig. 5.

Neither indomethacin nor mefenamic acid were completely esterified with BrMDC, even when a large amount of reagent was used, so the method seems inapplicable to their trace analysis, especially in biological specimens. The reason for this extremely low reactivity was suspected to be that each of the two compounds possessed a weakly basic nitrogen atom, which might prevent the formation of an anionic intermediate in aprotic solvents such as another carboxylic compound. We also ascertained that BrMDC could form corresponding ester derivatives with a variety of other substituted carboxylic acids, such as branched fatty acids, unsaturated acids, aryl acids, diacids and N-acylamino acids, but did not react with amino acids and peptides.

In conclusion, BrMDC might be applicable to the trace analysis of several series of acid compounds with satisfactory accuracy and reliability with slight modifications of the chromatographic condition. It is expected that its high sensitivity may provide a much more precise knowledge of biologically important organic acids, e.g., as a diagnostic technique for inherited metabolic diseases. The reagent is now being applied to the determination of prostaglandins, which are produced enzymatically from arachidonic acid by bovine seminal microsome preparations, and to some NSAIDs and their metabolites in biological fluids for pharmacokinetic studies.

REFERENCES

1 T. Goto and T. Nambara, in T. Nambara and N. Ikekawa (Editors), Modern High-Performance Liquid Chromatography, Hirokawa, Tokyo, 1982, p. 405.

2 A. Tsuji, in M. Hanano, K. Umemura and T. Iga (Editors), *Applied Pharmacokinetics, Theory and Experiments*, Soft Science, Tokyo, 1985, p. 37.
3 P. T. S. Pei, R. S. Henly and S. Ramachandran, *Lipids*, 10 (1975) 132.
4 C. R. Scholfield, *J. Am. Oil Chem. Soc.*, 52 (1975) 36.
5 J. D. Warthen, Jr., *J. Am. Oil Chem. Soc.*, 52 (1975) 151.
6 R. S. Henly and S. Ramachandran, in K. Tsuji (Editor), *GLC and HPLC Determination of Therapeutic Agents, Part 3*, Marcel Dekker, New York, 1979, p. 1341.
7 J. F. Lawrence, in R. W. Frei and J. F. Lawrence (Editors), *Chemical Derivatization in Analytical Chemistry*, Vol. 2, Plenum Press, New York, 1981, p. 191.
8 H. D. Durst, M. Milano, E. J. Kikta, S. A. Connelly and E. Grushka, *Anal. Chem.*, 47 (1975) 1797.
9 P. T. Pei, W. C. Kossa, S. Ramachandran and R. S. Henly, *Lipids*, 11 (1976) 814.
10 W. Dünges, *Chromatographia*, 9 (1976) 624.
11 W. Dünges, *Anal. Chem.*, 49 (1977) 442.
12 W. Dünges and N. Seiler, *J. Chromatogr.*, 145 (1978) 483.
13 S. Lam and E. Grushka, *J. Chromatogr.*, 158 (1978) 207.
14 S. Kamada, M. Maeda and A. Tsuji, *J. Chromatogr.*, 272 (1983) 29.
15 R. Farinotti, Ph. Siard, J. Bouson, S. Kirkiacharian, B. Valeur and G. Mahuzier, *J. Chromatogr.*, 269 (1983) 81.
16 N. Nimura and T. Kinoshita, *Anal. Lett.*, 13 (1981) 191.
17 H. Tuchiya, T. Hayashi, H. Naruse and N. Takagi, *J. Chromatogr.*, 234 (1982) 121.
18 M. Yamaguchi, S. Hara, R. Matsunaga, M. Nakamura and Y. Ohkura, *J. Chromatogr.*, 345 (1985) 227.
19 T. A. Stein, L. Angus, E. Borrero, L. J. Auguste and L. Wese, *J. Chromatogr.*, 385 (1987) 377.
20 J. Turk, S. J. Weiss, J. E. Davis and P. Needleman, *Prostaglandins*, 16 (1978) 291.
21 K. Kiyomiya, K. Yamaki, N. Nimura, T. Kinoshita and S. Oh-ishi, *Prostaglandins*, 31 (1986) 71.
22 A. Terada, S. Naruto, K. Wachi, S. Tanaka, Y. Izuka and E. Misaka, *J. Med. Chem.*, 27 (1984) 216.
23 K. Fukui and M. Nakayama, *J. Sci. Hiroshima Univ., Ser. A-2*, 26 (1963) 131.
24 G. Weber and F. W. J. Teale, *Trans. Faraday Soc.*, 54 (1958) 640.
25 W. Baker, C. N. Haksar and J. F. W. McOmie, *J. Chem. Soc.*, (1950) 170.
26 Y. Kawahara, in preparation.
27 C. E. Wheelock, *J. Am. Chem. Soc.*, 81 (1959) 1348.
28 T. Hinohara, K. Amano and K. Matsui, *Nippon Kagaku Kaishi*, (1976) 247.
29 Y. Kawahara, Y. Yamazaki and H. Naganuma, *Abstracts of the 43rd International Congress of Pharmaceutical Sciences, Montreux, 1983*, p. 78.
30 L. A. Sternson, in R. W. Frei and J. F. Lawrence (Editors), *Chemical Derivatization in Analytical Chemistry*, Vol. 1, Plenum Press, New York, 1981, p. 127.

CHROM. 21 636

PREPARATION OF ADSORBENTS FOR AFFINITY CHROMATOGRAPHY USING TSKGEL TRESYL-TOYOPEARL 650M

KOJI NAKAMURA*, KIYOHIRO TOYODA and YOSHIO KATO

Central Research Laboratory, Tosoh Corporation, Tonda, Shin-nanyo, Yamaguchi (Japan)

and

KIYOHITO SHIMURA and KEN-ICHI KASAI

Faculty of Pharmaceutical Sciences, Teikyo University, Sagamiko, Kanagawa (Japan)

(First received January 24th, 1989; revised manuscript received May 23rd, 1989)

SUMMARY

The optimum conditions for the coupling of proteins were investigated using TSKgel Tresyl-Toyopearl 650M. They were dependent on the proteins coupled. For example, when soybean trypsin inhibitor was coupled at pH 8 the coupling was completed within 1 h and the subsequent adsorption capacity for trypsin was maximal. Longer coupling times decreased the adsorption capacity due to multi-point attachment. The adsorbents obtained were successfully used for affinity chromatography in a short time.

INTRODUCTION

The preparation of adsorbents for affinity chromatography requires suitable matrices and effective coupling methods for attachment of ligands. Beaded agarose activated by cyanogen bromide is the most popular and versatile solid support for affinity matrices. Though the cyanogen bromide method discovered by Axen *et al.*[1] has contributed to the recent development of affinity chromatography, it has some problems such as the labile linkage between the ligands and the matrix[2,3] and the introduction of charged species[4,5]. In order to overcome these problems, Nilsson and Mosbach[6] developed a procedure using organic sulphonyl chlorides as activating agents. They activated agarose with tresyl chloride under relatively mild conditions for a short period of time. This yielded predominantly primary hydroxyl activation and the result was an excellent matrix for coupling proteins and affinity ligands. However, agarose is not a completely satisfactory matrix especially for industrial use and high-performance affinity chromatography because of its poor mechanical strength.

Very recently, a new support for affinity chromatography has become commercially available under the trade-name of TSKgel Tresyl-Toyopearl 650M. According to the supplier, it is prepared by introducing tresyl groups into TSKgel Toyopearl HW-65 (44–88 μm), which is a hydrophilic resin-based material of large pore size employed for gel filtration[7]. This paper describes the preparation of adsorbents for affinity chromatography using TSKgel Tresyl-Toyopearl 650M.

EXPERIMENTAL

Materials

Soybean trypsin inhibitor (STI), bovine trypsin, porcine trypsin, concanavalin A (Con A) and crude peroxidase were from Sigma. Purified peroxidase (RZ:3.48) was from Toyobo (Osaka, Japan). Human immunoglobulin (IgG) and human serum were from Miles, protein A from Repligen. TSKgel Tresyl-Toyopearl 650M was from Tosoh.

Coupling of proteins to Tresyl-Toyopearl

Proteins (5–80 mg) were dissolved in 4 ml of an appropriate coupling buffer at different pH values (0.1 M phosphate buffer containing 0.5 M NaCl for pH 6 and 7, 0.1 M carbonate buffer containing 0.5 M NaCl for pH 8 and 9) and mixed with 0.4 g dried Tresyl-Toyopearl (1 g dried Tresyl-Toyopearl gives a final gel volume of about 5 ml) at 4 or 25°C for 0.5–16 h. After washing three times with 20 ml of coupling buffer, the unreacted tresyl groups were deactivated by resuspending the gel in 10 ml of 0.1 M Tris–HCl (pH 8.5) for 1 h. Protein contents were determined by amino acid analysis.

Determination of adsorption capacity

The adsorption capacity of immobilized STI, Con A and protein A were determined by passing 10 mg of purified trypsin, peroxidase and human IgG, respectively, through each column (50 mm × 5 mm) equilibrated with the appropriate buffer [0.05 M Tris–HCl buffer containing 0.5 M NaCl and 20 mM CaCl$_2$ (pH 7.5) for the STI column, 0.1 M acetate buffer containing 0.5 M NaCl and 1 mM MgCl$_2$, MnCl$_2$ and CaCl$_2$ (pH 6.0) for the Con A column, 0.1 M phosphate buffer (pH 7.0) for the protein A column]. The excess of protein was removed with the equilibration buffer. Desorption of protein was achieved by an appropriate buffer [0.1 M acetic acid containing 0.5 M NaCl (pH 3.0) for the STI column, 0.11 M mannose in equilibration buffer for the Con A column, 0.1 M glycine–HCl (pH 2.2) for the protein A column]. The amounts of protein were calculated from the volume and absorption at 280 nm (trypsin and human IgG) and 403 nm (peroxidase).

Affinity chromatography

All chromatographic measurements were performed at 4 or 25°C with a CCPM pump (Tosoh) equipped with a variable-wavelength UV detector Model UV-8000 (Tosoh).

Measurement of trypsin activity

Trypsin activity was measured with benzoylarginine ethyl ester as a substrate, essentially according to the method of Schwert and Takenaka[8].

Measurement of peroxidase activity

Peroxidase activity was measured by the change in absorbance at 460 nm due to the oxidation of *o*-dianisidine in the presence of peroxidase and H$_2$O$_2$ as described by Shannon *et al.*[9].

Electrophoresis

Electrophoretic analysis of the fraction was performed in slabs of a 4–20% polyacrylamide gradient gel (Tefco, Tokyo, Japan) according to the manual supplied.

RESULTS AND DISCUSSION

Coupling of STI at different pH values

Table I shows the results of coupling of STI at different pH values. At pH 6 the coupling reaction was very slow and the coupling yield was only 12% after 16 h. At pH 7 the coupling yield was increased with coupling time, and the adsorption capacity for trypsin was maximal after 16 h. At pH 8 the coupling of STI was completed in 1 h and the adsorption capacity was maximal. However, longer coupling times decreased the adsorption capacity. At pH 9, although the coupling reaction was also completed in 1 h, the adsorption capacity was constant. Amino acid analyses indicated that tyrosyl, histidyl and lysyl residues of STI were coupled to Tresyl-Toyopearl and the lysyl residue was more reactive at higher pH values.

Immobilization of protein is generally thought to occur via several bonds per protein molecule (if the protein has many available functional groups). The coupling of STI at higher pH values (pH 8 or 9) might favour the multi-point attachment which decreases the biochemical activity due to distortion of STI or to steric hindrance of its binding site.

Effect of ligand concentration

Table II shows the effect of the ligand concentration on the amount coupled and

TABLE I

COUPLING OF STI AT DIFFERENT pH VALUES

STI applied: 5 mg/ml gel. Temperature: 25°C.

	Time (h)					
	0.5	*1*	*2*	*4*	*8*	*16*
pH 6						
Coupled STI (mg/ml gel)	0.2	0.3	0.4	0.5	0.5	0.6
Coupling yield (%)	4.0	6.0	8.0	10	10	12
Adsorption capacity (mg/ml gel)	0	0.1	0.1	0.1	0.2	0.3
pH 7						
Coupled STI (mg/ml gel)	0.5	0.9	1.4	2.4	3.3	4.1
Coupling yield (%)	10	18	28	48	66	82
Adsorption capacity (mg/ml gel)	0.2	0.5	0.7	1.1	1.5	2.0
pH 8						
Coupled STI (mg/ml gel)	4.5	4.9	5.0	5.0	5.0	5.0
Coupling yield (%)	90	98	100	100	100	100
Adsorption capacity (mg/ml gel)	2.1	2.1	1.5	1.3	1.1	1.0
pH 9						
Coupled STI (mg/ml gel)	4.7	4.8	5.0	5.0	5.0	5.0
Coupling yield (%)	94	96	100	100	100	100
Adsorption capacity (mg/ml gel)	1.5	1.5	1.4	1.5	1.4	1.5

TABLE II

EFFECT OF THE AMOUNT OF STI

Coupling buffer: 0.1 M carbonate + 0.5 M NaCl (pH 8). Temperature: 25°C.

	Time (h)					
	0.5	1	2	4	8	16
5 mg						
Coupled STI (mg/ml gel)	4.5	4.9	5.0	5.0	5.0	5.0
Coupling yield (%)	90	98	100	100	100	100
Adsorption capacity (mg/ml gel)	2.1	2.1	1.5	1.3	1.1	1.0
10 mg						
Coupled STI (mg/ml gel)	5.3	6.7	8.2	8.5	9.0	9.0
Coupling yield (%)	53	67	82	85	90	90
Adsorption capacity (mg/ml gel)	2.7	3.3	3.0	2.6	2.4	1.8
20 mg						
Coupled STI (mg/ml gel)	7.4	9.8	12	14	14	14
Coupling yield (%)	37	49	60	70	70	70
Adsorption capacity (mg/ml gel)	4.2	5.1	43	3.9	3.6	3.4
40 mg						
Coupled STI (mg/ml gel)	8.3	12	15	15	17	17
Coupling yield (%)	21	30	38	40	40	40
Adsorption capacity (mg/ml gel)	5.4	5.4	5.4	5.2	4.8	4.8

the adsorption capacity for trypsin. Although the amount of protein coupled increased with increasing concentration, the proportion of the protein which coupled fell and the coupling was less efficient at high protein concentration. As for the trypsin capacity, the maximum was obtained in 1–2 h at each ligand concentration, but the capacity decreased with increasing coupling time. At the lowest concentration, it was decrased to 50% after 16 h, but at the highest concentration it was decreased to 89% after 16 h. This is because the multi-point attachment was prevented due to the high ligand concentration.

TABLE III

TEMPERATURE EFFECT

STI applied: 5 mg/ml gel. Coupling buffer: 0.1 M carbonate + 0.5 M NaCl (pH 8).

	Time (h)					
	0.5	1	2	4	8	16
25°C						
Coupled STI (mg/ml gel)	4.5	4.9	5.0	5.0	5.0	5.0
Coupling yield (%)	90	98	100	100	100	100
Adsorption capacity (mg/ml gel)	2.1	2.1	1.5	1.3	1.1	1.0
4°C						
Coupled STI (mg/ml gel)	0.7	1.2	2.3	3.2	4.1	4.9
Coupling yield (%)	14	24	46	64	82	98
Adsorption capacity (mg/ml gel)	0.4	0.7	1.3	1.5	1.6	2.1

TABLE IV

COUPLING OF CON A AT DIFFERENT pH VALUES

Con A applied: 15 mg/ml. Temperature: 25°C.

	Time (h)				
	1	2	4	8	16
pH 7					
Coupled STI (mg/ml gel)				2.4	4.1
Coupling yield (%)				16	27
Adsorption capacity (mg/ml gel)				0.5	0.9
pH 8					
Coupled STI (mg/ml gel)	7.0	9.3	12	13	13
Coupling yield (%)	47	62	80	88	88
Adsorption capacity (mg/ml gel)	2.9	4.5	4.8	5.6	6.2

Temperature effect

Table III shows that, although the coupling of STI was effectively completed in 1 h at 25°C, it took 16 h to complete the coupling at 4°C.

Coupling of other proteins

Con A and protein A were coupled at different pH values. The matrices were then assayed for the protein content and adsorption capacity.

Con A from Jack bean was coupled at pH 7 and 8 (Table IV). Both the coupling yield and the adsorption capacity for peroxidase were increased as the pH was increased from 7 to 8. However, Con A seemed to be aggregated at pH 9 as judged from gel filtration (data not shown).

TABLE V

COUPLING OF PROTEIN A AT DIFFERENT pH VALUES

Protein A applied: 2.5 mg/ml gel. Temperature: 25°C.

	Time (h)				
	1	2	4	8	16
pH 8					
Coupled STI (mg/ml gel)	1.0	1.4	1.6	1.8	1.9
Coupling yield (%)	40	56	64	72	76
Adsorption capacity (mg/ml gel)	3.3	2.7	1.9	1.7	1.3
pH 9					
Coupled STI (mg/ml gel)	1.8	1.9	2.0	2.1	2.1
Coupling yield (%)	72	76	80	84	84
Adsorption capacity (mg/ml gel)	1.7	1.3	0.8	0.5	0.5
pH 8[a]					
Coupled STI (mg/ml gel)	0.3	0.6	0.8	1.0	1.1
Coupling yield (%)	12	24	32	40	44
Adsorption capacity (mg/ml gel)	3.2	4.6	4.6	4.4	4.3

[a] 50 mM Tris–HCl + 0.5 M NaCl.
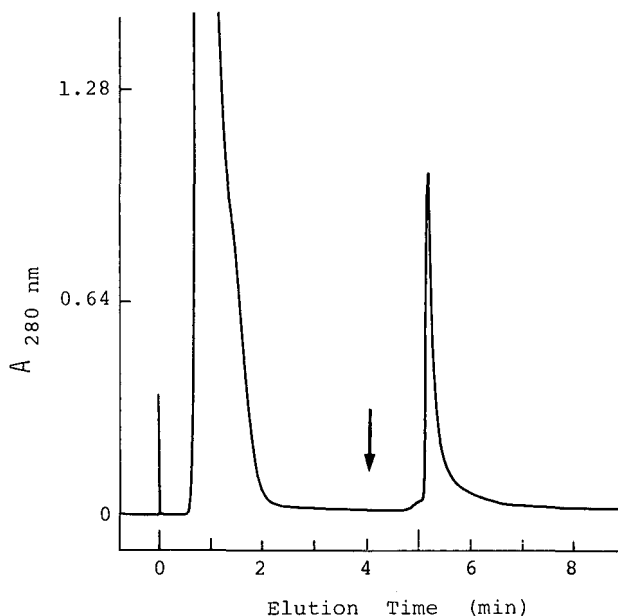
Fig. 1. Affinity chromatography of trypsin on STI-Toyopearl. Crude trypsin (5 mg in 500 μl) was loaded on the column (50 mm × 5 mm) previously equilibrated with 0.05 *M* Tris–HCl buffer (pH 7.5) containing 0.5 *m* NaCl and 20 m*M* CaCl$_2$ at a flow-rate of 1 ml/min at 4°C. After washing the column with the equilibration buffer, elution of adsorbed trypsin with 0.1 *M* acetic acid containing 0.5 *M* NaCl was started at the time indicated by the arrow.

Protein A, which binds to the Fc region of several classes of immunoglobulins[10,11], was coupled at pH 8 and 9. Table V shows the coupling yield increased with coupling time. The adsorption capacity for human IgG is the amount eluted with 0.1 *M* glycine–HCl buffer (pH 2.2). However, when 100 μg of human IgG were loaded and eluted with the acidic buffer, the recovery of human IgG was lower than 80% and it was difficult to elute all the bound human IgG. This result was in good agreement with that reported by Nilsson and Mosbach[12] (immobilizing protein A with too many linkages makes it difficult to elute all of the bound IgG). In order to prevent multi-point attachment, immobilization of protein A was carried out using Tris as a coupling buffer. The results are also shown in Table V, which indicates that although the coupling yield was decreased, the adsorption capacity was increased. Also, in this case, the recovery of human IgG was quantitative.

Demonstration of affinity chromatography

Fig. 1 shows the purification of porcine trypsin on STI-Toyopearl. A sample of commercial crude trypsin (5 mg in 500 μl) was loaded onto a STI-Toyopearl column (5 cm × 5 mm) and desorption of the bound trypsin was carried out with 0.1 *M* acetic acid containing 0.5 *M* NaCl (pH 3.0). Two major peaks were obtained from STI affinity chromatography of trypsin. The first peak (unbound fraction) had no trypsin acitivity and the second peak (bound fraction) had 90% of trypsin activity. This bound fraction gave a single band corresponding to a molecular weight of 23 000 according to
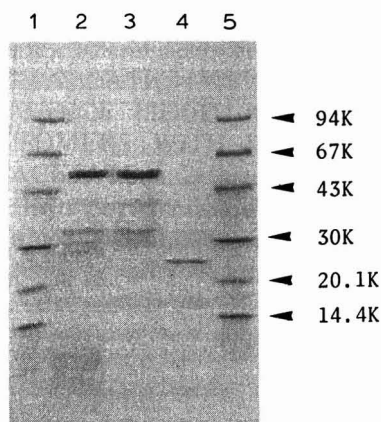
Fig. 2. SDS-polyacryl amide gradient gel (4–20%) electrophoresis. Lanes: 1 and 5 = low-molecular-weight marker (from Pharmacia); 2 = crude trypsin; 3 = unbound fraction; 4 = bound fraction. The gel was stained with 0.1% Coomassie Blue R250 in methanol–water–acetic acid (4:5:1, v/v/v). The anode is at the bottom. K = Kilodaltons.

sodium dodecyl sulphate polyacrylamide gel electrophoresis (SDS-PAGE) (see Fig. 2).

Fig. 3 shows the purification of peroxidase on Con A-Toyopearl. A crude peroxidase (5 mg in 0.5 ml) dissolved in equilibration buffer was loaded onto a Con A-Toyopearl column (5 cm × 5 mm). Desorption of the bound peroxidase was carried
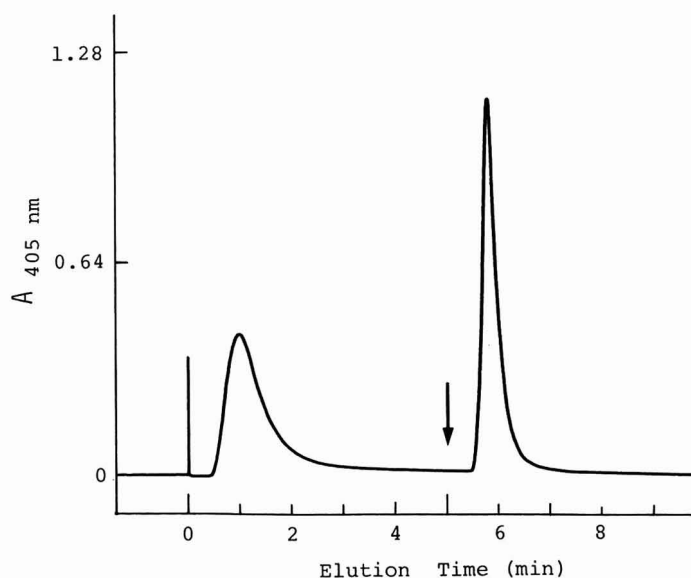
Fig. 3. Affinity chromatography of peroxidase on Con A-Toyopearl. Crude peroxidase (5 mg in 0.5 ml) was loaded on the column (50 mm × 5 mm) previously equilibrated with 0.1 M acetate buffer (pH 6.0) containing 0.5 M NaCl and 1 mM CaCl$_2$, MnCl$_2$ and MgCl$_2$ at a flow-rate of 1 ml/min at 25°C. After washing the column with the equilibration buffer, elution of adsorbed peroxidase with 0.11 M mannose in equilibration buffer was started at the time indicated by the arrow.
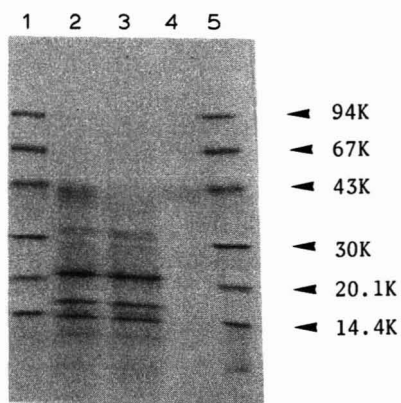
Fig. 4. SDS-polyacrylamide gradient gel (4–20%) electrophoresis. Lanes: 1 and 5 = low-molecular-weight marker (from Pharmacia); 2 = crude peroxidase; 3 = unbound fraction; 4 = bound fraction. Conditions as in Fig. 2.
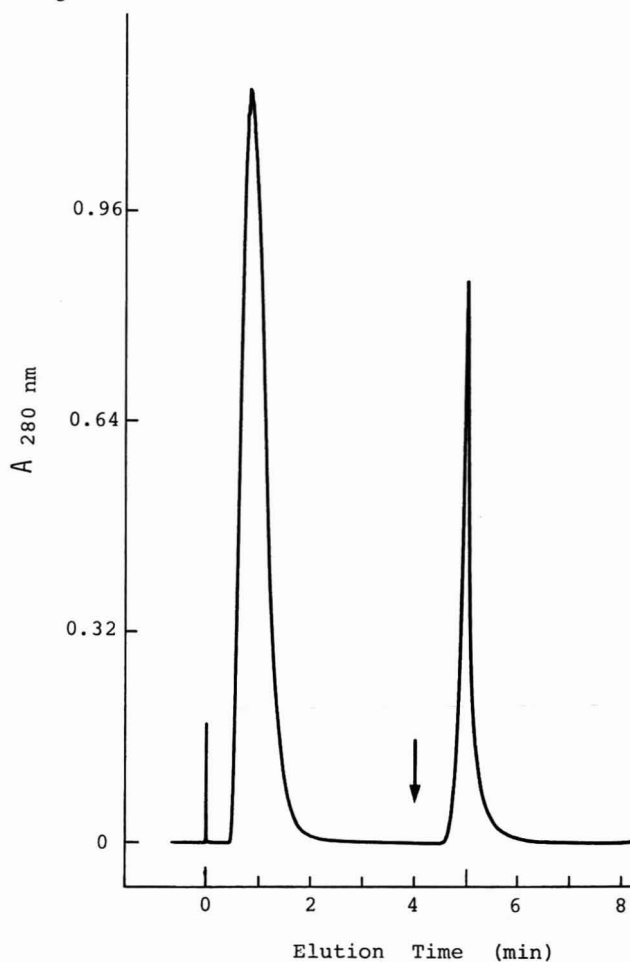
Fig. 5. Purification of human IgG on protein A-Toyopearl. Human serum (50 μl) was loaded on the column (50 mm × 5 mm) previously equilibrated with 0.1 *M* phosphate buffer (pH 7.0) at a flow-rate of 1 ml/min at 25°C. After washing the column with the equilibration buffer, elution of adsorbed IgG with 0.1 *M* glycine–HCl buffer (pH 2.2) was started at the time indicated by the arrow.
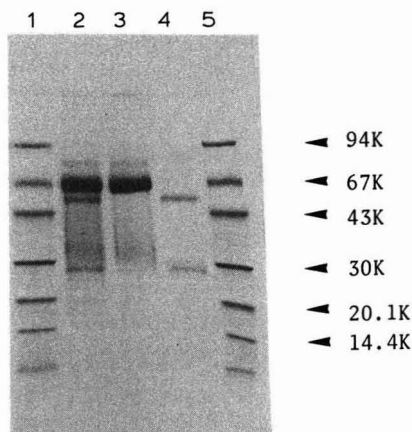
Fig. 6. SDS-polyacrylamide gradient gel (4–20%) electrophoresis. Lanes: 1 and 5 = low-molecular-weight marker (from Pharmacia); 2 = human serum; 3 = unbound fraction; 4 = bound fraction. Conditions as in Fig. 2.

out with 0.11 M mannose. The bound fraction had 70% of peroxidase activity and was also subjected to SDS-PAGE. Fig. 4 shows this fraction has several protein bands with a molecular weight of 42 000. However, this fraction gave a single peak in reversed-phase chromatography (data not shown).

Fig. 5 shows the purification of human IgG on protein A-Toyopearl. Human serum (50 μl) was loaded onto a protein A-Toyopearl column (5 cm × 5 mm) equilibrated in 0.1 M phosphate buffer (pH 7.0). Desorption of the bound IgG was performed with 0.1 M glycine–HCl buffer (pH 2.2). Judging from SDS-PAGE, the bound fraction contained only the light and heavy chain of human IgG (see Fig. 6). As demonstrated above, Tresyl-Toyopearl can be successfully used for affinity chromatography in a short time.

REFERENCES

1 R. Axen, J. Porath and S. Ernback, *Nature (London)*, 215 (1967) 1302.
2 J. Ludens, I. R. De Vries and D. D. Fanstiel, *J. Biol. Chem.*, 247 (1972) 7533.
3 V. Sica, E. Nola, I. Parikh, G. A. Puca and P. Cuatrecasas, *J. Biol. Chem.*, 248 (1973) 6543.
4 R. Lamed, Y. Levin and A. Oplatka, *Biochim. Biophys. Acta*, 305 (1973) 163.
5 A. H. Nishikawa and P. Bailon, *Arch. Biochem. Biophys.*, 168 (1975) 576.
6 K. Nilsson and K. Mosbach, *Biochem. Biophys. Res. Commun.*, 102 (1981) 449.
7 Y. Kato, K. Komiya and T. Hashimoto, *J. Chromatogr.*, 247 (1982) 184.
8 G. W. Schwert and Y. Takenaka, *Biochim. Biophys. Acta*, 16 (1955) 570.
9 L. Shannon, E. Kay and J. Y. Lew, *J. Biol. Chem.*, 244 (1966) 2166.
10 J. J. Langone, *J. Immunol. Methods*, 55 (1982) 277.
11 W. L. Bigbee, M. Vanderlaan, S. S. N. Fong and R. H. Jensen, *Mol. Immunology,* 20 (1983) 153.
12 K. Nilsson and K. Mosbach, *Methods Enzymol.*, 104 (1984) 56.

SEPARATION OF THE FOUR OPTICAL ISOMERS OF A DIHYDROPYRIDINE CALCIUM CHANNEL ANTAGONIST

KAREN D. WARD and LAWRENCE V. MANES*

Analytical and Environmental Research, Syntex USA Inc., 3401 Hillview Avenue, Palo Alto, CA 94304 (U.S.A.)

(First received April 5th, 1989; revised manuscript received May 17th, 1989)

SUMMARY

An isocratic high-performance liquid chromatography (HPLC) method is described for the separation of the four optical isomers of RS-93522-004, a racemic dihydropyridine-based drug containing two chiral centers. The drug is derivatized using (−)-camphanic acid chloride and the resulting four bis-camphanate diastereomers are separated on an achiral silica gel HPLC column. The precision, accuracy, and linearity of the method has been evaluated as applied to the determination of the isomer ratio of RS-93522-004. The method has also been evaluated to determine the limit of quantitation for the individual bis-camphanate diastereomers. Determination of the optical purity of the chiral derivatizing agent has also been addressed. No difference in the relative reactivity of the four individual RS-93522-004 optical isomers towards (−)-camphanic acid chloride is observed and the determination of the ratio of the RS-93522-004 bis-camphanate diastereomers has been shown to be unaffected by derivatization reaction yield. Attempts to resolve the optical isomers of several RS-93522-004 derivatives using various chiral HPLC columns are briefly discussed.

INTRODUCTION

In recent years, greater emphasis has been placed on the evaluation of differences in pharmacological effects of enantiomeric pharmaceutical compounds and the potential enantioselective metabolism of single isomers of racemic drug mixtures. This has led to the development of a wide array of chromatographic methods designed to separate and quantitate enantiomeric drug isomers[1].

Enantiomeric separations using high-performance liquid chromatography (HPLC) have been achieved by a variety of methods, which have led to two frequently used approaches. The first utilizes the classical technique of pre-column derivatization of enantiomers with chiral agents and separation of the resulting diastereomers on achiral stationary phases[2]. Inexpensive normal or reversed-phase HPLC columns are employed for this purpose. However, in this technique, important consideration must be given to enantiomeric purity of the chiral derivatizing agent and potential differences in reactivity of enantiomers towards the chiral reagent. The second in-

volves use of chiral stationary phases (CSPs)[3]. This approach is desirable because enantiomeric separations can be made directly, without pre-column derivatization steps, and because of the availability of several different types of commercial CSPs. However, commercially available CSP columns are expensive and, in some cases, derivatization of the analyte is still required to improve chromatographic properties and enhance enantiomeric selectivity.

RS-93522-004, 2-[4-(2,3-dihydroxypropoxy)phenyl]ethyl methyl 1,4-dihydro-2,6- dimethyl-4-(3-nitrophenyl)-3,5-pyridinedicarboxylate (**1**), is a synthetic dihydropyridine-based calcium channel antagonist under development for treatment of hypertension. It contains two chiral centers and is synthesized as a racemic mixture of four isomers consisting of two enantiomeric sets of diastereomers. Results from animal studies have shown the isomers with the (S)-configuration at C-4 of the dihydropyridine moeity display significantly greater pharmacological effects than the (4R)-isomers. Thus, the goal was to develop a method to separate and quantitate the individual isomers of RS-93522-004. Such a method would be of great utility for drug substance control, for the determination of the isomeric purity of single isomers, and as a means to probe for enantioselective metabolism of administered racemic drug.

The vast majority of the literature involving the two chromatographic strategies mentioned above describe separations of enantiomeric compounds containing only a single asymmetric carbon. Reports of the concurrent separation of both enantiomeric and diastereomeric isomers of racemic compounds containing multiple chiral centers are limited[4,5], and involve the separation of diastereomeric derivatives produced from derivatization of the optical isomers with chiral agents. Examples utilizing CSPs for this purpose are rare[6] and suggest the general inability of CSPs to simultaneously distinguish between both enantiomeric and diastereomeric components of isomeric mixtures. Column switching has been one approach used for such separations.[7] This technique utilizes conventional reversed-phase HPLC for separation of diastereomeric isomers followed by chiral HPLC separation of the enantiomeric components of an individual diastereomeric pair. This approach, however, suffers from the necessity for specialized equipment and still requires the use of costly CSP columns.

Several examples of the enantiomeric separation of dihydropyridine-based drugs using CSPs have been reported[8–12] yet all involve compounds containing only a single asymmetric carbon. Kern et al.[13] evaluated several commercially available CSPs to achieve separation of the four optical isomers of RS-93522-004, without success, and has reported a reversed-phase HPLC method which separates the diastereomeric components of RS-93522-004. Attempts, made in this study, to separate the optical isomers of a number of RS-93522-004 derivatives with the use of CSPs were also unsuccessful. This work describes the derivatization of RS-93522-004 with (−)-camphanic acid chloride and evaluates a normal-phase HPLC system which separates the resulting four bis-camphanate diastereomers. To our knowledge, no examples of enantiomeric resolution for this class of drugs using pre-column derivatization with chiral reagents has been reported.

EXPERIMENTAL

Apparatus

A Spectra-Physics (San Jose, CA, U.S.A.) 8100XR chromatograph, equipped

with a Valco (Houston, TX, U.S.A.) 20-μl fixed-loop injector, was used with a Kratos (Ramsey, NJ, U.S.A.) Spectroflow 757 UV absorbance detector set at 229 nm and 0.02 a.u.f.s. The oven temperature was set at 50°C. The detector output was monitored using a Spectra-Physics SP4270 integrator.

Materials

RS-93522-004 and its individual optical isomers were synthesized by the Institute of Organic Chemistry, Syntex Research, Palo Alto, CA, U.S.A. HPLC grade solvents were obtained from Burdick and Jackson (Muskegon, MI, U.S.A.) Hydrochloric acid was obtained from J. T. Baker (Phillipsburg, NJ, U.S.A.) and pyridine was obtained from Aldrich (Milwaukee, WI, U.S.A.). ($-$)-Camphanic acid chloride (98 + %) was obtained from Aldrich, and (R)-($+$)-1-(1-naphthyl)ethylamine (99.9 + %) and (S)-($-$)-1-(1-naphthyl)ethylamine (99.9 + %) were obtained from Norse Laboratories (Newbury Park, CA, U.S.A.)

Chromatographic conditions

A Nucleosil silica (5-μm, 25 cm × 4.6 mm I.D.) column was purchased from Alltech Assoc. (Deerfield, IL, U.S.A.) and used with a guard column (20 mm × 2.0 mm I.D.) packed with Alltech pellicular silica. The mobile phase consisted of 0.1% acetonitrile and 4% 2-propanol in isooctane (2,2,4-trimethylpentane). The addition of 0.1% acetonitrile is required to improve peak shape and reduce peak tailing. The flow-rate was maintained at 2.0 ml/min and the column pressure was approximately 2000 p.s.i. The sample concentration was approximately 0.3 mg/ml and the sample loading approximately 6 μg. HPLC solvents were filtered through 0.45-μm filters and the mobile phase was degassed by purging with helium.

Derivatization procedure

The derivatization reaction is shown in Scheme 1. A sample of 20 mg of RS-93522-004 or its single optical isomers and 40 mg of ($-$)-camphanic acid chloride are placed in a dry 12 × 75 mm test tube. The material is dissolved in 1 ml of anhydrous dichloromethane, and 30 μl of anhydrous pyridine is added to the solution. The test tube is then stoppered, shaken to mix the solution, and allowed to stand for 10 min at room temperature. A volume of 1 ml of 0.1 M hydrochloric acid is added to the test tube to quench the reaction. The organic layer is transferred with a pasteur pipette to a round bottomed flask and evaporated to dryness. The resulting residue is dissolved in approximately 5 ml of tetrahydrofuran and diluted with mobile phase to 100 ml to obtain a sample solution of approximately 0.3 mg/ml.

Modified derivatization procedure

A modified derivatization procedure was performed as above except the reaction was carried out with 30 mg of RS-93522-004 and 80 mg of ($-$)-camphanic acid chloride dissolved in 8 ml of anhydrous dichloromethane. Aliquots (1 ml) of the reaction mixture were taken at 0.5-min intervals for 5 min, and a final aliquot was taken at 240 min. Each aliquot was quenched with 0.5 ml of 0.1 M hydrochloric acid at the time of sampling. The HPLC analysis of each aliquot was performed using a Spherisorb ODS II (5 μm, 25 cm × 4.6 mm I.D.) column purchased from Alltech Assoc. (Deerfield, IL, U.S.A.) with a mobile phase consisting of methanol–water

(1) RS-93522-004

pyridine
dichloromethane
RT, 10 minutes

(-)-camphanic acid chloride

(2) RS-93522-004 bis-camphanate

* indicates chiral carbon
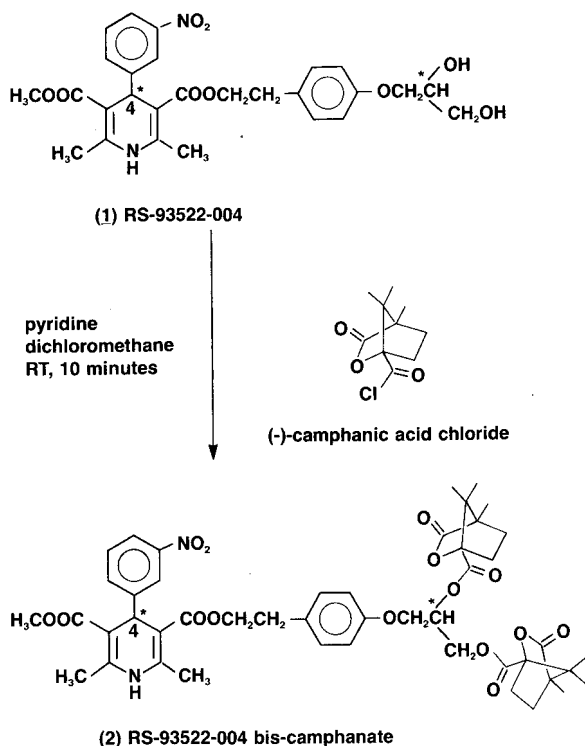
Scheme 1. Derivatization of RS-93522-004 with (−)-camphanic acid chloride. RT = reaction time.

(80:20). The column oven temperature was maintained at 40°C with a flow-rate of 1.0 ml/min and UV detection at 229 nm. The sample concentration was approximately 1.0 mg/ml in methanol and the sample loading was approximately 20 μg with a 20-μl sample loop.

Purity determination of (−)-camphanic acid chloride

Approximately 20 mg of (−)-camphanic acid chloride, as obtained from the manufacturer, was placed in a dry 12 × 75 mm test tube and dissolved in 0.5 ml of anhydrous dichloromethane. To this solution was added 20 μl of anhydrous pyridine and 20 μl of (R)-(+)-1-(1-naphthyl)ethylamine [(R)-NEA] or (S)-(−)-1-(1-naphthyl)-ethylamine [(S)-NEA]. The test tube was then stoppered, shaken to mix the solution, and allowed to stand for 30 min at room temperature. The reaction mixture was then quenched with 1 ml of 0.1 M hydrochloric acid. The organic layer was transferred with a pasteur pipette to a round bottomed flask and evaporated to dryness. The residue contained the corresponding NEA camphanamide diastereomers. The structure of each NEA camphanamide derivative was confirmed by both ^{1}H NMR and mass spectrometric (MS) analyses.

The NEA camphanamide derivatives were chromatographed using a Nucleosil

silica (5 μm, 25 cm $\times$ 4.6 mm I.D.) column with a mobile phase of hexane–ethyl acetate–acetonitrile (70:30:0.1) and UV detection at 254 nm. The flow-rate was maintained at 1.0 ml/min with a column oven temperature of 40°C. The sample concentration was approximately 0.5 mg/ml in ethyl acetate and the sample loading was approximately 10 μg with a 20-μl sample loop. The (S)-NEA camphanamide and (R)-NEA camphanamide derivatives were found to elute at 6.2 and 7.4 min, respectively.

The enantiomeric purity of ($-$)-camphanic acid chloride, as obtained from the manufacturer, was determined to be >99.3% by normal-phase HPLC analysis of the diastereomeric camphanamide components produced from its reaction with (R)-NEA, as described in the discussion of results.

RESULTS AND DISCUSSION

Chromatographic system development

In a previous report by Kern *et al.*,[13] several normal and reversed-phase HPLC methods were evaluated for their ability to separate the optical isomers of several derivatives of RS-93522-004. The derivatizing agents used in this work were all achiral. In addition, a number of commercially available CSPs were evaluated to separate the optical isomers of underivatized RS-93522-004 and the reported derivatives. However, none of the CSPs investigated resolved either the individual enantiomers or diastereomers of RS-93522-004 or its derivatives. The diastereomeric components of RS-93522-004 were found to separate as the bis-3,5-dinitrobenzoate esters by reversed-phase HPLC.

In the present work, RS-93522-004 was derivatized with a number of chiral acid chloride reagents to give the corresponding bis-esters. These included ($-$)-camphanic acid chloride, ($+$)-camphor-10-sulfonyl chloride, ($-$)-menthyloxyacetic acid chloride, (S)-($-$)-N-(trifluoroacetyl)prolyl chloride, (S)-($+$)-1-(1-naphthyl)ethyl isocyanate, (S)-N-1-(2-naphthylsulfonyl)-2-pyrrolidine carbonyl chloride. In all cases, an excess of the derivatizing reagent was used to obtain the bis-derivatives in order to minimize the number of potential reaction products. The bis-ester derivatives were chromatographed on several commercially available CSPs including Pirkle covalent phenylglycine DNB, Pirkle covalent naphthylalanine, Cyclobond β-cyclodextrin, Resolvosil BSA, Enantiopak α-1-glycoprotein, and Daicel OT($+$). The derivatives of ($-$)-menthyloxyacetic acid chloride and (S)-($+$)-1-(1-naphthyl)ethyl isocyanate were chromatographed only on the Cyclobond column. In most cases, no isomer separation was achieved and separation of diastereomeric components was accomplished in only a few instances[14,15]. This led to the evaluation of various normal and reversed phase HPLC systems. The normal-phase HPLC system reported here ultimately attained near baseline resolution of the four bis-camphanate diastereomers of RS-93522-004 (Fig. 1, Table I).

Identity of optical isomers

The four optical isomers of RS-93522-004 were individually derivatized following the described reaction conditions to give the corresponding bis-camphanate diastereomers. Their structures were confirmed by ^{1}H NMR, MS, and UV analyses, and their isomeric purity was established by the chromatographic method described here.
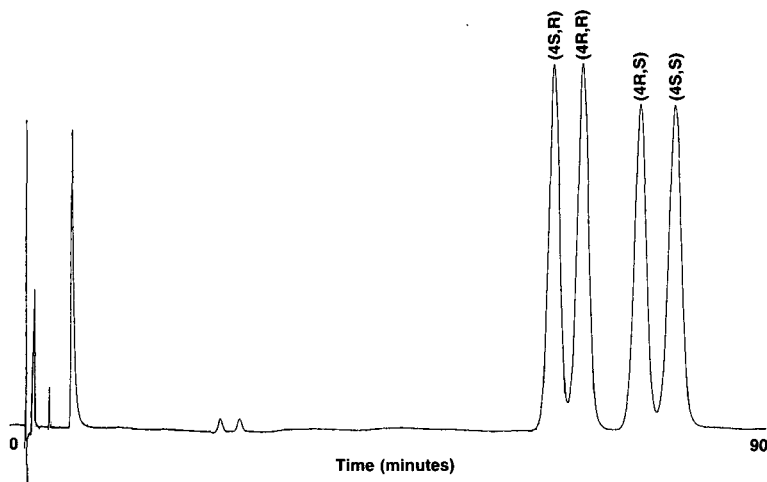
Fig. 1. HPLC separation of the RS-93522-004 bis-camphanate diastereomers.

The order of elution of the derivatized isomers was determined by chromatographic coinjection of the individual bis-camphanate diastereomers with the derivatized racemic drug. The order of elution was determined to be: the (4*S*,*R*) isomer first, the (4*R*,*R*) isomer second, the (4*R*,*S*) isomer third, and the (4*S*,*S*) isomer last (see Fig. 1).

Limit of quantitation

The limit of quantitation for individual bis-camphanate diastereomers was determined by chromatographing spiked solutions containing known amounts of the (4*R*,*R*) bis-camphanate isomer (peak 2) in the presence of the (4*S*,*R*) bis-camphanate isomer (peak 1). The concentration of the (4*S*,*R*) bis-camphanate isomer was held constant at 0.074 mg/ml (*i.e.* one-fourth of the specified concentration of 0.3 mg/ml) and the (4*R*,*R*) bis-camphanate isomer was spiked at levels equivalent to 0.25, 0.5, 1.0, 2.0, and 3.0% of the concentration of the former. The results appear in Table II. The limit of quantitation of the (4*R*,*R*) bis-camphanate isomer was found to be 0.5%, or 0.0075 μg for a given sample injection, under these chromatographic conditions. It should be noted that the (4*R*,*R*) bis-camphanate isomer elutes as a minor backside

TABLE I

SEPARATION OF THE RS-93522-004 BIS-CAMPHANATE DIASTEREOMERS

k' and R_s are the capacity factor and resolution, respectively. Chromatographic conditions are given in the Experimental section.

Isomer	k'	R_s
4*S*,*R*	37.6	
		1.28
4*R*,*R*	39.6	
		2.49
4*R*,*S*	43.7	
		1.41
4*S*,*S*	46.1	

TABLE II

ACTUAL AND OBSERVED PERCENTAGES OF THE RS-93522-004 (4R,R) BIS-CAMPHANATE
DIASTEREOMER SPIKED INTO THE (4S,R) BIS-CAMPHANATE DIASTEREOMER

Actual (%)	Observed (%)
0.25	nd
0.50	0.51
1.00	1.15
2.00	2.13
3.00	3.07

peak following the major (4S,R) bis-camphanate isomer peak (see Fig. 2). Therefore,
in this instance, the quantitation limit of 0.5% represents a worst case of detectability.
In addition, the limit of quantitation can be applied to the remaining bis-camphanate
diastereomers of RS-93522-004 because, at the detection wavelength of 229 nm, there
is no observed difference in their extinction coefficients.

Purity of chiral reagent

An important consideration in the validation of the method is to insure that the
chiral derivatizing agent is of sufficient enantiomeric purity so as not to affect the
accurate quantitation of the RS-93522-004 bis-camphanate single isomers. The
enantiomeric purity of (−)-camphanic acid chloride, as obtained from the manu-
facturer, was determined by normal-phase HPLC analysis of the diastereomeric cam-
phanamide components produced from its reaction with (R)-(+)-1-(1-naphthyl)eth-
ylamine [(R)-NEA], as described in the Experimental section. (−)-Camphanic
acid chloride was derivatized with (R)-NEA and (S)-(−)-1-(1-naphthyl)ethylamine
[(S)-NEA] to establish the HPLC retention times of the resulting diastereomeric (R)-
NEA and (S)-NEA camphanamide derivatives. The (S)-NEA camphanamide and
(R)-NEA camphanamide derivatives were found to elute at 6.2 and 7.4 min, respec-
tively. Normal-phase HPLC analysis of the (R)-NEA camphanamide derivative
showed the peak eluting at 6.2 min to integrate to 0.7% by area normalization. The
contributions to the area of this peak come from both the (R)-NEA derivative of

Fig. 2. HPLC chromatogram illustrating the limit of quantitation of the RS-93522-004 (4R,R) bis-campha-
nate diastereomer.

(+)-camphanic acid chloride, which arises from enantiomeric impurity of the (−)-camphanic acid chloride reagent, and from the enantiomeric (S)-NEA derivative of (−)-camphanic acid chloride, which arises from (S)-NEA contamination of the (R)-NEA reagent. Therefore, the enantiomeric purity of (−)-camphanic acid chloride was determined to be at least 99.3%.

This result was supported by derivatization of the RS-93522-004 (4S,R) isomer, available in high isomeric purity, with (−)-camphanic acid chloride and analysis using the HPLC procedure described here. Only the (4S,R) bis-camphanate diastereomer main peak was observed in the resulting HPLC chromatogram. No other diastereomeric components were observed which could be attributed to (+)-camphanate derivatives arising from enantiomeric impurity of the chiral derivatizing reagent. It should also be noted that the absence of the other bis-camphanate diastereomer peaks suggests that, under the derivatization reaction conditions, racemization of RS-93522-004 does not occur.

Relative reactivity of optical isomers

The potential for the individual optical isomers of RS-93522-004 to react with (−)-camphanic acid chloride at different rates during derivatization was evaluated by determining the bis-camphanate diastereomer ratios at incomplete reaction yields. To achieve intermediate reaction yields, the derivatization conditions were modified. Approximately four times the volume of dichloromethane specified was used in the derivatization, which slowed the reaction rate considerably. Under these conditions, the reaction did not reach completion after 4 h, and reaction mixtures containing differing yields of RS-93522-004, mono-camphanate ester, and bis-camphanate ester were obtained. Aliquots of the reaction mixture were taken at intervals and quenched to prevent further reaction. A reversed-phase HPLC method was developed to determine the percent of underivatized RS-93522-004, the percent of mono-camphanate ester, and the percent of bis-camphanate ester present in each quenched reaction aliquot (see Experimental). The yield of the bis-camphanate ester ranged from approximately 12 to 70% under these reaction conditions. The percent yield data is tabulated in Table III.

Each quenched reaction aliquot was also assayed using the described method to determine the ratio of the RS-93522-004 bis-camphanate diastereomers. The diastereomer ratios remained relatively constant at intermediate reaction yields as shown in Table IV. These data demonstrate that the ratio of the bis-camphanate diastereomers is unaffected by the derivatization reaction yield and that quantitative derivatization is not required. These data also support the determination that there is no difference in the relative reactivity of the four optical isomers of RS-93522-004 towards (−)-camphanic acid chloride.

Precision, accuracy, and linearity

The precision, accuracy, and linearity of the HPLC method were evaluated as applied to the determination of the isomer ratio of RS-93522-004. The precision was evaluated by performing six replicate injections of a single solution of the bis-camphanate diastereomers obtained from the reaction of RS-93522-004 with (−)-camphanic acid chloride. In a typical derivatization reaction, the resulting four bis-camphanate diastereomers are approximately equimolar with a composite concentration

TABLE III

PERCENT YIELD DATA

Reaction time (min)	RS-93522-004 (%)	Mono-camphanate (%)	Bis-camphanate (%)
0.5	14.3	73.9	11.8
1.0	13.7	74.7	11.5
1.5	11.9	75.5	12.6
2.0	7.1	76.4	16.5
3.0	2.7	74.6	22.8
5.0	1.6	69.0	29.4
240	0.5	29.8	69.7

of about 0.3 mg/ml. The area normalized percentages of the four individual bis-camphanate diastereomer peaks were determined and the results obtained were within 0.8% relative standard deviation, indicating good precision of the chromatographic method. The method reproducibility was assessed by performing duplicate injections from six separate reactions of RS-93522-004 and ($-$)-camphanic acid chloride and determining, individually, the area normalized percentages of the four bis-camphanate diastereomer peaks. The results obtained for each bis-camphanate diastereomer peak were within 0.4% relative standard deviation, indicating the reproducibility of the method.

The accuracy was assessed by derivatization of an accurately weighed mixture of the individual RS-93522-004 (4S,S), (4R,R), (4R,S), and (4S,R) isomers, in a ratio of approximately 1:1:1:1, with ($-$)-camphanic acid chloride, and subsequent determination of the diastereomer ratio of the bis-camphanate derivatives by the described HPLC method. Within the expected precision of the method, the observed bis-camphanate diastereomer ratio agreed well with the theoretical isomer ratio, as shown in Table V, thus demonstrating the accuracy of the method.

To determine the linearity of the method, sample solutions of the bis-camphanate derivatives at concentrations of approximately 5, 50, 85, 100, 115, and 200% of the specified concentration of 0.3 mg/ml were prepared. The total area of the four bis-camphanate diastereomer peaks versus known concentration were obtained and

TABLE IV

RS-93522-004 BIS-CAMPHANATE DIASTEREOMER RATIOS

% Yield	Peak 1	Peak 2	Peak 3	Peak 4
11.5	22.4	26.7	23.5	27.4
12.6	22.1	26.9	24.0	27.0
16.5	23.5	26.8	22.3	27.4
22.8	22.0	27.6	23.2	27.2
29.4	24.1	27.6	21.7	26.6
69.7	22.9	28.4	22.0	26.7
Mean	22.8	27.3	22.8	27.1
S.D.	0.8	0.6	0.9	0.3

TABLE V

RS-93522-004 BIS-CAMPHANATE DIASTEREOMER RATIOS

Peak	Experimental area (%)	Theoretical area (%)
4S,R	30.8	30.6
4R,R	25.5	25.6
4R,S	20.4	20.0
4S,S	23.3	23.9

used to prepare a linear regression line formula. Acceptable linearity was observed over the range tested, following the derived linear equation $y = 1.004x + 0.191$, where y = observed response and x = expected response. The average deviation from a theoretical calibration line having a slope of 1.00, expressed as the standard error of estimate, was 0.43%. The correlation coefficient found was 0.999, indicating the method is linear in the examined range of concentration. In addition, the relationship between the area ratios of (peak 1 + peak 2)/(peak 3 + peak 4) *versus* known concentration was also examined. A plot of area ratio *versus* concentration gave a slope of 0.053 demonstrating that the area ratio of the peaks remained relatively constant in the examined range of concentration. The individual area ratios of peaks 1/2 and peaks 3/4 *versus* concentration were similarly examined with parallel results.

CONCLUSION

A simple, normal-phase HPLC procedure has been described which separates the four optical isomers of RS-93522-004, a racemic dihydropyridine-based drug containing two asymmetric carbon centers, as their diastereomeric bis-camphanate derivatives. The method has been shown to be accurate, precise, and sensitive. In addition, no difference in the relative reactivity of the four individual RS-93522-004 optical isomers towards (−)-camphanic acid chloride is observed, and the determination of the ratio of optical isomers in RS-93522-004 is unaffected by derivatization reaction yield.

REFERENCE

1 D. W. Armstrong and S. M. Han, CRC Crit. Rev. Anal. Chem., 19 (1988) 175.
2 W. H. Pirkle and J. M. Finn, in J. D. Morrison (Editor), Asymmetric Synthesis, Vol. 1, Academic Press, New York, 1983, p. 87.
3 W. H. Pirkle and T. C. Pochapski, Adv. Chromatogr., 27 (1987) 73.
4 J. R. Kern, D. M. Lokensgard, L. V. Manes, M. Matsuo and K. Nakamura, J. Chromatogr., 450 (1988) 233.

5 R. Shimizu, T. Kakimoto, K. Ishii, Y. Fujimoto, H. Nishi and N. Tsumagari, *J. Chromatogr.*, 357 (1986) 119.
6 R. A. Chapman, *J. Chromatogr.*, 258 (1983) 175.
7 D. A. Roston and R. Wijayaratne, *Anal. Chem.*, 60 (1988) 950.
8 D. W. Armstrong, T. J. Ward, R. D. Armstrong and T. E. Beesley, *Science (Washington, D.C.)*, 232 (1986) 1132.
9 Y. Okamoto, R. Aburatani, T. Fukumoto, K. Hatano and K. Hatada, in preparation.
10 E. Delee, I. Jullien and L. Le Garrec, *J. Chromatogr.*, 450 (1988) 191.
11 Daicel Chemical Industries, Ltd., *Chiral HPLC Columns for Optical Resolution*, company literature (1988).
12 R. J. Bopp and J. H. Kennedy, *LC-GC, Mag. Liq. Gas Chromatogr.*, 6 (1988) 514.
13 J. R. Kern, D. M. Lokensgard and T. Yang, *J. Chromatogr.*, 457 (1988) 309.
14 J. R. Kern, unpublished results.
15 K. D. Ward, unpublished results.

SEPARATION OF PREPOLYMERS OF PHENOL–FORMALDEHYDE RESINS BY SUPERCRITICAL-FLUID CHROMATOGRAPHY

SADAO MORI*

Department of Industrial Chemistry, Faculty of Engineering, Mie University, Tsu, Mie 514 (Japan)

and

TOSHINORI SAITO and MAKOTO TAKEUCHI

New Project Development Office, JEOL Ltd., Akishima, Tokyo 196 (Japan)

(Received March 20th, 1989)

SUMMARY

Prepolymers of random novolac and resol resins were separated according to the number of nuclei (phenol groups) and the number of methylol groups attached to the nuclei. Temperature programming elution at a constant column pressure and constant flow-rates of both carbon dioxide and a modifier was applied in the order of decreasing column temperature. Two pumps were installed in a supercritical chromatography system to deliver carbon dioxide and a modifier independently. Ethanol was used as the modifier. The initial column temperature was 120 or 150°C and the programming rate was 3 or 4°C/min. The back pressure at the outlet of the UV detector was between 154 and 178 kg/cm². Nine oligomers for novolac resins from dihydroxydiphenylmethanes (DPM) (dimer, dinuclear) to decanuclear oligomers were separated. The percentages of three isomers, 2,2'-, 2,4'- and 4,4'-DPM, of dinuclear oligomers were 6, 26 and 68%, respectively. Seven isomers of trinuclear novolac oligomers were assigned. Molecular weight averages were calculated without any calibration standards, *e.g.*, $\bar{M}_w = 417$ and $\bar{M}_n = 366$ for the sample examined here. Mono- to pentanuclear resol oligomers were separated. Peaks for 2- and 4-methylol phenols, 2,4- and 2,6-dimethylol phenols and 2,4,6-trimethylol phenol were assigned. Di- and trinuclear resol oligomers were separated according to the number of methylol groups attached to the phenol groups.

INTRODUCTION

Prepolymers of phenolic resins, intermediate low-molecular-weight products, are obtained by the condensation of phenol (or substituted phenols) and formaldehyde. The prepolymers (oligomers) are then cured by heating or with a suitable cross-linking agent to produce hard and solvent-insoluble products. There are three types of phenolic resin prepolymers, random novolac, high-ortho novolac and resol, depending on the catalyst. The structures and the compositions of the reaction products are complex and considerably different depending on the catalyst and the experimental conditions.

The determination of the molecular species of these prepolymers often requires the application of several separation techniques, including high-performance liquid chromatography (HPLC), size-exclusion chromatography (SEC), and gas chromatography–mass spectroscopy (GC–MS). Resol resins were separated by SEC and the elution positions of several isomers of mono-, di- and trinuclear resol resins were estimated[1]. However, because of the limited separation capacity in SEC, only 2-methylol phenol (2-MP), 4-MP, 2,6-dimethylol phenol (2,6-DMP), 2,4-DMP and 2,4,6-trimethylol phenol (2,4,6-TMP) were separated by semi-micro HPSEC in a system which had 103 000 theoretical plates[2]. Novolac resins were also separated by the same SEC system and isomers of di-, tri-, tetra- and pentanuclear compounds were identified[2].

HPLC is the most suitable technique for the separation of such complex materials because of its high resolution. Reaction products from higher phenols and formaldehyde[3], ortho-novolac resins[4], phenol novolac and resol resins[5] and epoxy resins[6] were separated by HPLC and several isomers were characterized. However, the identification of the peaks separated is still a matter of debate. For the identification of complex structures of phenolic resins, the application of at least MS is required. GC–MS is capable of both the separation and identification of complex materials, if they can be separated by GC. Silylation of phenolic resins may enable the separation of these resins by GC[7–12]. Disadvantages of the silylation of phenolic resins followed by GC–MS are the unreliable silylation and the inability to apply this technique to higher-molecular-weight (higher nuclei) species because of their low vapour pressures.

Supercritical-fluid chromatography (SFC) has recently attracted serious attention because of its high resolution and its ease of application, similar to GC–MS. The analyses of relatively high-molecular-weight compounds have been reviewed[13]. Pressure programming to increase the pressure of the supercritical fluid (and increase its density) is usually required in the separation of oligomers which contain species with widely differing molecular weights. The addition of a polar solvent to the mobile phase is also effective in separating relatively high-molecular-weight materials[14] as well as polar oligomers[15].

This paper is concerned with a preliminary experiment on the separation of phenol–formaldehyde random novolac and resol resins by SFC. Temperature programmed elution (decreasing temperature) at a constant column pressure was applied and ethanol was added to the mobile phase as a modifier.

EXPERIMENTAL

Apparatus and elution

A JEOL supercritical-fluid chromatograph Model JSF-8800 (JEOL, Akishima, Tokyo, Japan) was used with an ultraviolet (UV) absorption detector Model CAP-UV01 operated at 210 nm. The volume of the flow cell was 1 μl and the path length was 5 mm. The pressure of the supercritical fluid was maintained constant at the detector outlet by using a constant pressure release valve actuated mechanically with a spring, screwdriver and a low-dead volume digital pressure meter. The SFC apparatus consists of two pumps, one for the delivery of liquefied carbon dioxide as the supercritical fluid (Model CAP-G03) and the other for the delivery of a modifier (Model CAP-L02). Ethanol was used as a modifier. One or two columns (25 cm × 1.7

mm I.D.) packed with silica-ODS (particle diameter 5 μm) were used and stored in a column oven to maintain the column temperature constant. A GC column oven (Hewlett-Packard Model HP 5980) was used after necessary modification for programming of descending column temperature.

The flow-rate of liquefied carbon dioxide was 300 μl/min and that of the modifier 100 or 50 μl/min. The initial column temperature was adjusted to 150 or 120°C and the column temperature was lowered at a rate of 3 or 4°C/min to 50 or 60°C. The pressure of the supercritical fluid flowing into a column was monitored at the inlet and recorded on a chart. The back pressure of the SFC system was read at the outlet of the UV detector.

Samples

Random novolac resins were prepared using 10 g of phenol, 7.4 g of a 37% formaldehyde aqueous solution (molar ratio of phenol to formaldehyde, 1:0.85) and 0.1 ml of a 3.5% hydrochloric acid solution as a catalyst. The reaction was performed at 85°C for 30 min and the reaction mixture was diluted in water, then allowed to cool. Unreacted phenol and formaldehyde were removed in vacuum together with water.

Resol resins were prepared using 10 g phenol, 15.7 g of a 37% formaldehyde aqueous solution (molar ratio of phenol to formaldehyde, 1:1.8) and 0.5 ml of a 10% sodium hydroxide solution as a catalyst. The reaction was performed at 80°C for 1 h and the reaction mixture was treated similarly to that for novolac resins.

These prepolymers were dissolved in tetrahydrofuran at about 5% concentration and the volume of these solutions injected on the column was 0.5 μl.

RESULTS AND DISCUSSION

Random novolac resins

Fig. 1 shows a typical SFC separation according to the number of nuclei. Nine oligomers from dihydroxydiphenylmethane (dimer, dinuclear) oligomers to decanuclear novolac oligomers were clearly separated and observed. The structure of novolac resins is depicted as polynuclear phenols with a methylene linkage between the aromatic nuclei[12]. The number of nuclei (the number of phenyl groups) is estimated as in Fig. 1; *i.e.*, peak c is dinuclear (dihydroxydiphenylmethanes), peak d trinuclear, peak e tetranuclear, etc.

According to the results obtained by GC–MS[12], methylol groups were not attached to each aromatic nucleus of novolac resins and the mass difference between each oligomer was 106 a.m.u. Therefore, molecular weight averages of the prepolymers can be calculated from the peak area of each oligomer and its molecular weight, if the UV response of each oligomer can be assumed to be equal. The molecular weight and relative peak intensity of each oligomer are listed in Table I. From these data, molecular weight averages can be calculated as the number average molecular weight, $\bar{M}_n = 366$ and the weight average molecular weight, $\bar{M}_w = 457$.

The content of phenol remaining in novolac resins used in this work was about 5%. The number average molecular weight calculated by including phenol was 319. The molecular weight obtained by vapour-pressure osmometry was equivalent to this value. Therefore, the method proposed here can calculate both molecular weight averages, including and excluding phenol. The calculation of molecular weight
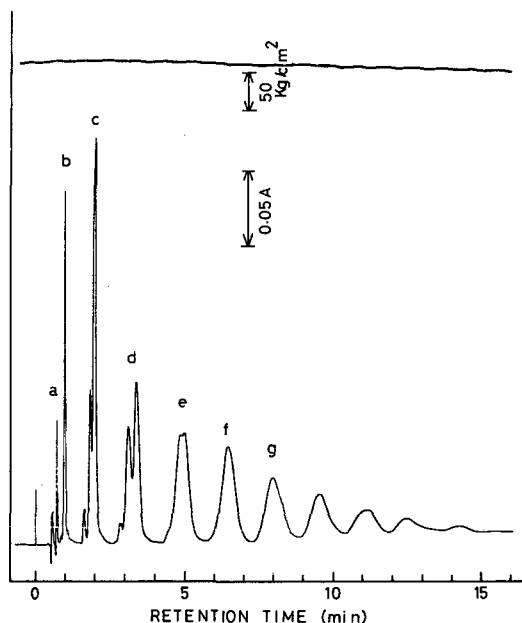
Fig. 1. SFC chromatogram of random novolac resins separated according to the number of nuclei. Flow-rates: carbon dioxide, 300 μl/min; ethanol, 100 μl/min. Column temperature: initial 120°C, final 50°C, programming rate 4°C/min. Back pressure: 162 kg/cm^2. Detector: UV at 210 nm, 0.5 a.u.f.s. Column: 250 mm × 1.7 mm. Peak identification: a = impurities; b = phenol; c = dinuclear; d = trinuclear; e = tetranuclear; f = pentanuclear; g = hexanuclear novolac resins.

averages by SEC requires the construction of a calibration graph of log molecular weight vs. retention volume and also the estimation of calibration parameters[16]. Our method does not require any calibration standards nor the estimation of calibration parameters. It is a direct method to obtain molecular weight averages (a self calibration method for calculating molecular weight averages) in contrast to SEC which requires calibration standards and is designated an indirect method.

TABLE I

MOLECULAR WEIGHT AND RELATIVE PEAK INTENSITY OF EACH OLIGOMER OF NOVOLAC RESINS

Number of nuclei	Molecular weight	Relative peak intensity (from Fig. 1) (%)
2	200	20.1
3	306	19.1
4	412	17.0
5	518	15.0
6	624	12.4
7	730	7.9
8	836	4.9
9	942	2.6
10	1048	1.0

The initial column temperature in Fig. 1 was 120°C and the column temperature 15 min after the injection of a sample solution was 60°C. The flow-rates of both carbon dioxide and ethanol were kept constant at 300 and 100 μl/min, respectively. The back pressure at the detector outlet was also kept constant, at 162 kg/cm². Therefore, the more condensed fluid flowed through the column at lower column temperature. Our (decreasing) temperature programming is a kind of density programming at constant column pressure.

Our SFC system has different features from other SFC systems for density programming and temperature programming. Density programming of other SFC systems utilizes the increase in flow-rate of a fluid or an increase in back pressure. Density programming in our SFC system arises from the result of temperature programming which is in the order of descending column temperature, though in other systems it is normally in the order of ascending column temperature. The cell block of the UV detector in this work is cooled to 20–25°C, and thus the fluid from the column becomes a liquid in an UV cell. Therefore, as far as the flow-rates at the two pumps and the back pressure at the outlet of the UV detector are constant, the liquid density at the UV cell is kept constant in spite of the change in column temperature, resulting in a stable baseline.

The column inlet pressure was monitored and recorded on a chart, and is shown at the top of Fig. 1. The initial column inlet pressure was 212 kg/cm² and the pressure 15 min after the sample injection was 220 kg/cm². The column pressure during the separation was very stable. As the back pressure in Fig. 1 was 162 kg/cm², the pressure drop between the column inlet and the detector outlet was 50 kg/cm² at the start.

The increase in column temperature results in a decrease in the density of the fluid, and therefore in an increase in retention time of a sample solute. In other words, the resolution of lower-molecular-weight solutes may be improved at the lower density of the fluid. An example is shown in Fig. 2. The initial temperature was 150°C and the back pressure was 178 kg/cm². Other experimental conditions were as in Fig. 1. The column temperature at the retention time of 15 min was 90°C, where hexanuclear novolac resins appeared. These oligomers appeared at a retention time of 8 min in Fig. 1, where the column temperature was 88°C. The column inlet pressure was 214 kg/cm² at the start and 220 kg/cm² 20 min after the sample injection. The pressure drop between the column inlet and the detector outlet was 36 kg/cm² at the start.

Besides the increase in retention time of these oligomers, the resolution of di- and trinuclear oligomers was much improved. Three peaks for dinuclear oligomers and more than three peaks including shoulder peaks were observed for trinuclear oligomers. According to the GC–MS analysis[8], peak c1 can be assigned to 2,2'-dihydroxydiphenylmethane (2,2'-DPM), peak c2 to 2,4'-DPM and peak c3 to 4,4'-DPM. The percentages of these isomers were calculated from the peak areas as 6 (peak 1), 26 (peak 2), and 68% (peak 3). Trinuclear novolac oligomers should have more than three isomers and seven isomers were separated and identified by using the results of GC–MS[8].

For further improvement of the separation of trinuclear oligomers the flow-rate of the modifier (ethanol) was decreased from 100 to 50 μl/min and two columns were connected. The results are shown in Fig. 3. The column inlet pressure at the start was 218 kg/cm². Five peaks including one shoulder peak were observed. Trinuclear oligomers appear at retention times between 19 and 24 min. Peaks can be assigned by
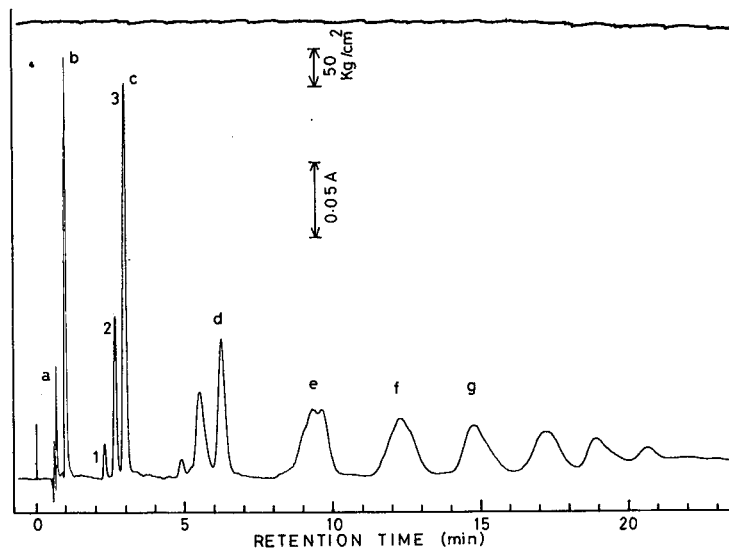
Fig. 2. SFC chromatogram of random novolac resins. Column temperature: initial 150°C, final 50°C, programming rate 4°C/min. Back pressure: 178 kg/cm². Other conditions and peak identification as in Fig. 1.
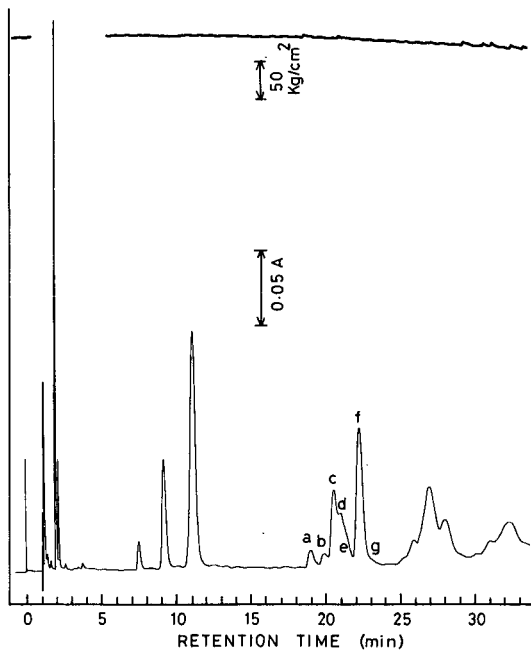
Fig. 3. SFC chromatogram of random novolac resins. Flow-rates: carbon dioxide, 300 μl/min; ethanol, 50 μl/min. Column temperature: initial 150°C, final 60°C, programming rate 3°C/min. Back pressure: 165 kg/cm². Detector: UV at 210 nm, 0.5 a.u.f.s. Column: 250 mm × 1.7 mm I.D. × 2. For peak identification, see text.

GC–MS[8] as follows: a is 3-(2-hydroxybenzyl)-2,2'-dihydroxydiphenylmethane (3,2-Bz-2,2'-DPM), b is 5,2-Bz-2,2'-DPM, c is 3,4-Bz-2,2'-DPM, d is 5,4-Bz-2,2'-DPM, e is 5,2-Bz-2,4'-DPM, f is 3,4-Bz-2,4'-DPM and g is 5,4-Bz-2,4'-DPM. Peaks e and g are observed by peaks d and f and are at the bottom of the right-hand side of those peaks. These assignments were based on the fact that the relative peak intensities of di- and trinuclear oligomers observed by SFC resembled those obtained by GC–MS[8] under the assumption that the elution order of novolac resin isomers by SFC was the same as that by GC.

Resol resins

The base-catalyzed condensation products of phenol with formaldehyde were resol-type resins comprised of mono- and polynuclear methylolated phenols[12] and their hemiformal isomers[10]. ^{1}H NMR spectrometric investigation of resol indicated the absence of methylene ether linkages and hemiformal groups[12].

SFC chromatograms of resol resins are shown in Fig. 4. The initial column temperature and other chromatographic conditions were as in Fig. 1. Peaks a are impurities in the sample solution and peak b is phenol. Peaks c–e are assigned to mononuclear resol oligomers, f–i to dinuclear, j–m to trinuclear and n to tetranuclear resol oligomers.

Similarly to the case of the novolac resins, the initial column temperature was increased in an attempt to improve the resolution of mono- and dinuclear resol oligomers. The results are shown in Fig. 5. The resolution of di- and trinuclear resol oligomers was not much improved as expected in contrast to novolac oligomers but
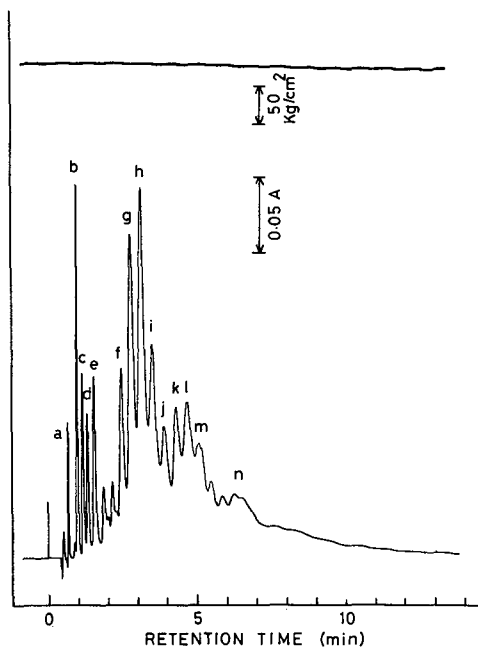
Fig. 4. SFC chromatogram of resol resins. Conditions as in Fig. 1. Column inlet pressure at the start: 200 kg/cm². For peak identification, see text.
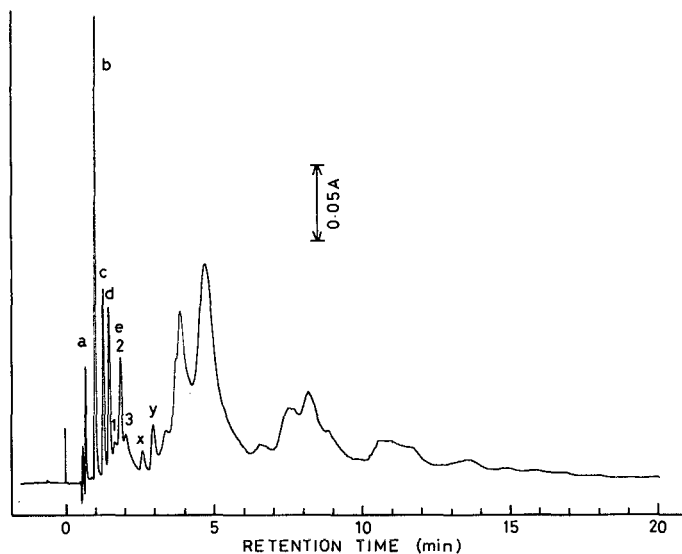
Fig. 5. SFC chromatogram of resol resins. Conditions as in Fig. 2 except the back pressure which was 173 kg/cm². For peak identification, see text.

peak e was split into three peaks. Peak c can be assigned to 2-MP, d to 4-MP from the results of GC–MS[9]. Similarly, peak e1 may be assumed to be 2,6-DMP, e2 to be 2,4-DMP and e3 to be 2,4,6-TMP. Oligomers from mono- to pentanuclear resols were separated under these SFC conditons.

Results obtained by decreasing the flow-rate of the modifier to 50 µl/min and connecting two columns as in Fig. 3 are shown in Fig. 6. Resol oligomers having different numbers of nuclei (aromatic groups) were clearly separated from each other. Novolac type oligomers were observed in resol resins by GC–MS[9]. Peaks x and y in Fig. 5 have the same retention times as those of 2,4′-DPM and 4,4-DPM in Fig. 2. However, the retention times of peaks x and y in Fig. 6 were not coincident with those of 2,4′-DPM and 4,4′-DPM in Fig. 3. Therefore, it was assumed that these DPMs were not included in the resol resins examined in our work. The resolution of mononuclear resol resins was not greatly improved, though the content of the modifier in the mobile phase was decreased. A peak at the front bottom of peak d and peaks x and y might be due to hemiformal isomers[10]. Peak e1 in Fig. 5. is assumed to be hidden in front of peak e in Fig. 6.

In dinuclear resol [methylolated dihydroxydiphenylmethanes (DMP)], fifteen isomers, i.e., four methylol DMP, five dimethylol DMP, four trimethylol DMP and two tetramethylol DMP, were confirmed by GC–MS[11]. Peak f in Fig. 6 may be provisionally assigned to methylol DMP, g to dimethyl DMP, h to trimethylol DMP and i to tetramethylol DMP. From the peak width, it can be assumed that several isomers are included in peaks f and g.

From a comparison of Fig. 4 with Fig. 6, peak j in Fig. 4 may belong to trinuclear resol oligmers as do peaks k, l and m. Trinuclear resol oligomers are composed of five different methylol groups such as mono-, di-, tri-, tetra- and pentamethylol trinuclear
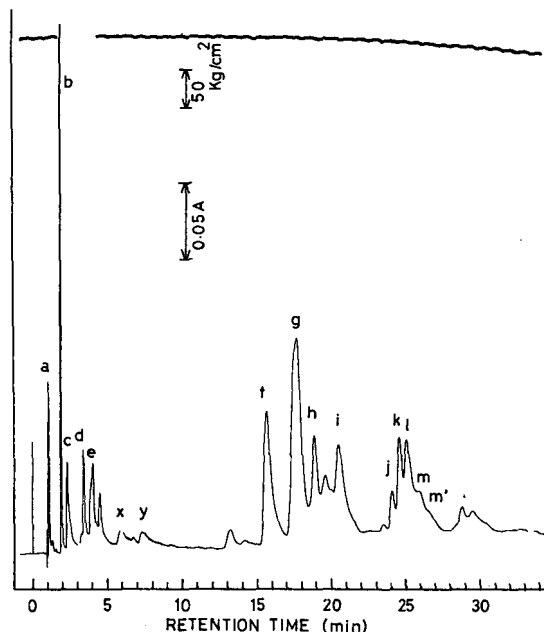
Fig. 6. SFC chromatogram of resol resins. Conditions as in Fig. 3 except the back pressure which was 154 kg/cm². The column inlet pressure at the start was 208 kg/cm². For peak identification, see text.

resol oligomers, including several isomers. Peaks j–m in Fig. 6 can be assigned to these oligomers in that order. Peaks n may be tetranuclear resol oligomers. Peaks f–n in Fig. 4 may correspond to peaks f–n in Fig. 6, though the assignment is not easy. The SFC conditions described in Fig. 4 (same as in Fig. 1) can separate resol oligomers according to the number of nuclei (phenol groups) and the number of methylol groups.

To conclude, the assignment of peaks in SFC chromatograms for both novolac and resol resins has been made by comparison with the results of GC–MS in the literature. However, these assignments are still provisional and SFC–MS is required for accurate assignments. SFC–MS is recognized to be easier than LC–MS and it is now under consideration. The technique described here is temperature programming SFC with decreasing column temperature at constant flow-rates of both carbon dioxide and a modifier and constant back pressure. This programming has the same effect as density programming SFC in increasing the fluid density, and has the advantage of a stable detector baseline because of the constant back pressure and constant temperature at the detector cell.

REFERENCES

1 M. Duval, B. Bloch and S. Kohn, J. Appl. Polym. Sci., 16 (1972) 1585.
2 S. Mori, J. Liq. Chromatogr., 9 (1986) 1329.
3 A. Ševenik, J. Chromatogr., 160 (1978) 205.
4 G. Gasiraghi, G. Sartori, F. Bigi, M. Cornia, E. Dradi and G. Casnati, Makromol. Chem., 182 (1981) 2151.

5 W. Werner and O. Barber, *Chromatographia*, 15 (1982) 101.
6 S.-T. Lai and L. Sangermano, *J. Chromatogr.*, 321 (1985) 325.
7 W. Lindner, *J. Chromatogr.*, 151 (1978) 406.
8 L. Prókai, *J. Chromatogr.*, 329 (1985) 290.
9 L. Prókai, *J. Chromatogr.*, 331 (1985) 91.
10 L. Prókai, *J. Chromatogr.*, 333 (1985) 161.
11 L. Prókai, *J. Chromatogr.*, 356 (1986) 331.
12 L. Prókai, *J. Appl. Polym. Sci., Polym. Lett.*, 24 (1986) 223.
13 P. Sandra, in R. M. Smith (Editor), *Supercritical Fluid Chromatography*, Royal Society of Chemistry, London, 1988, Ch. 5.
14 F. P. Schmits and E. Klesper, *Polym. Commun.*, 24 (1983) 142.
15 F. P. Schmitz and H. Hilgers, *Makromol. Chem., Rapid Commun.*, 7 (1986) 59.
16 S. Mori, *Anal. Chem.*, 53 (1981) 1813.

CHROM. 21 604

HIGH-PERFORMANCE LIQUID CHROMATOGRAPHIC DETERMINATION OF ALKYLAMIDOPROPYL-N,N-DIMETHYL-N-(2,3-DIHYDROXYPROPYL)AMMONIUM CHLORIDES IN AQUEOUS SOLUTIONS AND COSMETIC FORMULATIONS

ROLAND CAESAR[a], HENRY WEIGHTMAN and GILBERT R. MINTZ[*,b]

Inolex Chemical Company, Analytical Group, Philadelphia, PA (U.S.A.)

(First received December 12th, 1988; revised manuscript received April 26th, 1989)

SUMMARY

A reversed-phase high-performance liquid chromatographic method is described to determine the quaternary ammonium compounds myristamidopropyl-N,N-dimethyl-N-(2,3-dihydroxypropyl)ammonium chloride and oleamidopropyl-N,N-dimethyl-N-(2,3-dihydroxypropyl)ammonium chloride in aqueous solutions and cosmetic formulations. Fractions containing quaternary chlorides are isolated from their reactants and by-products by semi-preparative liquid chromatography and are used as standards to quantify the quaternium compound in selected samples. Analytical liquid chromatography is performed by an ion-pairing reversed-phase technique using two alkyl/cyano columns. This method is applicable as a quality control assay procedure to quantify these cationics in finished cosmetic formulations.

INTRODUCTION

Alkylamidopropyl-N,N-dimethyl-N-(2,3-dihydroxypropyl)ammonium chlorides were manufactured in 1952 as novel wetting and emulsifying agents[1]. Their use has extended into the personal care industry which results in a need to determine the amount of these quaternary ammonium compounds in aqueous solutions and cosmetic formulations[2–4]. These cationics offer excellent conditioning and emulsifying properties in a broad range of cosmetic formulations[4].

The quaternium chlorides are synthesized by alkylation of alkylamidopropyldimethylamines with α-monochlorohydrin in aqueous solution at 80–85°C and pH 8.0–8.5:

$$\underset{\underset{OH}{|}}{ClCH_2\overset{\overset{OH}{|}}{C}HCH_2} + \underset{\underset{CH_3}{|}}{R\overset{\overset{O}{||}}{C}NHCH_2CH_2CH_2\overset{\overset{CH_3}{|}}{N}} \longrightarrow [\underset{\underset{CH_3}{|}}{R\overset{\overset{O}{||}}{C}NHCH_2CH_2CH_2\overset{\overset{CH_3}{|}}{N}^+} \underset{\underset{OH}{|}}{CH_2\overset{\overset{OH}{|}}{C}HCH_2}] \quad Cl^-$$

---

[a] Present address: Ethyl Corporation, Orangeburg, SC, U.S.A.
[b] Present address: Centerchem, Inc., 660 White Plains Road, Tarrytown, NY 10591, U.S.A.

The possible impurities present in the product may be unreacted alkylamidopropyldimethylamine and α-monochlorohydrin. Other impurities that may be present are sodium chloride that results from the neutralization of sodium hydroxide with hydrochloric acid and glycerol that results from the nucleophilic substitution of chlorine in α-monochlorohydrin by hydroxide.

The determination of quaternary ammonium compounds is classically performed by potentiometric titration with anhydrous perchloric acid in the presence of mercury(II) acetate[5]. However, the presence of sodium chloride interferes with the determination because mercury(II) acetate complexes with chloride to form titratable acetate resulting in a falsely high result. Another classic determination involves titration of a quaternary ammonium chloride with standard sodium lauryl sulfate in a two phase water–chloroform system using methylene blue as the indicator[5]. Ideally the endpoint is observed when the intensity of the blue color is equally distributed between the two phases. However, with these particular quaternary compounds, the alkylamidopropyl-N,N-dimethyl-N-(2,3-dihydroxypropyl)ammonium–methylene blue complex is not soluble in chloroform and chloroform–alcohol solutions making endpoint detection impossible.

Another determination involves the formation of a water insoluble complex between the quaternary ammonium compound and hexacyanoferrate(III) ion[5]. Using this method, we determined the quaternary ammonium chloride concentration in an aqueous solution of Lexquat® AMG-O[a]. We found excellent correlation between this method and the quantity of desired product calculated from the amount of residual reactants remaining in the product. However, a low value was obtained in a complex cosmetic formulation containing additional surfactants.

In recent years, several papers have been published on the determination of quaternary ammonium compounds by high-performance liquid chromatography (HPLC) with reversed-phase packing containing octadecyl and alkylcyano silane groups chemically bonded to silica gel[6-8].

Ion-pair reversed-phase chromatography was chosen because without ion-pairing the quaternary ammonium chlorides gave tailing peaks when used with an alkylcyano stationary phase. The ion-pairing technique was also chosen because the capacity factor (k') of the analyte did not change with concentration when trifluoroacetic acid was used as a counter-ion.

A reversed-phase liquid chromatography method has been developed for quantitation of the surfactant(s) in the Lexquat® AMG product line. Furthermore, this procedure separates the alkylamidopropyl-N,N-dimethyl-N-(2,3-dihydroxypropyl)-ammonium chlorides from process impurities and was used to quantify the level of quaternary ammonium chloride in two cosmetic formulations.

EXPERIMENTAL

Reagents for synthesis of quaternaries

Myristic acid is commercially available at greater than 95% purity from Emery

---

[a] Lexquat AMG-O is a registered trade name for an aqueous solution of oleamidopropyl-N,N-dimethyl-N-(2,3-dihydroxypropyl)ammonium chloride.

and oleic acid was obtained from Witco with a greater than 70% $C_{18:1}$ content (Industrene 205). α-Monochlorohydrin at greater than 99% purity was obtained from Dixie (Houston, TX, U.S.A.).

Reagents and chemicals

HPLC grade acetonitrile, tetrahydrofuran (THF) and methanol (Burdick and Jackson Labs., Muskegon, MI, U.S.A.) and trifluoroacetic acid (Aldrich, Milwaukee, WI, U.S.A.) were used as components in various mobile phases.

Apparatus

The instrument employed was a Waters Assoc. high-performance liquid chromatography Model ALC-201 equipped with a Model 6000A pump and Model 401 differential refractometer. Chromatograms were obtained using a Waters Assoc. Model 730 data module. Infrared spectra were obtained using an IBM Model 32 IR spectrometer. NMR spectra were obtained using an Bruker WP 270 SY spectrometer at Betz Labs., Trevose, PA, U.S.A.

Semi-preparative chromatography

Separation of the quaternary ammonium chloride from impurities was accomplished using a 30 cm × 7.8 mm I.D. μBondapak C_{18} column. The mobile phase used was water–methanol (25:75, v/v) for Lexquat AMG-O and Lexquat AMG-M[a]. The flow-rate was 1.5 ml/min. The fraction containing the quaternary ammonium chlorides and mobile phase was allowed to dry by evaporation in a hood overnight to remove the bulk of the remaining solvent, and further dried at 80°C at atmospheric pressure for 8 h. The samples were then placed in a vacuum oven (25 mmHg) for three hours until a constant weight (agreed to between 0.04% of each other) was obtained[9,10].

Analytical chromatography

Oleamidopropyl-N,N-dimethyl-N-(2,3-dihydroxypropyl)ammonium chloride and myristamidopropyl-N,N-dimethyl-N-(2,3-dihydroxypropyl)ammonium chloride in aqueous systems were determined by reversed-phase ion-pairing liquid chromatography. Two alkyl/cyano columns (μBondapak CN, Waters Assoc.) 15 cm × 4 mm I.D. were used in series. The mobile phase used for the analytical HPLC in assaying the quaternary ammonium chloride in Lexquat samples was prepared by mixing 1100 ml of water, 900 ml of acetonitrile and 2 ml of trifluoroacetic acid. The same mobile phase was used to quantify oleamidopropyl-N,N-dimethyl-N-(2,3-dihydroxypropyl)-ammonium chloride in the skin moisturizer formulation containing Lexquat AMG-O. The mobile phase used for the determination of myristamidopropyl-N,N-dimethyl-N-(2,3-dihydroxypropyl)ammonium chloride in the clear conditioning shampoo containing Lexquat AMG-M was prepared by mixing 1140 ml of water and 840 ml of acetonitrile, 20 ml THF and 2 ml of trifluoroacetic acid.

---

[a] Lexquat AMG-M is a registered trade name for an aqueous solution of myristamidopropyl-N,N-dimethyl-N-(2,3-dihydroxypropyl)ammonium chloride.

Standard and sample preparation

Approximately 50 mg of standard obtained from the semi-preparative liquid chromatography, approximately 200 mg of aqueous Lexquat AMG sample, and approximately 650 mg of the prototype formulation were accurately weighed into separate 10-ml volumetric flasks and diluted to volume with the mobile phase.

Characterization of isolated quaternary chloride homologues

Elemental and infrared analyses. The evaporated fractions from the semi-preparative liquid chromatography containing the quaternary chlorides were dried at 80°C at atmospheric pressure for 8 h then placed in a vacuum oven (25 mmHg) for 3 h and until a constant weight (agreed to between 0.04% of each other) was obtained prior to submission to Galbraith Laboratories (Knoxville, TN, U.S.A.) for elemental analyses. The elemental analysis obtained for the myristyl and oleyl homologues were, respectively: calculated for $C_{22}H_{47}N_2O_3Cl$: C, 62.48%; H, 11.12%; N, 6.63%; O, 11.36%; Cl, 8.40%. Found: C, 62.00%; H, 11.30%; N, 6.50%; O, 11.75%; Cl, 8.45%. Calculated for $C_{26}H_{55}N_2O_4Cl$: C, 63.09%; H, 11.12%; N, 5.66%; O, 12.94%; Cl, 7.18%. Found: C, 63.11%; H, 10.71%; N, 5.58%; O, 13.23%; Cl, 7.75%.

An infrared spectrum was obtained on the dried residue of myristamidopropyl-N,N-dimethyl-N-(2,3-dihydroxypropyl)ammonium chloride isolated by semi-preparative procedures and the following peak assignments were made: 3299 cm^{-1} due to the hydroxyl stretch, 1653 cm^{-1} due to carbonyl stretch vibration of amide (amide I band), and 1545 cm^{-1} due to N–H bending vibration of amide (amide II band). The IR spectrum of the isolated oleamidopropyl-N,N-dimethyl-N-(2,3-dihydroxypropyl) ammonium chloride fraction provided the following peak assignments; 3286 cm^{-1} due to the hydroxyl stretch vibration, 1650 cm^{-1} due to the carbonyl stretch vibration of the amide (amide I bond), 1547 cm^{-1} due to the N–H bending vibration of amide (amide II bond), 3007 cm^{-1} due to the olefinic C–H stretch vibration and 985 cm^{-1} due to the C–H out of plane bending vibration.

NMR analysis. The isolated fractions from the semi-preparative liquid chromatography containing the myristyl and predominately the oleyl quaternary chlorides were subjected to ^{1}H NMR analysis in ^{2}H$_2$O. The proton assignments are as follows:

myristyl:
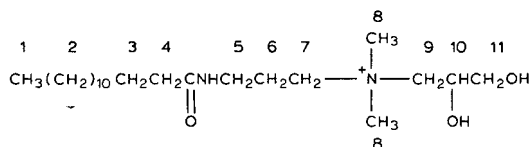
Myristamidopropyl-N,N-dimethyl-(2,3-dihydroxypropyl)ammonium chloride: ^{1}H NMR (^{2}H$_2$O) δ 0.92–0.94 (t, 3 H, No. 1 protons), δ 1.25 (m, 20 H, No. 2 protons), δ 1.58 (m, 2 H, No. 3 protons), δ 1.90–2.15 (m, 2 H, No. 4 protons), δ 2.15–2.35 (m, 2 H, No. 6 protons), δ 3.11–3.21 (d, 6 H, No. 8 protons), δ 3.21–3.38 (m, 2 H, No. 7 protons), 3.38–3.75 (m, 6 H, No. 5, No. 9, and No. 11 protons), 4.18–4.42 (m, 1 H, No. 10 proton).

oleyl:
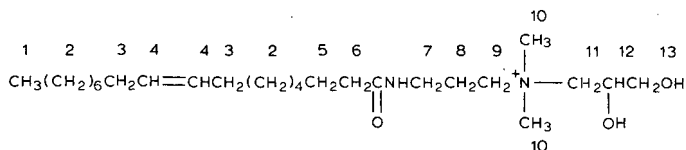
Oleamidopropyl-N,N-dimethyl-(2,3-dihydroxypropyl)ammonium chloride: ^{1}H NMR (^{2}H$_2$O) δ 0.82–0.94 (t, 3 H, No. 1 protons), δ 0.95–1.47 (m, 20 H, No. 2 protons), δ 1.48–1.70, (m, 2 H, No. 5 protons), δ 1.80–2.13 (m, 6 H, No. 3 and No. 6 protons), δ 2.20–2.38 (m, 2 H, No. 8 protons), δ 2.84–3.20 (d, 6 H, No. 10 protons), δ 3.20–3.35 (m, 2 H, No. 9 protons), δ 3.37–3.72 (m, 6 H, No. 7, No. 11 and No. 13 protons), δ 4.18–4.36 (m, 1 H, No. 12 proton), δ 5.18–5.41 (d, 2 H, No. 4 protons).

RESULTS AND DISCUSSION

The alkylamidopropyl-N,N-dimethyl-N-(2,3-dihydroxypropyl)ammonium chloride for myristic and oleic acids were synthesized and separated from unreacted impurities by semi-preparative liquid chromatography. Fig. 1A and B shows the preparative HPLC chromatogram of Lexquat AMG-M and Lexquat AMG-O, respectively. In separate chromatograms, we established the retention volumes of the possible reactants and any by-products: 3-chloro-1,2-propanediol, glycerol, sodium chloride and myristamidopropyl dimethylamine and oleamidopropyl dimethylamine and related alkylamidopropyl dimethylamine homologues present in commercially available oleic acid to ensure that these components were well resolved from the quaternary chloride of interest (see Fig. 1). We observed that the unalkylated alkyl-amidopropyldimethylamine does not elute using this particular column and mobile phase.

Having identified the peak(s) due to the alkylamidopropyl-N,N-dimethyl-N-(2,3-dihydroxypropyl)ammonium chlorides the chromatographic separation was repeated a number of times on a semi-preparative scale to obtain additional quantities of the myristyl quaternary present in Lexquat AMG-M and all homologues of alkyl-amidopropyl-N,N-dimethyl-N-(2,3-dihydroxypropyl)ammonium chlorides contained in Lexquat AMG-O, greater than 70% of which is the $C_{18:1}$ oleyl. The appropriate fractions containing the quaternary chloride(s) of interest were collected and the mobile phase evaporated to concentrate the desired ingredient(s).

As shown in Fig. 1B, the minor components (members of homologous series) present in Lexquat AMG-O were identified in the semi-preparative chromatogram of the figure legend.

As shown in Fig. 2, the absence of the reactants and by-products in the myristyl and oleyl amidopropyl-N,N-dimethyl-N-(2,3-dihydroxypropyl)ammonium chlorides was confirmed by reversed-phase ion-pairing liquid chromatography. Furthermore, Fig. 2A indicates that the myristamidopropyl-N,N-dimethyl-N-(2,3-dihydroxypro-pyl)ammonium chloride fraction contains only one peak. It should be noted that the oleyl fractions of fatty acids used to prepare these surfactants contain additional alkyl chain lengths and varying degrees of unsaturation. Therefore, the oleyl fraction (see Fig. 2B) contains many quaternary chlorides of different alkyl chain lengths which,
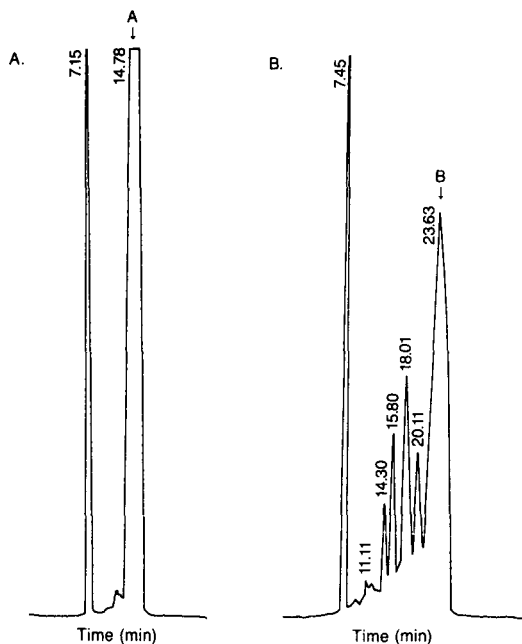
Fig. 1. Semi-preparative isolation of the surfactant components in Lexquat AMG-M and AMG-O on a μBondapak C_{18} reversed-phase column. (A) represents myristamidopropyl-N,N-dimethyl-N-(2,3-dihydroxypropyl)ammonium chloride and (B) is a chromatogram of oleamidopropyl-N,N-dimethyl-N-(2,3-dihydroxypropyl)ammonium chloride. The various quaternary homologues present in oleyl fraction were identified as follows: 14.30 min, myristyl; 15.80 min, palmitoleic; 18.01 min, linoleic; 20.11 min palmitic; 23.63 min oleic. The amount of each cationic injected onto the column was 15 mg.

within our limits of detection, is consistent with the known fatty acid composition of the starting material. As a manufacturer of large quantities of these quaternary chlorides for the cosmetics industry the economical considerations are such that we cannot use highly purified forms of the oleic acid, nor would it be necessary for specific applications in personal care formulations. We routinely use commercially available "oleic acid" which typically contains 2.4% myristic acid, 1.4% myristoleic acid, 0.2%
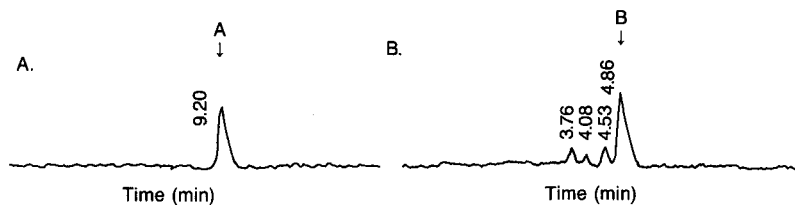
Fig. 2. Analytical chromatogram of (a) myristamidopropyl-N,N-dimethyl-N-(2,3-dihydroxypropyl)ammonium chloride and (B) oleamidopropyl-N,N-dimethyl-N-(2,3-dihydroxypropyl)ammonium chloride obtained by reversed-phase ion-pairing liquid chromatography. The amount of myristyl homologue injected onto the column was 52 μg and the amount of oleyl homologue was 48 μg. The various homologues present in the oleyl fraction have been identified as follows: 3.76 min, palmitoleic; 4.08 min, linoleic; 4.53 min, palmitic and 4.86 min, oleic.

myristolinoleic, 5.2% palmitic acid, 6.4% palmitoleic acid, 1.2% palmitolinoleic acid, 2.1% stearic acid, 72.7% oleic acid, 7.6% linoleic acid and 0.7% linolenic acid as determined by gas chromatography. The use of fatty acids containing other homologs to prepare the alkyl amidopropyldimethylamines prior to alkylation with α-monochlorohydrin will yield quaternary chlorides that contain various alkyl chain lengths. We have not attempted to identify and/or resolve in our chromatographic system the quaternary chlorides of the fatty acids that comprise less than 5% of the over all cationic species. We manufacture these products using the best available fatty acids with the highest concentration of alkyl groups of interest (*i.e.* myristyl and oleic) to prepare products with the desired functional properties. The presence of other alkyl homologues in the final product does not detract from the functional properties of these molecules.

Samples of the chromatographically isolated quaternary fractions and dried forms of the myristyl, oleyl and related homologues were subjected to elemental analysis (see Experimental). The results indicate that the desired compounds were obtained. Despite rigorous drying the oleyl homologue was dried consistently to the monohydrate as calculated from the elemental analysis.

Additional characterization of the isolated quaternary fractions was done by Fourier transform (FT)-IR and NMR (see Experimental). The FT-IR and NMR data indicate that the absorbances and signals observed from the respective instruments are consistent with the structures of the predominant cationic species in both standards. Furthermore, the absence of extraneous absorbances coupled with the expected integration values are consistent with the proposed structures of both standards.

The calibration plot for myristamidopropyl-N,N-dimethyl-N-(2,3-dihydroxypropyl)ammonium chloride is shown in Fig. 3. This calibration curve was obtained using acetonitrile–water (45:55) containing 0.1% trifluoroacetic acid as mobile phase and was used to assay Lexquat AMG-M. A separate calibration curve was generated using acetonitrile–water–THF (42:57:1) containing 0.1% trifluoroacetic acid as mobile phase for quantifying the myristyl homologue in the clear conditioning shampoo formulation (standard curve not shown). The linearity of response for the myristyl standards was tested between 50–420 μg equivalent to 5–40% for the Lexquat AMG-M in aqueous solutions and includes a concentration equivalent to 1–10% in cosmetic formulations. The correlation coefficient (r) by peak area was 0.999.

The calibration plot for the oleamidopropyl-N,N-dimethyl-N-(2,3-dihydroxypropyl)ammonium chloride containing fraction is shown in Fig. 4. This calibration curve was obtained using acetonitrile-water (45:55) containing 0.1% trifluoroacetic acid as mobile phase and was used to assay both the Lexquat AMG-O and the skin moisturizer formulation. The linearity of response of the oleyl standards was tested between 48–600 μg equivalent to 6–54% for Lexquat AMG-O in aqueous solutions and a concentration range equivalent to 1–16% in the cosmetic formulations. The correlation coefficient (r) by peak area measurements was 0.992.

As a routine procedure in the laboratory we were interested in establishing the accuracy and precision for determining alkylamidopropyl-N,N-dimethyl-N-(2,3-dihydroxypropyl) ammonium chloride levels in production batches of the aqueous solutions of Lexquat AMG-M and AMG-O. Table I summarizes the determination of each alkylamidopropyl-N,N-dimethyl-N-(2,3-dihydroxypropyl)ammonium chloride using the analytical HPLC methods described in this paper. The Lexquat
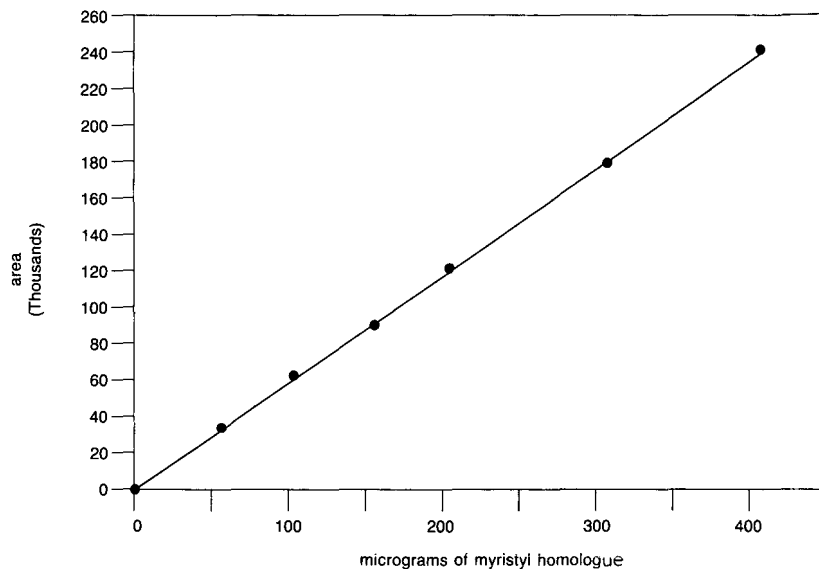
Fig. 3. Standard curve for the purified myristyl quaternary chloride. Chromatographic conditions were the same as Fig. 2A. Quantitative determination was based on peak area of the ion-pair.

AMG-M containing sample showed an error of 0.29% and relative standard deviation (R.S.D.) of 1.33% in six different runs. For the Lexquat AMG-O six different runs yielded an error of less than 1.41% and R.S.D. of 0.69%. The concentration of the analyte was measured by peak area. It is apparent that this analytical procedure
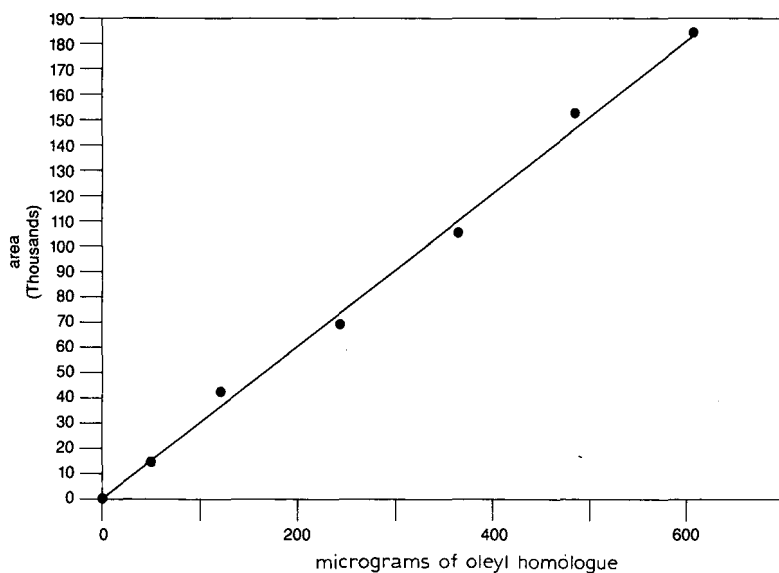
Fig. 4. Standard curve for the purified oleyl quaternary chloride. Chromatographic conditions were the same as Fig. 2B. Quantitative determination was based on peak area of the ion-pair.

TABLE I

ACCURACY AND PRECISION DATA FOR THE DETERMINATION OF QUATERNARY AMMONIUM CHLORIDES IN AQUEOUS SOLUTIONS

Weight percentages were determined by HPLC; the chromatographic conditions were the same as in Fig. 2. The analyses based on peak area of ion-pair.

Run no.	Weight(%)	
	Lexquat AMG-M	Lexquat AMG-O
1	34.5	28.7
2	33.5	28.8
3	34.1	28.8
4	34.2	28.6
5	34.8	29.0
6	33.9	28.6
Actual quaternary ammonium chloride level	34.1	28.4
Mean (%)	34.2	28.8
R.S.D. (%)	1.33	0.69
Error (%)	0.29	1.41

provides a reproducible method for quantifying the quaternary chlorides of interest in production batches.

The applicability of our analytical procedure for quantifying the quaternium ammonium compound in a complex cosmetic formula was demonstrated by determining the surfactant levels of Lexquat AMG-M and AMG-O in two different personal care prototypes. Two formulations were prepared according to methods described previously[4,11]; a clear conditioning shampoo containing Lexquat AMG-M (see Table II) and a skin moisturizer containing Lexquat AMG-O (see Table III). For purposes of this paper, we did not include fragrances usually found at low levels (< 1.0%) in preparing these formulations. With regard to the chromatographic separations, it should be noted that fragrances are usually composed of aldehydes, ketones or hydrocarbons. Non-polar compounds of this type would tend to be strongly retained on the column and thus not interfere with the cationics being quantified.

Determination of myristamidopropyl-N,N-dimethyl-N-(2,3-dihydroxypropyl) ammonium chloride in the clear conditioning shampoo required a change in solvent strength of the mobile phase. As shown in Fig. 5, a multiplicity of peaks due to various components was obtained in the analytical chromatogram for the clear conditioning shampoo. It is apparent that the myristyl quaternary component (A) was sufficiently resolved from the other components in the formulation for quantification. The resolution (R_s) equals 0.9. A list of the components in the shampoo is shown in Table II.

A chromatogram of the skin moisturizer containing Lexquat AMG-O is shown in Fig. 6. It is apparent that the major cationic species (B) present in this fraction (oleyl quaternary) was sufficiently resolved from the other components in the formulation for quantification. R_s was equal to 0.7. The components in this formulation are listed in Table III.

TABLE II

CLEAR CONDITIONING SHAMPOO CONTAINING LEXQUAT AMG-M

Procedure: add ingredients of part B to the water and heat to 60°C. When materials are completely dissolved, add part A to part B. Maintain temperature and mix. When uniform add Lexquat AMG-M to the mixture. Cool to room temperature and adjust the pH to 6 with citric acid. Fragrance was not included.

Component	Weight (%)
Part A	
Sodium C_{14-16} olefin sulfonate	4.63
Triethanolamine lauryl sulfate	9.85
Laura/myristamidopropyl betaine	9.82
Diethanolamide of coconut fatty acid	2.94
Potassium coco-hydrolyzed protein	2.94
Part B	
Water	64.37
Propylene glycol	2.90
Methyl paraben	0.29
Propyl paraben	0.10
Benzophenone-4	0.10
Tetrasodium EDTA	0.10
Myristamidopropyl-N,N-dimethyl-N-(2,3-dihydroxypropyl)ammonium chloride	1.76
Citric acid	0.20

TABLE III

SKIN MOISTURIZER CONTAINING LEXQUAT AMG-O

Procedure: add hydroxyethyl cellulose to water while mixing and heating to 78°C. When the cellulose is completely hydrated, add remaining material of part A. Combine part B in a separate vessel and heat to 78°C. When uniform slowly add part B to part A maintaining mixing and temperature. Allow to mix at 78°C for 15 min then cool to room temperature. Fragrance was not included.

Component	Weight (%)
Part A	
Water	69.76
Hydroxyethyl cellulose	0.88
Glycerol	2.93
Propylene glycol	1.95
Methylparaben	1.95
Oleamidopropyl-N,N-dimethyl-N-(2,3-dihydroxypropyl)ammonium chloride	1.91
Propylene glycol dinonanoate	14.66
Part B	
Glyceryl mono-, di-, and tristearates	1.95
Myristyl myristate	0.98
Stearyl alcohol	1.95
Cetyl alcohol	0.98
Propyl paraben	0.10
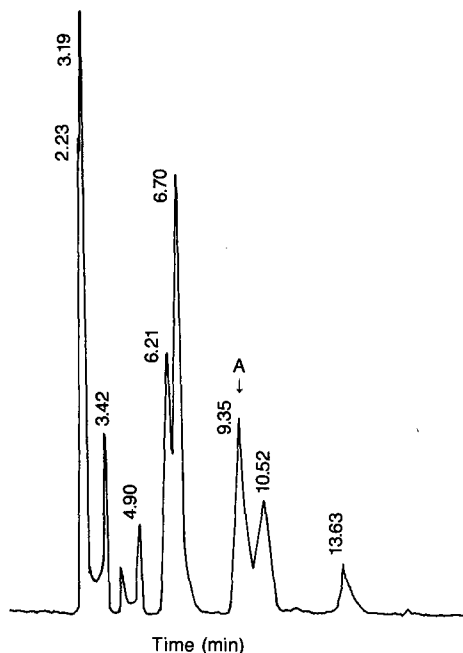
Fig. 5. Analytical separation and quantitation by HPLC of myristamidopropyl-N,N-dimethyl-N-(2,3-dihydroxypropyl)ammonium chloride (peak A) in a clear conditioning shampoo. Other components in the formulation were not identified. Chromatographic conditions were as described under Experimental, *Analytical chromatography*.

The resolution obtained by the chromatographic systems described was suited for both cosmetic formulas as demonstrated by the accuracy and precision of quantifying the myristyl and oleyl quaternaries in six separate runs, as indicated in Table IV.

For the myristyl quaternary present in the clear conditioning shampoo we observed an error of 1.14% and R.S.D. of 2.81% in six different runs. For the Lexquat AMG-O containing skin moisturizer six different runs yielded an error of 2.62% and R.S.D. of 3.78%. The concentration of each cationic, identified in separate chromatograms using the appropriate mobile phases was determined by peak area. This HPLC procedure provides a reliable and reproducible method for quantitating each of these quaternary chlorides in a complex cosmetic formulation. In contrast, classical wet analysis methods are currently not available for quantifying the different types of quaternary surfactants commonly used in formulations.

Given the complex nature of individual cosmetic formulations, different prototypes may require changes in mobile phase and/or columns to obtain the desired resolution of the quaternary ammonium chloride and thus accurately quantify the level of the alkylamidopropyl-N,N-dimethyl-N-(2,3-dihydroxypropyl)ammonium chloride in a personal care cosmetic formulation.
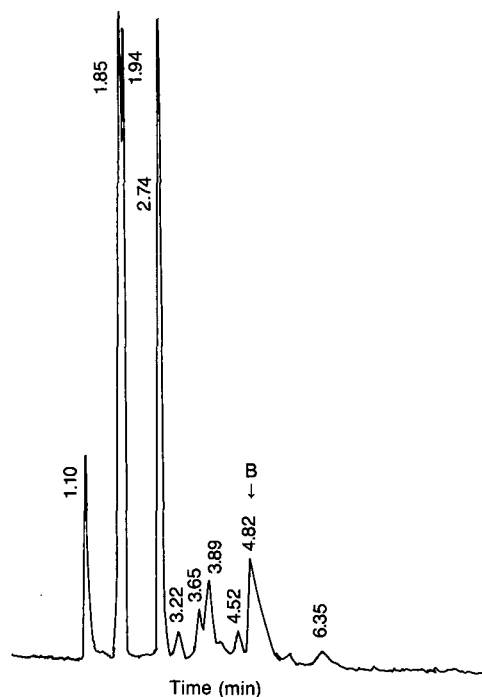
Fig. 6. Analytical separation and quantitation by HPLC of oleamidopropyl-N,N-dimethyl-N-(2,3-dihy-droxypropyl)ammonium chloride (peak B) in a skin moisturizer formulation. Other components in the formulation were not identified. Chromatographic conditions were as described under Experimental, *Analytical chromatography*.

TABLE IV

ACCURACY AND PRECISION FOR DETERMINATION OF ALKYLAMIDOPROPYL-N,N-DI-METHYL-N-(2,3-DIHYDROXYPROPYL)AMMONIUM CHLORIDE IN TWO COSMETIC FOR-MULATIONS

Weight percentages were determined by HPLC. Analyses based on peak area of the ion-pair.

Run No.	Weight (%)	
	Clear conditioning shampoo Lexquat AMG-M[a]	Skin moisturizer Lexquat AMG-O[b]
1	1.80	1.83
2	1.78	1.92
3	1.79	1.98
4	1.79	2.01
5	1.69	2.02
6	1.82	2.01
Amount (%) added to formulation	1.76	1.91
Mean (%)	1.78	1.96
R.S.D. (%)	2.81	3.78
Error (%)	1.14	2.62

[a] Chromatographic conditions were the same as in Fig. 5.
[b] Chromatographic conditions were the same as in Fig. 6.

CONCLUSIONS

The HPLC method described provides an accurate and reproducible procedure for quantifying the levels of two quaternary alkylamidopropyl-N,N-dimethyl-N-(2,3-dihydroxypropyl)ammonium chlorides in aqueous solutions and cosmetic formulations. Classical methods of potentiometric titrations and dye-binding methods were not suitable for quantitation of these quaternary compounds.

Accordingly, we used reversed-phase liquid chromatography to purify the myristyl and oleyl homologues from production batches of these cosmetic raw materials. Having isolated and identified the components of interest we used analytical ion-pairing chromatography to accurately quantify the levels of both quaternaries in production batches of the raw materials and two prototype personal care formulations.

ACKNOWLEDGEMENTS

REFERENCES

1 E. Cook and P. Moss, *U.S. Pat.*, 2,589,674 (1952).
2 A. Patel and H. Greenland, *U.S. Pat.*, 4,726,945 (1988)
3 D. E. Conner and A. W. Fogel, *U.S. Pat.*, 4,012,398 (1977).
4 J. J. Guth, G. M. Reinhart, L. R. Smith, B. W. Gesslein and G. R. Mintz, *U.S. Pat.*, pending (1988).
5 M. J. Rosen and H. A. Goldsmith, *Systemic Analysis of Surface-Active Agents*, Wiley, New York, 2nd ed., 1972, p. 445.
6 L. J. Cohn, V. J. Greely and D. L. Tibbetts, *J. Chromatogr.*, 321 (1985) 401.
7 N. Parris, *J. Liq. Chromatogr.*, 3(11) (1980) 1743.
8 G. Ambrus, L. T. Takahashi and P. A. Marty, *J. Pharm. Sci.*, 76(2) (1987) 174.
9 C. Paquot, *Standard Methods for the Analysis of Oils, Fats and Derivatives, Part 1*, Pergamon Press, New York, 6th ed., 1978, p. 8.
10 H. A. Boekenoogen, *Analysis and Characterization of Oils, Fats and Fat Products, Vol. 1*, Wiley, New York, 1964, p. 13.
11 B. Gesslein and L. Smith, *Inolex Technical Bulletin*, 1988, personal communication.

MONOCLONAL ANTIBODY-MEDIATED CLEAN-UP PROCEDURE FOR THE HIGH-PERFORMANCE LIQUID CHROMATOGRAPHIC ANALYSIS OF CHLORAMPHENICOL IN MILK AND EGGS

C. VAN DE WATER, D. TEBBAL and N. HAAGSMA*

Faculty of Veterinary Medicine, Department of the Science of Food of Animal Origin, University of Utrecht, P.O. Box 80 175, 3508 TD Utrecht (The Netherlands)

(First received February 13th, 1989; revised manuscript received May 3rd, 1989)

SUMMARY

A simple, rapid and specific sample preparation method based on antibody-mediated clean-up for the determination of chloramphenicol (CAP) in milk and eggs was developed. Skimmed milk and centrifuged egg homogenates were filtered and directly applied to immunoaffinity columns which were prepared by coupling monoclonal antibodies against CAP to a carbonyldiimidazole-activated support. Using a 0.2 M glycine, 0.5 M NaCl (pH 2.8) solution as an eluent, the immunoaffinity columns can be used more than 30 times without a decrease in column capacity. In subsequent high-performance liquid chromatographic analysis, no matrix interferences were observed. Good recoveries were obtained at spiking levels of 1–100 μg kg^{-1}. Due to the high specificity of the clean-up procedure, the limit of detection can be lowered by increasing the test portion. Concerning milk, the limit of detection was successfully lowered to 20 ng kg^{-1} by increasing the test portion to 1 l (recovery 99%). The method was applied to eggs produced by hens treated with CAP. The results are compared with those obtained by solid-phase extraction using silica gel.

INTRODUCTION

Various immunological methods for the detection and determination of residues of the broad-spectrum antibiotic chloramphenicol (CAP) have been described[1–8]. In these methods, antibodies against CAP were used in the final analysis. Recently we have demonstrated that these antibodies can also be used for a very specific clean-up and concentration of this compound from aqueous extracts of swine muscle tissue before high-performance liquid chromatographic (HPLC) analysis[9].

Usually, immunoaffinity columns are prepared by coupling antibodies to a cyanogen bromide (CNBr)-activated support[10,11]. However, this procedure has some disadvantages[11]: charged isourea groups are formed which are responsible for undesirable ion-exchange effects, and the isourea linkage is rather unstable. Therefore attention was paid, by Bethell *et al.*[12] and also by Hearn *et al.*[13], to an alternative coupling procedure using carbonyldiimidazole (CDI). The urethane linkage formed

by this coupling procedure proved to be much more stable (leak resistant) than the isourea linkage introduced by the cyanogen bromide coupling procedure. Moreover, the urethane linkage is uncharged[11,14]. Therefore, non-specific binding due to ion-exchange effects does not occur.

In our earlier procedure the immunoaffinity columns were prepared by coupling monoclonal antibodies against CAP to a CNBr-activated support[9]. No decrease in CAP recovery at the 10 μg kg^{-1} level was observed after using these columns eleven times. On closer investigation, however, the column capacity was found to be decreased. Nevertheless, this capacity was high enough to guarantee good recoveries at the 10 μg kg^{-1} level. When the immunoaffinity columns were reused more often a continuous decrease in the column capacity led to lower recoveries. For that reason a CDI-activated support, which is now commercially available, was chosen for the preparation of the immunoaffinity columns. Other aspects with respect to reuse of the columns were also studied, such as the type of eluent and storage of the columns. Moreover, factors influencing the binding of CAP to the immunoaffinity columns such as the bed volume and the CAP concentration on the CAP capture efficiency were also investigated.

This paper describes the modified antibody-mediated clean-up procedure for the determination of CAP in eggs and milk. The method was also applied to eggs of hens to which CAP had been administered. The results obtained were compared with those obtained by a solid-phase extraction (SPE) procedure developed earlier[15].

EXPERIMENTAL

Reagents and chemicals

Water was purified by demineralization (conductivity <1 μS). Glycine and CAP were from Sigma (St. Louis, MO, U.S.A.), ammonium acetate, hexane, hydrogen chloride, sodium monohydrogenphosphate, potassium chloride, silica gel (average particle diameter 40 μm, for flash chromatography) and sodium acetate from Baker (Phillipsburgh, NJ, U.S.A.), ammonium sulphate, boric acid, citric acid monohydrate, isooctane, sodium chloride, sodium hydrogencarbonate, potassium dihydrogenphosphate from Merck (Darmstadt, F.R.G.), acetonitrile and methanol (both HPLC grade) from Rathburn (Walkerburn, U.K.), sodium azide from BDH (Poole, U.K.) and carbonyldiimidazole (CDI)-activated trisacryl GF-2000 (in acetone slurry) and bicinchoninic acid (BCA) protein assay reagent from Pierce (Rockford, IL, U.S.A.). Filter-paper circles (S&S 589.1, diameter 90 mm; S&S 589.3, diameter 125 mm and S&S 589.1/2, diameter 125 mm) were obtained from Schleicher and Schüll (Dassel, F.R.G.). The 125-ml polypropylene beakers were from Sarstedt (Eindhoven, The Netherlands).

A standard solution was prepared by dissolving 25.0 mg of CAP in 10.0 ml of methanol. Working standards for HPLC were prepared in the range of 10–1500 ng ml^{-1} by diluting the standard solution in the HPLC eluent. Spiking solutions containing 0.10, 1.00 and 10.00 μg ml^{-1} of CAP were prepared by diluting the standard solution in methanol. The mobile phase solvent for HPLC was acetonitrile–0.01 M sodium acetate buffer pH 5.4 (25:75, v/v).

Concentrated phosphate-buffered saline (PBS) was prepared by dissolving 80 g of NaCl, 14.33 g of Na$_2$HPO$_4$ · 2H$_2$O, 2 g of KH$_2$PO$_4$, 2 g of KCl and 2 g of NaN$_3$ in

1 l of demineralized water. The PBS (pH 7.4; 0.1368 M NaCl, 0.0015 M KH$_2$PO$_4$, 0.0081 M Na$_2$HPO$_4$ · 2H$_2$O, 0.0027 M KCl, 0.0031 M NaN$_3$) was prepared by diluting concentrated PBS 1:10 in demineralized water.

The coupling buffer solution (pH 8.5) was 0.13 M boric acid. The blocking buffer solution (pH 8.0) contained 0.2 M glycine; the acetate buffer (pH 4.0) contained 0.1 M sodium acetate and 0.5 M sodium chloride. Monoclonal antibodies against CAP are described below. The eluent used in the antibody-mediated clean-up procedure was a 0.2 M glycine, 0.5 M sodium chloride (pH 2.8) solution.

Apparatus

The instruments used were a Moulinette homogenizer (Moulinette, Gouda, The Netherlands), a spectrophotometer (Uvichem MK2; Rank Hilger, London, U.K.), a Prepspin 50 ultracentrifuge (Measuring and Scientific Equipment, Crawley, U.K.), a table centrifuge (Rotina/S; Hettich, Tuttlingen, F.R.G.), an Ultra-Turrax (Janke and Kunkel, Staufen, F.R.G.), a shaking apparatus (Janke and Kunkel, Type S50), a Reacti-Vap evaporating unit Model 18780, connected to a Reacti-Therm heating module, Model 18790 (Pierce), a vortex mixer (Scientific Industries, Bohemia, NY, U.S.A.), a magnetic stirrer (Pt 800; Protherm, Etten-Leur, The Netherlands), a sintered-glass funnel, diameter 40 mm, porosity 16–40 μm (P. M. Tamson, Zoetermeer, The Netherlands) and Visking dialysis tubing size 2 18/32 in. (Medicell, London, U.K.).

In order simultaneously to perform the antibody-mediated extractions, a proportioning pump III from a Technicon AutoAnalyzer II system was used in combination with Tygon calibrated flow-rated pump tubes, flow-rate 1.20 ml min^{-1}, 0.056 in. I.D. (Technicon, New York, NY, U.S.A.). The pump tubes were connected to immunosorbent packed Econo-columns (No. 737-122, 10 cm × 0.7 cm; Bio-Rad Labs., Richmond, CA, U.S.A.). The HPLC system used was the same as that described earlier[15].

Preparation and purification of monoclonal antibodies

The preparation and production of the monoclonal antibodies against CAP were performed in the hybridoma laboratory of the Department of Infectious Diseases and Immunology (Faculty of Veterinary Medicine, University of Utrecht, The Netherlands). These monoclonal antibodies possess the immunoglobulin G$_1$ (IgG$_1$) isotype. They were originally selected for an enzyme-linked immunosorbent assay (ELISA) and purified by ammonium sulphate precipitation as described earlier[8], but with the aid of boric acid solution as a coupling buffer. After dialysis the concentration of monoclonal antibodies in the purified solution, expressed as the amount of IgG per millilitre, was determined spectrophotometrically using the BCA protein determination[16].

Preparation of immunoaffinity columns

The excess of acetone of the CDI-activated support was removed by suction on a sintered glass funnel. The gel was washed with five bed volumes of ice-cold water. A 10-ml volume of the drained gel cake was transferred to 20 ml of the purified monoclonal antibody solution containing 5 mg ml^{-1} IgG. In this aqueous medium the 10-ml gel cake was swollen to a volume of 15 ml. The gel suspension was gently mixed

in a 50-ml polypropylene tube for 24 h at 4°C using a shaking apparatus. The suspension was centrifuged at 300 g for 3 min; the supernatant was used for the determination of the coupling efficiency (see below). The pellet was gently mixed with 20 ml of blocking buffer for 2 h at room temperature using a shaking apparatus. The gel suspension was centrifuged at 300 g for 3 min. The pellet was successively washed with 20 ml of coupling buffer, 20 ml of acetate buffer and 20 ml of coupling buffer. Finally the gel was washed with 50 ml of PBS and transferred to the columns (bed volume 0.5 ml per column).

The efficiency of the monoclonal antibody conjugation to CDI-activated trisacryl GF-2000 was determined from the concentration of IgG in the diluted purified monoclonal antibody solution before and after the coupling procedure. The concentration of IgG was determined as described above. The dynamic and specific column capacities were determined in an analogous manner to that described earlier[9]. Instead of elution with methanol, the saturated immunosorbent was eluted with 0.2 M glycine, 0.5 M NaCl (pH 2.8) as described.

Samples

Spiking studies. Full-cream milk and whole eggs were used for spiking studies. The milk and homogenized egg samples were spiked with CAP at 1, 10 and 100 μg kg^{-1} at least 15 min before sample preparation.

Animal studies. Four laying hens (Hubbard golden comet, 25 weeks old) were treated with CAP through their drinking water during 5 successive days. The dosages were 0.05 (group A) and 0.5 g l^{-1} (group B) respectively; two animals for each group. Two laying hens served as the control group. The eggs were collected each day. Eggs produced within one group on the same day were pooled and homogenized using an Ultra Turrax for 45 s. Portions were frozen until analysis.

Sample preparation (antibody mediated clean-up)

Milk. Approximately 10 g of homogenized milk were accurately weighed in a 20-ml polypropylene tube. The milk sample was centrifuged at 3000 g for 15 min. Fat (upper layer) was removed. The skimmed milk sample was filtered through S&S 595. ½ filter-paper. The polypropylene tube was rinsed with 5 ml of PBS. The wash liquid was filtered through the same filter. The total filtrate was subjected to antibody-mediated clean-up.

Eggs. Approximately 10 g of spiked homogenized whole egg were accurately weighed in a 14-ml polycarbonate tube. With respect to samples in the animal study, however, smaller test portions must be used in some cases to avoid overloading of the immunoaffinity columns. For the egg homogenates from day 1 up to day 12 (group A), day 13 and day 14 (group A) and day 1 up to day 9 (group B) the amounts were lower (0.5, 1.0 and 5.0 g respectively). To these samples, blank egg homogenate was added up to 10 g.

The homogenates (spiking study and animal study) were centrifuged at 10 000 g for 10 min. The supernatant was filtered through S&S 589.1 filter-paper. The pellet was washed with 5 ml of PBS. The wash liquid was filtered through the same filter. The total filtrate was subjected to antibody-mediated clean-up.

Antibody-mediated clean-up. The total sample solution was pumped through the immunoaffinity column at a rate of 1.2 ml min^{-1} using a Technicon proportioning

pump. The column was washed with 25 ml of PBS; CAP was eluted subsequently with 20 ml of glycine–NaCl eluent at a flow-rate of 1.2 ml min^{-1}. The eluate was collected in a 50-ml polypropylene tube. It was extracted twice with ethyl acetate (1 × 15 ml, 1 × 10 ml) using a shaking apparatus for 15 min. The upper organic layers were successively evaporated to dryness in a stream of nitrogen at 45°C using the evaporating unit and heating module (position 3, high). The residue was dissolved in 1 ml of the mobile phase solvent using a vortex mixer for 15 s. This solution was used for HPLC analysis.

Before regeneration, the risk of cross-contamination was minimized by washing the column with 20 ml of the glycine–NaCl eluent at a flow-rate of 1.2 ml min^{-1}. The columns were regenerated by washing with 20 ml of PBS at a flow-rate of 1.2 ml min^{-1}. If not in use the columns should be stored in PBS at 4°C. The columns were not allowed to run dry during the antibody-mediated clean-up and regeneration. If air-bubbles are present the immunosorbent should be shaken until a gel suspension is formed. Then the gel was allowed to settle again.

Sample preparation (solid-phase extraction)

Approximately 10 g of the homogenized egg sample were subjected to a solid-phase extraction procedure which comprises sonication-aided extraction with ethyl acetate, addition of hexane to the extract and cleaning up and concentration of the extract on a small column packed with silica gel. Compared to the solid-phase extraction described earlier for the determination of CAP in swine muscle tissue[15], some modifications were introduced[17]. After solid-phase extraction, all samples (dissolved in mobile phase solvent) were extracted three times with 1-ml volumes of isooctane. The remainder solution was subjected to HPLC analysis.

Chromatography

The samples were subjected to HPLC analysis. The HPLC conditions were as described earlier[15], except for the pH of the mobile phase. Aliquots of the sample and standard solution (40 μl) were injected by means of the loop injector. For low concentrations (below 10 μg kg^{-1}), 100-μl volumes were injected.

RESULTS AND DISCUSSION

Spiking studies

Recovery experiments were carried out on full-cream milk and eggs at spiking levels of 1, 10 and 100 μg kg^{-1}. The samples, including the blank samples, were subjected eight-fold to antibody-mediated clean-up followed by HPLC analysis according to the procedure described. The results are presented in Table I. At the spiking level of 1 μg kg^{-1} the recoveries are nearly 100%. However, at higher spiking levels the recoveries are somewhat lower. A logarithmic relationship exists between the spiking level and the recovery found, the coefficient of correlation being 1.0000 for milk and 0.9919 for egg.

The lowest standard deviations were obtained at the spiking level of 10 μg kg^{-1}. The higher standard deviations at 1 μg kg^{-1} may be attributed to the fact that the HPLC analysis was performed quite close to the limit of detection of the CAP standard, being 0.6 ng (signal corresponding three times the noise level). The cause of the

TABLE I

RECOVERY OF CHLORAMPHENICOL FROM SPIKED MILK AND EGGS

	Added $(\mu g\ kg^{-1})$	Recovery (%)	Standard deviation (%)
Milk	1	100	8.5 ($n = 8$)
	10	91	5.5 ($n = 8$)
	100	82	7.4 ($n = 8$)
Eggs	1	98	12.2 ($n = 7$)[a]
	10	91	3.2 ($n = 7$)[a]
	100	80	6.1 ($n = 8$)

[a] One sample was lost during sample preparation.

higher standard deviations at the spiking level of 100 $\mu g\ kg^{-1}$ and the lower recoveries at higher spiking levels will be discussed below. Typical chromatograms from spiked egg and milk samples are shown in Fig. 1. Very clean chromatograms were obtained. In this way, CAP can be determined in full-cream milk and eggs at the spiking level of 1 $\mu g\ kg^{-1}$.

Due to the absence of matrix interferences, a greater amount of sample can be subjected to antibody-mediated clean-up. This opens up the possibility to determine lower CAP contents. For example, a milk solution spiked with 20 ng kg^{-1} can be analysed when 1 l instead of 10 ml is subjected to antibody-mediated clean-up (recovery 99%). The chromatograms obtained after HPLC analysis were as clean as those in Fig. 1. In the analysis of egg homogenates, however, it was not possible to enlarge the test portion for antibody-mediated clean-up due to clogging of the column.

Antibody-mediated clean-up

Conjugation efficiency and column capacity. The efficiency of the monoclonal antibody conjugation to CDI-activated trisacryl GF-2000 was 59%. The protein loading was calculated as 3.10 mg of monoclonal antibody per ml of gel. The dynamic column capacity was found to be 2.73 μg of CAP per ml of gel, and the specific column capacity was 0.88 μg of CAP per mg of immobilized monoclonal antibody.

Reuse of immunoaffinity columns. To investigate the effect of reuse of immunoaffinity columns, the total column capacities were determined. Immunoaffinity columns with a bed volume of 1.5 ml were saturated by passing 20 ml of a 1 $\mu g\ ml^{-1}$ CAP solution in PBS at a flow-rate of 1.2 ml min^{-1}. After washing with 25 ml of PBS, the columns were eluted with the glycine–NaCl solution or with methanol as described earlier[9]. The eluate was analysed for CAP by HPLC. After regeneration, the cycle (saturation, washing, elution, analysis and regeneration) was repeated several times. The experiments covered a period of 1 month. When not in use the columns were stored in PBS at 4°C.

The results are presented in Fig. 2. Glycine–NaCl does not significantly influence the column capacity during 33 cycles, whilst using methanol the column capacity decreased strongly. After 6 cycles only 15% of the original column capacity is left; after 17 cycles the column capacity is only 100 ng. Therefore glycine–NaCl solution is
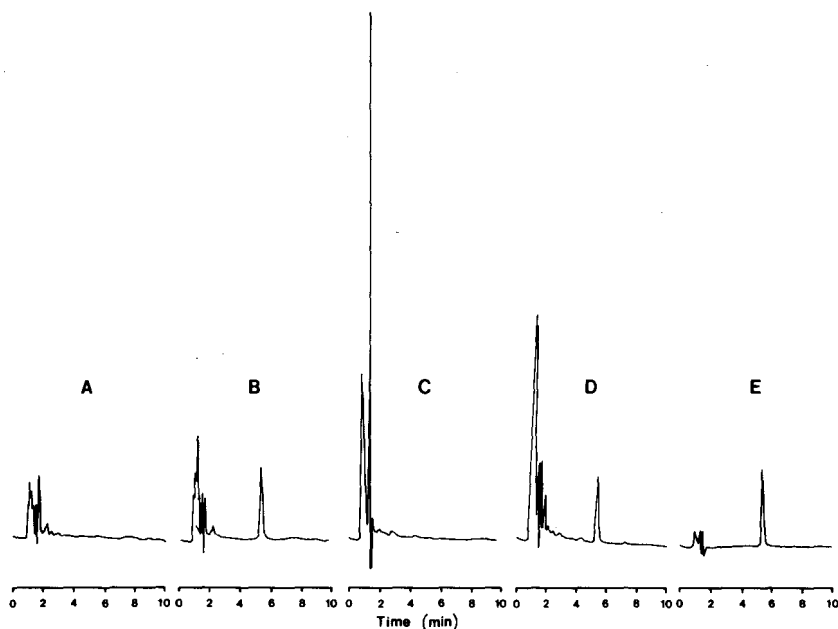
Fig. 1. Chromatograms of milk and egg samples purified by means of antibody-mediated clean-up followed by HPLC analysis. (A) Blank milk sample; (B) spiked (10 μg kg^{-1}) milk sample; (C) blank egg sample; (D) spiked (10 μg kg^{-1}) egg sample and (E) standard solution of CAP. Absorbance range settings: 0.016 a.u.f.s.

preferred as an eluent when the columns have to be reused many times. For single-use columns, methanol is the elution solvent of choice due to the easier pretreatment before HPLC analysis. Furthermore, the column capacity was slightly restored after storage in PBS (viz., Fig. 2).

   Capture efficiency. In the procedure described earlier for the determination of CAP residues in swine muscle tissue[9], addition of PBS to the aqueous tissue extracts before the antibody-mediated clean-up was necessary. In the case of milk and egg homogenates, however, the samples can be subjected to antibody-mediated clean-up directly after centrifugation and filtration. Extraction and dilution in PBS was not necessary for obtaining an high capture efficiency of CAP. However, as is seen from Table I, the recovery at the highest spiking level is lowered to 80%. This was caused by a lowering of the CAP capture by the column and not by incomplete elution. At that spiking level the amount of CAP for capture approximates the total column capacity for CAP.

   To investigate how to improve the capture efficiency, in particular at amounts of CAP close to the column capacity, the following study was carried out. A fixed amount of CAP, i.e., 1250 ng, was dissolved in respectively 2, 10 and 50 ml of PBS or skimmed milk. Antibody-mediated extractions were performed using columns with a 0.5-ml bed volume. For CAP in PBS the capture efficiency increased from 56% for the most concentrated solution (1250 ng CAP per 2 ml) to 90% for the most diluted solution (1250 ng CAP per 50 ml). For skimmed milk the same tendency was observed: 72% for the most concentrated solution and 88% for the most diluted solution.
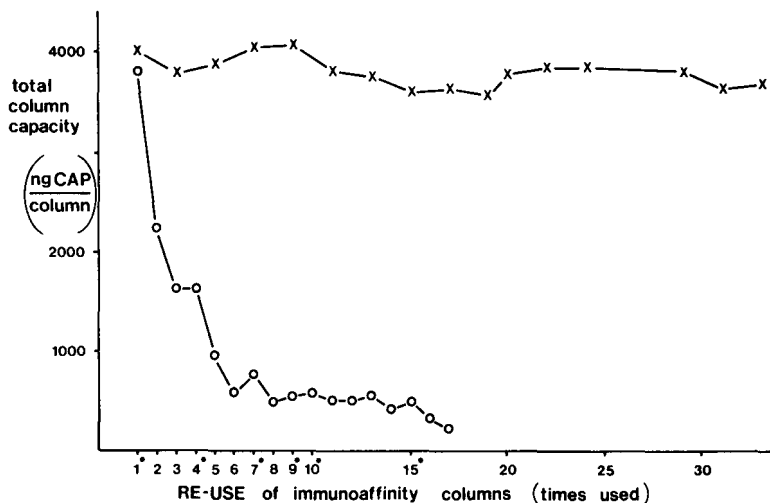
Fig. 2. The effect of storage of the immunosorbent in PBS at 4°C and of the type of eluent used on the total column capacity by reuse of the immunoaffinity columns. The successive antibody-mediated extraction cycles (saturation, washing, elution and regeneration) were performed with two identical immunoaffinity columns (bed volume 1.5 ml). One column was used for the methanol elution (O—O), the other column for the glycine–NaCl elution (×—×). The numbers provided with an asterisk are the first capacity determinations performed on a new day. The capacity determinations were made over a period of 1 month.

Similar experiments were carried out using immunoaffinity columns with a bed volume of 1.0 ml.

An increase in the bed volume of the immunoaffinity columns from 0.5 to 1.0 ml slightly improved the capture efficiency at all concentrations. The results indicate that at a fixed bed volume a more efficient binding of CAP can be reached by lowering the CAP flux through the column or, in other words, when the same amount of CAP was extracted from a greater volume. This holds especially when the amount of CAP to be extracted approximates the total column capacity. This means that dilution of the sample solution which is subjected to antibody-mediated clean-up and/or lowering of the flow through the column will result in an higher recovery of CAP. However, these modifications were not introduced in the antibody-mediated clean-up described due to the increase in the analysis time. Apart from the lower recoveries at higher spiking levels, the higher standard deviation at the spiking level of 100 μg kg^{-1} can also be explained by the antibody-mediated clean-up described. If the amount of CAP which is subjected to antibody-mediated clean-up approximates the total column capacity, it is a matter of course that small changes in conditions (such as the bed volume, temperature and sample composition) cause greater differences in recovery.

By comparing the results of the capture of CAP from skimmed milk with those from PBS, it is remarkable that a more efficient capture is obtained from skimmed milk. In general, PBS is considered to give the optimum condition for antigen–antibody interaction.

TABLE II

CHLORAMPHENICOL CONTENT OF EGGS PRODUCED BY LAYING HENS TREATED WITH CHLORAMPHENICOL VIA THEIR DRINKING WATER DURING 5 SUCCESSIVE DAYS

AMC = Antibody-mediated clean-up; SPE = solid-phase extraction.

Days after starting the CAP treatment	CAP dosage = 0.05 g l^{-1}		CAP dosage = 0.5 g l^{-1}	
	AMC ($\mu g\ kg^{-1}$)	SPE ($\mu g\ kg^{-1}$)	AMC ($\mu g\ kg^{-1}$)	SPE ($\mu g\ kg^{-1}$)
1	41.8	62.0	568.1	835.6
2	48.8	58.9	775.5	884.0
3	47.5	71.3	861.2	1107.2
4	63.8	98.7	1214.8	1392.5
5	75.4	119.1	1321.9	1565.5
6	55.5	79.2	774.7	980.0
7	52.1	79.1	891.3	1021.2
8	37.3	61.4	854.4	997.2
9	27.2	57.5	1003.0	973.5
10	21.5	38.1	428.1	565.4
11	10.4	19.4	266.4	374.4
12	2.5	6.2	171.7	228.1
13	1.7	3.3	29.3	53.0
14	<1.0	<1.0	6.2	10.5
15	<1.0	<1.0	1.4	1.6
16	<1.0	<1.0	<1.0	<1.0
17	<1.0	<1.0	<1.0	<1.0

Animal study

The eggs of treated hens were analysed for CAP after antibody-mediated clean-up and solid-phase extraction using silica gel, respectively, according to the procedures described. The results shown in Table II indicate that, even after 1 day of CAP administration, considerable amounts of CAP were eliminated into eggs. CAP levels under 1 $\mu g\ kg^{-1}$ were observed 14–16 days after starting the CAP treatment. All values were obtained by one replicate determination. The mean recovery for CAP-spiked eggs obtained after solid-phase extraction was identical to those described earlier[15] for spiked swine muscle tissue, *i.e.*, 79%. The CAP contents of eggs obtained by the solid-phase extraction procedure are corrected for this recovery. In the case of antibody-mediated clean-up, each value is corrected for a recovery obtained from the logarithmic relationship between the CAP content and recovery (see Spiking studies). The results obtained by the antibody-mediated clean-up and solid-phase extraction correlate well with each other (*viz.*, Fig. 3), the coefficient of correlation being 0.9932. It is remarkable, however, that nearly all results obtained with the aid of the antibody-mediated clean-up procedure are lower than those obtained by the solid-phase extraction procedure (*viz.*, Table II). The explanation for this phenomenon may be as follows: in the solid-phase extraction procedure the eggs are sonication-aided extracted with ethyl acetate. This solvent may cause a disruption of protein-bound drugs[18,19]. Therefore a more complete extraction of CAP may be possible. In the antibody-mediated extraction, on the other hand, the samples are applied to the
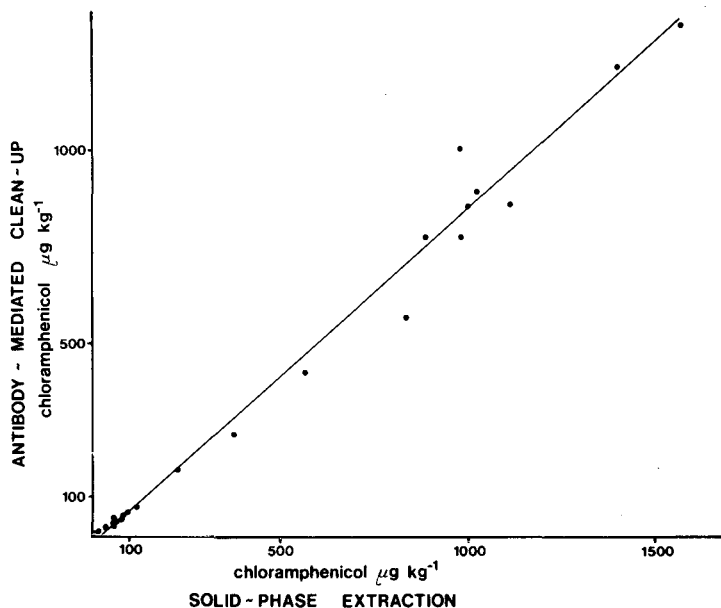
Fig. 3. Correlation between antibody-mediated cleaned and solid-phase extracted egg samples. Eggs were collected from treated hens; 0.05 and 0.5 g CAP l^{-1} drinking water during 5 successive days. The line is given by $y = 0.87x - 20.38$ ($n = 28$, correlation coefficient 0.9932).

immunoaffinity column after centrifugation and filtration. In that case no disruption of the protein-bound CAP may occur. It is probable that at least a part of the protein-bound CAP remains in the precipitate after centrifugation. Another possibility may be that protein-bound CAP cannot be bound by the immunoaffinity column. The cause of the lower results obtained with the aid of the antibody-mediated clean-up will be studied in detail.

ACKNOWLEDGEMENTS

REFERENCES

1 G. S. Campbell, R. P. Mageau, B. Schwab and R. W. Johnston, *Antimicrob. Agents Chemother.*, 25 (1984) 205.
2 D. Arnold, D. vom Berg, A. K. Boertz, U. Mallick and A. Somogyi, *Arch. Lebensmittelhyg.*, 35 (1984) 131.
3 D. Arnold and A. Somogyi, *J. Assoc. Off. Anal. Chem.*, 68 (1985) 984.
4 C. Hock and F. Liemann, *Arch. Lebensmittelhyg.*, 36 (1985) 125.

5 O. Agthe and F. Scherk, *Arch. Lebensmittelhyg.*, 37 (1986) 97.

6 M. von Beck, E. Märtlbauer and G. Terplan, *Arch. Lebensmittelhyg.*, 38 (1987) 99.

7 E. Märtlbauer and G. Terplan, *Arch. Lebensmittelhyg.*, 38 (1987) 3.

8 C. van de Water, N. Haagsma, P. J. S. van Kooten and W. van Eden, *Z. Lebensm.-Unters.-Forsch.*, 85 (1987) 202.

9 C. van de Water and N. Haagsma, *J. Chromatogr.*, 411 (1987) 415.

10 *Affinity Chromatography —Principles and Methods*, Pharmacia, Uppsala, 1983.

11 P. D. G. Dean, W. S. Johnson and F. A. Middle, *Affinity Chromatography, a Practical Approach*, IRL Press, Oxford, 1985.

12 G. S. Bethell, J. S. Ayers, M. T. W. Hearn and W. S. Hancock, *J. Chromatogr.*, 219 (1981) 361.

13 M. T. W. Hearn, E. L. Harris, G. S. Bethell, W. S. Hancock and J. A. Ayers, *J. Chromatogr.*, 218 (1981) 509.

14 M. T. W. Hearn, G. S. Bethell, J. S. Ayers and W. S. Hancock, *J. Chromatogr.*, 185 (1979) 463.

15 N. Haagsma, C. Schreuder and E. R. A. Rensen, *J. Chromatogr.*, 363 (1986) 353.

16 P. K. Smith, R. I. Krohn, G. T. Hermanson, A. K. Mallia, F. H. Gartner, M. D. Provenzano, E. K. Fujimoto, N. M. Goeke, B. J. Olson and D. C. Klenk, *Anal. Biochem.*, 150 (1985) 76.

17 N. Haagsma *et al.*, in preparation

18 M. von Petz, *Dtsch. Lebensm. Rundsch.*, 78 (1982) 396.

19 H. Büning-Pfaue and T. Schmidt, *Arch. Lebensmittelhyg.*, 36 (1985) 87.

SEPARATION OF DERIVATIZED BLACK TEA THEARUBIGINS BY HIGH-PERFORMANCE LIQUID CHROMATOGRAPHY

B. L. WEDZICHA* and T. J. DONOVAN[a]

Procter Department of Food Science, University of Leeds, Leeds LS2 9JT (U.K.)

(First received April 6th, 1989; revised manuscript received May 23rd, 1989)

SUMMARY

SI thearubigins were extracted from black tea infusions and converted into acetyl and methyl derivatives. Both derivatives gave rise to discrete components upon thin-layer chromatography on silica and were eluted in high yield from silica high-performance liquid chromatographic columns using mixtures of chloroform and methanol. Acetyl derivatives tended to undergo time-dependent changes in chromatographic behaviour, whilst methyl derivatives appeared to be stable.

INTRODUCTION

Thearubigins play an important role in the quality of black tea infusions. Together with theaflavins, they determine the strength and colour of the infusion[1], play a role in its mouthfeel[2] presumably due to their astringency[3] and are involved in the quality-related ability of the infusion to form "tea cream", a precipitate of complexes of caffeine with theaflavins and thearubigins[4–6]. Thearubigins are the most abundant phenolic fraction of black tea.

Thearubigins is the name originally assigned to all the acidic brown pigments of black tea[1]. A broad classification of these compounds is those extractable into ethyl acetate, the SI thearubigins, and those remaining in the aqueous phase, the SIa and SII thearubigins with the SIa group being more soluble in diethyl ether[7]. Other separations based on extractability have also been carried out[8–11]. Other separation attempts include the use of cellulose column chromatography[9], Toyopearl chromatography[12], ion exchange and paper electrophoresis[13], reversed-phase high-performance liquid chromatography (HPLC)[14] and gel chromatography media, *e.g.*, Pharmacia LH20[15]. However, none has proved entirely satisfactory.

One problem with the chromatographic systems involving a stationary phase is the high affinity of the thearubigins for the stationary phase; this can potentially be controlled by derivatizing the phenolic groups. The purpose of this work was to investigate the potential for normal phase HPLC of derivatized SI thearubigins.

---

[a] Present address: Lyons Tetley Limited, 325/347, Oldfield Lane, Greenford, Middlesex, UB6 0AZ, U.K.

EXPERIMENTAL

Extraction of SI thearubigins

An infusion of black tea leaf (25 g) in boiling water (1 l) was maintained at 95°C for 5 min. The infusion was filtered (glass fibre paper) and freeze dried. The tea solids (50 g) obtained from several pooled freeze-dried extracts were dissolved with stirring in hot aqueous methanol (1 l, 25% methanol). The presence of methanol was necessary to prevent the formation of tea cream and to reduce the tendency for emulsion formation on addition of chloroform. The solution was extracted exhaustively with chloroform to remove caffeine in a continuous liquid–liquid extraction apparatus. To test for the satisfactory removal of caffeine, a further extraction of the whole of the aqueous phase was carried out in a separating funnel containing chloroform (1 l), the extract was dried over anhydrous $MgSO_4$ and its absorbance measured at 276 nm in 1-cm silica cells. This procedure was repeated unil the absorbance of the extract was <0.1. Chloroform remaining in the aqueous phase was removed under reduced presure at 30°C. The solution was extracted repeatedly with an equal volume of water-saturated ethyl acetate until no more colour was extracted. The ethyl acetate extracts were pooled, dried over $MgSO_4$ and evaporated to dryness under reduced pressure at 30°C. To ensure complete removal of ethyl acetate, the solids were dissolved in acetone and evaporated to dryness as before. These solids were dissolved in the minimum volume of acetone (1 volume) and the solution added dropwise with stirring to chloroform (10 volumes) cooled in ice. The precipitate was removed by centrifugation (15 000 g, 10 min), redissolved in the minimum volume of acetone and reprecipitated in chloroform as before. The precipitate was dissolved in the minimum volume of acetone (1 volume) and precipitated three times by adding to peroxide-free diethyl ether (5, 10 and 15 volumes) with stirring in ice. To ensure complete removal of diethyl ether, the final precipitate was dissolved in acetone and evaporated to dryness under reduced pressure at 30°C to give the SI thearubigin fraction.

The product was shown to be free from low-molecular-weight impurities by thin-layer chromatography (TLC) and gas chromatography (GC). The TLC method was a variation of the paper chromatographic method of Roberts *et al.*[7] and Ratnaike[13] in which the paper was replaced with a 0.1-mm cellulose thin layer on a polymer film backing (Polygram Cel 300, 20 cm × 20 cm; Macherey-Nagel, F.R.G.) sheets. These sheets gave better resolution, shorter development time and easier handling than the papers. The components were separated by two-dimensional chromatography with butanol–acetic acid–water (4:1:2.2) in the first direction and aqueous acetic acid (2%) in the second. The components were visualized by spraying with an aqueous solution of a mixture of ferric chloride (0.3%, w/w) and potassium ferricyanide (0.3%, w/w). The plates were fixed in dilute acid (HCl) and excess of ferricyanide was removed by washing in water. The GC method was as used for the analysis of tea flavanols as their trimethylsilyl derivatives[16].

Acetylation of thearubigins

The acetylation procedure was a modification of that used by Cattell[15]. The sample (0.1 g) was dissolved in dry pyridine (1 ml), acetic anhydride (6 ml) added and the mixture warmed at 30°C for 1 h. Water (10 ml) was added with cooling and the precipitate filtered off. The product was dissolved in chloroform (5 ml) and the

solution extracted with aqueous $NaHCO_3$ (10%, w/v; 2 × 5 ml) and water (2 × 5 ml) before being evaporated to dryness.

The degree of acetylation was assessed by carrying out the reaction using half the amounts of reagents given above and adding the reaction mixture to water (20 ml) followed by pyridine (50 ml). The resulting solution was titrated with 0.5 M NaOH to pH 9.2 using a pH meter, and a blank titration was carried out on a solution omitting the thearubigin sample. In order to check the efficiency of acetylation, a sample of (−)epicatechin (Sigma) was treated similarly.

Methylation of thearubigins

The methylation of thearubigins using diazomethane has been described by Ratnaike[13]. Diazomethane was prepared as a solution in diethyl ether from N-methyl-N-nitrosotoluene-p-sulphonamide according to the method described by Vogel[17]. The thearubigin sample (20 mg) was dissolved in methanol (2 ml) in an ice-bath and excess of diazomethane solution was added. The presence of the excess of reagent was demonstrated by adding a few drops of glacial acetic acid to an aliquot of the reaction mixture, when gas was immediately evolved. The reaction mixture was immediately evaporated to dryness under reduced pressure at 30°C.

Separation of derivatized thearubigins

A preliminary choice of the solvent system for HPLC separations on silica was made by means of TLC (silica gel G $60F_{254}$, 0.25 mm, activated at 110°C for 30 min). Components were located under UV light. High-performance liquid chromatographic separations (ACS liquid chromatography system LC750 with two reciprocating pumps and a decilinear programmer; Applied Chromatography Systems, Macclesfield, U.K.) were carried out on a Partisil 10 column (HPLC Technology, Macclesfield, U.K.; particle size 10 μm, 25 cm × 0.46 cm) at 1 ml min^{-1} with the column effluent monitored spectrophotometrically (1-cm path length cell, ACS 750-11 monitor at 254 nm or Cecil CE212A spectrophotometer at 330 nm). The recovery of samples from the column was measured by comparing the UV spectrum of the sample applied to the column with that of the eluted mixture, at the same dilutions.

RESULTS AND DISCUSSION

When subjeced to two-dimensional TLC analysis on cellulose the thearubigin preparation was found as a streak (R_F 0.3–0.9) in butanol–acetic acid–water as the solvent, and no evidence of components showing mobility in both solvents was seen at any level of application of the sample. This is consistent with the chromatographic behaviour of SI thearubigins[18]. Similarly, no evidence of the presence of monomeric tea polyphenols was seen from GC analysis of trimethylsilyl derivatives of the thearubigin sample.

The acetyl derivative of the thearubigin preparation formed readily and it was found that 20 ± 2% (mean of three determinations ± standard deviation) of the mass of the original thearubigin was due to OH groups which became acetylated. Acetylation of (−)-epicatechin indicated that 28.3 ± 2.3% of its mass was due to OH groups, compared with the expected value of 29.3% corresponding to five OH groups in the molecule. Whilst it is not possible to use this result to predict the degree of

acetylation per monomer in thearubigins, it shows that a substantial number of OH groups had been derivatized; there would have been approximately three acetyl groups per monomer unit if the thearubigin consisted of catechin repeating units.

A characteristic of thearubigins is their lack of mobility when examined by TLC on silica and no resolution of components on cellulose. The behaviour of thearubigins, acetylated thearubigins and acetylated instant green tea (mixture of flavanols) on silica is shown in Table I for a wide range of solvents. In all cases, derivatization has allowed chromatograms to be obtained, with particularly high mobility in ethyl acetate–methyl ethyl ketone–formic acid–water (5:3:1:1) and chloroform–methanol (3:2). Also, the appearance of the chromatograms was different from those of the low-molecular-weight components of green tea, indicating that the spots observed were not due to the low-molecular-weight precursors of thearubigins present in green tea, which can be released by hydrolysis of thearubigins during the acetylation procedure. Of the two solvents capable of moving all the sample away from the origin, that which did not

TABLE I

TLC ANALYSIS OF ACETYLATED GREEN TEA (ACETYLATED MIXTURE OF GREEN TEA FLAVA-NOLS), SI THEARUBIGINS AND ACETYLATED SI THEARUBIGINS ON SILICA ($60F_{254}$) USING A VARIETY OF SOLVENTS

All components identified under UV ligh. Mobility shown as R_F value; those values underlined refer to coloured (yellow/brown) spots.

Solvent	R_F		
	Acetylated green tea	Thearubigins	Acetylated thearubigins
Benzene–ethyl formate–formic acid (72:24:1)	0, 0.050, 0.09, 0.14, 0.18	0 + short dark streak	0, 0.10, 0.92 + short dark streak
Toluene–ethyl formate–formic acid (50:40:10)	0.43, 0.46, 0.52, 0.54	0 + short dark streak	0, 0.35, 0.41 + short dark streak
Methyl ethyl ketone	0.73, 0.81 + pale streak	0 + long dark streak	0, 0.47, 0.49, 0.91, + long pale streak
Benzene–ethanol (75:25)	0.26, 0.67, 0.77, 0.81, 0.88	0 + short dark streak	0, 0.63, 0.64, 0.71 + long pale streak
Cyclohexane–acetone (20:25)	0, 0.34, 0.50, 0.53, 0.56, 0.58, 0.61 + pale streak	0 + short dark streak	0, 0.53, 0.58, 0.92 + long pale streak
Cyclohexane–chloroform–pyridine (10:30:25)	0.80, 0.85, 0.88 + pale streak	0	0, 0.69 + long pale streak
Cyclohexane–chloroform–acetic acid (20:25:5)	0, 0.04, 0.07, 0.12, 0.15, 0.17, 0.24	0	0, 0.12, 0.25 + short dark streak
Chloroform–ethyl acetate–formic acid (25:20:5)	0.57, 0.61, 0.66, 0.69, 0.73	0	0, 0.60, 0.75, 0.98 + long dark streak
Ethyl acetate–methyl ethyl ketone–formic acid–water (50:30:10:10)	0.99	0 + long dark streak	0.97
Benzene–ethyl acetate (75:25)	0, 0.16, 0.24, 0.33, + pale streak		0, 0.05, 0.08, 0.21, 0.97
Chloroform–methanol (30:20)	0.99	0 + short dark streak	0.96 + pale streak
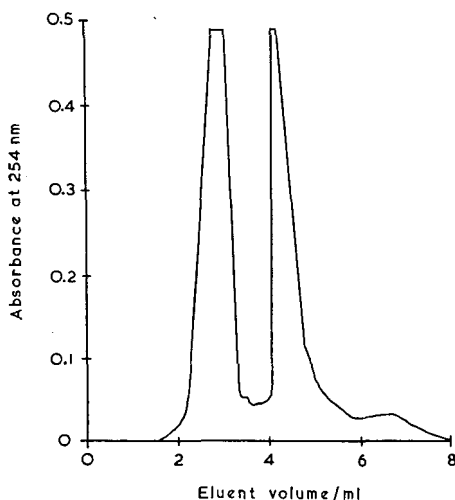
Fig. 1. Separation of acetylated SI thearubigins by HPLC on Partisil 10 (25 cm × 0.46 cm) with chloroform–methanol (4:6) at 1 ml min^{-1}.

contain acid was preferred because the risk of possible modification of thearubigin was avoided and HPLC analysis was, therefore, attempted using chloroform–methanol mixtures. The best separation shown in Fig. 1 was achieved using chloroform–methanol (4:6, v/v). When the UV spectrum (250–700 nm) of the sample for analysis was compared with that of the pooled fractions eluted from the column, the absorbances at any wavelength were within ±5% (from three sets of experiments) and

TABLE II

TLC ANALYSIS OF METHYLATED SI THEARUBIGINS ON SILICA (60F$_{254}$)

All components identified under UV light. Mobility shown as R_F value; those values underlined refer to coloured (yellow/brown) spots.

Solvent	R_F
Ethyl acetate	0 + long dark streak
Ethyl acetate–methyl ethyl ketone (25:15)	0, 0.03, 0.05, 0.15 + long dark streak
Ethyl acetate–methyl ethyl ketone–formic acid–water (25:15:5:5)	0.12, 0.20, 0.28, 0.37, 0.45, 0.49, 0.54, 0.60, 0.64, 0.95
Ethyl acetate–methyl ethyl ketone–water (25:15:5)	0, 0.03, 0.05, 0.09, 0.12, 0.15, 0.18, 0.34, 0.94 + long dark streak and early spots overlapped
Ethyl acetate–methyl ethyl ketone–formic acid (25:15:5)	0, 0.04, 0.06, 0.09, 0.13, 0.94 + long pale streak and early spots overlapped
Ethyl acetate–methyl ethyl ketone–methanol (25:15:5)	0, 0.04, 0.12, 0.19, 0.29, 0.39, 0.95 + long dark streak
Ethyl acetate–methyl ethyl ketone–methanol (25:15:10)	0, 0.17, 0.25, 0.39, 0.46, 0.56, 0.66, 0.73, 0.94 + long dark streak and early spots overlapped
Ethyl acetate–methyl ethyl ketone–methanol (25:15:10)	0, 0.11, 0.40, 0.52, 0.60, 0.66, 0.75, 0.96 + long dark streak and early spots overlapped
Chloroform	0, 0.94
Methanol	0, 0.57, 0.62, 0.66, 0.79 + long pale streak

it is concluded that the chromatogram represents an high proportion of the thearubigin applied. A feature of the acetyl derivatives was their apparent instablity. When left to stand over a period of hours, samples of acetylated thearubigin showed a progressive increase in colour remaining at the point of application in TLC experiments when analysed using any of the solvents given in Table I. Similarly, the slowest migrating peak in the chromatogram in Fig. 1 becomes more prominent with ageing of the sample and it is likely that acetylation does not afford complete protection of the sample.

The analysis of methylated thearubigins by TLC is summarized in Table II. As was the case for acetylation, methylation allows components of thearubigins to be resolved and, in general, it was possible to separate the mixture into a greater number of spots than was the case for acetylated samples. The best separation by HPLC was obtained using a chloroform–methanol gradient as follows: initially chloroform–methanol (9:1) was used for 5 min followed by an increasing concentration of methanol at 1% min^{-1} for 10 min, 2% min^{-1} for 5 min, 5% min^{-1} for 5 min and finally 10% min^{-1} until the solvent was pure methanol. A typical chromatogram for methylated thearubigins from a sample of Lipton's yellow label tea bags is illustrated in Fig. 2 where up to fourteen components may be discerned. Thearubigins from an instant tea of SriLankan origin showed a similar chromatogram but the peaks appeared to be of different sizes. Table III shows a comparison of the positions and intensities of the peaks measured from two separate experiments for each of the methylated thearubigins from the two teas, with the errors shown as standard deviations. When the UV spectrum of the methylated sample for analysis was
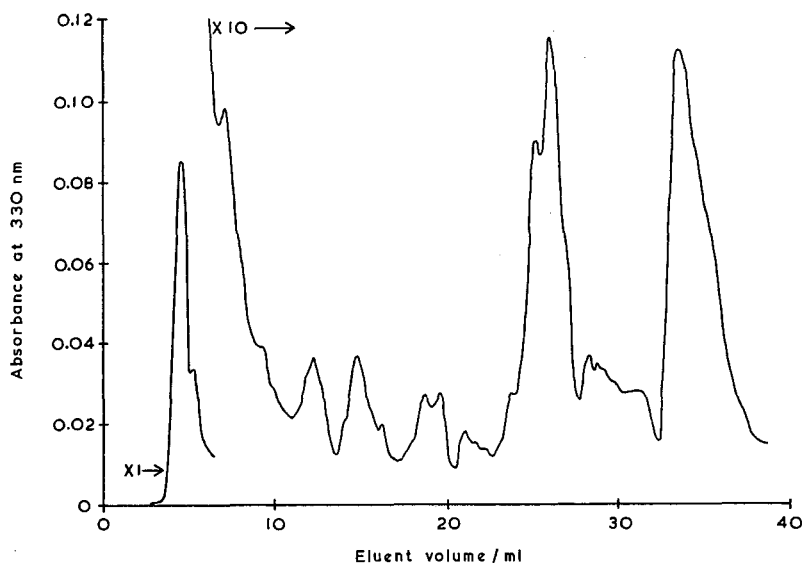
Fig. 2. Separation of methylated SI thearubigins by HPLC on Partisil 10 (25 cm × 0.46 cm) at 1 ml min^{-1} using the following gradient system: chloroform–methanol (9:1) for 5 min followed by gradient elution increasing the concentration of methanol at 1% min^{-1} for 10 min, 2% min^{-1} for 5 min, 5% min^{-1} for 5 min and finally at 10% min^{-1} until the solvent was pure methanol.

TABLE III

COMPARISON OF RETENTION VOLUMES AND PEAK HEIGHTS OF COMPONENTS PRESENT IN METHYLATED SI THEARUBIGINS FROM TWO BLACK TEAS

Teas: 1 = Liptons yellow label tea bags; 2 = SriLankan instant tea. All analyses were carried out on a Partisil 10 column (25 cm × 0.46 cm) at 1 ml min^{-1} using the following gradient system: chloroform–methanol (9:1) for 5 min followed by gradient elution increasing the concentration of methanol at 1% min^{-1} for 10 min, 2% min^{-1} for 5 min, 5% min^{-1} for 5 min and finally at 10% min^{-1} until the solvent was pure methanol.

Tea 1		Tea 2	
Elution volume (ml)	Absorbance at 330 nm	Elution volume (ml)	Absorbance at 330 nm
4.9 ± 0.5	0.084 ± 0.003	4.6 ± 0.2	0.046 ± 0.004
5.4 ± 0.3	0.034 ± 0.004	6.2 ± 0.2	0.024 ± 0.002
7.3 ± 0.1	0.013 ± 0.001	7.1 ± 0.1	0.022 ± 0.002
9.7 ± 0.2	0.007 ± 0.001	9.6 ± 0.4	0.014 ± 0.002
11.9 ± 0.3	0.007 ± 0.001	10.8 ± 0.5	0.011 ± 0.001
14.3 ± 0.3	0.007 ± 0.001	14.0 ± 0.3	0.010 ± 0.001
		15.3 ± 0.3	0.007 ± 0.003
17.5 ± 0.1	0.006 ± 0.001	17.7 ± 0.1	0.008 ± 0.001
18.4	0.011	18.8 ± 0.2	0.011 ± 0.001
19.7	0.007	20.0 ± 0.1	0.014 ± 0.002
		21.7 ± 0.4	0.013 ± 0.001
23.7 ± 0.1	0.010 ± 0.003		
25.0 ± 0.1	0.009 ± 0.003	24.4 ± 0.5	0.011 ± 0.001
26.0	0.015	26.8	0.012
27.8 ± 0.1	0.010 ± 0.004		
		29.7	0.020
		30.7 ± 0.3	0.016 ± 0.002
32.7 ± 0.4	0.010 ± 0.002	32.2	0.013

compared with that of the pooled fractions eluted from the column, the absorbances at any wavelength were within ±10% (from three sets of measurements) and the chromatograms observed therefore represent a large proportion of the thearubigin. It was noticed, however, that a small amount of sample was retained irreversibly, reducing the life of columns and therefore necessitating the use of the minimum amount of derivatized thearubigin sample. This led generally to the need for high sensitivity in detection. It is now appropriate to consider these separations as a means of identification of different tea varieties or blends.

In general, HPLC of methylated thearubigins with a methanol–chloroform solvent gradient was able to achieve better separation than TLC with any of the solvents tried. When chloroform or methanol was used as TLC solvents some of the sample always remained at the origin. If mobility in TLC is indicative of mobility under HPLC conditions, then the components at the origin probably represent less than 10% of the absorbance of the sample at 330 nm.

CONCLUSION

Thearubigins are regarded as polymeric polyphenols and a reason for their high affinity towards silica which prevents its use for their analysis is likely to include polar interactions with OH groups on the polymer. This is supported by the observations made here that acetylation or methylation of these groups causes thearubigins to become mobile on silica in a variety of solvents. We report here the first partial separation of thearubigins as their derivatives by HPLC which should now form the basis of a renewed attempt to characterize these polymers.

REFERENCES

1 E. A. H. Roberts, *J. Sci. Food Agric.*, 9 (1958) 381.
2 D. J. Millin, D. J. Crispin and D. Swaine, *J. Agric. Food Chem.*, 17 (1969) 717.
3 G. W. Sanderson, A. S. Ranadive, L. S. Eisenberg, F. J. Farrell, R. Simms, C.H. Manley and P. Coggon, *ACS Symp. Ser.*, 26 (1976) 14.
4 E. A. H. Roberts, *J. Sci. Food Agric.*, 14 (1963) 700.
5 R. F. Smith, *J. Sci. Food Agric.*, 19 (1968) 530.
6 R. L. Wickremasinghe and K. P. Perera, *Tea Q.*, 37 (1966) 131.
7 E. A. H. Roberts, R. A. Cartwright and M. Oldschool, *J. Sci. Food Agric.*, 8 (1957) 72.
8 E. A. H. Roberts, D. W. Rustige and C. Randell, *Ann. Rep. Toklai Station*, (1960) 341.
9 L. Vuataz and H. Brandenberger, *J. Chromatogr.*, 5 (1961) 17.
10 A. G. Brown, W. B. Eyton, A. Holmes and W. D. Ollis, *Phytochemistry*, 8 (1969) 2333.
11 A. G. Brown, W. B. Eyton, A. Holmes and W. D. Ollis, *Nature (London)*, 221 (1969) 742.
12 J. Ozawa, *Agric. Biol. Chem.*, 46 (1982) 1079.
13 S. I. Ratnaike, *Ph. D. Thesis*, University of Leeds, 1980.
14 A. Robertson and D. S. Bendall, *Phytochemistry*, 22 (1983) 883.
15 D. J. Cattell, *Ph. D. Thesis*, University of Leeds, 1972.
16 P. D. Collier and R. Mallows, *J. Chromatogr.*, 57 (1971) 29.
17 A. I. Vogel, *Practical Organic Chemistry*, Longmans, London, 3rd ed., 1957, p. 967.
18 E. A. H. Roberts and R. F. Smith, *J. Sci. Food Agric.*, 14 (1963) 689.

Note

Model compound sorption by the resins XAD-2, XAD-8 and diethyl-aminoethylcellulose

An useful application to flavonoids isolation

LUIGINO MAGGI, RENATO STELLA and MARIA T. GANZERLI VALENTINI

Dipartimento di Chimica Generale e Centro di Radiochimica e Analisi per Attivazione del CNR, Università di Pavia, Viale Taramelli 12, 27100 Pavia (Italy)

and

PIERGIORGIO PIETTA*

Dipartimento di Scienze e Tecnologie Biomediche, Sezione di Chimica Organica, Università di Milano, Via Celoria 2, 20133 Milan (Italy)

(Received March 15th, 1989)

High recoveries of aromatic acids and phenols from water are possible by adsorption on macroreticular resins such as XAD and diethylaminoethyl (DEAE) cellulose[1]. However, due to the lack of data on the distribution coefficients, K_D, as a function of pH, a more systematic study is desirable.

The sorption of model compounds, phenol (P), cinnamic acid (C), benzoic acid (B), 3,5-dihydroxybenzoic acid (DH), 3,5-dimethoxy-4-hydroxybenzoic acid (DM), coumarin (CM), rutin (RU), isoorientine (IO) and isovitexine (IV) on XAD-2, XAD-8 and DEAE-cellulose was then investigated. Among these compounds, rutin, isoorientine and isovitexine belong to the group of flavonoids, which are found ubiquitously in plants and have many pharmacological properties[2]. Standards are not available for many of the flavonoids and the traditional methods for their isolation are based on thin-layer or column chromatography using different supports (silica, cellulose, polyamide, Sephadex LH-20) and aqueous organic solvents[3,4].

In recent years, semipreparative high-performance liquid chromatography (HPLC) has been applied for the purification of flavonoids, mainly using reversed-phase columns[5]. Nevertheless, the isolation of flavonoids from crude plant extracts through simple column chromatography has potential as confirmed by the results described in this paper.

EXPERIMENTAL

Materials

Coumarin and rutin were obtained from C. Roth (Karlsruhe, F.R.G.). All other test compounds were from Carlo Erba (Milan, Italy). Isoorientine and isovitexine were isolated from *Passiflora incarnata* L. extracts according to the literature[6]. These extracts were obtained from different commercial sources. All chemicals used were of reagent grade.

Resins

XAD-2 and XAD-8 macroreticular resins (Rohm & Haas, Philadelphia, PA, U.S.A.) were thoroughly purified by sequential solvent extraction with methanol, acetonitrile and diethyl ether in a Soxhlet extractor for 8 h per solvent. The purified resins were stored under methanol in glass stoppered bottles to maintain their purity.

DEAE-cellulose (Bio-Rad, Richmond, CA, U.S.A.) was pretreated by the following procedure: about 50 g of dry cellulose were mixed in 10 ml of 0.5 M HCl for 1 h. The cellulose was rinsed with deionized water in a Büchner funnel until the pH was neutral; it was then suspended in 0.5 M NaOH for 1 h and rinsed with deionized water until the pH was neutral. Pretreated DEAE-cellulose was stored in the dark at 4°C.

Instrumentation

A Perkin-Elmer scanning spectrophotometer Model 550 SE was used for standard and eluate analysis.

HPLC was performed with a Waters M-501 pump fitted with a μBondapak C_{18} column (25 cm × 4.6 mm I.D.). Peaks were monitored with a Waters M-481 absorbance detector at 340 nm: output was measured with a Shimadzu Model CR3A integrator, using the external standard quantitation method. The eluent was 2-propanol–tetrahydrofuran–water (5:15:80, v/v/v) at a flow-rate of 0.7 ml/min.

Batch experiments

Batch distribution coefficients, K_D

$$K_D = \frac{\text{mg material adsorbed per g of resin}}{\text{mg material in solution per ml solution}}$$

were obtained by shaking overnight in stoppered flasks approximately 100 mg of resin with 25 ml of sample at a fixed pH, adjusted to a value between 2 and 9 by adding 0.1 M HCl or 0.1 M NaOH. After equilibration for 24 h at 25°C, suitable aliquots were taken from the unknown and standard flasks and the concentration of the solute in each was determined spectrophotometrically.
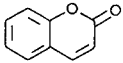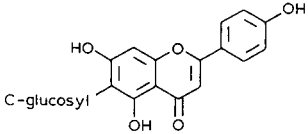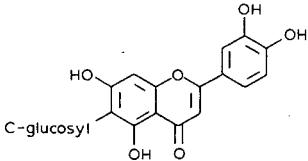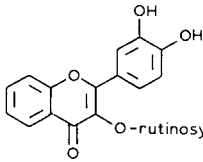
Column experiments

For the experiments on artificial samples glass columns (10 mm I.D.) were packed by using a water–XAD-2, water–XAD-8 or water–DEAE-cellulose slurry rinsed with 500 ml of distilled water to remove methanol. The DEAE-cellulose bed was 50 mm, those of the XADs was 220 mm and the reservoir volume was 250 ml. The flow-rate was maintained and controlled by a peristaltic pump and was set to 1 ml/min for DEAE-cellulose and 5 ml/min for XADs. The eluting agent was passed through the column and the effluent was collected by a fraction collector and monitored with the Perkin-Elmer spectrophotometer.

The isolation of isovitexine and isoorientine from the *Passiflora incarnata* extract was performed by loading 2 g of the extract on a DEAE-cellulose column (bed height 270 mm, 16 mm I.D.) and eluting with 0.01 M HCl at a flow-rate of 1.2 ml/min.

Final purification was effected by passing the eluates through a column of XAD-2, same size as that of the DEAE-cellulose, and desorbing the flavonoids with methanol.

TABLE I

COMPOUNDS EXAMINED

Compound	Abbreviation	Compound	Abbreviation	Formula
Phenol	P	Coumarin	CM	
Benzoic acid	B			
		Isovitexine	IV	
Cinnamic acid (*trans*)	C			
3,5-Dihydroxybenzoic acid	DH	Isoorientine	IO	
3,5-Dimethoxy-4-hy-droxybenzoic acid	DM			
		Rutin	RU	
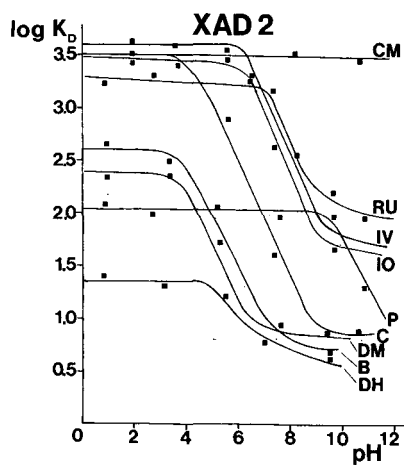
Fig. 1. Effect of pH on K_D for the uptake by XAD-2. Symbols as in Table I.
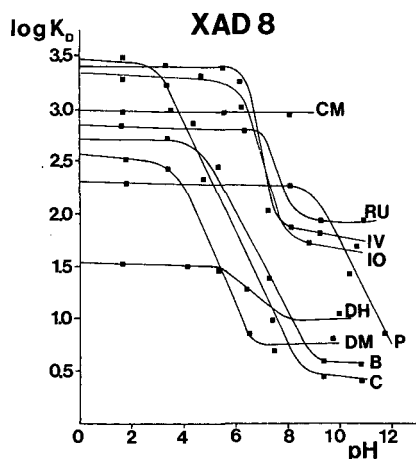
Fig. 2. Effect of pH on K_D for the uptake by XAD-8.

Solutions

Test solutions of aromatic acids and phenol (30–100 mg/l) in water were prepared. Samples of 200 μl of *Passiflora incarnata* L. aqueous extract (total flavones approximately 1%) were used without any previous treatment.

RESULTS AND DISCUSSION

The adsorptive forces involved when using XAD-2 and XAD-8 resins are mainly van der Waal interactions[7]. However, since the compounds examined (Table I) contain phenolic or/and carboxylic groups, their sorption on XAD-2 and XAD-8 is influenced by the pH as shown in Figs. 1 and 2. The K_D values of phenol, benzoic acid and cinnamic acid decrease sharply in a pH range which is close to the pK_a of each compound. On the other hand, 3,5-dimethoxy-4-hydroxybenzoic and 3,5-dihydroxy-
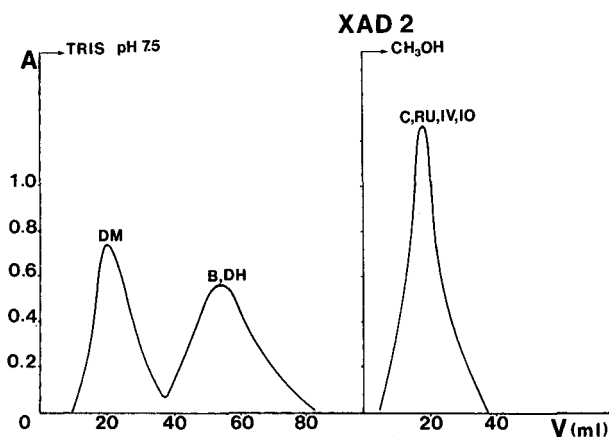
Fig. 3. Desorption from XAD-2.

TABLE II

SORPTION OF SELECTED AROMATIC ACIDS AND FLAVONOIDS ON DEAE-CELLULOSE RESIN (BATCH EXPERIMENTS)

H_nA	pH_a	K_D	
		$H_nA–NaOH$ pH 7.5	10^{-2} M Tris–HCl pH 7.5
Phenol	9.89	—	—
Benzoic acid	4.19	800	80
Cinnaic acid (trans)	4.44	1480	420
3,5-Dihydroxybenzoic acid	4.04	5050	580
3,5-Dimethoxy-4-hydroxybenzoic acid	—	4200	500
Coumarin	—	100	8
Isovitexine	—	57 000	15 600
Isoorientine	—	81 000	24 100
Rutin	—	11 800	2800

benzoic acid exhibit a slope change at higher pH values, while the behaviour of the neutral coumarin is represented by a "flat" curve. As shown in Fig. 3, only three compounds are removed from XAD-2 resin using a pH 7.5 buffer and the others can be eluted as a single large fraction with methanol. This means that an effective separation is not possible and the purification of the flavonoids rutin, isoorientin and isovitexin cannot be attained by means of XAD resins. Unlike the XAD resins, the mechanism of retention by DEAE-cellulose is based on charge rather than on hydrophobic interactions. To measure k_D values the intermediate pH of 7.5 was chosen, so that most of the model compound were in their anionic forms. The data in Table II indicate that the molecular complexity plays an important role in determining the extent of sorption as confirmed by the uptakes of rutin, isoorientin and isovitexin. An efficient separation of these flavonoids from the other aromatic compounds was then achieved (Fig. 4). As
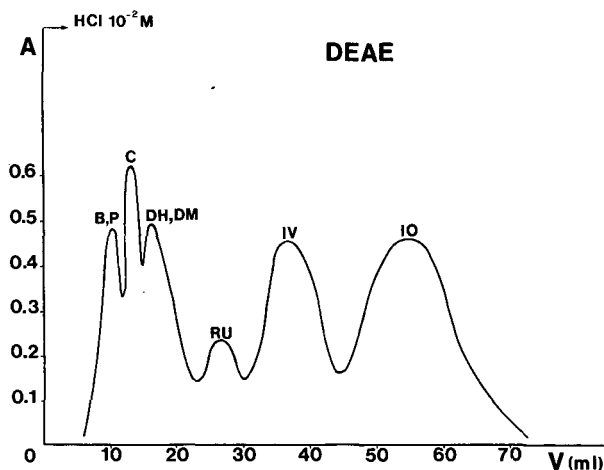
Fig. 4. Desorption from DEAE-cellulose.
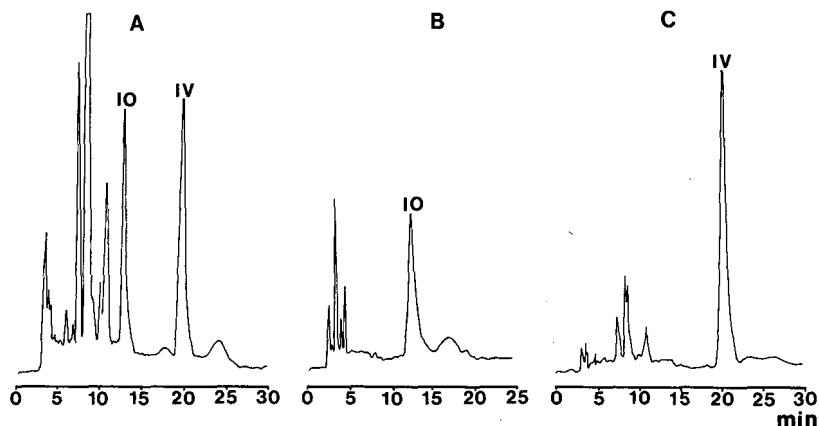
Fig. 5. HPLC analysis before and after the isolation of isoorientin and isovitexin from *Passiflora incarnata* L. extracts. (A) *Passiflora incarnata* L. extract; (B) and (C) components eluted from DEAE-cellulose with 0.01 *M* HCl.

far as the ionic strength is concerned, a small increase produces a sharp decrease in K_D values, as shown in Table II.

In conclusion, the sorption of aromatic acids and phenols on XAD resins is favoured by pH values in the range of the pK_a of the adsorbed compound, but desorption is aspecific. On the other hand the interactions between the same compounds and DEAE-cellulose at pH 7.5 are so enhanced by the molecular complexity that a selective elution from the resin can be performed using 0.01 *M* HCl. By this approach, isooriention and isovitexin have been isolated from the other carboxylic and phenolic components in a 2-g *Passiflora incarnata* L. extract (Fig. 5). The amounts recovered, after removal of HCl by adsorption chromatography on XAD-2, were 37 and 25 mg of isovitexine and isoorientine, respectively. The extension of this approach to other plant extracts is under investigation.

REFERENCES

1 E. M. Thurman, R. L. Malcolm and G. R. Aiken, *Anal. Chem.,* 50 (1978) 775.
2 V. Cody, E. Middleton, Jr. and J. B. Harborne (Editors), *Plant Flavonoids in Biology and Medicine. Biochemical, Pharmacological and Structure–Activity Relationship*, Alan R. Liss, New York, 1986.
3 K. R. Markham, *Techniques of Flavonoid Identification*, Academic Press, London, 1982.
4 E. Stahl and W. Schild, *Pharmazeutische Biologie, 4. Drogenanalyse II: Inhaltsstoffe und Isolierung*, Gustav Fischer Verlag, Stuttgart, 1981.
5 V. Cheynier and J. Rigaud, *Am. J. Enol. Vitic.*, 37 (1986) 248.
6 H. Geiger and K. R. Markham, *Z. Naturforsch., Teil C*, 41 (1986) 949.
7 M. D. Grieser and D. J. Pietrzyk, *Anal. Chem.*, 45 (1973) 1348.

Note

Chromatographic behaviour and determination of orellanine, a toxin from the mushroom *Cortinarius orellanus*

DANIELLE CANTIN*

Laboratoire de Chimie Analytique, U.F.R. de Pharmacie, Université J. Fourier de Grenoble, Domaine de La Merci, 38 700 La Tronche (France)

JEAN-MICHEL RICHARD

Laboratoire de Toxicologie et Ecotoxicologie, U.F.R. de Pharmacie, Université J. Fourier de Grenoble, B.P. 138, 38 243 Meylan Cedex (France)

and

JOSETTE ALARY

Laboratoire de Chimie Analytique, U.F.R. de Pharmacie, Université J. Fourier de Grenoble, Domaine de La Merci, 38 700 La Tronche (France)

(First received April 4th, 1989; revised manuscript received May 18th, 1989)

Several species of *Cortinarius* mushrooms have been reported to be highly toxic for animals and man[1]. We have shown that orellanine is the true principal toxin of *C. orellanus* and that it causes the same kind of nephrotoxicity as does the whole mushroom[2–4]. This compound was shown[5] to be an hydroxylated and amine oxidized bipyridine which has also been obtained by synthesis[6]. The purity of our samples of orellanine enabled us to confirm its structure by X-ray crystallography as (2,2'-bi-pyridine)-3,3',4,4'-tetrol-1,1'-dioxide (see Fig. 1)[7]. The detection, separation and quantitation of orellanine are of great importance with regard to its toxicity. Thin-layer chromatographic methods have been previously reported for quantitation[8,9]. We think that they are not suitable for this purpose. More recently, Holmdahl *et al.*[10] succinctly suggested the use of a reversed-phase ion-pair high-performance liquid chromatograhic (HPLC) system at pH 4.5 with electrochemical detection. Taking into account our knowledge about the physico-chemical behaviour of orellanine, we were not convinced by such a procedure. The chromatographic behaviour of this bipyridine structure bearing six acido-basic functions is extremely complicated. A detailed study of this behaviour appeared necessary. This paper describes the optimization of two rapid and very sensitive HPLC methods for the separation and determination of orellanine, on the basis of its acido-basic properties. The procedure was applied to the quantitation of the toxin in the mushroom, using an UV detector.

EXPERIMENTAL

Apparatus

The liquid chromatograph used was a Shimadzu (Kyoto, Japan) Model LC-6A,
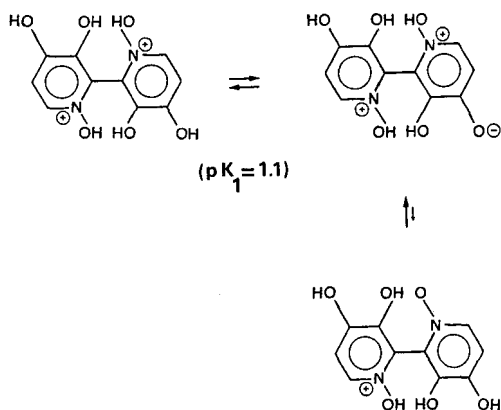
Fig. 1. Ionic forms of orellanine in equilibrium in aqueous solutions below pH 3.

equipped with an UV spectrophotometric detector SPD-6A and a Rheodyne (Cotati, CA, U.S.A.) Model 7 010 injection valve with a 20-μl loop. Retention times and peak areas were measured by a CR-3A Chromatopac (Shimadzu).

Chemicals and reagents

All reagents, solvents and acids used were of analytical reagent grade (SDS, Peypin and Prolabo, Paris, France). Water was deionized and twice distilled in a quartz glass still. Ion-pairing agents (1-hexane- and 1-octanesulphonic acids) were of HPLC reagent grade (Kodak, Rochester, NY, U.S.A.).

Extraction of orellanine

The toxin was extracted from dry powdered carpophores of *C. orellanus* collected locally. Extraction was carried out either at room temperature (method 1) or with a Soxhlet apparatus (method 2). In method 1, fatty material and apolar pigments were removed by successive extractiosns with hexane, chloroform and acetone. Orellanine was extracted with methanol. In method 2, orellanine was extracted according to ref. 11, but that methanolic extraction was carried out with a Soxhlet apparatus for 2 h and repeated ten times.

Purification of orellanine

The toxin was precipitated after standing 48 h at 4°C from an aqueous solution of the dried extract (0.1 g/ml, adjusted pH to 4.5–5). Crude crystals were collected by centrifugation at 2000 g for 10 min). After removal of a colloidal layer by aspiration, the crystals were rinsed twice with cooled water. Then, orellanine was suspended in water (0.1 g/ml) and the pH adjusted to 8.5–9 with concentrated ammonia. After centrifugation at 3500 g for 10 min to remove insoluble material, the pH was adjusted to 4.5–5 with 3.5 *M* acetic acid. The solution was left to crystallize at 4°C for 48 h. Orellanine was collected by centrifugation. The above recrystallization process was repeated twice. The colourless crystals obtained were rinsed successively with cooled ethanol and cooled diethyl ether and were collected by centrifugation at 3500 g for 5 min.

Sample handling

Standard solutions of orellanine. These were prepared by dissolving a known weight in phosphoric acid pH 0, to give a concentration of about $5 \cdot 10^{-4}$ M (126 mg/l) checked by UV spectrophotometry after 1/10 dilution ($\varepsilon = 10\ 900\ 1\ mol^{-1}\ cm^{-1}$ at 262 nm and 9100 1 $mol^{-1}\ cm^{-1}$ at 288 nm at pH 1). Stock solutions of this photosensitive and easily oxidable product were stored in the dark at 4°C and used in the following 2 days. They were diluted in a suitable mobile phase, to give a concentration range of 10^{-6}–10^{-4} M.

Solutions of mushroom extracts. Dried methanolic extracts (0.5–1.5 mg/ml) were dissolved in phosphoric acid pH 0. Direct assay solutions were made by 1/10 dilution in a suitable mobile phase (pH 1). For the standard addition method, they were added with an equal volume of a solution of orellanine ($5 \cdot 10^{-5}$–$10 \cdot 10^{-5}$ M), in a suitable mobile phase at pH 1.

For all assays, 20 μl were injected into the chromatograph.

Chromatographic conditions

Thin-layer chromatography. TLC and HPTLC plates were obtained from Merck (Darmstadt, F.R.G.). Orellanine is easily detected by its absorption at 254 nm or by the blue fluorescence of its spot after 2 min UV irradiation at 366 nm.

High-performance liquid chromatography. Two chromatographic systems were used. The first stationary phase was Rosil CN 5 μm prepacked in a 150 mm × 4.6 mm stainless-steel cartridge from Alltech (Paris, France). The mobile phase consisted of phosphoric acid adjusted to pH 1.0 ± 0.1. Elution was at a flow-rate of 0.5 ml/min. Chromatographic peaks were monitored at 260 or 290 nm, the wavelengths of the UV maxima for orellanine at pH 1.0. The second stationary phase was μBondapak C_{18} 5 μm (150 mm × 3.9 mm) from Waters (Northwich, U.K.). The mobile phase was phosphoric acid adjusted to pH 1.0 ± 0.1–acetonitrile (94:6, v/v) and 1-octane-sulphonic acid $2.5 \cdot 10^{-3}$ M. It was pumped at a flow-rate of 0.8 ml/min unless stated otherwise. The ion pair was detected at 290 nm.

The solutions were filtered through a 0.5-μm Millipore filter and degassed. All analyses were carried out isocratically at room temperature.

RESULTS AND DISCUSSION

Considerable attention has to be paid to sample preparation. Orellanine has poor solvent solubility and stability. It is better to dissolve the toxin in water. Insoluble between pH 1 and 8.4, it is largely soluble at pH values above 8.4 and below 1. Nevertheless, we noted the low stability of orellanine at alkaline pH. To overcome these solubility and stability problems, we propose a number of precautions. Orellanine should be dissolved at pH 0 and diluted at pH 1. Occasionally, additional spots or peaks were noticed when orellanine solutions were exposed to daylight. To avoid any photolytic decomposition, we recommended that the chromatography be carried out in a fume cupboard.

The choice of a thin chromatographic layer was very difficult. Prast et al.[8] recommended a silica gel layer with a mixed polar solvent added with organic acid. We have found that orellanine does not undergo any migration on such a layer. We have investigated many other layers (silica, aluminium oxide, cellulose, silica bonded with

diol, amino, cyano, methylsilane and octylsilane functionalities) and eluents. Most systems tested do not give successful separations. On the generally used polar layers, orellanine does not migrate at all, due to its very high polarity. On the non-polar ones, the toxin migrates with the solvent front or gives a diffuse streak. A cellulose layer allows a separation. Methanolic eluents give hardly reproducible results with diffuse spots. Furthermore, orellanine is of low stability in methanol. Butanolic eluents, added with acetic acid, give successful separations with the water–butanol ratio ranging from 1:3 to saturation. The R_F values obtained with butanol–acetic acid–water (3:1:1 to 4:1:5) eluents are between 0.7 and 0.3 respectively. To transpose the chromatographic system to HPLC, we have tried Si-CN HPTLC plates, the polarity of which is known to be medium. Non-polar solvents give no migration at all while highly polar ones give no compact spots but large diffuse streaks starting from the application point. To obtain suitable spots, the pH has to be lowered to 1–2. Addition of acetonitrile or dioxane reduces the R_F value, for instance, $R_F = 0.5$ with dioxane–phosphoric acid pH 2 (1:1). Decreasing the pH value increases the R_F value.

The pH was shown to be the key to resolving the chromatographic determination. A study of the ionic species of orellanine and the corresponding different pK values was undertaken using electrochemical[12] and spectrometric methods[13]. The first pK value of orellanine is 1.1. At this pH value, contrary to what is observed at pH > 3, only a few ionic forms of the toxin are present in solution (Fig. 1). At lower pH values the fully protonated form is predominant. This bicationic species is hydrophilic though it is not so polar as the other ones present at higher pH. Thus the lowest pH value usable is required to chromatograph that molecule.

For the determination of orellanine, we propose two reversed-phase HPLC systems using columns with different polarities (Si-CN and Si-C$_{18}$). These bonded phases are known to be stripped by strong acids (pH below 2). Nevertheless, they are usable up to pH 1 if they are rinsed every night with twice distilled water. With these precautions, we used these columns for more than 6 months without any change in the number of theoretical plates. The precision of the HPLC methods employing an UV detector was investigated by calculating the coefficient of variation of the peak area following ten injections of a known quantity onto the column. The chromatographic characteristics are given in Table I.

First system with Si-CN bonded phase

This system allows a rapid, acute, sensitive and economical quantitation of the toxin. With this medium-polar phase, the recommended eluent is phosphoric acid at pH 1. Under these severe conditions, orellanine is swiftly eluted as a very sharp, symmetrical and reproducible peak (retention time, $t_R = 4.4$ min). Addition of a medium-polar solvent (dioxane) from 5 to 50% only slightly reduces the retention time with this reversed-phase system (from 4 to 3.5 min). Increasing the pH results in a lengthening of the retention time ($t_R = 10$ min at pH 2) with a consequent effect on the peak width. The asymmetry of the trailing peaks obtained probably indicates the presence of several ionic forms of orellanine. At pH 1, the peak areas are highly stable during a day and reproducible from day to day. The detector response for orellanine was linear within a wide concentration range with an excellent correlation coefficient, r, and a low detection limit.

TABLE I

HPLC OF ORELLANINE

Systems: 1, Si-CN, eluent H_3PO_4, pH 1, 0.5 ml/min; 2, Si-C_{18}, eluent H_3PO_4, pH 1–CH_3CN (94:6, v/v), $2.5 \cdot 10^{-3}$ M 1-octanesulphonic acid, 0.8 ml/min. Other chromatographic conditions as described in Experimental. Detection limit based on a signal-to-noise ratio of 3.

Sys-tem	Retention time, t_R (min) $\pm$ C.V. (%)	Quantitation linearity[a] (calibration range: 5–500 ng)		Repeatability, C.V. (%)	Reproducibility, C.V. (%)	Detection limit (pg)
		$y = ax + b$	r			
1	4.43 ± 0.09	$y = 2120\,x + 1720$	0.9994	0.61	1.70	40
2	6.58 ± 1.0	$y = 2260\,x - 7080$	0.9994	0.90	0.55	50

[a] y = Peak area; x = amount injected (ng); a = integrator response factor; b = intercept with y axis; r = regression correlation coefficient; C.V. = coefficient of variation.

Second system with Si-C_{18} bonded phase

The same eluent (phosphoric acid, pH 1) permits the separation of orellanine with a substantially longer retention time (8 min at a flow-rate of 0.5 ml/min). Addition of small amounts of medium-polar solvents strongly reduces the retention time (3.1 min with 2% dioxane).

In order to obtain a still longer retention time, one must use paired-ion chromatography which allows strongly ionic compounds, poorly retained in reversed-phase HPLC systems, to be separated. The pH should be adjusted so that the sample is present in its bicationic form and gives an ion-pair complex with a large and strongly ionic organic counter ion added in the mobile phase. This will make the ionized sample behave as a non-ionic species with some non-polar (lipophilic) characteristics. The resulting species can easily be chromatographed by a reversed-phase system.

Holmdahl *et al.*[10] proposed the use of the following mobile phase: 0.05 M citrate–phosphate buffer, pH 4.5–15.4% methanol and $5 \cdot 10^{-3}$ M 1-hexane-sulphonic acid. It should be noted that citrate buffers are known to dissolve the silica in the column because of their chelating properties and again that orellanine is of low stability in methanol. We found that orellanine is not retained with that eluent at pH 4.5. At this pH value, more than seven polar species, non-ionic or bearing positive and/or negative charges, are present in solution[13]. Amphoteric compounds, such as orellanine, are often difficult to chromatograph. Classically, they can readily be chromatographed using either cationic or anionic reagents. The counter ion in the reagent should ion-pair with one functionality of the amphoteric compound while the other one should remain in its electrically neutral form due to the pH of the reagent. That is not the case with orellanine at pH 4.5: non-neutral ion-pair complexes and non-ionic forms of orellanine are present in solution and all behave as non-complexed polar oralline.

Positively charged ion-pairing agents are of no practical interest owing to the low stability of orellanine and of the silica base at the alkaline pH required for their utilization. To have in solution the bicationic form (Fig. 1), able to form a neutral ion pair with negatively charged ion-pairing agents, one must use the lowest pH value possible. We propose phosphoric acid, pH 1. Addition of medium-polar water-
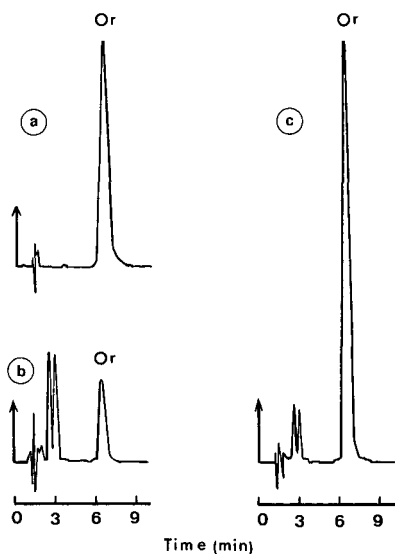
Fig. 2. Typical chromatograms of (a) standard solutions of orellanine (0.25 μg injected), (b) solutions of dried mushroom extract (1.2 μg injected), (c) dried mushroom extract (0.6 μg) spiked with standard orellanine (0.125 μg). Column: Si-C_{18}. Eluent: H_3PO_4 pH 1–CH_3CN (94:6, v/v), 2.5 · 10^{-3} M 1-octane-sulphonic acid; 0.8 ml/min. Other chromatographic conditions as described in Experimental. Or = Orellanine.

miscible solvents in the eluent and variation in the relative size of the lipophilic portion of the counter ion will affect the degree of retention obtained as it is well known for reversed-phase systems. For the evaluation of the method, we used a mobile phase of phosphoric acid pH 1–6% acetonitrile and 2.5 · 10^{-3} M 1-octanesulphonic acid. The ion pair has maxima at 260 and 290 nm. The latter was chosen as the optimum wavelength permitting both high sensitivity and high selectivity. With a flow-rate of 0.5 ml/min, orellanine is eluted late with a retention time of 11.4 min which greatly lengthens the analysis time. However, certain applications may require the use of this method. With a flow-rate of 0.8 ml/min, calibration graphs were linear over a wide range of standards. Stable and reproducible peak areas and an excellent linearity are obtained, thus allowing the quantitation of the toxin (Fig. 2). With the low detection limit, one can avoid the use of the delicate electrochemical detection which gave Holmdahl et al.[10] a ten times higher detection limit (at +900 mV vs. Ag/AgCl). Note that, at such an oxidation potential, not only orellanine can be detected, but also every 3,4-dihydroxylated pyridinic compound. Among these products, orellinine and orelline, respectively the monoamine oxidized and the non-amine oxidized compounds, are particularly likely to be present with orellanine as contamination or degradation products.

Quantitation of orellanine in mushroom extracts

The Si-CN chromatographic system does not allow the separation of orellanine from some other constituents of the mushroom extracts. Hence, it cannot be used for the determination of their orellanine contents. We used the Si-C_{18} chromatographic

system to quantitate the toxin in several dried mushroom extracts stored for 1 year (Fig. 2). The same content of 4.0 ± 0.2% (w/w) was assessed either by the direct method or by the standard addition method in these extracts, corresponding to a content of 1.2% (w/w) in the dried powder of *Cortinarius orellanus*. The accuracy of the determination is 1.8%.

CONCLUSION

Two efficient methods of separation and quantitation are now at our disposal to assess the content of orellanine. With the medium-polar or apolar phases chosen, orellanine, or its ion-pair complex respectively, is eluted either rapidly or with retention times which can be lengthened for the purpose in hand. This allows the separation of orellanine from molecules with different polarities in different media with a low detection limit (40 and 50 pg on column).

ACKNOWLEDGEMENT

REFERENCES

1   T. Schumacher and K. Høiland, *Arch. Toxicol.*, 53 (1983) 87.
2   J.-M. Richard, J. Louis and D. Cantin, *Arch. Toxicol.*, 62 (1988) 242.
3   G. Klein, J.-M. Richard and M. Satre, *Microbiol. Lett., Fed. Eur. Microbiol. Soc.*, 33 (1986) 19.
4   J.-M. Richard, P. Ravanel and D. Cantin, *Toxicon*, 25 (1987) 350.
5   W. Z. Antkowiak and W. P. Gessner, *Tetrahedron Lett.*, 21 (1979) 1931.
6   M. Tiecco,, M. Tingoli, L. Testaferri, D. Chianelli and E. Wenkert, *Tetrahedron*, 42 (1986) 1475.
7   C. Cohen-Addad, J.-M. Richard and J. C. Guitel, *Acta Crystallogr., Sect. C.*, 43 (1987) 504.
8   H. Prast, E. R. Werner, W. Pfaller and M. Moser, *Arch. Toxicol.*, 62 (1988) 81.
9   C. Andary, S. Rapior, A. Fruchier and G. Privat, *Cryptogamie, Mycol.*, 7 (1986) 189.
10 J. Holmdahl, J. Ahlmen, S. Bergek, S. Lundberg and S.-A. Persson, *Toxicon*, 25 (1987) 195.
11 W. Z. Antkowiak and W. P. Gessner, *Bull. Acad. Pol. Sci., Ser. Sci. Chim.*, 23 (1975) 729.
12 D. Cantin, J.-M. Richard, D. Serve and J. Alary, *Electrochim. Acta*, 33 (1988) 1047.
13 J.-M. Richard, D. Cantin and J.-L. Benoit-Guyod, in preparation.

Note

Capillary isotachophoretic separation of phosphate, arsenate, germanate, silicate and molybdate ions using complex-forming equilibria

MASAHIKO KAN, FUMIO KOMATSU, SHUNITZ TANAKA, HITOSHI YOSHIDA and MITSU-HIKO TAGA*

Department of Chemistry, Faculty of Science, Hokkaido University, Sapporo 060 (Japan)

Capillary isotachophoresis (CITP) is an excellent technique for the separation and determination of ionic species, requiring only a short period of time and small amounts of samples.

In a previous paper[1], we have shown that CITP in combination with an enrichment technique is useful for the determination of phosphate ion at the 1 μM level. Phosphate ion was collected on a membrane filter by a facile and rapid procedure as the ion pair of molybdophosphate with bis[2-(5-chloro-2-pyridylazo)-5-diethylaminophenolato]cobalt(III). The ion pair was dissolved in N,N-dimethylformamide and the solution was injected into the CITP analyzer. In this method, however, the separation of phosphate ion from arsenate ion, which was also enriched, was not achieved.

Phosphate and arsenate ions resemble each other in chemical properties. Therefore, the determination of one of these ions is often subject to interference by the other ion in some methods, such as spectrophotometry based on the formation of an heteropoly acid with molybdate[2,3]. The separation of phosphate and arsenate by chromatographic methods has been reported[4,5]. However, there is no report of the separation of these ions by CITP. Such a separation is difficult because of the resemblance in chemical properties and, therefore, the similarity in effective mobilities.

Some attempts have been made to improve the separability in CITP[6–9], of which the use of complex-forming or ion-pairing equilibria is most effective. We have also developed some migration systems using complex-forming or ion-pairing equilibria for the separation of ionic species whose effective mobilites were similar[10–13] or for electrically neutral species such as catechol derivatives[14].

In the present paper, the separation of phosphate and arsenate as well as of germanate, silicate and molybdate is described. The complex-forming equilibria of phosphate and arsenate ions with magnesium ion added to the leading electrolyte are effective for the separation. The difference in the effective mobilities of phosphate and arsenate ions increases with the difference in stabilities of the complexes.

EXPERIMENTAL

Apparatus

A Shimadzu Model IP-1B capillary isotachophoretic analyzer with a potential gradient detector was used. The separation was carried out in a polytetrafluoroethylene isotachophoretic tube consisting of a precapillary tube (50 mm × 1.0 mm I.D.) and a main capillary tube (150 mm × 0.5 mm I.D.).

Reagents

The stock solutions of phosphate, arsenate and molybdate ions were prepared by dissolving potassium dihydrogenphosphate, disodium hydrogenarsenate and ammonium molybdate in water, respectively. For the stock solutions of germanate and silicate ions, standard solutions of germanium and silicon (Wako Pure Chemical Industries, Osaka, Japan, atomic absorption spectrophotometry grade) were used. The stock solution of germanium was an aqueous solution of germanium(IV) oxide and that of silicon was a 0.02 M sodium carbonate aqueous solution of sodium silicate.

The leading electrolyte was prepared by diluting stock solutions of 1 M hydrochloric acid, 1 M magnesium chloride solution and 1% poly(vinyl alcohol), and the pH was adjusted by adding tris(hydroxymethyl)aminomethane (Tris). The pH of the terminating electrolyte was adjusted by adding potassium hydroxide.

The leading and terminating electrolyte systems are listed in Table I.

RESULTS AND DISCUSSION

Selection of electrolyte systems

For the migration of germanate and silicate ions which are conjugate bases of weak acids, alkaline electrolyte systems were used. As the buffering counter ions in these systems, Tris and ammonia were examined. Ammonia was not suitable because the difference in the effective mobilities of the leading and terminating ions is small. Tris is useful as a buffering counter ion up to pH *ca.* 9 and has an adequate migration velocity.

In the alkaline solutions, a zone of carbonate ion penetrated from the terminating electrolyte across the sample zones, and therefore the time required for analysis

TABLE I

LEADING AND TERMINATING ELECTROLYTE SYSTEMS

	Leading electrolyte	Terminating electrolyte
Ion	10 mM Cl$^-$ (added as HCl and MgCl$_2$)	10 mM β-alaninate
Counter ion	TrisH$^+$	K$^+$ (added as KOH)
pH	8.5	10.4
Additives	0.01% poly(vinyl alcohol)	
	3 mM Mg^{2+} (added as MgCl$_2$)	
	5% Methanol	

increased. To shorten this zone barium hydroxide was added to the terminating electrolyte[15] but the zone length of carbonate ion was little affected. This is explained by the fact that the major part of the carbonate ion comes from the injected sample solution containing silicate ion. The stock solution of silicate contains sodium carbonate.

Effect of pH

The effect of the pH in the leading electrolyte on the effective mobilities of the ions is shown in Fig. 1. The R_E value represents the ratio of the potential gradient of the sample ion or terminating ion to that of the leading ion. The R_E values of germanate and silicate ions decreased with increasing pH. An increase of the pH of the leading electrolyte suppresses the protonation of the silicate and germanate ions, so the effective mobilities of these ions increase. These was little variation of the R_E values of phosphate, arsenate and molybdate ions with change of pH because the degree of protonation of these ions is not so greatly influenced by the change in pH within the range mentioned here.

At pH 8, the difference in the effective mobilities of the silicate and terminating ions was small and high voltage was applied because of their low degree of ionization. At pH 9, on the other hand, arsenate and hydrogencarbonate ions had similar effective mobilities. For the separation of the ions mentioned, the leading electrolyte was adjusted to pH 8.5.

Effect of complex-forming equilibria

For the separation of phosphate and arsenate, the utility of complex-forming equilibria between these ions and magnesium ion was investigated. The effect of the concentration of magnesium ion in the leading electrolyte on the R_E values is shown in Fig. 2.

Without magnesium ion, the R_E values of arsenate and hydrogencarbonate ions were equal and that of phosphate ion was somewhat smaller. Upon addition of magnesium ion to the leading electrolyte, the R_E value of phosphate ion increased. The R_E value of arsenate also increased, but not so much as that of phosphate.
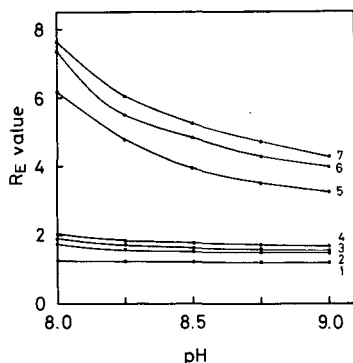
Fig. 1. Effect of the pH of the leading electrolyte on the R_E values of molybdate (1), hydrogencarbonate (2), arsenate (3), phosphate (4), germanate (5), silicate (6) and β-alanine (7) ions. Electrolyte systems as in Table I except for the pH of the leading electrolyte.
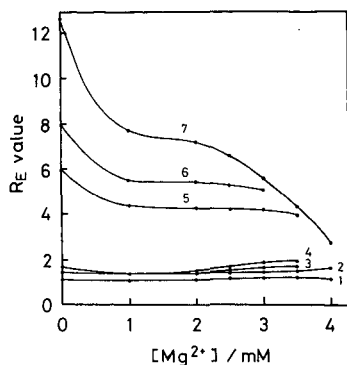
Fig. 2. Effect of the concentration of magnesium ion in the leading electrolyte on the R_E values. Curves as in Fig. 1. Electrolyte systems as in Table I except for the concentration of magnesium ion.

With increasing concentration of magnesium ion, complexes are formed between phosphate and arsenate ions with magnesium ion and the net charges of the complexes decrease. The difference in the effective mobilities of phosphate and arsenate is caused by the difference in the stabilities of the complexes.

The R_E values of germanate, silicate and molybdate ions were little influenced by the complex-forming equilibria with magnesium ion. The R_E value of the terminating ion decreased with increasing concentration of magnesium ion. The zone of silicate disappeared at 3.5 mM magnesium ion and those of phosphate, arsenate and germanate ions disappeared at 4 mM because of their effective mobilities were lower than that of the terminating ion.

Calcium ion was not suitable as a complexing agent because of the formation of a precipitate with phosphate.

Effect of organic solvents

To enhance the interaction between the above ions and magnesium ion, methanol was added to the leading electrolyte. The effect of the methanol concentration on the R_E values is shown in Fig. 3.
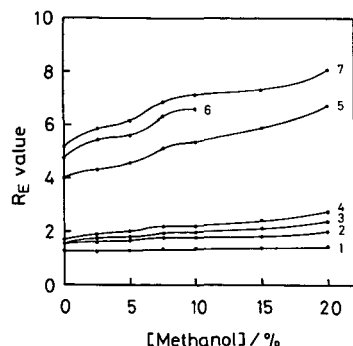
Fig. 3. Effect of the concentration of methanol in the leading electrolyte on the R_E values. Curves as in Fig. 1. Electrolyte systems as in Table I except for the concentration of methanol.
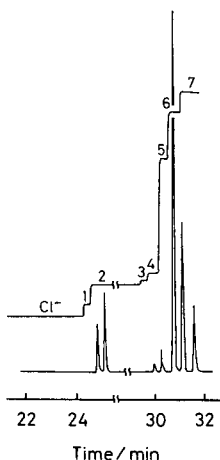
Fig. 4. Isotachopherogram: 1 = molybdate (2.5 nmol); 2 = hydrogencarbonate; 3 = arsenate (1.1 nmol); 4 = phosphate (2.5 nmol); 5 = germanate (3.6 nmol); 6 = silicate (6.4 nmol); 7 = β-alanine ions. Electrolyte systems as in Table I. Driving current: 50 μA.

Without addition of methanol, there was no difference in the R_E values of arsenate and hydrogencarbonate ions. By the addition of only 2.5% methanol, the zone of arsenate ion was completely separated from that of hydrogencarbonate ion. With the increasing methanol concentration, the difference in the R_E values became larger. This is due to the increase in the interaction of arsenate ion with magnesium ion.

The zone of silicate disappeared at more than 15% methanol because its effective mobility is lower than that of the terminating ion.

Acetone was not suitable as an organic solvent because its boiling point is lower and migrations were often interrupted by the generation of bubbles.

Calibration graphs

An isotachopherogram obtained under the optimum conditions is shown in Fig. 4. The separation of phosphate, arsenate, germanate, silicate and molybdate ions is achieved and the boundaries of each zone are very sharp.

Calibration graphs for each ion were constructed by linear regressions and their parameters are given in Table II. Although it is known that silicate ion forms a

TABLE II

PARAMETERS OF LINEAR REGRESSIONS FOR CALIBRATION GRAPHS

Ion	Intercept(s)	Slope (s nmol^{-1})	Correlation coefficient	Range (nmol)
Phosphate	0.55	10.29	0.994	0.5–2.5
Arsenate	1.21	14.14	0.994	0.5–2.5
Germanate	1.48	4.97	0.997	0.5–3.6
Silicate	1.98	3.75	0.996	2.0–12
Molybdate	1.19	5.88	0.999	2.5–21

TABLE III

RELATIVE STANDARD DEVIATIONS OF ZONE LENGTHS

Ion	R.S.D. (%)	Replicate	Amount (nmol)
Phosphate	2.0	9	2.5
Arsenate	2.6	9	1.1
Germanate	8.4	10	3.6
Silicate	3.8	10	6.4
Molybdate	3.2	10	2.5

precipitate with magnesium ion, it had no influence within the concentrations studied. Relative standard deviations of the zone lengths for each ion are listed in Table III. The linearities of calibration graphs and the reproducibilities of the zone lengths for each ion are satisfactory for the determination of these ions.

REFERENCES

1 M. Taga, M. Kan, F. Komatsu, S. Tanaka and H. Yoshida, *Anal. Sci.*, 5 (1989) 219.
2 M. Taga and M. Kan, *Bull. Chem. Soc. Jpn.*, 62 (1989) 1482.
3 T. Nasu and M. Kan, *Analyst (London)*, 113 (1988) 1683.
4 T. Takamatsu, M. Kawashima and M. Koyama, *Bunseki Kagaku*, 28 (1979) 596.
5 R. J. Williams, *Anal. Chem.*, 55 (1983) 851.
6 F. M. Everaerts, J. L. Beckers and T.P.E.M. Verheggen, *Isotachophoresis, Theory, Instrumentation and Applications*, Elsevier, Amsterdam, 1976, Chs. 16 and 17.
7 H. Miyazaki and K. Katoh, *Tohsoku Denki Eidoh Hoh*, Kohdansha, Tokyo, 1980, Ch. 7.
8 P. Boček, M. Deml, P. Gebauer and V. Dolnik, *Analytical Isotachophoresis*, VCH, Weinheim, 1988, Ch. 9.
9 P. Boček, I. Miedziak, M. Deml and J. Janák, *J. Chromatogr.*, 137 (1977) 83.
10 I. Nukatsuka and H. Yoshida, *J. Chromatogr.*, 237 (1982) 506.
11 H. Yoshida, M. Hida and M. Taga, *J. Chromatogr.*, 325 (1985) 179.
12 Y. Hirama and H. Yoshida, *Nippon Kagaku Kaishi*, 1986, 943.
13 S. Tanaka, T. Kaneta and H. Yoshida, *J. Chromatogr.*, 447 (1988) 383.
14 S. Tanaka, T. Kaneta and H. Yoshida, *Anal. Sci.*, 5 (1989) 217.
15 P. Boček, M. Deml, P. Gebauer and V. Dolnik, *Analytical Isotachophoresis*, VCH, Weinheim, 1988, Ch. 10, p. 191.

Note

Analytical high-performance liquid chromatography system for separation of components in nonoxynol-9 spermicidal agents[a]

D. BRUCE BLACK, BRIAN A. DAWSON and GEORGE A. NEVILLE*

Bureau of Drug Research, Health Protection Branch, Health and Welfare Canada, Tunney's Pasture, Ottawa, Ontario K1A 0L2 (Canada)

(First received February 6th, 1989; revised manuscript received May 8th, 1989)

Extensive use of high-performance liquid chromatography (HPLC) has been made during the past decade to investigate a wide range of ethoxylated non-ionic surfactants[1–8] and anionic surfactants[1,9,10]. HPLC has been particularly valuable for analysing industrial and domestic waste water for levels and distributions of linear alkylbenzenesulphonates (LASs), alkylphenol polyethoxylates (APEOs), and nonylphenol (NP) for environmental control[11–13], for determination of non-ionic surfactants used in tertiary oil recovery[14], and for determining dodecylbenzenesulphonates and ethoxylated alkylphenols in liquid pesticide formulations[15].

Nonoxynol-9 (nonylphenoxypolyethoxyethanol, $CH_3(CH_2)_8C_6H_4(OCH_2CH_2)_nOH$), as commercially produced, is a complex non-ionic surfactant consisting of mixtures of oligomers of polyethoxylated nonylphenol. The average value of n is said to be about 9 (ref. 16), although this value appears to be more coincidental to its name than the fact its oligomers bear chiefly the nonylphenoxy terminal group as compared to the diisobutylphenoxy terminus of octoxynol-9, another widely used nonionic surfactant. In principal, any number of nonoxynol-X mixtures can be produced for each of which X represents the average number of repeating polyethyleneglycol units, which, in tern, affect the viscosity, solubility, polarity, and dispersant properties of the particular surfactant formulation[17]. In particular, nonoxynols-4, -15, and -30 are used as pharmaceutical formulating aids (surfactants)[18]. Our interest in nonoxynol-9 arises over its use as a spermicidal agent, as found in most vaginal contraceptive jellies, creams, aerosol foams and lubricated (coated) condoms sold over-the-counter in many countries including Canada. The purpose of this investigation was to characterize the claimed active spermicidal agent of a new product, a soft polyurethane vaginal contraceptive sponge containing nonoxynol-9, being prepared for introduction to the Canadian market, and to compare its chemical features with those of other commercial nonoxynol-9 raw samples.

---

[a] Presented in part at the *169th Annual Canadian Chemical Conference, Saskatoon, Saskatchewan, Canada,* 1–4 June, 1986.

EXPERIMENTAL

Materials

A vaginal sponge, known as Today Vaginal Contraceptive Sponge (VLI Corp., Irvine, CA, U.S.A.) was trimmed of its string loop and soaked in methanol (200 ml, HPLC grade) with occasional agitation for 3 h after which the extract was reduced to a viscous fluid (almost 100% recovery of product claim) in a rotary evaporator under pumping vacuum. For comparison, a sample of the raw nonoxynol-9 (Lot RM-1065-22), as used in manufacture of the Today sponge, was obtained from the VLI Corp. and samples of raw nonoxynol-9 were obtained from Ortho Pharmaceutical (Canada), Don Mills, Ontario, Canada (Lot T1623) and from Rougier, Chambley, Quebec, Canada (Lot 11A30RR). All materials were examined by ^{1}H NMR spectroscopy and by HPLC analysis.

Instrumentation

HPLC analyses of the raw nonoxynol-9 samples, as well as that extracted from the vaginal sponge, were performed with a Chromatography Sciences Company silica S5W 5-μm column (25 cm $\times$ 4.6 mm I.D.) employing an ethyl acetate–methanol (1:1, v/v) mobile phase at a flow-rate of 1 ml/min. A Spectra-Physics SP8000B liquid chromatograph was used with a Schoeffel 770 UV–VIS detector at 280 nm.

^{1}H NMR spectra were obtained at 80 MHz and ambient temperature (22°C) from the nonoxynol-9 samples in acetone-d_6 (containing 1% tetramethylsilane internal reference) using a Bruker WP-80 spectrometer.

RESULTS AND DISCUSSION

^{1}H NMR spectral analysis

Acetone-d_6 was found to be the solvent which resulted in the richest ^{1}H NMR spectra (Fig. 1) of the nonoxynol-9 samples, and all samples, including the material extracted from the sponge, gave essentially identical proton spectra. By this analysis, no other component appeared to have been extracted from the urethane sponge. Exchange with ^{2}H$_2$O resulted in simplification of the bands near δ 3.6 and suggests that the downfield peaks seen here may arise from the various oligomer hydroxy protons. The integration is supportive of the gross structural features, *i.e.*, on the basis of the low field pattern (δ 7) arising from 4 aromatic protons, the principal band near δ 3.6 accounts surprisingly well for the 36 protons of the archetypal polyethoxy group (OCH$_2$CH$_2$)$_n$ where $\bar{n}$ = 9, and likewise the integral for the two high-field patterns accounts for the 19 protons of the *para*-nonyl substituent. In dimethyl sulfoxide-d_6 (DMSO-d_6), the sponge extract showed somewhat similar proton spectral features found in acetone-d_6 except for some loss of band character, probably due to increased viscosity of the solution. In ^{2}H$_2$O solution (also at ambient temperature), the proton spectrum of the sponge extract suffered serious loss of band character, probably due to the formation of micellar colloids.

HPLC analysis

The chromatograms obtained from analysis of the sponge extract and the three raw nonoxynol-9 samples are shown in Fig. 2. Both the sponge extract and the Rougier
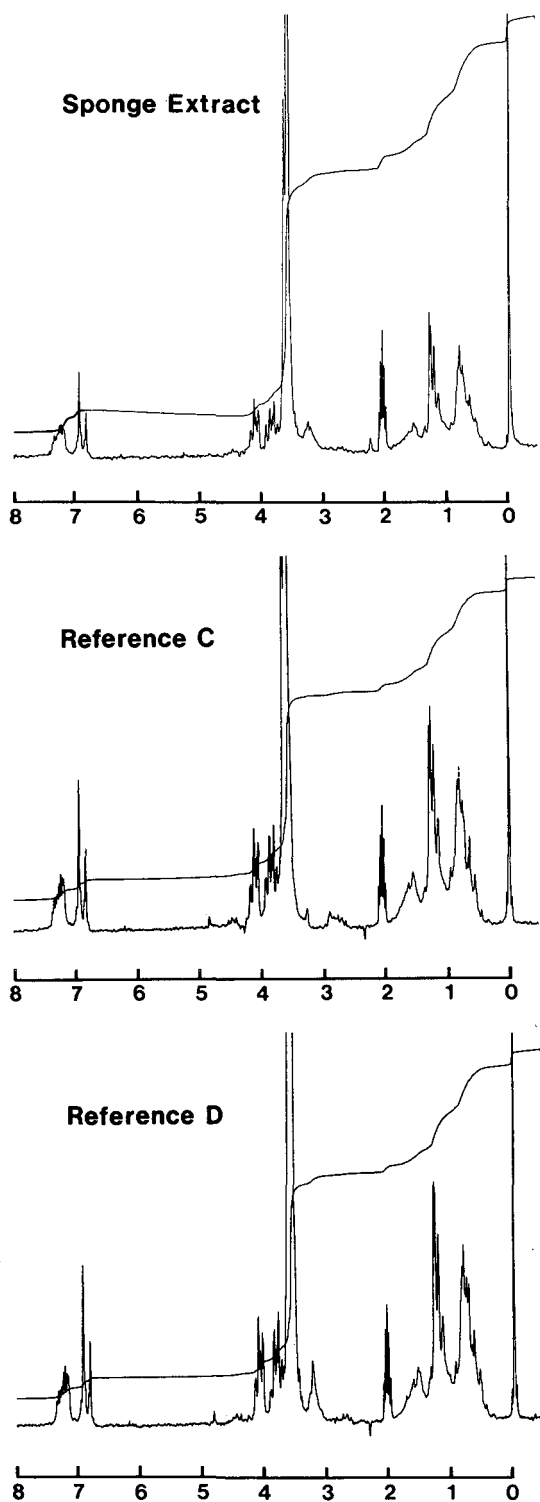
Fig. 1. ^{1}H NMR spectra (80 MHz) of nonoxynol-9 extracted from the sponge (top) and of reference materials C (Rougier, Lot 11A30RR) and D (Ortho, Lot T1623) in acetone, d_6. Chemical shift scale B in ppm.
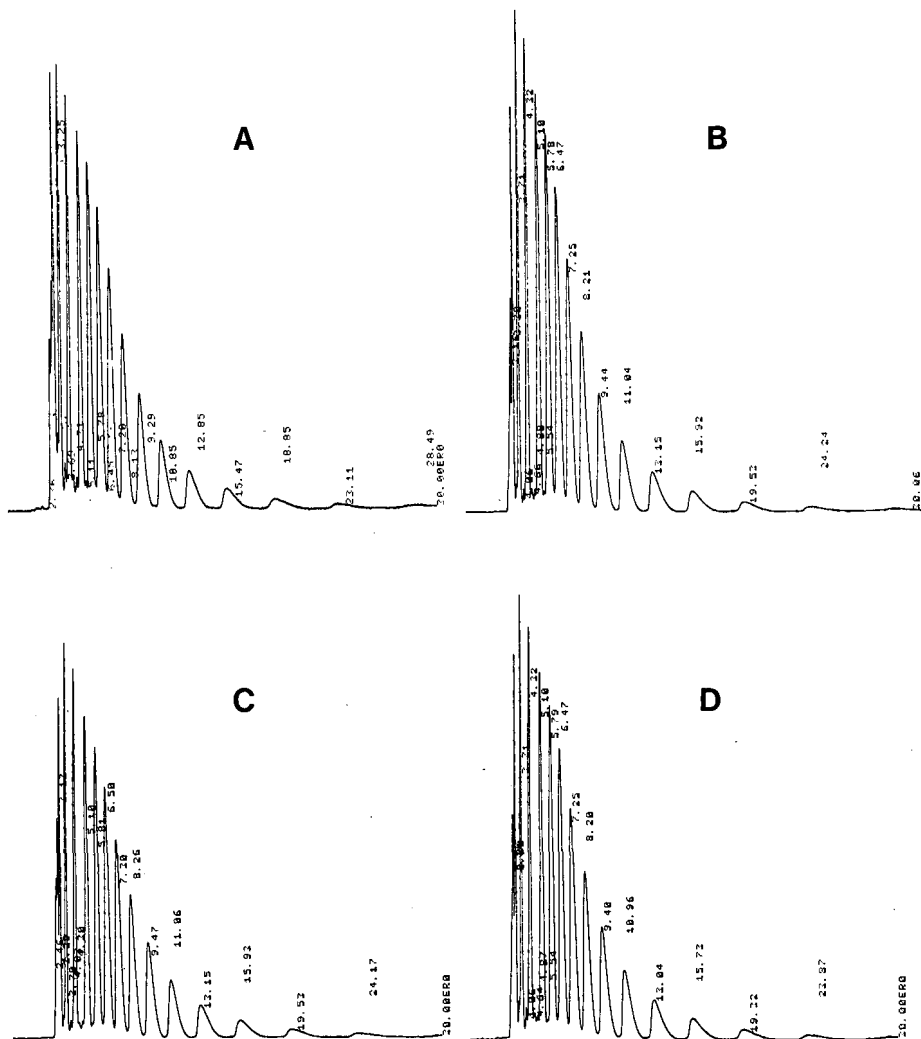
Fig. 2. Chromatograms of nonoxynol-9. (A) Extracted from the Today Vaginal Contraceptive Sponge, (B) raw material (Lot RM-1065-22) used by VLI Corp. for the Today Sponge, (C) Rougier raw material (Lot 11A30RR), and (D) Ortho raw material (Lot T1623). Elution times for individual peaks are given in min.

material showed 17 component peaks, whereas 16 peaks were seen for the raw VLI and the Ortho nonoxynol-9 samples. In each instance, the last component to be eluted was minute (peak 17 for the sponge extract and Rougier material, and peak 16 for the raw VLI and Ortho materials). Interestingly, both the sponge extract and the raw Rougier nonoxynol-9 showed an extra initial peak at the beginning of their chromatograms that was not seen in the chromatograms for the raw VLI and Ortho samples. Apart from these small differences, the four chromatograms showed remarkable similarity in overall profile and retention times, indicative of clean extraction of nonoxynol-9 from

the sponge with no apparent carryover of other components from the urethane material.

The forward phase (normal-phase) non-gradient HPLC system used to obtain the chromatograms shown in Fig. 2, with near baseline separation, constitutes a simpler and faster HPLC procedure for characterizing the oligomeric composition of nonoxynol-9 than reported in the literature to date. While Schreuder and Martijn[15] obtained excellent baseline separation of the oligomers of an ICI (U.K.) ethoxylated nonylphenol (NPEO) with an ethoxylation degree ($\bar{n}$) of 8.5, their procedures required double the time (> 50 min) at the same flow-rate of 1.0 ml/min using an aminopropyl-modified silica column (Hypersil APS, 250 mm $\times$ 4.6 mm I.D.) with a linear gradient of propan-2-ol–water (90:10) in a mobile solution of hexane–tetrahydrofuran (70:30) with increased ratio of the former to the latter from 0.05 at time 0 to 0.5 in 60 min. Similarly, Marcomini and Giger[12] separated Marlophen 810, containing NPEO oligomers with an average of 11 and a range of 1–18 ethoxy units, over a 30-min interval using an aminosilica 3-μm column (Hypersil APS, 100 mm $\times$ 4 mm I.D.) employing initially a 2-min elution of 100% n-hexane–2-propanol mixture (H/IP, 98/2) followed by a 25-min linear elution gradient leading to "50% H/IP (98/2) and 50% H/IP (98/2)" (erroneously reported — a more polar second solvent mix would have to have been used), at a flow-rate of 1.5 ml/min. Using the same normal-phase HPLC system, Marcomini and Giger[12], however, were able to separate 16 components of an NPEO in about 20 min from an unidentified granular laundry detergent in a chromatogram whose peaks were better resolved than those obtained from Marlophen 810, which they had used as an NPEO standard mixture.

In our HPLC analysis of the nonoxynol-9 spermicidal materials, UV detection was effected at 280 nm, very close to the absorption at 277 nm employed by Marcomini and Giger[12] for normal-phase HPLC analyses, because the response factors of NPEO and nonylphenol (NP) were available from the literature[19]. For investigation of more complex detergent systems, Marcomini and Giger[12] used UV at 225 nm to benefit from about a five-fold increase in intensity of absorption by APEOs and NP in the presence of LASs. Schreuder and Martijn[15] also employed UV detection at 225 nm; however, polyethylene glycol (PEG), having no absorbance at 225 nm, was not detected. For HPLC analysis of any of the PEGs, refractometric detection is required as demonstrated by Zeman[2]. We chose, instead, to characterize the oligomers, separated under other conditions, using preparative HPLC, by ^{1}H NMR and MS[20].

In retrospect, simpler, direct forward phase HPLC systems employing silica columns for analysis and separation of APEO preparations were undoubtedly tried, but with little apparent success[21,22]. Subsequent analytical development for such non-ionic surfactants was directed more towards investigation of properties of modified silica columns and gradient elution systems. The better specification and consistancy of manufacture of silica columns in more recent years, together with greater exploration of solvent conditions, now make it possible to employ the simpler, direct approach of non-gradient silica HPLC analyses for these substances.

We believe that the analytical HPLC system reported herein constitutes a convenient and rapid, non-gradient method for assessing pharmaceutical nonoxynol-9 preparations.

REFERENCES

1 J. A. Pilc and P. A. Sermon, *J. Chromatogr.*, 398 (1987) 375–380.
2 I. Zeman, *J. Chromatogr.*, 363 (1986) 223–230.
3 N. Garti, V. R. Kaufman and A. Aserin, *Sep. Purif. Methods*, 12 (1983) 49–116.
4 A. Aserin, N. Garti and M. Frenkel, *J. Liq. Chromatogr.*, 7 (1984) 1545–1557.
5 M. Kudoh, *J. Chromatogr.*, 291 (1984) 327–330.
6 A. Aserin, M. Frenkel and N. Garti, *J. Am. Oil Chem. Soc.*, 61 (1984) 805–809.
7 M. Kudoh, S. Fudans and S. Yamaguchi, *J. Chromatogr.*, 205 (1981) 473–477.
8 M. C. Allen and D. E. Linder, *J. Am. Oil Chem. Soc.*, (1981) 950–957.
9 P. K. G. Hodgson and N. J. Stewart, *J. Chromatogr.*, 387 (1987) 546–550.
10 R. E. A. Escott, S. J. Brinkworth and J. A. Steedman, *J. Chromatogr.*, 282 (1983) 655–661.
11 A. Marcomini, S. Capri and W. Giger, *J. Chromatogr.*, 403 (1987) 243–252.
12 A. Marcomini and W. Giger, *Anal. Chem.*, 59 (1987) 1709–1715.
13 M. S. Holt, E. H. McKerrell, J. Perry and R. J. Watkinson, *J. Chromatogr.*, 362 (1986) 419–424.
14 P. L. Desbène, B. Desmazières, J. J. Basselier and L. Minssieux, *Chromatographia*, 24 (1987) 588–592.
15 R. H. Schreuder and A. Martijn, *J. Chromatogr.*, 435 (1988) 73–82.
16 *Seventh Supplement to U.S. Pharmacopeia XXI and to National Formulary XVI*, United States Pharmacopeial Convention, Rockville, MD, 1988 p. 2811.
17 W. B. Satkowski, S. K. Huang and R. L. Liss in M. J. Schick (Editor), *Nonionic Surfactants*, Vol. 1, Marcel Dekker, New York, 1967, Ch. 4.
18 *Merck Index*, Merck & Co., Rahway, NJ, 10th ed., 1983, item No. 6518, p. 6522.
19 M. Ahel and W. Giger, *Anal. Chem.*, 57 (1985) 2584–2590.
20 D. B. Black, B. A. Dawson, J.-C. Ethier and G. A. Neville, submitted for publication.
21 K. J. Bombaugh, R. F. Levangie, R. N. King and L. Abrahams, *J. Chromatogr. Sci.*, 8 (1970) 657–663.
22 J. F. K. Huber, F. F. M. Kolder and J. M. Miller, *Anal. Chem.*, 44 (1972) 105–110.

CHROM. 21 624

Note

Separation of pirimicarb and its metabolites by high-performance liquid chromatography

PAOLO CABRAS*, LORENZO SPANEDDA and CARLO TUBEROSO

Istituto di Chimica Farmaceutica, Tossicologica ed Applicata, Viale Diaz 182, 09100 Cagliari (Italy)

and

MARA GENNARI

Istituto di Chimica Agraria, Via P. Giuria 15, 10126 Turin (Italy)

(Received March 28th, 1989)

Pirimicarb, 2-dimethylamino-5,6-dimethylpyrimidin-4-yl dimethylcarbamate (I) (Fig. 1) is a selective aphicide with rapid contact and translaminar actions; it is taken up by roots and translocated in the xylem system[1]. Its highly selective action makes it especially suitable for integrated control programmes. A rapid reduction of pirimicarb occurs in plants after spraying, mainly by volatilization but also by photochemical and metabolic degradation, the major products being compounds II and III (Fig. 1). Some of the residue cannot be extracted from cabbage leaves (14%) or from lettuce (25%) by conventional techniques[2].

Pirimicarb is extensively degraded in soil, the principal route being the hydrolysis of the carbamate moiety either by biological or chemical means. Compounds V, VI and III are the major metabolites (Fig. 1); compound V is the major product (84%) of the photochemical degradation on the soil surface[2].

Even in animals, the principal degradation route of pirimicarb is the hydrolysis of the carbamate moiety: the hydroxypyrimidines V–VII are the major products whereas the carbamate-containing metabolites are absent or in very low amount (8%)[3].

For residue analysis, gas chromatography (GC) has been employed in order to determine pirimicarb[4] and its carbamate-containing metabolites II and III[5]. High-performance liquid chromatography (HPLC) has recently been used with UV–VIS detection[6,7] and with fluorescence detection[8]; with this technique, pirimicarb and its metabolite desmethyl-pirimicarb (III) were determined in various crops.

In this paper an HPLC separation of pirimicarb and its major metabolites is reported.

EXPERIMENTAL

Apparatus

A Varian (Palo Alto, CA, U.S.A.) Model 5020 liquid chromatograph was employed, equipped with a variable-wavelength UV-100 UV–VIS detector and
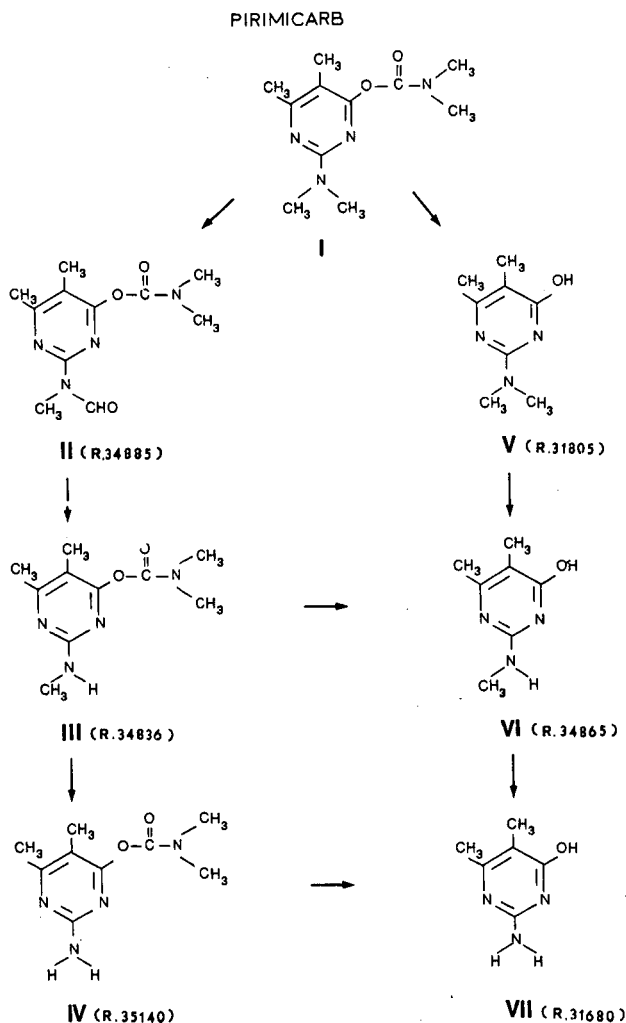
Fig. 1. Metabolic pathway of pirimicarb.

a Rheodyne injector (50-μl loop), connected to an H.P. (Hewlett-Packard, Avondale, PA, U.S.A.) Model 3390 A reporting integrator.

Chromatography

Hibar (Merck, Darmstadt, F.R.G.) RP-8, RP-18 and NH$_2$ columns (250 mm × 4.0 mm I.D., 10 μm) were used; the mobile phase was water–acetonitrile (NH$_2$) or phosphate buffer–acetonitrile (RP-8 and RP-18) in various ratios (Table I). The detector wavelength was programmed during the analyses according to the UV spectra of pirimicarb and its metabolites (245 nm for I and II, 236 nm for III, 226 nm for IV, 295 nm for V–VII).

TABLE I

RETENTION TIMES OF PIRIMICARB (I) AND ITS METABOLITES (II–VII) WITH DIFFERENT
COLUMNS AND ELUENTS

Column	Mobile phase	Retention time (min)						
		VII	VI	V	IV	III	II	I
	Buffer– acetonitrile (v/v)							
RP-8	60:40	2.26	2.46	2.75	3.27	4.29	5.80	7.14
	65:35	2.30	2.43	2.81	3.61	4.79	7.26	8.75
	70:30	2.45	2.57	2.92	4.04	5.72	9.91	11.37
RP-18	60:40	2.06	2.25	2.62	3.00	4.23	5.91	8.66
	65:35	2.15	2.30	2.69	3.34	4.89	7.78	11.37
	70:30	2.21	2.48	2.84	3.79	5.98	10.95	15.56
	Water– acetonitrile							
NH$_2$	10:90	7.89	5.03	3.48				
	8:92	10.59	6.02	3.61				
	5:95	20.07	9.50	4.01				

Chemicals and materials

Acetonitrile was of HPLC grade (Carlo Erba, Milan, Italy); water was doubly distilled and filtered through a Milli Q apparatus (Millipore, Milan, Italy) before use. The buffer solution was made from 10^{-2} M KH$_2$PO$_4$ with 5 ml/l acetic acid; potassium dihydrogenphosphate and glacial acetic acid were of analytical grade (Carlo Erba).

Pirimicarb (I) and its metabolites II (2-methylformylamino-5,6-dimethyl-pyrimidin-4-yl dimethylcarbamate, R. 34885), III (2-methylamino-5,6-dimethyl-pyrimidin-4-yl dimethylcarbamate, R. 34836), IV (2-amino-5,6-dimethylpyrimidin-4-yl dimethylcarbamate, R. 35140), V (2-dimethylamino-5,6-dimethyl-4-hydroxy-pyrimidine, R. 31805), VI (2-methylamino-5,6-dimethyl-4-hydroxypyrimidine, R. 34865) and VII (2-amino-5,6-dimethyl-4-hydroxypyrimidine, R. 31680) were obtained from ICI Solplant (Milan, Italy).

RESULTS AND DISCUSSION

A water–acetonitrile mixture was initially used as the mobile phase with reversed-phase (RP) columns and a good separation was achieved for the carbamate-containing metabolites I–IV. However, the hydroxypyrimidine (V–VII) peaks were very close but still resolved. After several analyses the columns showed an un-accountable loss of efficiency; compounds V–VII were not resolved and IV and V were overlapped.

Water was then replaced in the eluent mixture by a phosphate buffer solution, so achieving a greater reproducibility of retention times at the same resolution than with water–acetonitrile as the mobile phase.

   As shown by the retention times on RP-8 and RP-18 columns (Table I), the carbamate-containing metabolites I–IV were greatly influenced by the percentage of buffer in the mobile phase (in decreasing order from I to IV) whereas the hydroxypyrimidines V–VII appeared less sensitive to such changes. Using mobile phases with a buffer content equal or greater than 65%, a good resolution of compound V from IV was achieved, but peaks V–VII were so close that any loss of efficiency of the column caused them to overlap.

   Owing to the incomplete separation of the most polar compounds V–VII on RP columns, a normal phase NH_2 column was used that gave a good separation of V–VII with water–acetonitrile as the mobile phase, whereas I–IV were rapidly eluted and not resolved. The retention times changed considerably by increasing the polarity of the eluent mixture, especially for compounds VI and VII, whereas V was less influenced by changes in the water content of the mobile phase.

   Calibration graphs for each compound were constructed by plotting concentrations vs. peak areas. An RP-8 column for compounds I–IV and an NH_2 column for V–VII were used, with respectively buffer–acetonitrile (65:35, v/v) and water–acetonitrile (8:92, v/v) as the mobile phase (Fig. 2). Good linearities were achieved in the range 0–1.5 ppm with correlation coefficients between 0.9991 and 0.9997. Under the optimum conditions, the detection limit was 0.005 ppm for each compound.

   The method described allows the separation of pirimicarb and its metabolites and may be useful for the determination of these compounds, after appropriate extraction and clean-up in different matrices.
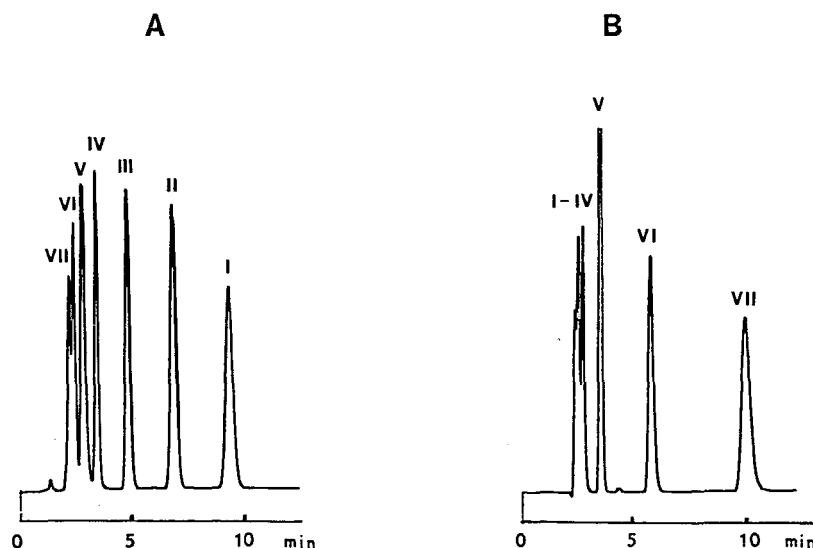
Fig. 2. Chromatography of pirimicarb (I) and its metabolites (II–VII): (A) on an RP-8 column, mobile phase, phosphate buffer–acetonitrile (65:35, v/v), flow-rate 1 ml/min, UV detection at 226, 236 and 245 nm: (B) on an NH_2 column, mobile phase, water–acetonitrile (8:92, v/v), flow-rate 1 ml/min; UV detection at 295 nm.

ACKNOWLEDGEMENTS

REFERENCES

1 C. R. Worthing (Editor), *The Pesticide Manual*, The British Crop Protection Council, Lavenham, 8th ed., 1987.
2 *Pesticides Residues in Food: 1976 Evaluations*, FAO/WHO, Rome, 1977, p. 535.
3 *Pesticides Residues in Food: 1978 Evaluations*, FAO/WHO, Rome, 1979, p. 209.
4 J. E. Bagness and W. G. Sharples, *Analyst (London)*, 99 (1974) 225.
5 D. J. W. Bullock, in G. Zweig (Editor), *Analytical Methods for Pesticides, Plant Growth Regulators and Food Additives*, Vol. VII, Academic Press, New York and London, 1973, p. 399.
6 M. D. Osselton and R. D. Snelling, *J. Chromatogr.*, 368 (1986) 265.
7 P. Cabras, M. G. Lalli, M. Meloni, F. M. Pirisi, F. Cabitza, M. Cubeddu and M. Porcu, *Riv. Soc. Ital. Sci. Alim.*, 17 (1988) 61.
8 J. W. Dornseiffen and W. Verwaal, *6th International Congress of Pesticide Chemistry IUPAC, Ottawa, August 10–15, 1986*, Abstracts SE-15 (Internal Report of the Governmental Food Inspection Service, Amsterdam).

Note

Isolation of an antimicrobial bromoditerpene from a marine alga aided by improved bioautography

SALVATORE CACCAMESE*, ORAZIO CASCIO and ANNA COMPAGNINI

Dipartimento di Scienze Chimiche, Università di Catania, Viale Doria 6, 95125 Catania (Italy)

(Received April 7th, 1989)

Bioautography is a technique familiar to microbiologists in the search for antibiotics from microorganisms and different procedures have been used to improve its performance[1–3]. Most of the published procedures are based on the "contact" technique where the antibacterial compound is transferred from the chromatographic layer to an inoculated agar plate through a diffusion process. These procedures suffer several disadvantages such as low sensitivity, spurious inhibition of the contact area and are not suitable for water-insoluble compounds. Recently, a "direct" bioautographic detection on the chromatographic layer which makes use of an appropriate device for spreading the agar on the plate has been published[4].

We describe here a simple "contact" bioautography assay to isolate easily a strong antimicrobial bromoditerpene, sphaerococcenol A, from the marine red alga *Sphaerococcus coronopifolius:*

I
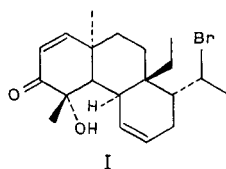
Although the compound and the extract were water-insoluble, it was possible to perform bioautography by improving the diffusion process that takes place through the contact of the chromatographic layer with the inoculated agar plate.

Compound I was isolated from material collected in Spain[5] and Yugoslavia[6] but not from *S. coronopifolius* collected in the bay of Naples and Sicily from which other diterpenoids were isolated[7,8]. However, it was reported that a lipophilic extract of this species collected along the eastern coast of Sicily exhibited good *in vitro* antimicrobial activity[9]. We show here, through its isolation aided by bioautography, that compound I is the major component responsible for that activity.

In the disc-diffusion agar test, sphaerococcenol A exhibited a strong antibacterial activity against *Bacillus subtilis* and *Escherichia coli* and against the fungus *Phoma tracheiphila* which causes a destructive disease of *Citrus* trees in the Mediterranean region.

EXPERIMENTAL

TLC plates and conditions

Commercially available 20 cm × 20 cm thin-layer chromatographic (TLC) aluminium sheets (layer thickness 0.2 mm) precoated with silica gel 60 were obtained from Merck (Darmstadt, F.R.G.). They were divided into sizes of 10 cm × 5 cm. Before use, the plates were washed with the elution solvent in the developing tank. About 20 or 50 μg of methanolic solution containing 1 mg/ml of compound I or the extract were applied to the TLC plates to form spots. Camag Microcap micropipettes were used for sample application. The spot size was minimized by applying the sample volume in small increments on top of each other, with complete drying of the solvent after each application. Chromatography was effected by using a 10 cm × 10 cm twin-trough chamber (Camag, Muttenz, Switzerland), preequilibrating the layer with the vapours of the elution solvent and then developing up to 9 cm. The plates were thoroughly dried in a stream of air.

Preparative TLC was performed on 20 cm × 20 cm glass supported plates (thickness 0.5 mm, Merck) precoated with silica gel 60. The extract was applied as an acetone solution using a laboratory-made 2-ml dispenser. The chromatography was performed in 20 cm × 20 cm twin-trough Camag chambers with the same precautions as in analytical TLC. All solvents were of analytical grade and mixtures were made up on a v/v basis.

Chemical visualization

A solution of 1% ceric sulphate in 1 M H_2SO_4 was used. Intensification of the different colours of the spots was obtained by heating in an oven at 115°C for 10 min. Visualization on the preparative TLC plates was done only at an edge, the remaining silica layer being protected with a clean glass plate.

Culture medium and microorganisms

For bioautography, antibiotic medium No. 1 (Difco, Detroit, MI, U.S.A.) was dissolved in a phosphate saline buffer at pH 7.3 (ref. 10) and sterilized by autoclaving at 121°C for 15 min. After cooling at 45°C, 1 ml of *Bacillus subtilis* ATCC 6633 spore suspension (Difco) or *Escherichia coli* strain B ATCC 11303 inoculum (Sigma, St. Louis, MO, U.S.A.) was added to 200 ml culture medium. Before congealing, 15 ml of the inoculated agar were added to sterile 15-cm glass Petri plates, swirling carefully.

In addition to the above bacteria, the fungus *Phoma tracheiphila* was used in the disc-diffusion agar plate tests. The microorganism was obtained from the Institute of Plant Pathology of the University of Catania as a 12-days-old pycnidiospores suspension.

Plant material

S. coronopifolius (fresh weight 2 kg) was collected at a depth of 4–5 m at Castelluccio, eastern Sicily in September 1988. A voucher specimen is deposited in the Herbarium of the Algology Laboratory of the Institute of Botany of the University of Catania.

RESULTS AND DISCUSSION

The fresh alga was immediately soaked in isopropanol. The solution was concentrated to give a residue that was partitioned between a 1 M sodium nitrate solution and diethyl ether. The ether layer yielded, after desiccation and concentration, 1.91 g of deep green semisolid extract which was strongly active against $B.$ $subtilis$ and $E.$ $coli$ in the disc-diffusion agar plate test.

Silica gel TLC [dichloromethane–light petroleum (b.p. 40–70°C), 6:4] of the extract showed, after visualization, about 15 differently coloured spots. However, a much simpler pattern was observed by bioautographic detection. Only the spots at R_F 0.32 and 0.44 were antimicrobially active as well as the origin spot. This selectivity was a guide for the preparative TLC.

However, practical difficulties were encountered using the classical bioautographic procedure. The use of glass-supported TLC plates is not advisable since air-bubbles form easily. The interposition of a sheet of lens-tissue paper, as is usual, prevents the bubbles and avoids the detachment of a portion of the silica layer when the TLC plate is removed from the agar, but strongly decreases the sensitivity. Thus, the use of aliminium-supported plates is crucial.

These plates can be slightly bent longitudinally in the middle and placed carefully on the agar layer in the Petri dish. In this way, wetting of the silica gel layer proceeds homogeneously in 20–30 s from the middle to the edge of the plate, avoiding trapping of air-bubbles between the agar surface and the thin-layer plate.

Antibiotic medium No. 1 was the culture agar. However, it was prepared in a phosphate saline buffer instead of water. This detail prevents the growth-inhibiting effect of residual solvent or acidic silica sites that causes an initial diffuse inhibition of the contact trace left by the plate on the agar layer. The TLC plate is kept at 4°C for 1 h to allow diffusion from the silica gel into the inoculated agar. It is then gently removed and the bioautographic Petri plate is incubated at 25°C for 14–18 h in sealed plastic bags. Antimicrobial substances are visible on the plates as clear zones without growth of the microorganism.

Although the spaerococcenol A and the extract are insoluble in water, clear inhibition spots have been obtained using moistured agar plates. These, prepared in a few days in advance and stored at 2–8°C, were reequilibrated at 25–30°C to improve their wettability before using for bioautography. In this case an efficient diffusion process takes place from the TLC plate to the agar layer.

The information gained by bioautography led us to a preparative TLC dedicated to the isolation of the active compounds from the extract, avoiding collection of the inactive compounds. Thus, 450 mg of the extract were distributed in four silica gel plates and eluted with the same solvent. The band at R_F 0.32 when scraped off and eluted with diethyl ether gave, after crystallization from n-hexane, 35 mg of sphaerococcenol A identified by comparison of its physical (m.p.) and spectral (infrared, mass and ^{1}H nuclear magnetic resonance) properties with those reported in the literature[5,6]. The TLC band at R_F 0.44 gave instead a mixture (8 mg) of two inseparable brominated compounds with molecular weight 462.

Sphaerococcenol A is still detectable by bioautography when 10 μg of it are spotted and eluted on the TLC plate. Its activity in the diffusion test from a 6-mm antibiotics disc to a Müller-Hinton agar plate is (μg applied), mm zone of inhibition:

against *B*. subtilis, (10) 9; streptomycin sulphate as control, (0.15) 15; against *E. coli*, (10) 8; streptomycin sulphate as control, (1.5) 12; against *P. tracheiphila*, (10) 9; filipin as control, (20) 11.

ACKNOWLEDGEMENTS

REFERENCES

1   J. C. Touchstone and M. F. Dobbins, *Practice of Thin Layer Chromatography*, Wiley, New York, 2nd ed., 1983, pp. 361–365.
2   V. Betina, *J. Chromatogr.*, 78 (1973) 41.
3   G. H. Wagman and M. J. Weinstein, *Chromatography of Antibiotics*, Elsevier, Amsterdam, 1973, p. 7.
4   M. O. Hamburger and G. A. Cordell, *J. Nat. Prod.*, 50 (1987) 19.
5   W. Fenical, J. Finer and J. Clardy, *Tetrahedron Lett.*, (1973) 731.
6   S. De Rosa, S. De Stefano, P. Scarpelli and N. Zavodnik, *Phytochemistry*, 27 (1988) 1875.
7   F. Cafieri, L. De Napoli, E. Fattorusso and C. Santacroce, *Phytochemistry*, 27 (1988) 621; and references cited therein.
8   F. Cafieri, L. De Napoli, E. Fattorusso, M. Piattelli and S. Sciuto, *Tetrahedron Lett.*, (1979) 963; and references cited therein.
9   S. Caccamese and R. Azzolina, *Planta Med.*, 37 (1979) 333.
10 C. H. Collins and P. M. Lyne, *Microbiological Methods*, Butterworths, London, 1970, pp. 113–153.

Note

High-performance liquid chromatographic analysis of β-escin

PIERGIORGIO PIETTA* and PIERLUIGI MAURI

Dipartimento di Scienze e Tecnologie Biomediche, Sezione Chimica Organica, Via Celoria 2, 20133 Milan (Italy)

and

ROBERTO MAFFEI FACINO and MARINA CARINI

Istituto Chimica Farmaceutica Tossicologica, Viale Abruzzi 42, 20131 Milan (Italy)

β-Escin, the active constituent of *Aesculus hippocastanum* L., is a mixture of saponins derived from the triterpenes protoescigenin and barringtogenol[1] (Fig 1). Because of its antiinflammatory, antiedematous and capillaro-protective properties, β-escin is largely employed in the therapy of peripheral vascular disorders[2,3]. In recent years, it has found wide application also in the cosmetic field, mainly for the prevention/treatment of panniculopatia edemato-fibrosclerotica (so-called cellulitis)[4].

In spite of its widespread use, there have been few reports on the high-performance liquid chromatographic (HPLC) analysis of β-escin[5,6] and, due to the lack of standards, the assays described are based on determination of the aglycone
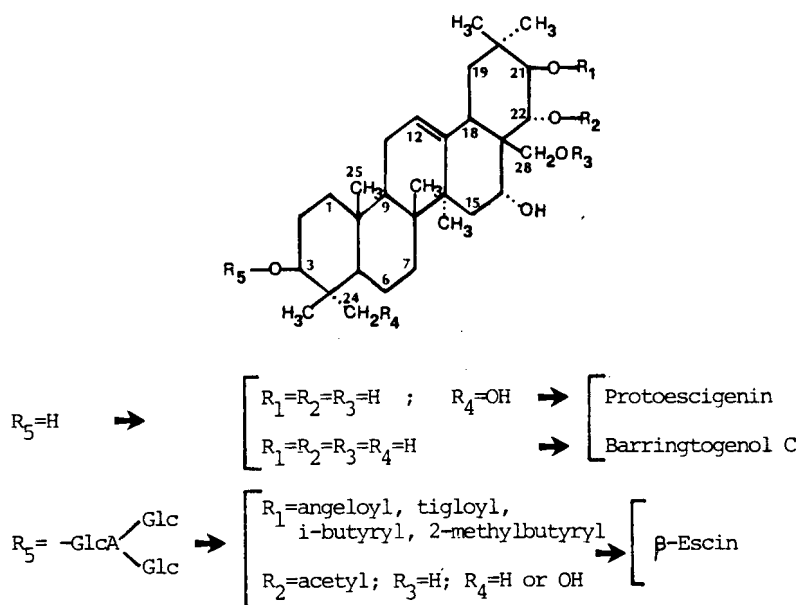
Fig. 1. Chemical structures of β-escin saponins. GlcA = Gluconic acid; Glc = glucose; i = iso.

after alkaline hydrolysis or on relative peak areas. Furthermore, none of the reported methods offers a satisfactory separation of the components, to allow their isolation/characterization.

In this work we describe an efficient isocratic HPLC procedure for the isolation of the main saponin[7] 3-[2″-(β-D-glucopyranosido)-4′-(β-D-glucopyranosido)-β-D-glucuronopyranosido]-21-β-tigloyl-22-α-acetylprotoescigenin (I) and it 21-β-angeloyl analogue (II). These compounds have been used as reference standards for the analysis of β-escin samples.

EXPERIMENTAL

Materials

β-Escin was obtained from different commercial sources (Fluka-Schrepfer and Indena, Milan, Italy). Commercial samples were dissolved in water at a concentration of 0.3 mg/ml and centrifuged at 2500 g for 5 min to remove any particulate material. Acetonitrile and water were of HPLC grade (J. T. Baker, Deventer, The Netherlands).

Chromatographic conditions

The liquid chromatograph consisted of a Model U6K universal injector, a Model 510 pump, a Model Lambda Max 480 UV detector and a Model 990 photodiode array detector (Waters Assoc., Milford, MA, U.S.A.) connected to a CR3A integrator (Shimadzu, Kyoto, Japan).

Chromatographic experiments were performed on Spheri-5 RP-18 (100 mm × 4.6 mm, 5 μm; Brownlee Labs., Santa Clara, CA, U.S.A.) and on Microsorb 3-μm Spherical C_{18} (100 mm × 4.6 mm; Rainin, Woburn, MA, U.S.A.). To preserve the column life, precolumns (RP-18, 5 μm, OD-GU, Brownlee Labs.; Microsorb 3 μm C_{18}, guard No. 80-200-G3, Rainin) were used. The Rainin column and guard-column were supplied by Biolabo Instrument (Milan, Italy).

The mobile phase was acetonitrile–water–20% phosphoric acid (33.5:66.5:0.1), pH 3.2; the flow-rate was 1.0 ml/min. Samples (20 μl) were applied on the column and the peaks were monitored at 205 nm (a.u.f.s. = 0.032).

Isolation of saponins I and II

Aliquots (50 μl) of an aqueous solution of β-escin (2 mg/ml) were repetitively (four or five times) injected and eluted as described above. The major peaks [14.8 (I) and 18.1 (II) min] were collected by means of a Model 201 fraction collector (Gilson, Biolabo, Milan, Italy) and the corresponding fractions were dried under vacuum. Their purity was confirmed by rechromatography.

Mass spectrometry

Fast atom bombardment (FAB) mass spectra were obtained on a VG Analytical Model 70-70 EQ instrument, employing argon atoms with kinetic energy 7 keV. Recordings in the negative ion mode were taken at a resolution of 3000, with a speed of 20S/decade. Data were processed by a Digital PDP 8/A computer system. Matrix: thioglycerol.

RESULTS AND DISCUSSION

The purpose of the present investigation was to develop a simple and rapid HPLC procedure for the isolation of the main saponins (I and II) of β-escin. This required a determination of the chromatographic conditions suitable for a well resolved fingerprinting of β-escin under isocratic conditions. The Brownlee Labs. RP-18 and Microsorb C_{18} columns provided the best resolution in comparison with Bio-Rad C_{18} Nova-pak and Hypersil columns, so confirming the results obtained during a study of Ginseng saponins[8].

To avoid peak broadening due to the presence of carboxyl groups in the escin,
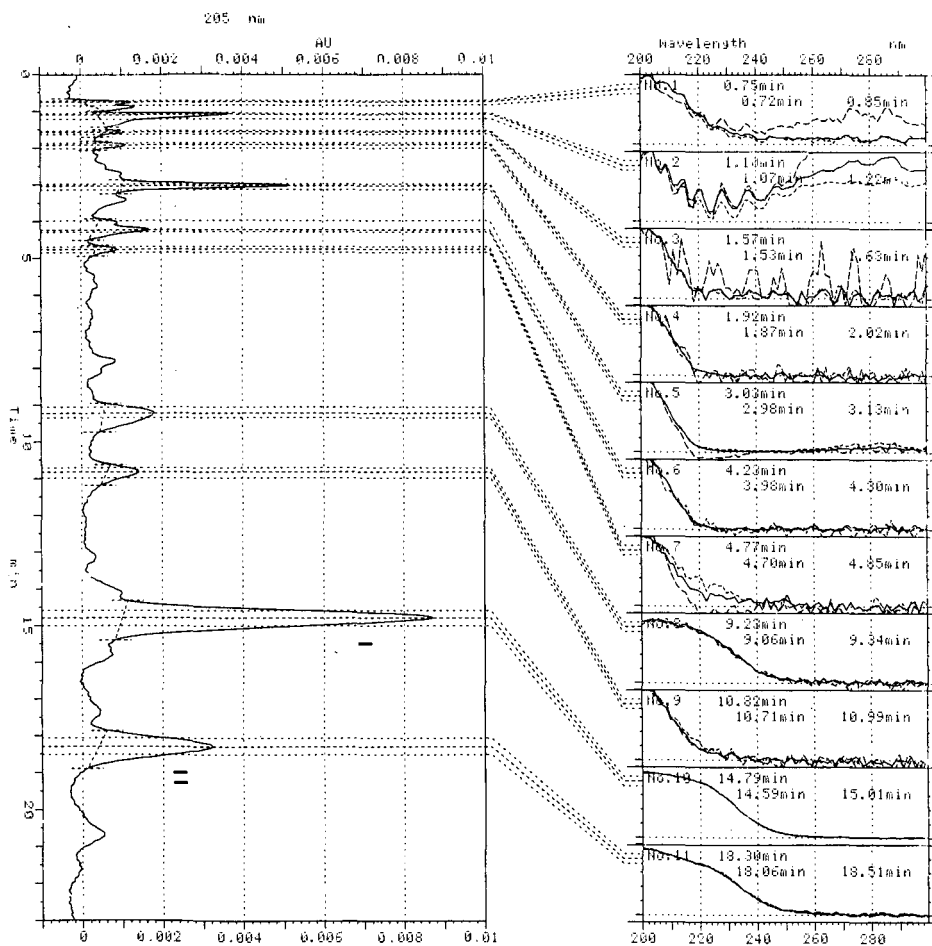
Fig. 2. Chomatogram of β-escin. Peaks: I = 3-[2″-(β-D-glucopyranosido)-4′-(β-D-glucopyranosido)-β-D-glucuronopyranosido]-21-β-tigloyl-22-α-acetylprotoescigenin; II = 3-[2″-(β-D-glucopyranosido)-4′-(β-D-glucopyranosido)-β-D-glucuronopyranosido]-21-β-angeloyl-22-α-acetylprotoescigenin. Eluent: acetonitrile–water 20%–phosphoric acid (33.5:66.5:0.1), pH 3.2; flow-rate, 1.0 ml/min. UV detection at 205 nm. On the right, the spectra of the ascending slopes (·····), the descending slopes (------) and the maxima of the various peaks are shown, together with the respective retention times.

the mobile phase was brought to acidic pH (3.2). Different percentages of acetonitrile and flow-rates were tested. A sharp separation was achieved with 33.5% acetonitrile in water (pH 3.2) over 20 min at a flow-rate of 1.0 ml/min (Fig. 2).

The main peak related to saponin I and the secondary peak related to saponin II were eluted with retention times of 14.8 and 18.1 min, respectively and they were easily collected automatically.

The negative ion FAB mass spectrum of saponin I (Fig. 3a) shows an abundant deprotoned molecular ion at m/z 1130 (the base peak) and fragment ions at m/z 1100 (which arises from the molecular ion by loss of a CH_2OH residue) and at m/z 1088, due to the loss of a $COCH_3$ residue. The other abundant fragment ion at m/z 968 corresponds to cleavage of the glycosidic bond accompanied by transfer of a hydrogen atom from the leaving sugar $[M - H - glucose]^-$. No significant fragment ions were detectable in the lower mass range of the spectrum.

Saponin II shows in the negative ion mode a deprotonated molecular ion at m/z 1130 (the base peak) and a fragmentation pattern perfectly superimposable on that of saponin I (Fig. 3b).

The average contents of saponins I and II were 30–40 and 10–15%, respectively using the isolated, pure compounds as standards.

It is known[7] that of 3-[2''-(β-D-glucopyranosido)-4'-(β-D-glucopyranosido)-β-D-
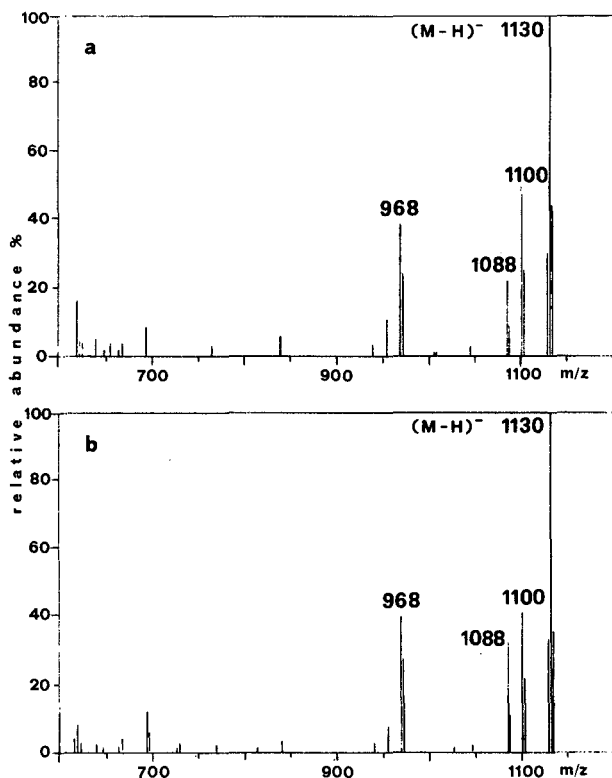
Fig. 3. Negative ion FAB mass spectra of saponin I (a) and saponin II (b).

glucuronopyranosido]-21-β-tigloyl-22-α-acetylprotoescigenin(I) and 3-[2″-(β-D-glu-copyranosido)-4′-(β-D-glucopyranosido)-β-D-glucuronopyranosido]-21-β-angeloyl-22-α-acetylprotoescigenin the first is the major component. Therefore, on this basis and quantitation data, saponins I and II can be assigned as the tigloyl and angeloyl analogues, respectively.

In conclusion, the results of this study show the effectivenes of the method described for the separation of β-escin saponins. The isolation of the major constituents allows a new approach to the assay of β-escin in pharmaceutical and cosmetic formulations, and furthermore gives the possibility of a deeper insight into the pharmacological activity of each component.

REFERENCES

1 E. Stahl and W. Schild, *Pharmazeutische Biologie, 4. Drogenalyse II: Inhaltsstoffe und Isolierung*, G. Fischer Verlag, Stuttgart, 1981.
2 V. M. Rothkopf and G. Vogel, *Arzneim.-Forsch. (Drug Res.)*, 26 (1976) 225.
3 F. Annoni, A. Mauri, F. Marincola, and L. F. Resele, *Arzneim.-Forsch. (Drug Res.)*, 29 (1979) 672.
4 G. Proserpio, S. Gatti and P. Genesi, *Fitoterapia*, 51 (1980) 113.
5 H. Wagner, H. Reger and R. Baurer, *Dtsch. Apoth.-Ztg.*, 124 (1985) 1513.
6 M. Burnouf-Radosevich and N. E. Delfel, *J. Chromatogr.*, 368 (1986) 433.
7 J. Wagner, W. Schlemmer and H. Hoffman, *Arzneim.-Forsch. (Drug Res.)*, 20 (1970) 205.
8 P. G. Pietta, P. L. Mauri and A. Rava, *J. Chromatogr.*, 356 (1986) 212.

Note

Separation of DNA restriction fragments by high-performance ion-exchange chromatography on a non-porous ion exchanger

YOSHIO KATO*, YOSUKE YAMASAKI, AKANE ONAKA, TAKASHI KITAMURA and
TUSTOMU HASHIMOTO

Central Research Laboratory, Tosoh Corporation, Tonda, Shinnanyo, Yamaguchi 746 (Japan)

and

TOMOAKI MUROTSU, SHINICHI FUKUSHIGE and KENICHI MATSUBARA

Institute for Molecular and Cellular Biology, Osaka University, Yamadaoka, Suita, Osaka 565 (Japan)

(First received March 6th, 1989; revised manuscript received May 11th, 1989)

Separation of DNA restriction fragments is often necessary in the field of molecular biology and gene technology. Agarose or polyacrylamide gel electrophoresis has been mainly employed for this purpose. Although conventional and high-performance liquid chromatography was also examined, its resolution was not satisfactory in most cases, particularly for large DNA fragments[1].

Recently, we demonstrated that proteins and oligonucleotides can be separated rapidly with very high resolution by ion-exchange chromatography on a non-porous anion exchanger[2,3]. We have now tested the usefulness of ion-exchange chromatography on the same support for the separation of DNA restriction fragments.

EXPERIMENTAL

Chromatographic measurements were performed with a system consisting of a double plunger pump, Model CCPM, and a variable-wavelength UV detector, Model UV-8000, operated at 260 nm (Tosoh, Tokyo, Japan). The column was TSKgel DEAE-NPR (35 mm × 4.6 mm I.D.) (Tosoh) packed with non-porous spherical hydrophilic resin particles of 2.5 μm diameter whose surfaces are chemically bonded with diethylaminoethyl groups[2]. DNA fragments were separated by gradient elution of sodium chloride in 20 mM Tris–HCl buffer (pH 9.0). All eluents were filtered through a 0.22-μm membrane filter.

A pBR322 DNA-Hae III digest (Sigma, St. Louis, MO, U.S.A.) and a λ DNA-Hind III digest (Pharmacia, Uppsala, Sweden) were used as model samples of small and large DNA restriction fragments. pBR322 DNA-Hae III digest contains 22 fragments of 7 (14), 11 (45), 18 (50), 21 (33), 51 (29), 57 (39), 64 (33), 80 (41), 89 (39), 104 (36), 123 (44), 124 (35), 184 (41), 192 (53), 213 (39), 234 (41), 267 (49), 434 (42), 458 (57), 504 (47), 540 (44) and 587 (57%) base pairs; the numbers in parentheses are the nucleotide compositions (A–T content). λ DNA-Hind III digest contains eight fragments of 125, 564, 2027, 2322, 4361, 6557, 9416 and 23 130 base pairs. A 1 kb DNA ladder from Bethesda Research Labs. (Gaithersburg, MD, U.S.A.) was also used

although some components are not restriction fragments. It contains 23 fragments with a wide range of chain lengths: 75, 142, 154, 200, 220, 298, 344, 394, 506, 516, 1018, 1635, 2036, 3054, 4072, 5090, 6108, 7126, 8144, 9162, 10 180, 11 198 and 12 216 base pairs. These samples were heated at 65°C for 5 min and then cooled quickly in ice–water before injection.

RESULTS AND DISCUSSION

Fig. 1 shows a chromatogram of pBR322 DNA-Hae III digest. Peaks were estimated as indicated in the figure by considering that DNA fragments are mainly eluted in order of increasing chain length; fragments having high A–T contents are eluted slightly later than expected from their chain lengths and the peak areas are approximately proportional to the chain lengths[4]. (Fragments of 7 and 11 base pairs were not assigned although two of several peaks appearing before 2 min are supposed to correspond to them.) This assignment is considered to be correct by comparison between this result and one reported previously for the separation of the same sample on a porous ion exchanger, where peaks were assigned by polyacrylamide gel electrophoresis[5]. Therefore, small DNA fragments (less than 600 base pairs) can be separated almost completely when they differ in chain length by 5–10%.

Fig. 2 shows a chromatogram of λ DNA-Hind III digest. Five large peaks were collected and examined by agarose gel electrophoresis. The first peak contained two fragments of 2027 and 2322 base pairs. Another four peaks contained only single fragments of 4361, 6557, 9416 and 23 130 base pairs, respectively. This result suggests that ion-exchange chromatography on a non-porous ion exchanger is also very effective even for large DNA fragments over 1000 base pairs. It is possible to achieve almost baseline separations in a very short time, e.g., 5 min, for large fragments differing in chain length by more than 50%. It is also possible to improve the separation to some extent by employing a flow-rate lower than 1.0 ml/min, as explained later, although the separation time becomes slightly longer.

Fig. 1. Chromatogram of pBR322 DNA-Hae III digest (4.8 μg in 8 μl). The separation was performed on a TSKgel DEAE-NPR column with a 0.1-min linear gradient from 0.25 to 0.45 M sodium chloride followed by a 2.9-min linear gradient from 0.45 to 0.5 M and a 57-min linear gradient from 0.5 to 1.0 M in 20 mM Tris–HCl buffer (pH 9.0) at a flow-rate of 1.5 ml/min and 25°C. The numbers on the peaks are the estimated chain lengths of the DNA fragments in base pairs.

Hecker et al.[6] and Westman et al.[5] recently reported separations of DNA restriction fragments. They employed porous anion exchangers having large pores and obtained good separations. However, their applications were limited to rather small fragments, mostly smaller than 1000 base pairs in chain length, and took much langer times (1–8 h with some exceptions) than in Figs. 1 and 2. Stowers et al.[7] and Merion et al.[8] recently reported quite nice separations of a wide range of nucleic acids including large DNA restriction fragments by high-performance ion-exchange chromatography. The resolutions attained by them and those here seem to be equivalent, while the separation times in Figs. 1 and 2 are shorter.

The recovery of DNA restriction fragments from the column was examined for the separations in Figs. 1 and 2. The recovery was estimated from the areas of the peaks eluted. As controls, we used peak areas observed when the column was replaced with an empty 1 mm I.D. stainless-steel tube of 1 ml total inner volume. Both samples were recovered in high yield, more than 85%.

The effect of some operational variables was studied. In the separation of small fragments with constant gradient time, the resolution increased with increasing flow-rate up to around 1.0 ml/min and then decreased with further increase in the flow-rate. On the other hand, the flow-rate required to obtain the highest resolution was lower than 1.0 ml/min in the separation of large fragments, although the flow-rate dependence of the resolution was not so significant. It seemed to be 0.5–0.8 ml/min for 1000–5000 base pair fragments and 0.3–0.5 ml/min for 5000–20000 base pair fragments. Although the resolution continuously increases with decreasing gradient
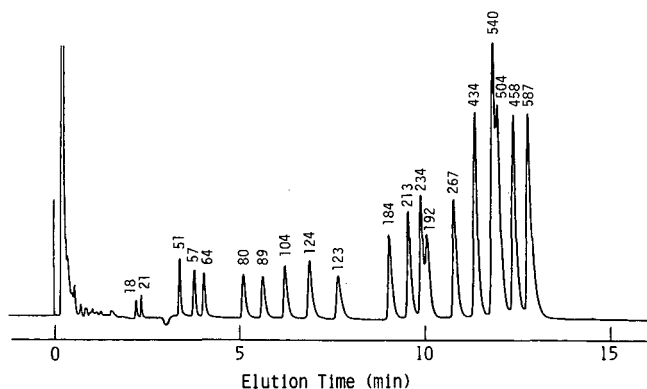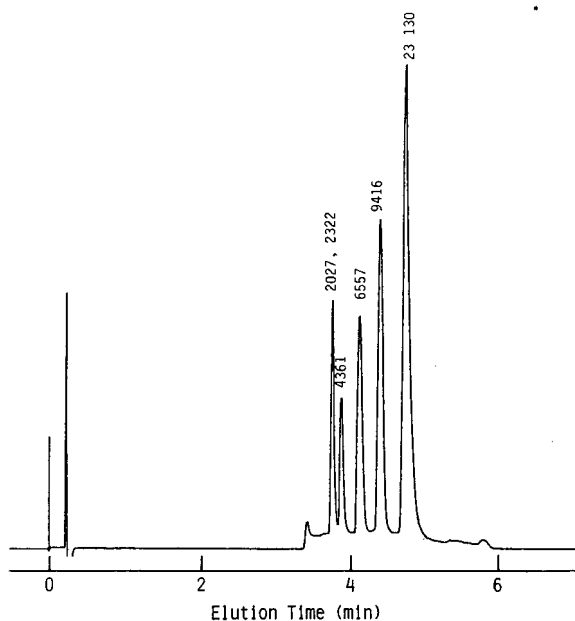

Fig. 2. Chromatogram of λ DNA-Hind III digest (2 μg in 4 μl). The separation was performed on a TSKgel DEAE-NPR column with a 10-min linear gradient from 0.5 to 1.0 M sodium chloride in 20 mM Tris–HCl buffer (pH 9.0) at a flow-rate of 1.0 ml/min and 25°C. Numbers are chain lengths of DNA fragments in base pairs identified by agarose gel electrophoresis.

steepness in general, there existed a certain gradient steepness which provided the highest resolution. This depended on the size of the fragment. It was 10–20 mM NaCl/min for fragments less than 1000 base pairs, 20–30 mM NaCl/min for 1000–5000 base pair fragments and 30–50 mM NaCl/min for 5000–20 000 base pair fragments. Accordingly, gradients shallower than these values should not be employed because there is no advantage. They result in not only lower resolution but also longer separation times and greater dilution of the sample. Steeper gradients should be selected of course when more rapid separations are required. The separation in Fig. 1 was carried out with a rather complicated gradient constructed with three linear portions for speed and yet satisfactory resolution. The column length had little influence on the resolution, particularly in the separation of large fragments. Slightly better separations were achieved with longer columns. Therefore, separations can be improved by using two or three columns connected in series, as exemplified in Fig. 3. The resolution was almost independent of temperature in the range of 25–65°C, while the elution of DNA fragments was slightly delayed with increasing temperature. The maximum sample load in order to obtain the highest resolution was rather low, as anticipated. In the separation of λ DNA-Hind III digest the resolution was almost constant at sample loads up to 10 μg, and then gradually decreased with further increase in the sample load.
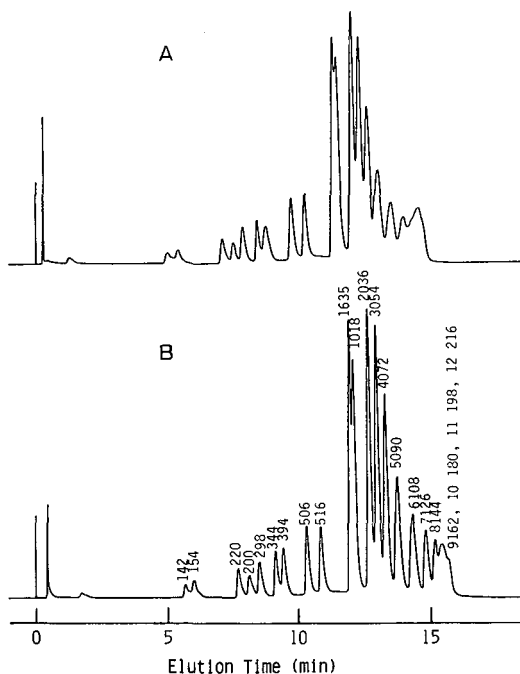
Fig. 3. Chromatograms of a 1 kb DNA ladder (6.3 μg in 6 μl). The separations were performed on one (A) and two (B) TSKgel DEAE-NPR columns with a 60-min linear gradient from 0.5 to 1.0 M sodium chloride in 20 mM Tris–HCl buffer (pH 9.0) at a flow-rate of 1.0 ml/min and 25°C. Numbers are the chain lengths of the DNA fragments in base pairs, estimated by comparing this result with one obtained by Merion et al.[8], who separated the same sample and identified peaks by agarose gel electrophoresis of collected fractions.

As demonstrated, ion-exchange chromatography on the non-porous anion exchanger, TSK gel DEAE-NPR, is very useful for the separation of DNA restriction fragments. A wide range of DNA fragments, from small to very large ones, can be separated in 5–15 min with high resolution. The recovery of DNA fragments was also high ($>85\%$). Although gel electrophoresis is the most common technique used to separate DNA fragments owing to its high resolution, it has some problems in quantitative measurements of the components, scaling up, recovery of the separated components, etc. On the other hand, ion-exchange chromatography does not have such problems. Accordingly, ion-exchange chromatography on TSK gel DEAE-NPR should be a good alternative to gel electrophoresis for the analysis and purification of DNA fragments.

REFERENCES

1 Y. Kato, M. Sasaki, T. Hashimoto, T. Murotsu, S. Fukushige and K. Matsubara, *J. Chromatogr.*, 320 (1985) 440.
2 Y. Kato, T. Kitamura, A. Mitsui and T. Hashimoto, *J. Chromatogr.*, 398 (1987) 327.
3 Y. Kato, T. Kitamura, A. Mitsui, Y. Yamasaki, T. Hashimoto, T. Murotsu, S. Fukusige and K. Matsubara, *J. Chromatogr.*, 447 (1988) 212.
4 Y. Kato, M. Sasaki, T. Hashimoto, T. Murotsu, S. Fukushige and K. Matsubara, *J. Chromatogr.*, 265 (1983) 342.
5 E. Westman, S. Eriksson, T. Låås, P.-Å. Pernemalm and S.-E. Sköld, *Anal. Biochem.*, 166 (1987) 158.
6 R. Hecker, M. Colpan and D. Riesner, *J. Chromatogr.*, 326 (1985) 251.
7 D. J. Stowers, J. M. B. Keim, P. S. Paul, Y. S. Lyoo, M. Merion and R. M. Benbow, *J. Chromatogr.*, 444 (1988) 47.
8 M. Merion, W. Warren, C. Stacey and M. E. Dwyer, *BioTechniques*, 6 (1988) 246.

Note

High-performance liquid chromatographic determination of zearalenone and ochratoxin A in cereals and feed

W. LANGSETH*, Y. ELLINGSEN, U. NYMOEN and E. M. ØKLAND

Department of Pharmacology and Toxicology, National Veterinary Institue/The Norwegian College of Veterinary Medicine, P.O. Box 8146 Dep., 0033 Oslo 1 (Norway)

(First received February 27th, 1989; revised manuscript received May 23rd, 1989)

Cereals and mixed feed are frequently contaminated with mycotoxins produced by different fungi. Two of the more important ones are ochratoxin A and zearalenone[1–3]. In Norway ochratoxins are normally produced by *Penicillium verrucosum* and the A type is predominant. Zearalenone is like the trichothecenes a fusarium toxin. The gas chromatographic method normally used for the trichothecenes gives, however, low recovery[4].

Zearalenone and ochratoxin A can be analyzed by high-performance liquid chromatography (HPLC) under very similar conditions[5]. Howell and Taylor[6] have described a method for determination of aflatoxins, ochratoxin A and zearalenone in feed. The recoveries of ochratoxin A achieved by using this method are, however, sometimes poor.

In this paper a modified method for the determination of zearalenone and ochratoxin A is described. Aflatoxin is omitted because it is of minor importance in cereals grown in northerns countries like Norway. Modern solid phase extraction columns were used for clean up. These minicolumns are convenient to use and the solvent consumption is less than 1/10 of that of traditional columns. The procedure given was optimized for different types of cereals and feed.

One hundred samples of wheat, barley, oats and mixed feed have been analyzed by the procedure described. The detection limits were 2–5 μg/kg for zearalenone, depending on the type of feed, and 0.1–0.3 μg/kg for ochratoxin A.

EXPERIMENTAL

Reagents

Ochratoxin A and zearalenone were obtained from Sigma. The following stock solutions were made: (a) zearalenone, 20 mg/l in acetonitrile; (b) ochratoxin A, 1 mg/l in toluene–acetic acid (9:1).

Other chemicals were obtained from the following sources: Celite from Supelco; clean-up columns were Bond Elut, SI (silica), 500 mg, from Analytichem International.

All solvents used for the clean-up procedure were of p.A. grade (Merck), while the solvents used as the mobile phase for HPLC were of HPLC grade (Rathburn).

Apparatus

The flask shaker was a universal shaking machine from Edmund Bühler, Type SM 2.5. The vacuum manifold used in connection with the clean-up columns were obtained from Supelco. The HPLC equipment was obtained from Perkin-Elmer, and consisted of a dual-pump module (Series 2) with a Rheodyne injector (Model 7125) or a Series 10 pump with an ISS-101 autoinjector. The detector was an LS-4 fluorescence spectrophotometer. The integrator system was either a LC-100 integrator or an Omega-2 data system.

The analytical column was a Nucleosil C_8, 5 μm reversed-phase column, 125 mm × 4 mm I.D. The 50-mm guard column was dry packed with LC-8 pellicular packing, 40 μm (Supelco).

Sample preparation

The samples were kept in a deep freezer at $-18°C$ until analyzed. The whole sample was ground and mixed well before an analytical sample was taken.

Extraction and clean up

A 50-g amount of ground sample was mixed with 250 ml chloroform and 25 ml 0.1 M phosphoric acid in a 1-l flask. Celite (10 g) was added to wheat and barley samples. The flask was shaken automatically for 45 min. Wheat and barley samples were filtered through folded filters, while the mixture of extraction solvent and solid material of oat and mixed feed samples was transferred to a 250-ml centrifuge-tube and centrifuged for 10 min at 9000 g before filtration. The centrifugate was then decanted and filtered through a folded filter containing 2 g Celite.

A 25-ml volume of the wheat and barley extracts, and 15 ml of the oat and mixed feed extracts, was transferred to pear-shaped flasks and evaporated almost to dryness on a rotary evaporator. Dichloromethane (10 ml) was added to the residues.

Column clean up

The column was connected to the vacuum manifold after addition of about 2 g dried Na_2SO_4 to the top of it. A 5-ml volume of hexane and 5 ml dichloromethane were washed through the column before the sample extract was transferred quantitatively to the column. The solvent was drained to the top of the layer of Na_2SO_4 and the column was washed with 10 ml dichloromethane, 10 ml hexane and 10 ml toluene. Thereafter, zearalenone was eluted with 8 ml toluene–acetone (95:5). Ochratoxin A was eluted with 6 ml toluene–acetic acid (9:1). The two fractions were collected in separate 12-ml conical centrifuge-tubes.

The eluates were evaporated to dryness under a stream of nitrogen. A 250-μl volume of acetonitrile and 250 μl 0.1 M phosphoric acid were added to each residue and mixed on a Whirlimixer for 1 min. The samples were then sonicated for 5 min and mixed once more on the Whirlimixer before centrifugation for 10 min at 2000 g. An 100-μl volume of the supernatant was transferred to an HPLC sample vial.

HPLC analysis

A 20-μl volume of the extract was injected into the chromatograph. Methanol–0.01 M orthophosphoric acid (58:42) was used as the mobile phase. The flow-rate was 1 ml/min, and the excitation wavelength of the fluorescence detector was set at 270 nm

for zearalenone and 340 nm for ochatoxin A, while the emission wavelength in both cases was 465 nm.

RESULTS AND DISCUSSION

Chloroform–phosphoric acid (250:25) is an effective extraction medium for ochratoxin and zearalenone[6,7].

Oat samples and mixed feed samples did not become clear after filtration, not even after addition of Celite. A clear extract was required for the further clean-up procedure on the minicolums. Centrifugation of the extract including the feed followed by filtration gave, however, a clear extract.

Minicolumns or solid phase extraction columns were used. Up to twelve samples were easily handled at the same time. From wheat and barley samples extracts equivalent to 5 g of cereals can be placed on columns containing 500 mg of packing material. In extracts from oats and mixed feed the amount of contamination is higher, thus extracts equivalent to only 3-g samples can be placed on the columns. Otherwise a reduced recovery was observed, especially for zearalenone.

Sodium sulphate was added to the top of the silica minicolumn to reduce the water content of the dichloromethane extract, and thereby also the elution strength of the solution.

The necessity for each washing step was examined. Omission of the dichloromethane step gave a less clean chromatogram for zearalenone. Washing with toluene can in some cases be omitted, but not always. The procedure originally contained a washing step with chloroform–methanol (97:3) after the elution of zearalenone as described by Howell and Taylor[6]. A very low recovery was then occasionally obtained for ochratoxin; the toxin had been washed out with the chloroform–methanol solution.

Of the zearalenone 95% was found in the 2–6 ml fraction when eluted with 10 ml toluene–acetone (95:5), while 95% of the ochratoxin was eluted with 4 ml toluene–acetic acid (9:1). Aflatoxins may at this state be eluted with 10 ml chloroform–methanol (97:3)[6,8].

The eluate of zearalenone was normally coloured, often green. When evaporated to dryness, green drops were seen which did not dissolve in acetonitrile–phosphoric acid. Sonication and mixing with a Whirlimixer ensured the dissolution of zearalenone. By centrifugation a clear extract was obtained which can be injected directly into the HPLC system. Filtration of the extract can then be omitted.

Both a reversed-phase[6,7,9] and a normal-phase[10,11] chromatographic system have been used for the determination of zearalenone by HPLC, while only a reversed-phase has been used for ochratoxin A[6,7]. Elution of ochratoxin A, containing a carboxylic acid group, requires an acidic mobile phase. Even though zearalenone and ochratoxin A cannot be chromatographed at the same time, it is preferable to use the same mobile phase. Both acetonitrile and methanol can be used as the organic modifier of the mobile phase. Either methanol–0.01 M phosphoric acid (58:42) or acetonitrile–0.01 M phosphoric acid (40:60) was used when the Nucleosil C_8 column was used. A Supelcosil C_{18} column was also tried. This column can be used when the washing step with dichloromethane in the clean-up procedure is not omitted.

Both 275 (ref. 6) and 236 nm (refs. 9–12) have been used as excitation wavelength
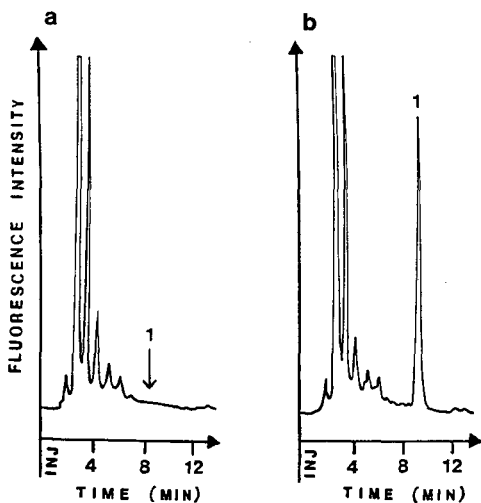
Fig. 1. Chromatogram of (a) barley sample containing no zearalenone and (b) the same sample spiked to contain 100 μg/kg zearalenone (1). Column: Nucleosil C_8, 5 μm, 50 mm × 4.6 mm + 125 mm × 4 mm I.D. Mobile phase: methanol–0.01 M phosphoric acid (58:42). Detector: fluorescence spectrophotometer; excitation at 270 nm, emission at 465 nm.

for zearalenone. A similar or higher signal-to-noise ratio was obtained with 275 nm as with 236 nm. The former was chosen because of the higher selectivity.

About 100 samples have been analyzed by the method described: 36 samples contained detectable amounts of zearalenone and 54 samples contained detectable amounts of ochratoxin. The highest amounts were found to be 137 and 1300 μg/kg,
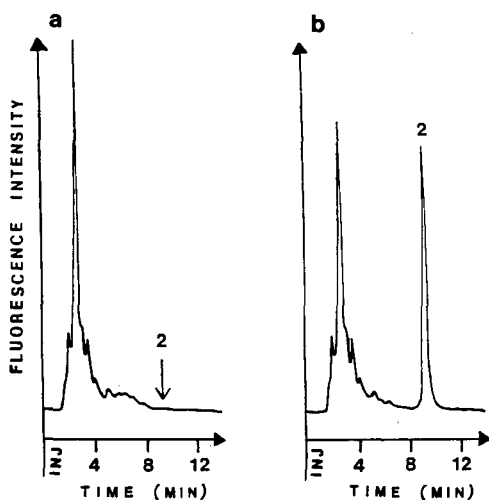
Fig. 2. Chromatogram of (a) barley sample containing no ochratoxin and (b) the same sample spiked to contain 5 μg/kg ochratoxin (2). Chromatographic conditions as in Fig. 1, except that 340 nm was used as the excitation wavelength.

TABLE I

RECOVERY TESTS DONE ON DIFFERENT TYPES OF SAMPLES

Wheat and barley samples were spiked to contain 100 μg/kg zearalenone and 5 μg/kg ochratoxin A in addition to the natural contamination by these mycotoxins. The figures were 167 and 8.3 μg/kg, respectively, for oat and mixed feed samples. See text for further information.

Recovery (%)	Zearalenone				Ochratoxin			
	Wheat	Barley	Oat	Feed[a]	Wheat	Barley	Oat	Feed
Mean	83	89	78	77	96	92	81	77
S.D.	8	6	6	10	8	15	15	21
n[b]	9	10	15	9	11	9	14	6

[a] Mixed feed.
[b] Number of samples.

respectively. The identity of the HPLC peaks was verified by fluorescence spectra when samples contained high amounts of the mycotoxins. These results will be published elsewhere.

Typical chromatograms of samples containing no zearalenone and ochratoxin and samples spiked to contain the same mycotoxins are shown in Figs. 1 and 2.

At least one recovery test was done for each set of samples analyzed. A 500-ng amount of zearalenone and 25 ng ochratoxin A were added to an extra aliquot of a chloroform extract of the sample. The same clean up and HPLC method was used for these extracts as for the other ones. The standard solution was added to the chloroform extract instead of to the cereal sample itself in routine analysis to save time and solvent. We found no significant difference in recovery between the two methods, the average being 8% in favour of addition to the cereals. The standard deviation was 9% for eight samples. The average of the recovery tests obtained for zearalenone and ochratoxin in different types of samples are shown in Table I.

The reproducibility of the method was checked for different types of samples.

TABLE II

REPRODUCIBILITY TEST ON FOUR DIFFERENT SAMPLES

Mean relative standard deviation: 18% (15%[a]).

Sample	Zearalenone				Ochratoxin			
	Wheat	Barley	Oat	Feed[b]	Wheat	Barley	Oat	Feed
1 (μg/kg)	34	4	<5	15	<0.1	86	4.5	0.8
2 (μg/kg)	41	6	<5	20	<0.1	119	4.8	0.4
3 (μg/kg)	42	6	<5	16	<0.1	105	4.0	0.5
4 (μg/kg)	29	5	<5	13	<0.1	123	4.0	0.5
Mean (μg/kg)	37	5	—	16	—	108	4.3	0.6
S.D. (μg/kg)	6	1	—	3	—	17	0.4	0.2
R.S.D. (%)	17	18	—	18	—	15	9	31

[a] Ochratoxin in feed is not included, because of its low content.
[b] Mixed feed.

Four samples were analyzed four times each for zearalenone and ochratoxin A. The results are given in Table II. The samples were ground especially well before the analysis, to remove the inhomogeneities that always exist in mycotoxin samples. Some variations in the results may nevertheless reflect inhomogeneities in the samples.

The detection limit depended on the type of sample, being highest for mixed feed and oat samples. It was found to vary between 2 and 5 μg/kg for zearalenone and between 0.1 and 0.3 μg/kg for ochratoxin.

CONCLUSIONS

A rapid, sensitive and selective method for the determination of the important mycotoxins zearalenone and ochratoxin A is presented.

The clean-up procedure given is optimized for modern solid phase extraction columns, which are much easier to handle than conventional columns. The method involves no liquid–liquid extraction or other time-consuming steps. The identification and quantification is by HPLC. Clean chromatograms are obtained in most cases, making it easy to identify the zearalenone and ochratoxin peaks. Even with complicated mixed feed samples, the mycotoxins can be determined without further purification of the eluate from the minicolumn, which is recommended by other workers[5,6].

REFERENCES

1 R. J. Cole, *Modern Methods in the Analyis and Structural Elucidation of Mycotoxins*, Academic Press, New York, 1986.
2 J. E. Smith and M. O. Moss, *Mycotoxins, Formation, Analysis and Significance*, Wiley, New York, 1985.
3 P. Krogh, *Mycotoxins in Food*, Academic Press, London, 1987.
4 C. E. Kientz and A. Verweij, *J. Chromatogr.*, 355 (1986) 229.
5 E. Josefsson and T. Möller, *J. Assoc. Off. Anal. Chem.*, 62 (1979) 1165.
6 M. V. Howell and P. W. Taylor, *J. Assoc. Off. Anal. Chem.*, 64 (1981) 1356.
7 E. Josefsson and T. Möller, *J. Assoc. Off. Anal. Chem.*, 62 (1979) 1165.
8 W. Langseth, unpublished results.
9 G. A. Bennett, O. L. Shotwell and W. F. Kwolek, *J. Assoc. Off. Anal. Chem.*, 68 (1985) 958.
10 M. E. Olsen, H. I. Pettersson, K. A. Sandholm and K.-H. C. Kiessling, *J. Assoc. Off. Anal. Chem.*, 68 (1985) 632.
11 T. Tanaka, A. Hasegawa, Y. Matsuki, U.-S. Lee and Y. Ueno, *J. Chromatogr.*, 328 (1985) 271.
12 D. L. Orti, R. H. Hill, J. A. Liddle and L. L. Needham, *J. Anal. Toxicol.*, 10 (1986) 41.

Note

Chromatographic method for determination of hexuronic acid in dermatan sulphate

HIDEKI UCHIYAMA, AKIRA OGAMO and KINZO NAGASAWA*

School of Pharmaceutical Sciences, Kitasato University, 5-9-1, Shirokane, Minato-ku, Tokyo 108 (Japan)

(First received March 6th, 1989; revised manuscript received May 23rd, 1989)

A number of dermatan sulphate–chondroitin sulphate copolymers (so-called dermatan sulphates) having different hexuronic acid contents, degrees of sulphation and molecular weights, have been reported[1]. The hexuronic acid contents in these polysaccharides were conventionally estimated by the carbazole–orcinol ratio[2], which has been widely used for approximate estimation of the ratio of D-glucuronic acid to L-iduronic acid in glycosaminoglycans containing both hexuronic acids. Later, an enzymatic procedure using chondroitinase AC and ABC[3,4] was frequently utilized for microdetermination of hexuronic acid in the above-mentioned copolymers.

Recently we required a method to check the reliability of the enzymatic procedure. The method described herein was devised to satisfy our requirements, but it turned out to be useful as a general method for the chemical assay of the hexuronic acid content with the aid of a combination of gel filtration and ion-exchange chromatography.

EXPERIMENTAL

Materials and methods

Rooster-comb dermatan sulphates (sodium salts, RC-20 and RC-30 fractions) were as described previously[4]. Pig-skin dermatan sulphate (sodium salt, M_r 20 000) was obtained as a 20% ethanol fraction by fractionation with ethanol of the calcium salt according to the procedure of Meyer *et al.*[5]. Derivatives of these dermatan sulphates, which had been labelled with a 2-aminoethylamino group at the reducing end of the polysaccharide chain, were as described previously[6].

Standard N-acetylchondrosine and N-acetyldermosine were as described previously[7]. 1,2-Isopropylidene-L-iduronolactone was obtained from Nakarai Chemicals (Kyoto, Japan), and D-glucurono-6,3-lactone from Sigma (St. Louis, MO, U.S.A.). Chondroitinase AC-II from *Arthrobacter auresens* and chondroitinase ABC from *Proteus vulgaris* were obtained from Seikagaku Kogyo (Tokyo, Japan). AG 1-X4 anion-exchange resin (200–400 mesh) and Sephadex G-25 were obtained from Bio-Rad Labs. (Richmond, CA, U.S.A.) and Pharmacia Fine Chemicals (Uppsala, Sweden), respectively.

Hexuronic acid was determined by the method of Bitter and Muir[8], modified by increasing the borate concentration to 0.2 M, and by using D-glucurono-6,3-lactone and 1,2-isopropylidene-L-iduronolactone as standards[9].

Enzymatic determination of hexuronic acid in dermatan sulphates and their 2-amino-
ethylamino derivatives

To a solution of the sample (100 µg in 20 µl of water) were added enriched Tris buffer[10], pH 8.0 (10 µl) and chondroitinase AC-II (0.5 units in 20 µl of water), and the mixture was incubated at 37°C for 5 h. To another sample of the material (100 µg in 20 µl of water) were added enriched Tris buffer (10 µl) and chondroitinase ABC (0.2 units in 20 µl of water), and the mixture was incubated for 5 h at 37°C. The absorbance at 232 nm was measured for each incubation mixture to obtain the ratio of A_{232} (chondroitinase AC-II) to A_{232} (chondroitinase ABC) which gave the proportion of D-glucuronic acid in the total hexuronic acid content (%)[3].

Determination of hexuronic acid in dermatan sulphates and their 2-aminoethylamino
derivatives

Hydrolysis of the polysaccharide materials with dimethyl sulphoxide containing
10% water. A solution of the sample ($\approx$ 6 mg per 0.4 ml water) was passed through a column of Dowex 50W-X2 (H$^+$, 50–100 mesh) at 0–4°C. The eluent and washings were pooled, neutralized (pH 6.0) by the addition of pyridine and lyophilized to give the pyridinium salt as a white powder. A solution of the pyridinium salt ($\approx$ 6 mg) in dimethyl sulphoxide containing 10% of water (1.5 ml) was heated in a Pyrex test-tube (10 cm × 0.7 cm) fitted with a PTFE screw-cap and stirred with PTFE stirrer (diameter 0.5 cm) for 30 h at 108 $\pm$ 1°C. After cooling in an ice-batch, the contents of the test-tube were diluted in an equal volume of water and transferred to a distillation flask (volume 20 ml), then neutralized (pH 6.0) with 0.1 M NaOH. The solution obtained was evaporated to dryness at 30–35°C under reduced pressure.

Separation on Sephadex G-25 and AG 1-X4 anion-exchange resin, of the
hydrolysate into N-acetyldermosine, N-acetylchondrosine, L-iduronic acid and D-glu-
curonic acid, and determination of the ratio of D-glucuronic acid to total hexuronic acid.
The hydrolysate obtained above was dissolved in 0.1 M ammonium hydrogen-carbonate (0.5 ml) and loaded on a column (85.5 cm × 1.5 cm) of Sephadex G-25 prepared in the same solvent. The column was eluted at 20–25°C with the same solvent at a flow-rate of 34 ml/h. Each fraction (2 ml) was analyzed for hexuronic acid (the elution diagrams are shown in the insets of Fig. 1a, b). The fractions corresponding to the disaccharide and monosaccharide peaks (tube Nos. 46–65 of the elution diagrams in the insets of Fig. 1a, b) were pooled and lyophilized. The residue was dissolved in water (0.5 ml) and loaded on a column (85.5 cm × 1.0 cm) of AG 1-X4 (HCO$_2^-$, 200–400 mesh) prepared in water. The column was eluted at 40°C with 0.2 M formic acid at a flow-rate of 24 ml/h. Each fraction (3.9 ml) was analyzed for hexuronic acid (Fig. 1a, b). The sum of the peak areas due to N-acetylchondrosine and D-glucuronic acid in each elution diagram of Fig. 1 provides an estimate of the content of D-glucuronic acid in the sample, and the sum of the peak areas due to N-acetyl-dermosine and L-iduronic acid affords that of L-iduronic acid in the sample.

RESULTS AND DISCUSSION

One of us reported previously that the reaction of the pyridinium salts of dermatan sulphates in dimethyl sulphoxide containing 10% of water at 105°C for 30 h afforded higher oligosaccharide ($\geq$ tetrasaccharide, 18.3%), disaccharide (69.2%)

and monosaccharide fractions (12.5%, based on hexuronic acid determination, respectively), and recommended this procedure as an improved method for preparing N-acetyldermosine and L-iduronic acid from dermatan sulphates[7]. The essential feature of the hydrolysis in dimethyl sulphoxide containing a small amount of water is the initial rapid cleavage of the sulphate groups of sulphated mucopolysaccharides under moderately acidic conditions. This probably results from the solvation between protons and dimethyl sulphoxide molecules in the reaction medium: the 2-acetamido-2-deoxy-β-D-hexosyl linkages of the resulting desulphated mucopolysaccharides are
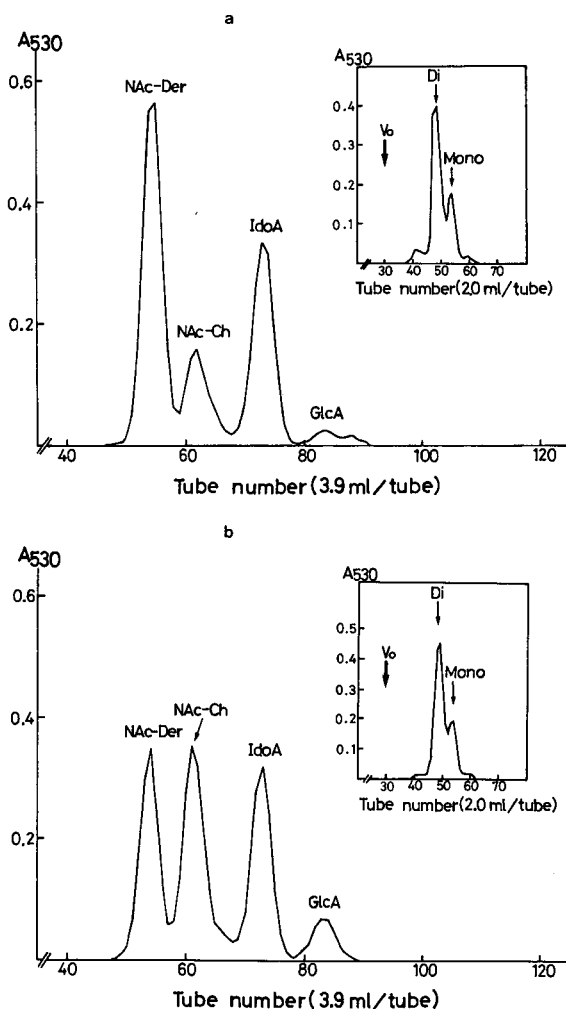
Fig. 1. Anion-exchange chromatography, on AG 1-X4 resin(HCO_2^-), of the mono- and disaccharide reaction products of dermatan sulphates treated with water–dimethyl sulphoxide (1:9, v/v) for 30 h at 108 $\pm$ 1°C. (a) Pig-skin dermatan sulphate; (b) rooster-comb dermatan sulphate, RC-30 fraction. Gel filtration diagrams, on Sephadex G-25, of the whole reaction products from dermatan sulphate are shown in each inset. NAc-Der = N-acetyldermosine; NAc-Ch = N-acetylchondrosine; IdoA = L-iduronic acid; GlcA = D-glucuronic acid; Di = disaccharide fraction; Mono = monosaccharide fraction; V_o = void volume.

preferentially cleaved and gradual liberation of the hexuronic acid residues takes place without any marked decomposition of them.

We have investigated an optimum reaction condition to minimize the amount of unreacted oligosaccharide (18.3% of the total material subjected to hydrolysis) without decomposition of hexuronic acid components, especially of L-iduronic acid, and have succeeded in obtaining the disaccharide and monosaccharide fractions almost quantitatively by heating the pyridinium salts of the polysaccharides in water–dimethyl sulphoxide (1:9, v/v) at 108 ± 1°C for 30 h. As shown in Fig. 1, pig-skin and rooster-comb (RC-30) dermatan sulphates were almost completely hydrolyzed to the constitutional disaccharide and monosaccharide species under the conditions described. Although the elution data are not shown here, rooster-comb (RC-20) dermatan sulphate and 2-aminoethylamino derivatives of these dermatan sulphates all give results similar to those of Fig. 1. A small peak (tube Nos. 35–45) before the disaccharide peak is mainly due to unreacted oligosaccharides, and another small peak (tube Nos. 57–65) after the monosaccharide peak is due to lactones of D-glucuronic acid and L-iduronic acid (the insets of Fig. 1). The carbazole–orcinol ratio of the small peak (tube Nos. 35–45) was assayed to determine the approximate hexuronic acid content, and the value roughly agreed with those obtained by the method proposed herein (experiments and data not shown), indicating no appreciable error due to neglect of this small peak from the whole procedure. All the fractions except the first small peak (tube Nos. 35–45) were subjected to subsequent separation on AG 1-X4 ion-exchange resin. The separation was satisfactory as shown in Fig. 1. HPLC with a Whatman Partisil-10 SAX or Partisil-10 PAC column using a linear gradient of potassium dihydrogenphosphate, or with a reversed stationary phase column (ODS) using an acetonitrile–water system, did not resolve the mono- and disaccharide reaction products from dermatan sulphate (data not shown).

The hexuronic acid contents of the dermatan sulphates and of their 2-amino ethylamino derivatives determined by the above method were in close agreement with those obtained by the enzymatic method as shown in Table I. Our method, which

TABLE I

RATIOS OF D-GLUCURONIC ACID CONTENT TO TOTAL HEXURONIC ACID CONTENT (%) IN DERMATAN SULPHATES AND THEIR 2-AMINOETHYLAMINO DERIVATIVES, ASSAYED BY BOTH ENZYMATIC AND THE PRESENT METHODS

Sample	Ratio of D-glucuronic acid to total hexuronic acid(%)	
	Enzymatic method	Present method
Pig-skin dermatan sulphate	18.6	19.1
Rooster-comb dermatan sulphate		
RC-20 fraction	21.5	23.7
RC-30 fraction	40.9	42.8
2AEA pig-skin dermatan sulphate[a]	19.1	21.6
2AEA rooster comb dermatan sulphate		
RC-20 fraction	22.6	22.1
RC-30 fraction	41.4	42.8

[a] 2AEA = 2-aminoethylamino.

consists of acid hydrolysis and chromatographic separation, is necessarily accompanied by some errors due to these two processes. One of them would be a deviation from the stoichiometry of the acid hydrolysis, and another would be non-ionic irreversible adsorption on the AG 1 anion-exchange resin. On the other hand, the enzymatic determination using chondroitinase AC and ABC[3] has been demonstrated by us (data not shown) to be susceptible to varous factors specific to the enzymatic reactions, such as variance in the structures of the substrates (the existence of a variety of dermatan sulphate–chondroitin sulphate copolymers) or in the enzyme source (condroitinase AC-I from *Flavobacterium*[3] and AC-II from *Arthrobacter*[11]. Accordingly, we thought that the data on the hexuronic acid content obtained by the enzymatic method need to be supported by some other method differing in principle from the enzymatic method. However, there was only a semiquantitative method based on the carbazole–orcinol ratio[2]. As described above, the method proposed here is very simple both in principle and practice, and the data in Table I show that the values obtained are reliable. Thus, our method is considered to be useful for investigators in the biochemical and medical fields as a complement to the existing methods.

REFERENCES

1 L.-Å. Fransson, in G. O. Aspinall (Editor), *The Polysaccharides*, Vol. 3, Academic Press, New York, 1985, p. 338.
2 P. Hoffman, A. Linker and K. Meyer, *Arch. Biochem. Biophys.*, 69 (1957) 435.
3 T. Yamagata, H. Saito, O. Habuchi and S. Suzuki, *J. Biol. Chem.*, 243 (1968) 1523.
4 K. Nagasawa, A. Ogamo, H. Ichihara and K. Yoshida, *Carbohydr. Res.*, 131 (1984) 301.
5 K. Meyer, E. Davidson, A. Linker and P. Hoffman, *Biochim. Biophys. Acta*, 21 (1956) 506.
6 H. Uchiyama and K. Nagasawa, *Carbohydr. Res.*, 159 (1985) 263.
7 Y. Inoue and K. Nagasawa, *Carbohydr. Res.*, 97 (1981) 263.
8 T. Bitter and H. M. Muir, *Anal. Biochem.*, 4 (1962) 330.
9 M. Kosakai and Z. Yosizawa, *Anal. Biochem.*, 93 (1979) 295.
10 H. Saito, T. Yamagata and S. Suzuki, *J. Biol. Chem.*, 243 (1968) 1536.
11 K. Hiyama and S. Okada, *J. Biol. Chem.*, 250 (1975) 1824.

Note

Adsorption chromatographic separation of ^{125}I-labelled derivatives of 3'-azido-3'-deoxythymidine

I. MUCHA, B. TANÁCS and G. TÓTH*

Institute of Isotopes of the Hungarian Academy of Sciences, P.O. Box 77, H-1525 Budapest (Hungary)

(First received February 22nd, 1989; revised manuscript received April 26th, 1989)

A sensitive radioimmunoassay of 3'-azido-3'deoxythymidine (AZT) requires a tracer of high specific activity. When ^{125}I is used for labelling, the maximum specific activity is 2200 Ci/mmol, provided that one radioiodine atom is introduced into the AZT molecule. Despite the fact that a higher specific activity of the tracer gives a higher sensitivity of the radioimmunoassay in question, the incorporation of two radioiodine atoms in the starting material, which would result in a specific activity of 4400 Ci/mmol, should be avoided as doubly labelled tracers usually exhibit poor binding to the antibody. As AZT cannot be directly labelled with radioiodine, a tyrosine methyl ester (TME) side-chain was coupled through either a succinyl or a carboxymethyl group at the 5'- position and ^{125}I was introduced into the 3- and/or 5-position of TME (Fig. 1) via electrophilic substitition.

In order to suppress the formation of the doubly labelled 3,5-diiodo-TME derivative, the inactive compounds to be labelled should be applied in large excess relative to radioiodine and care should be taken to ensure complete separation of the ^{125}I-labelled monoiodo derivatives, otherwise the specific activity is drastically decreased.

A decrease in the specific activity (expressed as radioactivity of the labelled molecule per unit mass, *e.g.*, Ci/g or Ci/mmol) results in a decrease in the sensitivity of the radioimmunoassay, *i.e.*, an increase in the detection limit.

Fig. 1. 3'-Azido-3'-deoxythymidine-5'-succinyl-TME (AZT-S-TME) and 3'-azido-3'-deoxythymidine-5'-O-carboxymethyl oxime-TME (AZT-C-TME).
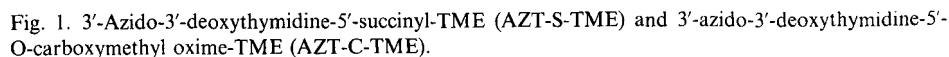
Previously, it was shown for several small molecules that the introduction of iodine substitutent(s) into the phenolic ring gives rise to a considerable increase in the adsorption affinity towards Sephadex LH-20 dextran gel compared with the parent molecules[1–4]. Based on this finding, we report an adsorption chromatographic separation of ^{125}I-labelled AZT from the inactive parent compounds using Sephadex LH-20 as adsorbent.

EXPERIMENTAL

Sample preparation

In order to examine the chromatographic behaviour of AZT-S-TME and AZT-C-TME (Fig. 1), used for radioiodination, these compounds were synthesized using tritium-labelled AZT. The latter was prepared from AZT (Sigma, St. Louis, MO, U.S.A.) according to the method of Hill and Freeman[5]. From tritium-labelled AZT the carboxymethyl oxime or hemisuccinate derivative was produced by the use of aminooxyacetic acid (Sigma) and succinic anhydride (Sigma). Tyrosine methyl ester (Sigma) was coupled to these derivatives by the use of the carbodiimide method.

Labelling with [125]I

The labelling of AZT-S-TME and AZT-C-TME with ^{125}I was performed by the use of the chloramine T method[6]. To 10–20 μg of AZT-S-TME or AZT-C-TME, 1–2 mCi of ^{125}I in slightly alkaline solution were added, followed by 200–300 μg of chloramine T in 50 μl of phosphate buffer (pH 7.4). After 30–60 s, the labelling reaction was quenched with 700 μg of sodium metabisulphite in 100 μl.

Chromatography

Sephadex LH-20 dextran gel (Pharmacia, Uppsala, Sweden) was swollen in distilled water prior to being packed in the column (130 × 10 mm I.D.). The height of the packing was 100 mm. The sample (0.1–0.2 ml) was placed on the top of the column and allowed to soak in and, 10–20 min later, *i.e.*, when adsorption equilibrium had been attained, elution was performed with ethanol–water (flow-rate 22–24 ml/h).

The pH of the eluent, when not indicated otherwise, was adjusted to 4 with 0.1 M citrate buffer so as to suppress the dissociation of the phenolic hydroxyl group of the tyrosine methyl ester residue. At higher pH ionization of the OH group may take place, which decreases or cancels the adsorption of the TME residue[1–4].

Radioactivity measurement

To measure the elution volume of tritium-labelled derivatives, the effluent was collected with a fraction collector (LKB 2211) in 0.5-ml fractions and its radioactivity was determined by liquid scintillation counting (LKB 1214).

In the case of chromatography of ^{125}I-labelled compounds, the effluent was passed over a NaI(Tl) scintillation crystal and the count rate was monitored by a ratemeter and registered by an x–y plotter. A peristaltic pump, flow-rate 22–24 ml/h, delivered the eluent.

The distribution coefficient was calculated according to the equation

$$k = \frac{V_e - V_0}{W} = \frac{V_e - 5.44}{1.46} \qquad (1)$$

where V_e, V_0 and W are the elution volume, the dead volume and the weight of the adsorbent, respectively.

RESULTS

The elution volume of tritium-labelled AZT-S-TME and AZT-C-TME was 10–11 ml and proved to be independent of the ethanol concentration. For ^{125}I-labelled AZT-S-TME and AZT-C-TME the elution volumes obtained for different ethanol concentrations are given in Table I.

From the data in Table I, the conclusion can be drawn that at any ethanol concentration investigated the ^{3}H-labelled compounds are eluted first, followed by the ^{125}I-labelled compounds. With ^{125}I-labelled AZT-S-TME and AZT-C-TME the elution volume decreases with increasing ethanol concentration. With the exception of dilute eluents (10 and 20% ethanol), the distribution coefficient depends on the ethanol concentration of the eluent as follows:

$$\log k = \log k_0 - n \log X \tag{2}$$

where k is the distribution coefficient, X is the concentration of the organic solvent expressed as a molar fraction in the binary eluent and k_0 and n are constants for a given binary eluent and iodo compound.

$$\log k = 1.33 \log X \; (^{125}\text{I-AZT-S-TME}) \tag{3}$$

$$\log k = 0.004 - 1.24 \log X \; (^{125}\text{I-AZT-C-TME}) \tag{4}$$

The distribution coefficient as a function of the ethanol concentration expressed as a molar fraction is shown in Fig. 2. Comparison of the data in Table I and the elution volume of the ^{3}H-labelled AZT-S-TME and AZT-C-TME reveals that the introduction of the radioiodine atom into position 3 of the TME residue considerably increases the elution volume. Consequently, the adsorption affinity of the ^{125}I-labelled molecules towards the LH-20 gel can mainly be attributed to the ^{125}I-labelled TME

TABLE I

ELUTION VOLUME OF ^{125}I-LABELLED AZT-S-TME AND AZT-C-TME

Eluent: aqueous ethanol (pH 4)

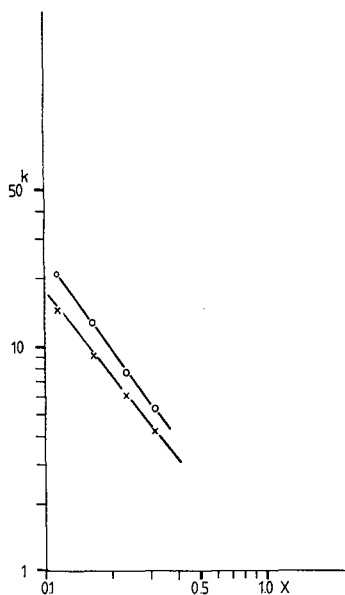| Ethanol concentration		Elution volume (ml)	
% (v/v)	Molar fraction, X	[^{125}I]AZT-S-TME	[^{125}I]AZT-C-TME
10	0.032	35	52
20	0.07	33	44
30	0.115	28	36
40	0.166	19	25
50	0.23	14	17
60	0.312	12	14

Fig. 2. Distribution coefficient as a function of ethanol concentration. Eluent: aqueous ethanol (pH 4). $\times$ = AZT-S-TME; $\bigcirc$ = AZT-C-TME.

residue and only to a negligible extent to the AZT itself. On the other hand, the linear $\log k$ vs. $\log X$ relationship which proved to be valid in the ethanol concentration range 30–60% (v/v) (molar fraction 0.115–0.312) makes possible the adjustment of the optimum distribution coefficient and the complete separation of ^{125}I-labelled AZT-S-TME and AZT-C-TME from the parent molecule.

REFERENCES

1 G. Tóth, *J. Radioanal. Chem.*, 46 (1978) 201.
2 G. Tóth, *J. Chromatogr.*, 238 (1982) 476.
3 G. Tóth and J. Zsadányi, *J. Radioanal Nucl. Chem. Lett.*, 86 (1984) 25.
4 G. Tóth, *J. Radioanal. Nucl. Chem.*, 121 (1988) 17.
5 J. A. Hill and G. A. Freeman, *J. Labelled Compd. Radiopharm.*, 25 (1988) 278.
6 W. M. Hunter and F. C. Greenwood, *Nature (London)*, 194 (1962) 495.

Book Review

Advances in chromatography, Vol. 28, edited by J. C. Giddings, E. Grushka and P. R.
Brown, Marcel Dekker, New York, Basle, 1989, XVIII + 317 pp., price
US$ 99.75 (U.S.A. and Canada), US$ 119.50 (rest of world), ISBN 0-8247-
7878-2.

This year's volume of this excellent series is made up of seven reviews:

(1) Theoretical aspects of quantitative affinity chromatography, by Alain Jaulmes and Claire Vidal-Mad-
jar;
(2) Column switching in gas chromatography, by Donald E. Willis;
(3) The use and properties of mixed stationary phases in gas chromatography, by Gareth J. Price;
(4) On-line small-bore chromatography for neurochemical analysis in the brain, by William H. Church
and Joseph B. Justice, Jr.;
(5) The use of dynamically modified silica in HPLC as an alternative in chemically bonded materials, by
Per Helboe, Steen Honoré Hansen and Mogens Thomsen;
(6) Gas chromatographic analysis of plasma lipids, by Arnis Kuksis and John J. Myher; and
(7) HPLC of penicillin antibiotics, by Michel Margosis.

These are all very satisfactory reviews, with only one observation, namely that
some authors reviewed their field recently in the form of a monograph and thus cover
the same ground here in another form.

Without wanting to carp unduly, it should be noted that in the last review,
dealing with penicillin, it is stated: "The application of liquid chromatography to the
analysis of antibiotics was first performed by Fischbach." Now Fischbach's papers
date from 1946–1947, while liquid chromatography was used already in 1942 by
Abraham and Chain and by Catch, Cook and Heilbron in purifying penicillins, and
by Levi in 1946–1949 for their analysis. This might perhaps have been mentioned
here.

Unfortunately, the reference lists have not been checked; thus, there are numer-
ous typing errors, such as "Syprynowicz", "Guichon", "Di Corcici".

M. LEDERER

Book Review

Neuromethods, Vol. 7, lipids and related compounds, edited by A. Boulton, G. Baker and L. Horrocks, Humana Press, Clifton, NJ, 1988, 360 pp., price US$ 64.50 (U.S.A.), US$ 74.50 (export).

Volume 7 of this successful series contains ten chapters dealing with

(1) Lipid extraction;
(2) Preparation and analysis of acyl and alkenyl groups of glycerophospholipids from brain subcellular membranes;
(3) Quantitative analysis of acyl group composition of brain phospholipids, neutral lipids and free fatty acids;
(4) Steroids and related isoprenoids;
(5) Phospholipids;
(6) Determination of phospholipases, lipases and lysophospholipases;
(7) Isolation, separation and analysis of phosphoinositides from biological sources;
(8) Analysis of prostaglandins, leukotrienes and related compounds in retina and brain;
(9) HPLC analysis of neutral glycosphingolipids and sulfatides; and
(10) Methods to study the biochemistry of gangliosides.

Each chapter was written by a different author (or group of authors). They all seem adequate as a first orientation for neurochemists. But none of them is exhaustive; for example, the chapter on phospholipids lists altogether 41 references and none later than 1986. So one can hardly call these chapters reviews nor can the tome be called a handbook.

In the chapter on "Steroids and related isoprenoids" the main topic is stated as "Cholesterol is quantitatively the major steroid synthesised within neural tissue and methodologies relating to the metabolism of cholesterol will consequently be a major focus of this review". So the reader will certainly not find a coverage of the literature of steroid chromatography. One has the impression that all chapters are interesting, well written and informative. It is, however, not quite clear whether the authors are addressing themselves to research workers or to students. For the first the literature coverage seems scanty, for the latter the topic is too specialised.

M. LEDERER

PUBLICATION SCHEDULE FOR 1989

Journal of Chromatography and Journal of Chromatography, Biomedical Applications

MONTH	J	F	M	A	M	J	J	A	S	
Journal of Chromatography	461 462 463/1	463/2 464/1	464/2 465/1 465/2	466 467/1 467/2	468 469 470/1 470/2	471 472/1 472/2 473/1	473/2 474/1 474/2 475	476 477/1 477/2	478/1 478/2 479/1	The publication schedule for further issues will be published later
Bibliography Section		486/1		486/2		486/3		486/4		
Biomedical Applications	487/1	487/2	488/1 488/2	489/1 489/2	490/1 490/2	491/1	491/2	492 493/1	493/2 494	495

INFORMATION FOR AUTHORS

(Detailed *Instructions to Authors* were published in Vol. 445, pp. 453–456. A free reprint can be obtained by application to the publisher, Elsevier Science Publishers B.V., P.O. Box 330, 1000 AH Amsterdam, The Netherlands.)

Types of Contributions. The following types of papers are published in the *Journal of Chromatography* and the section on *Biomedical Applications:* Regular research papers (Full-length papers), Notes, Review articles and Letters to the Editor. Notes are usually descriptions of short investigations and reflect the same quality of research as Full-length papers, but should preferably not exceed six printed pages. Letters to the Editor can comment on (parts of) previously published articles, or they can report minor technical improvements of previously published procedures; they should preferably not exceed two printed pages. For review articles, see inside front cover under Submission of Papers.

Submission. Every paper must be accompanied by a letter from the senior author, stating that he is submitting the paper for publication in the *Journal of Chromatography*. Please do not send a letter signed by the director of the institute or the professor unless he is one of the authors.

Manuscripts. Manuscripts should be typed in double spacing on consecutively numbered pages of uniform size. The manuscript should be preceded by a sheet of manuscript paper carrying the title of the paper and the name and full postal address of the person to whom the proofs are to be sent. Authors of papers in French or German are requested to supply an English translation of the title of the paper. As a rule, papers should be divided into sections, headed by a caption (*e.g.*, Summary, Introduction, Experimental, Results, Discussion, etc.). All illustrations, photographs, tables, etc., should be on separate sheets.

Introduction. Every paper must have a concise introduction mentioning what has been done before on the topic described, and stating clearly what is new in the paper now submitted.

Summary. Full-length papers and Review articles should have a summary of 50–100 words which clearly and briefly indicates what is new, different and significant. In the case of French or German articles an additional summary in English, headed by an English translation of the title, should also be provided. (Notes and Letters to the Editor are published without a summary.)

Illustrations. The figures should be submitted in a form suitable for reproduction, drawn in Indian ink on drawing or tracing paper. Each illustration should have a legend, all the *legends* being typed (with double spacing) together on a *separate sheet*. If structures are given in the text, the original drawings should be supplied. Coloured illustrations are reproduced at the author's expense, the cost being determined by the number of pages and by the number of colours needed. The written permission of the author and publisher must be obtained for the use of any figure already published. Its source must be indicated in the legend.

References. References should be numbered in the order in which they are cited in the text, and listed in numerical sequence on a separate sheet at the end of the article. Please check a recent issue for the layout of the reference list. Abbreviations for the titles of journals should follow the system used by *Chemical Abstracts*. Articles not yet published should be given as "in press" (journal should be specified), "submitted for publication" (journal should be specified), "in preparation" or "personal communication".

Dispatch. Before sending the manuscript to the Editor please check that the envelope contains three copies of the paper complete with references, legends and figures. One of the sets of figures must be the originals suitable for direct reproduction. Please also ensure that permission to publish has been obtained from your institute.

Proofs. One set of proofs will be sent to the author to be carefully checked for printer's errors. Corrections must be restricted to instances in which the proof is at variance with the manuscript. "Extra corrections" will be inserted at the author's expense.

Reprints. Fifty reprints of Full-length papers, Notes and Letters to the Editor will be supplied free of charge. Additional reprints can be ordered by the authors. An order form containing price quotations will be sent to the authors together with the proofs of their article.
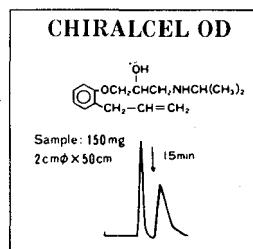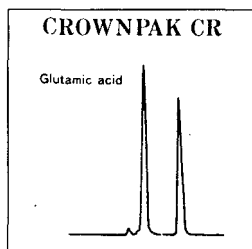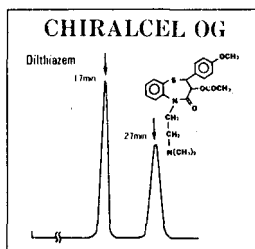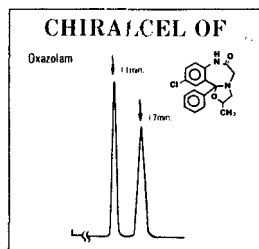
Advertisements. Advertisement rates are available from the publisher on request. The Editors of the journal accept no responsibility for the contents of the advertisements.

For Superior Chiral Separation

CHIRALCEL, CHIRALPAK and CROWNPAK are now available from DAICEL and include 15types of HPLC columns which provide superior resolution of racemic compounds.

Drugs directly resolved on our DAICEL columns are given as follows;

SUBSTANCE	α	column	SUBSTANCE	α	column	SUBSTANCE	α	column
Alprenolol	3.87	OD	Gauifenesin	2.40	OD	Oxapadol	complete	CA-1
Amphetamine	1.2	CR	Hexobarbital	1.7	CA-1		resolution	
Atenoloi	1.58	OD	Homatropine	3.13	OD	Oxazepan	4.36	OC
Atropine	1.62	OD	Hydroxyzine	1.17	OD	Oxazolam	1.67	OF
Baclofen	1.39	CR	Indapamide	. 1.58	OJ	Oxprenolol	6.03	OD
Carbinoxamine	1.39	OD	Ketamine	complete	CA-1	Perisoxal	1.33	OF
Carteolol	1.86	OD		resolution			1.27	OD
Chlophedianol	2.82	OJ	Ketoprofen	1.46	OJ	Pindolol	5.07	OD
Chlormezanone	1.47	OJ	Mephobarbital	5.9	OJ	Piprozolin	1.7	CA-1
Cyclopentolate	2.47	OJ		2.3	CA-1	Praziquantal	complete	CA-1
Diltiazem	1.46	OD	Methaqualone	2.8	CA-1		resolution	
	2.36	OF		7.3	OJ	Propranolol	2.29	OD
	1.75	OG	Methsuximide	2.68	OJ	Rolipram	complete	CA-1
Disopyramide	2.46	OF	Metoprolol	complete	OD		resolution	
Ethiazide	1.54	OF		resolution		Sulconazole	1.68	OJ
Ethotoin	1.40	OJ	Mianserin	1.75	OJ	Suprofen	1.6	OJ
Fenoprofen	1.3 .	OJ	Nilvadipine	complete	OT	Trimebutine	1.81	OJ
Glutethimide	2.48	OJ		resolution		Warfarin	1.96	OC

CHIRALCEL OF — Oxazolam

CHIRALCEL OG — Dilthiazem

CROWNPAK CR — Glutamic acid

CHIRALCEL OD — Sample: 150mg 2cmφ×50cm

In addition to the drugs listed above, our chiral columns permit resolution also of the following :
FMOC amino acids and Carboxylic acids, and Pesticides, for example Isofenfos, EPN and Acephate, and Synthetic intermediate 4-hydroxy cyclophentenone etc, Many other compounds besides these can be readily resolved.

▶ Separation Service
● A pure enantiomer separation in the amount of 100g～10kg is now available.
● Please contact us for additional information regarding the manner of use and application of our chiral columns and how to procure our separation service.

For more information about our Chiral Separation Service and Columns, please contact us !

DAICEL CHEMICAL INDUSTRIES, LTD.

Tokyo
8-1, Kasumigaseki 3-chome,
Chiyoda-ku, Tokyo 100, Japan
Phone : 03(507)3151, 3189
Telex: 222-4632 DAICEL J
FAX: 03(507)3193

DAICEL (U.S.A.) INC.
Fort Lee Executive Park
Two Executive Drive Fort Lee,
New Jersey 07024
Phone : (201)461-4466
FAX : (201)461-2776

DAICEL (U.S.A.), INC.
611 west 6th Street, Room 2152
Los Angeles California 90017
Phone: (213)629-3656
Telex: 215515 DCIL UR
FAX: (213)629-2109

DAICEL (EUROPA) GmbH
Königsallee 92a.
4000 Düsseldorf 1, F. R. Germany
Phone: (0211)134158
Telex: (41)8588042 DCEL D
FAX: (0211)879-8329

425 A